AMINO ACID PLATINUM(II) COMPLEXES: SYNTHESIS, CHARACTERISATION AND COUPLING TO PORPHYRINS

by

Jacquline Bond

A thesis
presented to the
University of Western Sydney, Macarthur
in partial fulfillment of the requirements
for the degree of
Doctor of Philosophy

April, 2000

PLEASE NOTE

The greatest amount of care has been taken while scanning this thesis,

and the best possible result has been obtained.

ACKNOWLEDGEMENTS

The completion of a PhD project is a huge task involving the help and support of many people. I would especially like to acknowledge the assistance of my supervisor, Dr Trevor D. Bailey, for providing helpful suggestions, comments and constructive criticism on style and content.

My profuse thanks to goes to Dr Narisimha Redi for his helpful discussions and generous assistance with many of the NMR spectra. I would also like to express my appreciation of the valuable advice and assistance given to me by Dr Michael Antolovich, Dr Herman Hombrecher, Professor John Hubbard and Dr Robyn Crumbie.

I wish to express deep gratitude to many people who, although they were not directly involved in the project, provided ideas, recognition and simply good company in the laboratory. Special thanks are due to the small number of fellow postgraduates without whose understanding and company would have made my studies far less enjoyable - Dale Jones, Paul Pelligrini, Alex Szyczew, Ivan Greguric and Gary Bowman. I would also like to thank Chris Turville for his patience, understanding and most of all, smiles and good cheer at just the right times.

Finally, I must thank my Mum and Dad for giving me the unreserved encouragement and support I needed to finish this task. Throughout the final year, my Mum asked repeatedly, "When are you going to finish your PhD and graduate? ". She asked once too often, so I did. Her enthusiastic support and repeated urgings to graduate helped bring this thesis to fruition. This thesis owes its existence more to my Mum than any other person. To Mum and Dad, I dedicate this thesis.

STATEMENT OF AUTHENTICATION

The work, presented in this thesis is, to the best of my knowledge and belief, original except as acknowledged in the text. I hereby declare that I have not submitted this material, either in whole or in part, for a degree at this or any other institution.

[redacted]

TABLE OF CONTENTS

LIST OF TABLES

LIST OF DIAGRAMS

ABBREVIATIONS

9-AA	9-aminoacridine orange
adria	adriamycin
AgI	silver iodide
amac	amino acid
AO	acridine orange
AQ	anthraquinone
BCl_3	boron trichloride
BF_3-etherate	boron trifluoride diethyl etherate
carboplatin	cis-diammine(1,1-cyclobutanedicarboxylato)platinum(II)
CBDCA	cyclobutanedicarboxylate
$CDCl_3$	deuterochloroform
CH_2Cl_2	dichloromethane
$CHCl_3$	chloroform
$(C_6H_5)_4BNa$	sodium tetraphenylborate
$(COCl)_2$	oxalyl chloride
cisplatin	cis-diamminedichloroplatinum(II)
D_2O	deuterium oxide
d_6-DMSO	d_6-dimethylsulfoxide
dach	1,2-diaminocyclohexane
dbn	3,4-diaminobenzoic acid
DCC	N,N-dicyclohexylcarbodiimide
DDQ	2,3-dichloro-5,6-dicyanobenzoquinone
DDTC	diethyldithiocarbamate
DEPT	distortionless enhancement by polarisation transfer
DHE	dihematoporphyrin ether/ester
DMF	N,N-dimethylformamide
DNA	deoxyribonucleic acid
2D-NMR	two-dimensional nuclear magnetic resonance
EDAC	1-ethyl-3-(3-dimethylaminopropyl)carbodiimide
en	1,2-diamino-ethane (also known as ethylenediamine)
ESI	electrospray ionisation
$H[Pt(L\text{-lysine})Cl_2]$	dichloro(L-lysine)platinum(II)

H_2SO_4	sulfuric acid
HCl	hydrochloric acid
HMG	high-mobility group proteins
HMQC	Hetero Correlation through Quantum Coherence
HOBT	1-hydroxybenzotriazole hydrate
HPD	hematoporphyrin derivative
IR	infrared
JM-40	[Pt(malonato)(en)]
$K[Pt(L\text{-}asp\text{-}N,O)Cl_2]$	dichloro(L-aspartic acid)platinum(II)
$K[Pt(L\text{-}glu.OMe)Cl_2]$	dichloro(L-glutamic acid-methyl ester)platinum(II)
$K[Pt(L\text{-}glu\text{-}N,O)Cl_2]$	dichloro(L-glutamic acid)platinum(II)
$K[Pt(L\text{-}serine)Cl_2]$	dichloro(L-serine)platinum(II)
$K_2[PtCl_4]$	potassium tetrachloroplatinate(II)
KCl	potassium chloride
L-asp	L-aspartic acid
LDL	low density lipoproteins
L-glu	L-glutamic acid
L-glu.OMe	L-glutamic acid, methyl ester
$MgSO_4$	magnesium sulfate
Na_2CO_3	sodium carbonate
Na_2SO_4	sodium sulfate
NaCl	sodium chloride
n-BuLi	n-butyllithium
NH_4Cl	ammonium chloride
NHS	N-hydrosuccinimide
NMR	nuclear magnetic resonance
o-nitro-phen	o-nitro-phenylenediamine
P_2O_5	phosphorus pentaoxide
PCl_3	phosphorus trichloride
PCl_5	phosphorus pentachloride
PDT	photodynamic therapy

PF_6^-	pentafluorophosphate
ppm	parts per million
[Pt(*cis*-R,S-dach)Cl_2]	dichloro(*cis*-R,S-1,2-diaminocyclohexane)platinum(II)
[Pt(dbn)Cl_2]	dichloro(3,4-diaminobenzoic acid)platinum(II)
[Pt(en)Cl_2]	dichloro(ethylenediamine)platinum(II)
[Pt(L-asp-N,O)(*cis*-R,R-dach)]	(L-aspartic acid)(*cis*-R,S-1,2-diaminocyclohexane)platinum(II)
[Pt(L-asp-N,O)(en)]Cl	(L-aspartic acid)(ethylenediamine)platinum(II) chloride
[Pt(L-asp-N,O)$(NH_3)_2$]Cl	bis(ammine)(L-aspartic acid)platinum(II) chloride
[Pt(L-asp-N,O)(*trans*-R,R-dach)]	(L-aspartic acid)(*trans*-R,R-1,2-diaminocyclohexane)platinum(II)
[Pt(L-glu-N,O)$(NH_3)_2$]Cl	bis(ammine)(L-glutamic acid)platinum(II) chloride
[Pt(L-lysine)$(NH_3)_2$]Cl	bis(ammine)(L-lysine)platinum(II) chloride
[Pt(L-serine)(en)]Cl	(ethylenediamine)(Lserine)platinum(II) chloride
[Pt(L-serine)$(NH_3)_2$]Cl	bis(ammine)(L-serine)platinum(II) chloride
[Pt(o-nitro-phen)Cl_2]	dichloro(o-nitro-phenylenediamine)platinum(II)
[Pt(*trans*-R,R-dach)Cl_2]	dichloro(*trans*-R,R-1,2-diaminocyclohexane)platinum(II)
[Pt(*trans*-S,S-dach)Cl_2]	dichloro(*trans*-S,S-1,2-diaminocyclohexane)platinum(II)
$SOCl_2$	thionyl chloride
tba	tert-butylamine
[(terpy)-Pt(HET)]$^+$	2-hydroxyethanethiolato-2,2',2"-terepyridineplatinum(II)
TFA	trifluoroacetic acid
THF	tetrahydrofuran
3THPP	tetra(3-hydroxyphenylporphyrin)
TLC	thin layer chromatography
TMePP-COOH	5-(p-carboxylphenyl)-10,15,20-tri(p-methylphenyl)porphyrin
TMePP-COOMe	5-(p-methoxycarbonylphenyl)-10,15,20-tri(p-methyl-phenyl)porphyrin
TMePP-COOMe	5-(p-methoxyphenyl)-10,15,20-tri(p-methylphenyl)porphyrin
TMesPP-COOMe	5,10,15-trimesityl-20-(4-methoxycarbonylpheny)porphyrin
TMS	tetramethylsilane
TMSP	2,2,3,3-tetradeutero-3-(trimethylsily)propionate
TPP	5,10,15,20-tetraphenylporphyrin

TPP-NH_2	5-(p-aminophenyl)-10,15,20-triphenylporphyrin
TPP-NO_2	5-(4-nitrophenyl)-10,15,20-triphenylporphyrin
$TPPS_3$-NH_2	5-(4-aminophenyl)-10,15,20-tris(4-sulfonatophenyl)porphyrin
$TPPS_4$	tetraphenylporphyrin tetrasulfonate
TTP	tetratolyporphyrin
UV	ultra-violet
WR2721	amifostine
XP	xeroderma pigmentosum

ABSTRACT

Anti-cancer treatment using existing cytotoxic drugs is far from being tumour-specific. The ultimate way to achieve tumour-selectivity is to use the tumour-localising capabilities of porphyrins to direct the active platinum components. The present study describes the synthesis and characterisation of novel platinum-porphyrin conjugates that have the potential of binding specifically to the DNA of cancer cells.

The first stage involves the synthesis of a series of platinum(II) complexes. Initially, the 1:1 dichloro complexes of the formula $[Pt(amac\text{-}N,O)Cl_2]^-$ were isolated from reactions of $K_2[PtCl_4]$ with the amino acids L-asp, L-glu, L-glu.OMe, L-serine and L-lysine. These complexes were characterised with elemental analysis, infrared, ^{1}H NMR and ^{13}C NMR spectra. The X-ray structure of $[Pt(L\text{-}lysine)Cl_2]^-$ has been determined. Crystals of $[Pt(L\text{-}lysine)Cl_2]^-$ are monoclinic, spacer group P2(1), with two independent molecules in the asymmetric unit and unit dimensions a = 9.634 (8) Å, b = 11.113 (11) Å, c = 11.057 (9) Å and β = 102.02 (6)°. Many of the dichloro complexes were then used to produce $[Pt(amac\text{-}N,O)(A)]^+$ derivatives where A = 2 x NH_3, ethylenediamine or diaminocyclohexane (*cis*-R,S- and *trans*-R,R-). Various diamine platinum(II) complexes were also synthesied and characterised by ^{1}H and ^{13}C NMR spectroscopy. The results were applied to the analysis of the $[Pt(amac\text{-}N,O)(A)]^+$ derivatives.

The second stage describes the synthesis of a set of four porphyrins containing suitable linker groups. Three of these porphyrins were prepared by mixed aldehyde condensations with pyrrole and substituted benzaldehydes. The other was prepared by aryl nitration of TPP followed by reduction to give an amino-porphyrin. Each porphyrin bears a functional group that can react directly in coupling reactions. These groups include an amine, a carboxyl and a methyl ester. All

porphyrins have been characterised by spectral methods such as UV-Visible, ^{1}H NMR, ^{13}C NMR and mass spectroscopy.

Finally, an investigation into the use of carbodiimide reagents in the coupling of TPP-NH_2 and $TPPS_3$-NH_2 with $[Pt(L\text{-}asp\text{-}N,O)(NH_3)_2]^+$ has been explored. The reaction of TPP-NH_2 with $[Pt(L\text{-}asp\text{-}N,O)(NH_3)_2]^+$ in the presence of DCC and HOBT afforded the amide linked platinum-porphyrin conjugate in 43% yield. Correspondingly, the reaction of $TPPS_3$-NH_2, $[Pt(L\text{-}asp\text{-}N,O)(NH_3)_2]^+$ and EDAC gave a water-soluble conjugate in 53% yield. The structures of the platinum-porphyrin conjugates were mainly determined by infrared, ^{1}H NMR and ^{13}C NMR spectroscopy.

CHAPTER

1

GENERAL INTRODUCTION

The study of cancer plays an important role in modern medical science. Over the years, a lot has been learnt about the properties and treatment of cancer cells. Despite the remarkable progress made in understanding the genesis of cancer, the work so far has had very little impact in the clinic especially the design of new and improved drugs.

Platinum-based drugs such as cis-diamminedichloroplatinum(II) and its analogue, carboplatin, are the most effective chemotherapeutic agents used in the treatment of testicular, ovarian, bladder and lung cancers. Nevertheless, the emergence of toxic side-effects compromises its clinical effectiveness. It is generally agreed that most of the toxic effects of platinum-based drugs arise from their lack of selectivity.

This thesis reports on the development of new platinum(II) complexes bound to carrier molecules with the hope of obtaining compounds which display the cytotoxic effects only in tumour tissue. In addition, some information is included about what is known about the causes of cancer, how it kills and the current methods of treatment.

Cancer: A Review

Cancer is an ancient disease. It has afflicted our ancestors throughout history. Cancer has always been a much feared disease, but until recently it was seldom encountered. In the last decade, the situation has changed dramatically. Cancer is now Australia's leading cause of death followed by ischaemic heart disease. In 1998, cancer accounted for 27% (33 560 deaths) of total deaths.[1] The leading primary site of male cancer deaths was the trachea, bronchus and lung of which there were 4,820 deaths. For females, the primary site was the breast with 2,542 deaths. Other major sites are shown in the Diagram 1.1.

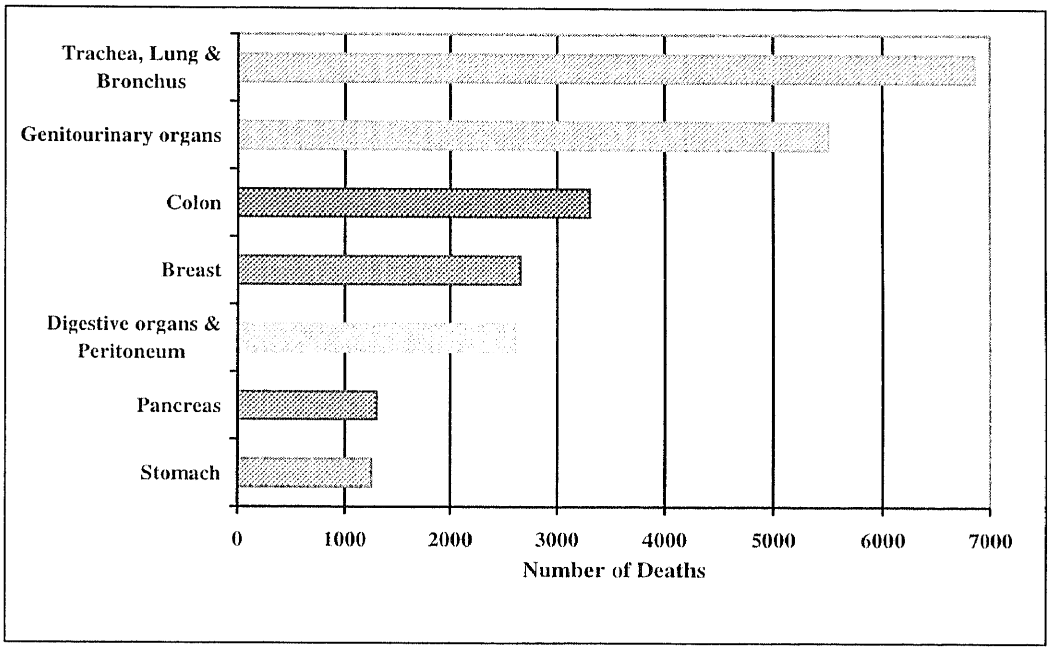

Diagram 1.1: Deaths due to cancer-main sites, Australia 1998.

There are many reasons for the substantial increase in the incidence of cancer. Firstly, many years of exposure to carcinogenic materials are usually required to produce cancer. The average life span of people in the 20th century has increased during the last fifty years, and therefore more people now live long enough to develop cancer. Secondly, modern life-styles and the contemporary environment result in longer exposures to more kinds of carcinogens and in greater amounts.

1.1 CHARACTERISTICS OF A CANCER CELL

Cancer results from the malfunctioning of one of the many cells that make up the body. Cancer generally begins when a single normal cell converts to a cancer cell, that is it undergoes transformation. Each descendant of the cell is also a cancer cell and all, in turn, produces more cancer cells. Whatever the nature of the conversion, it is transmitted from one cell generation to the next at each cell division.

Cancer cells have heritable properties[2,3] that underlie the nature of the disease they cause. It is the combination of these features that makes cancers peculiarly dangerous.

(a) Regulation of reproduction is defective in cancer cells. In an adult the reproduction of normal cells occurs only to replace cells that are lost. The insidious property of cancer cells is that they are unresponsive to feedback mechanisms from neighbouring cells. As a consequence, cell division is no longer regulated, leading to uncontrolled proliferation.

(b) Cancer cells are effectively immortal. Many kinds of normal cells have limited life spans, for example, lymphocytes, intestinal epithelial cells and epidermal cells of skin. In cancer cells, the genetic control of life span is lost, resulting in immortality.

Cancer begins when a single cell becomes defective in the characteristics described above as a result of a change in its genetic make-up. These genetic changes appear to consist of mutations in the expressions of genes involved in the control of reproduction, differentiation and life span of a cell.

1.2 CANCER CELLS AND DISEASE

The two classes of genes[2] in which mutations cause transformation include proto-oncogenes and tumour suppressers.

Proto-oncogenes

Proto-oncogenes are normal cellular genes which are critical for normal cell proliferation and differentiation. Proto-oncogenes are present in every normal cell in the body, and encode for growth factors, nuclear proteins, regulatory enzymes and components of intracellular pathways of signal transduction. When proto-oncogenes are normally regulated, their functions are essential to the cell; it is only when they become transformed into an active oncogene that they contribute to the development of cancer. There are many conceivable modes of genetic disruption that can activate a proto-oncogene. The gene can be altered by point mutation, or through chromosomal abnormalities called "translocation," in which two chromosomes exchange segments. Expression of genes on that segment had been precisely regulated by virtue of its normal chromosomal location, but controls are lost at the new location. A change in the expression of a single amino acid is sufficient[2,4] for conversion to an oncogene.

Tumour Suppressers

The emergence of cancer appears to involve the accumulation of genetic damage in a target cell. To help prevent such damage, cells have machinery to repair deoxyribonucleic acid (DNA) after it has been damaged. Tumour suppressers such as the p53 protein have the job of temporarily stopping cell division, allowing the DNA to be repaired before copying.[5] The p53 protein is also identified with a process of programmed cell death that may be important in killing cancer cells. It has been found that mutations in this gene contribute to the development of 50% of all human cancers.[5] Cancer researchers have convincing evidence that shows that loss of the growth inhibition exerted by these genes plays a major role in cancer.

1.3 SPREAD OF CANCER CELLS AND DEATH

Cancer requires months or even years to give rise to a cancer mass that produces disease symptoms. Immortality and failure to stop reproducing causes cancer cells to accumulate. Accumulation of these functionally defective cells results in disease. Eventually the growing mass interferes with the function of an essential organ, leading to death. Commonly the function of the liver, lungs, brain or kidney is impaired.

The malignancy is often enhanced by the invasion of the cancer cells in to the adjacent normal tissue and by the spread of cancer cells to the other sites. This spreading occurs when detached cancer cells travel in the blood and lymphatic system, a process called *metastasis*.[2] Many of these wandering cancer cells are probably destroyed by the immune system. However, a minute proportion of these cells often succeed in founding metastatic colonies in the liver, bone, lungs, brain and lymph nodes. Development of new sites greatly complicates the problem of treatment.

A large number of cancer deaths result from infection. An impaired immune system means that patients are highly susceptible to bacteria, molds and other infectious organisms. These organisms which are normally destroyed by the immune system of a healthy individual can form fatal infections in cancer victims.

1.4 DNA REPAIR AND CANCER

DNA is a long polymer of nucleotide subunits. Each nucleotide contains phosphate, the sugar deoxyribose and one of four nucleic acid bases: adenine, thymine, guanine or cytosine.[6] It is these bases that carry the information that specifies the composition of all the organisms protein molecules.

DNA is organised in two chains that form a double helix (Diagram 1.2). Given the structure and size of the bases this arrangement requires the sequence of bases to follow the Watson-Crick pairing rules.[7] This specifies that wherever an adenine appears on one chain it is linked with thymine on the other. Similarly guanine is matched with cytosine. The adenine-thymine pair is stabilised by two hydrogen bonds whilst the guanine is stabilised by three hydrogen bonds.[7] This consistent pairing of complementary bases is crucial for maintaining the genetic code.

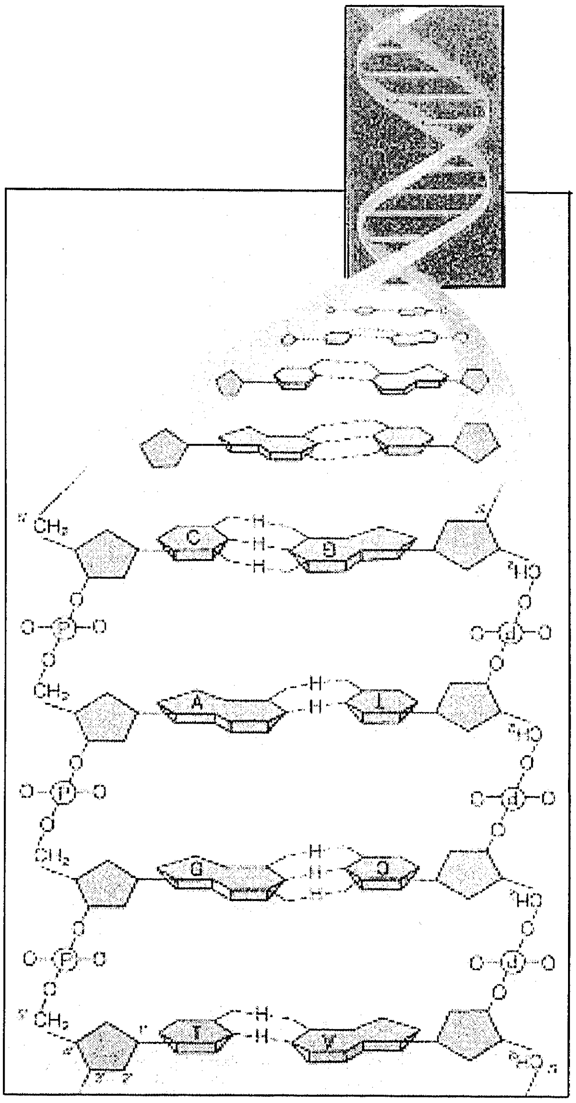

Diagram 1.2: DNA strand.

Genetic material is at constant risk of malfunctioning, both because of errors introduced during its manufacture and damage caused by environmental insults such as chemicals and ultra-violet radiation. To deal with this threat, cells possess repair mechanisms that correct mutational lesions before they become part of the inherited genetic inventory. There are two types of repair systems, mismatch repair and excision repair.[8]

Mismatch Repair

Mismatch repair specialises in errors made during DNA replication. The common DNA biosynthetic errors include insertion of an incorrect base or the addition of an extra nucleotide, resulting in unpaired bases within the helix. It is the job of the mismatch repair system to scan newly synthesised DNA strands for violations of the Watson-Crick pairing rules, cut out mistakes and then fill in the gaps with the correct sequence.[9]

Nucleotide Excision Repair

Lesions made by outside agents such as ultra-violet light and chemicals are handled by nucleotide excision repair pathway (NER). NER recognises bulky lesions in the DNA strand and is crucial for humans. Individuals with defects in their NER processes have the genetic disease xeroderma pigmentosum (XP) and are so sensitive to ultra-violet radiation that the slightest exposure of the skin to sunlight is liable to provoke skin cancer.[10] NER is much more complicated than mismatch repair using the production of twelve genes to recognise and clip out damaged DNA segments. The steps involved in the removal of a lesion by NER[11,12] are shown in Diagram 1.3.

The loss of DNA repair proficiency may result in genetic destabilisation leading to mutations that activate proto-oncogenes or inactivate tumour suppresser genes, and thus cause cancer. Not only has the intense study of repair systems provided molecular geneticists with much needed information, but it also has an impact in the clinic. New anti-cancer drugs have to be designed so that insertion on a DNA strand produces lesions that are subtle enough to escape recognition by the cells repair systems.

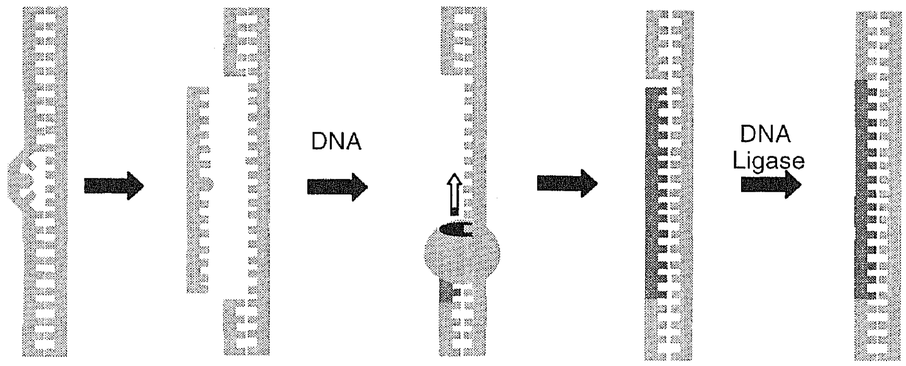

(1) Recognition of lesion followed by excision of the damaged region with concomitant degradation of excised DNA Strand.

(2) DNA Polymerase binds to the 3'-OH end of the cut DNA strand and synthesises a new strand to fill in the gap.

(3) DNA Ligase seals the nick left in the damaged strand, thus completing the restoration process.

Diagram 1.3: Steps of NER.

1.5 TREATMENT OF CANCER

Without treatment, virtually all cancers are sooner or later fatal. The objective of cancer treatment is to eliminate all cancer cells from an individual. Elimination of every trace of cancer cell is necessary because cancer can regrow from a single surviving cancer cell. The three traditional methods of treatment include:

(a) Surgery: the surgical removal of discrete masses of cancerous tissue. This method works when a tumour is fully accessible and has not spread, but it offers little hope when the cancer cells have begun to disseminate through the body.

(b) Radiation: shrinks or kills cancers not amenable to surgery.

(c) Chemotherapy: drug regimes that systematically attack metastasis. Such treatments have severe side effects because the drugs are highly toxic and cannot discriminate between normal and cancer tissue.

Unfortunately, by the time the disease has been discovered clinically most cancers already consists of billions of cells and usually have already moved to other sites. To remove, or destroy every last cell is difficult and usually impossible with presently available methods. Development of new ways of treating cancer is centred on the manipulation of components that deliver a drug specifically to cancer cells. Without such specificity, drugs will also bind to normal cells, producing unacceptable side-effects.

Platinum Based Chemotherapeutic Drugs

1.6 DISCOVERY OF CISPLATIN

Platinum-based drugs are among the most active and commonly used clinical agents for the treatment of advanced cancer. The first platinum drug to be used clinically was cis-diamminedichloroplatinum(II), commonly known as cisplatin (Diagram 1.4).

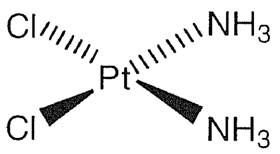

Diagram 1.4: cis-Diamminedichloroplatinum(II).

Barnett Rosenberg serendipitously discovered the anti-cancer properties of cisplatin in 1965.[13] Rosenberg was studying the influence of weak alternating currents on the growth of *Escherichia coli*. During the course of his experiments, he observed that when the current was applied across platinum electrodes immersed in media containing the bacteria and ammonium chloride (NH_4Cl), cell division ceased and the bacterial cells grew long filaments up to 300 times their normal length. This filamentous growth is indicative of the ability of an agent to react with DNA.[3] Further studies revealed that it was not the electric current itself but trace amounts of a cis-configurated chloro complex that were responsible for this biological effect. The complex that resulted from the oxidation of the platinum electrode was identified as cisplatin. Six years later, the anti-proliferative effect of cisplatin was applied to the treatment of human cancer.

Cisplatin is routinely used for the treatment of ovarian, testicular, bladder, head and neck, and small-cell lung carcinomas.[7,14] Although cisplatin is an active anti-cancer agent, it is also extremely toxic. The major toxicities induced by cisplatin include nephrotoxicity, neurotoxicity, nausea and vomiting, myelosuppression (bone marrow suppression) and ototoxicity.[3,15] All toxicities appear to be dose related, with neurotoxicity, nephrotoxicity and ototoxicity appearing to be cumulative. The maximum tolerated dose of cisplatin is 100mg/day for up to five consecutive days.[16]

Neurotoxicity is the major dose-limiting problem associated with cisplatin.[14,17] After several treatment cycles patients experience a loss of vibration sense, paraethesia and sensory ataxia.[18] The use of neuroprotective drugs has been explored as a potentially useful method to deliver higher doses of cisplatin without the development of cisplatin-induced peripheral neuropathy. Of those tried, the administration of glutathione concomitant with cisplatin was found to significantly reduce the incidence of neurotoxicity without lowering the therapeutic index of cisplatin.[17,19]

In early clinical trials, nephrotoxicity was the primary dose-limiting adverse effect. Nowadays, nephrotoxic effects have become more manageable through the use of intravenous saline hydration[14] and subsequent mannitol diuresis[16] during cisplatin administration. Nucleophilic sulfur-containing compounds also appear promising in attenuating kidney and gastro-intestinal problems. These include sodium thiosulfate,[20] thiourea[21] and amifostine (WR2721)[22,23] The protective effect of these thiol compounds can be attributed to the formation of inactive mobile metabolites, resulting in a reduction in the amount of unchanged cisplatin in the kidney. Studies on animal systems have shown that diethyldithiocarbamate (DDTC) is also capable of protecting against cisplatin-induced nephrotoxicity.[20] Unfortunately, the usefulness of DDTC in the clinic is significantly reduced, partly due to chemotherapy-related toxicities. Toxicities related to DDTC infusion include burning of the mouth, chest tightness and central nervous toxicity.[20,24]

Depression of bone marrow diminishes the body's ability to produce the white blood cells, leaving patients open to secondary infections. Protection from cisplatin-induced bone marrow suppression may be controlled by the prophylactic use of hematopoietic growth factors and bone marrow transplantation.[25]

1. 7 DEVELOPMENT OF CARBOPLATIN

Due to cisplatin's inherent activity but unfortunate side-effects, extensive research has been done to find a derivative with greater activity and/or decreased toxicity. Among the plethora of platinum agents synthesised and evaluated, only one additional compound, carboplatin has received worldwide acceptance in the clinic. Carboplatin (cis-diammine(1,1-cyclobutanedicarboxylato)platinum(II), Diagram 1.5) was formally recognised as a second-generation platinum anti-cancer compound in 1990.[26]

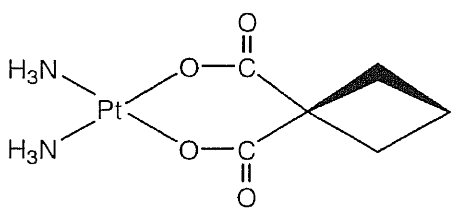

Diagram 1.5: cis-Diammine(1,1-cyclobutanedicarboxylato)platinum(II).

Like cisplatin, carboplatin shows similar activity against ovarian and small cell lung cancer but with significant reduction of side effects to the kidneys and the nervous system.[3] The dose-limiting toxicity of carboplatin is myelosuppression.[27] Carboplatin is said to be approximately four times less toxic than cisplatin.[28] This lower toxicity means that doses of up to 400mg/day can be administered without a need for forced hydration and diuresis.[28,29] The decreased toxicity appears to be strongly related to its greater pharmo-kinetic stability in solution.[25] Degradation of carboplatin to potentially damaging derivatives occurs at much slower rates.[26] Tests performed in vivo have shown that at 37°C the retention half-life in blood plasma for carboplatin is 30 hours compared with only 1.5-3.6 hours for cisplatin.[3,30] In patients treated with carboplatin, 65% of the drug is excreted through the kidney within the first 24 hours (compared to 16-35% for cisplatin), with at least 32% in its free unchanged form.[31]

1.8 CISPLATIN ANALOGUES

While the side-effects of cisplatin have been reduced by the development of carboplatin, both drugs are limited by the emergence of acquired resistance.[14] Resistance to platinum anti-cancer drugs has been investigated in many cell lines. From these studies the major mechanisms have been identified as reduced cellular drug transport, enhanced DNA repair of the critical platinum-DNA lesions and enhanced intracellular detoxification through glutathione and metallothioneins systems.[27,28] To overcome this problem of resistance, efforts have focused on developing a third-generation of platinum complexes with activity against cisplatin-resistant tumour systems preferentially with oral bioavailability. Advances in this area led to the development of JM216, the first orally administratable platinum(IV) drug to enter clinical trials.

JM216 entered into phase II clinical trials in 1994 after phase I trials proved encouraging. It showed superior activity against ovarian cancer xenographs compared to cisplatin and carboplatin.[32] Moreover, it was capable of circumventing acquired cisplatin resistance in ovarian and cervical carcinoma cell lines. The toxicity profile is similar to that of carboplatin rather than cisplatin. No neurotoxicity or nephrotoxicity was observed. Myleosuppression was the dose-limiting adverse effect.[28]

JM216 has the added advantage in that it can be administered orally, giving rise to the possibility of treatment on an outpatient basis. The first phase of testing demonstrated that the anti-tumour effect was schedule-dependant. Initial trials used an oral schedule consisting of a single dose given every 21 days without hyperhydration.[32] However, further trials showed that a greater activity could be achieved when doses are administered on days 1 to 5, repeated every 21 days.[28] If phase II clinical trials are as encouraging as phase I trials then JM216 may emerge as the most interesting new drug to be developed since cisplatin and carboplatin.

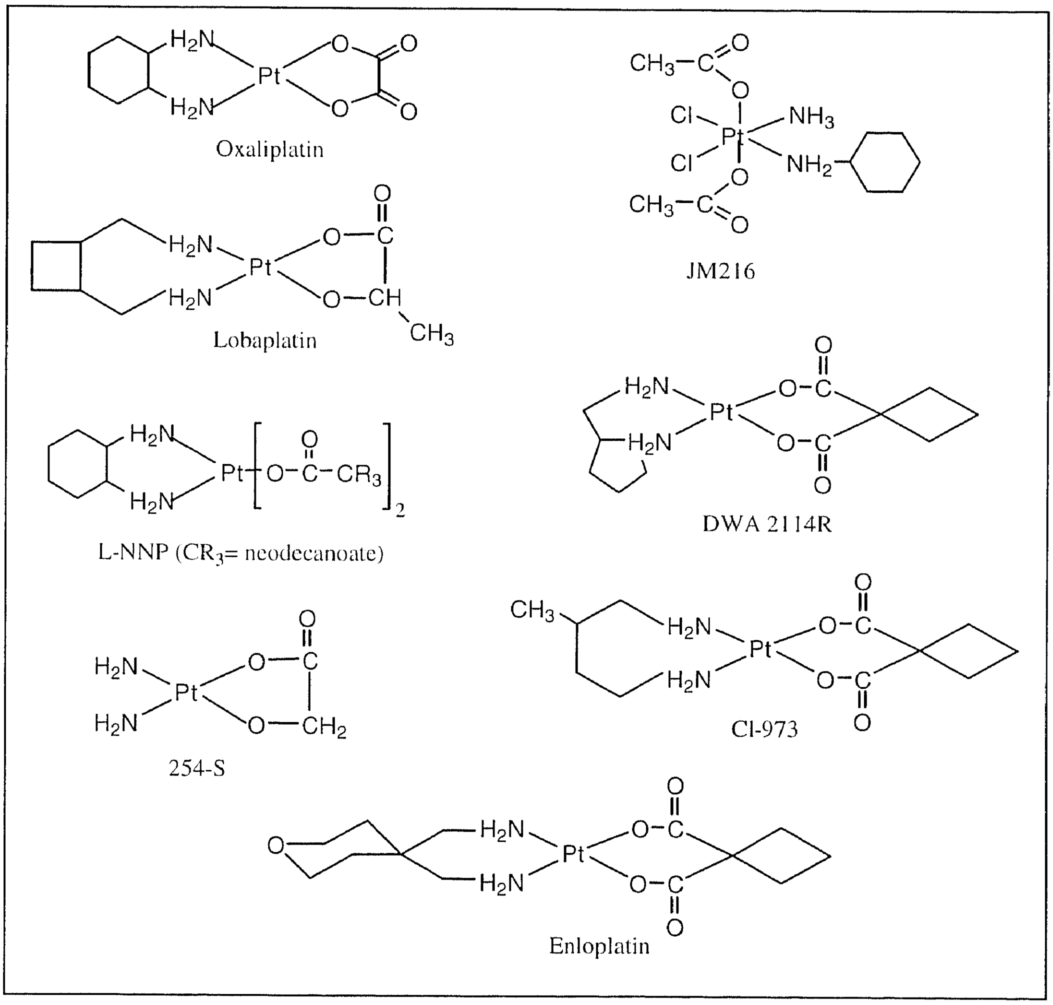

Diagram 1.6: Structures of cisplatin analogues currently in clinical development.

At present, seven other platinum analogues are currently undergoing clinical evaluation. Five of these compounds (DWA2114R, Cl-973, 254-S, lobaplatin and enloplatin) are essentially 'carboplatin-like' drugs. Whilst the remaining drugs (oxaliplatin and L-NNP) are based on the 1,2-diaminocyclohexane ligand. The structures of these cisplatin analogues are displayed in Diagram 1.6.

1.9 STRUCTURE-ACTIVITY RELATIONSHIPS

Out of the large number of analogs that have been synthesised and tested, no drug has qualities superior to both cisplatin and carboplatin. The improved drugs still suffer narrow range of activity and from the phenomenon of acquired resistance. Thus, the search for more effective analogues still continues. A structure-activity relationship is yet to be unequivocally established, but according to the classical criteria[33] certain structural features appear necessary for their therapeutic activity.

Oxidation State

The platinum complexes may be square-planar platinum(II) or octahedrally configured platinum(IV). The platinum(IV) complexes show a lower cytostatic activity and it is thought that these complexes are reduced to platinum(II) in vivo by cysteine.[34]

Geometry

The complexes must be cis-configured. Transplatin which differs from cisplatin only in its ligand coordination, is less toxic and ineffective as an anti-cancer agent. Cis-geometry is considered to be important for the formation of bifunctional DNA lesions that disrupt replication.

Charge

Electrical neutrality was once regarded as a criterion for anti-tumour activity on the basis that electrically neutral complexes would penetrate cell membranes more easily than charged compounds.[34] However, there are a number of cationic and anionic platinum complexes that contravene the original structure-activity rules in that they exhibit a low but significant degree of anti-tumour activity. The cationic platinum(II) complexes that display anti-tumour activity include cis-$[Pt(NH_3)_2(inosine)_2]Cl_2$ and cis-$[Pt(NH_3)_2(guanosine)_2]Cl_2$.[35] Anionic complexes such as $[PtCl_3NH_3]^-$ and $[Pt(tert\text{-}butylamine)Cl_3]^-$ also show promise as anti-tumour agents.[34,36]

Physio-Chemical Properties

The complexes should possess favourable physio-chemical properties such as solubility and stability in aqueous solution. One of the problems associated with the use of cisplatin is its low solubility in water, which is less than 3 g per litre.[37]

Components of Cisplatin Analogues

The components of active complexes consist of two non-leaving groups in the cis position and two monodentate or one bidentate leaving group. Refer to Diagram 1.7 for a schematic representation. The terms leaving and non-leaving refer only to the relative reactivity since no ligand is completely inert to substitution.

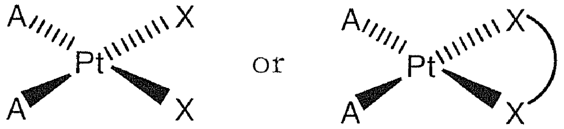

Diagram 1.7: Components of a cisplatin analogue where X is the leaving group and A is the non-leaving group.

The non-leaving groups should be inert amines. They range from the simplest one, ammonia, to linear, branched or cyclic amines and diaminocycloalkanes (see Table 1.1). Platinum complexes with ammonia and primary amines display the highest anti-tumour activity. Complexes with tertiary amines are inactive. The most promising alternatives to cisplatin appear to be the chelates in which the ammonia ligand has been replaced by ethylenediamine[3,38] or cis-diaminocyclohexane.[34,39]

The leaving groups are typically anionic with a restricted range of lability. They must exhibit intermediate bond stability with platinum allowing them to exchange under biological conditions. Complexes with very labile ligands are extremely toxic while those containing inert Pt-X bonds are rendered inactive.[34] Some typical leaving groups are shown in Table 1.1.

Table 1.1: A selection of leaving and non-leaving groups.

Non-Leaving Groups	Leaving Groups
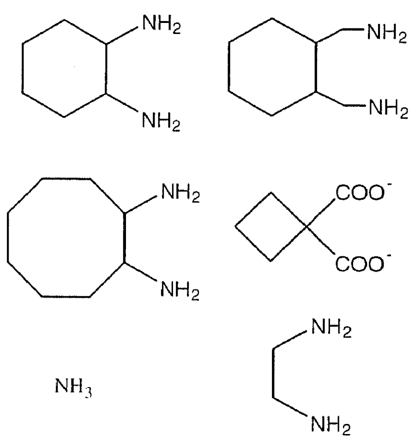	Cl^- Br^- SCN^- NO_3^- NO_2^- H_2O OH^- 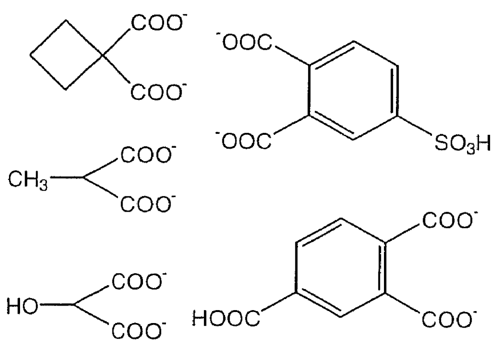

1.10 MODE OF ACTION OF CISPLATIN

The pathways of cisplatin in the body are schematically outlined in Diagram 1.8. After administration by injection or infusion, cisplatin may be bound through the sulfur sites of a variety of biomolecules. In fact, the dose-limiting nephrotoxicity of cisplatin may be attributed to the coordination of platinum(II) to the sulfhydryl group in enzymes and other proteins.[40,41] Examples of sulfur-donor biomolecules include cysteine, histidine methionine, glutathione, and metalothioneine.[3,16,42] The remaining fraction of cisplatin is circulated in the blood almost unchanged. Its reactivity is suppressed by the high chloride ion concentration of 100mM in blood.[3,7]

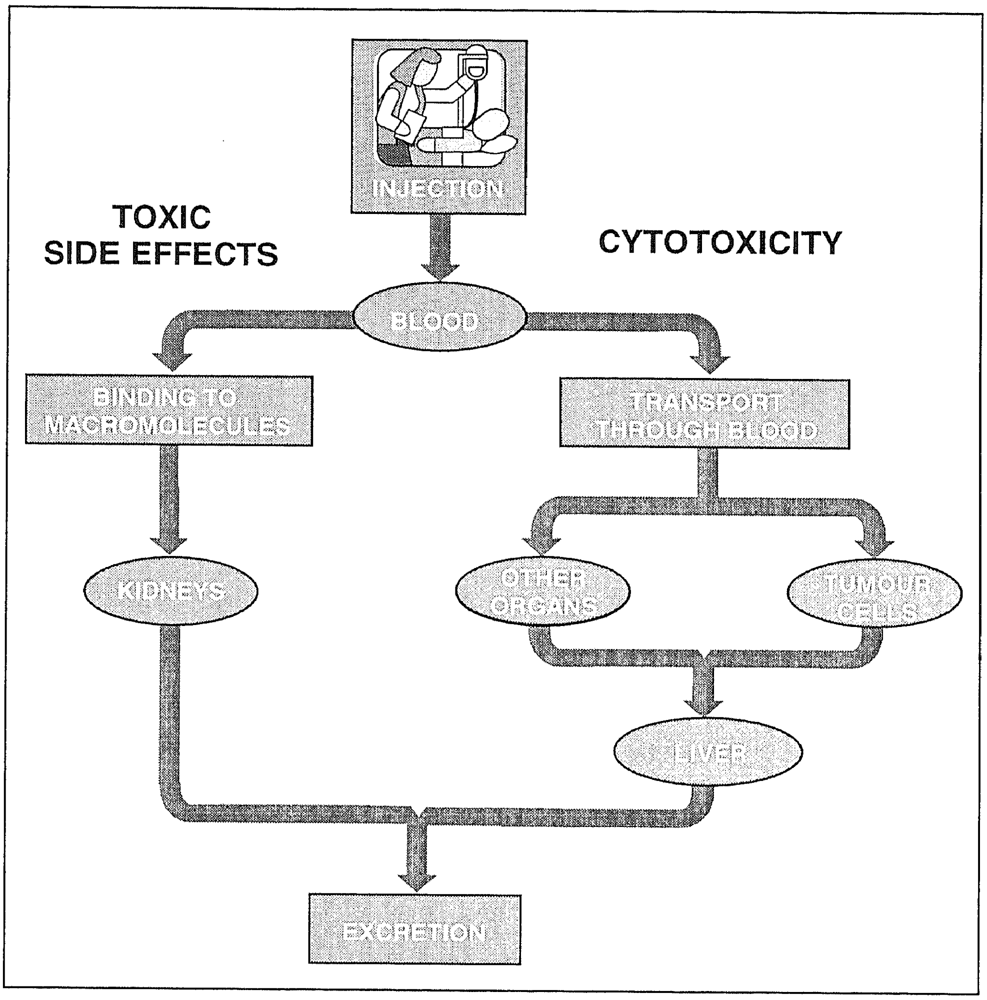

Diagram 1.8: Pathways of cisplatin in the human body.

After passive transport of neutral cisplatin across the cytoplasmic membrane, it encounters a markedly lower chloride concentration of 4mM and undergoes a series of hydrolysis reactions (Diagram 1.9).[3,43] Within the cell about 40% of the hydrated species exists as cis-$[Pt(NH_3)_2Cl(H_2O)]^+$.[26] The positive charge on this substituted complex makes it a particularly active form of the cytostatic agent because it is more likely to approach and coordinate to the negatively charged DNA helix.

Other species such as $[Pt(NH_3)_2(H_2O)(OH)]^+$ have been shown to oligomerize producing hydroxy-bridged polymeric species.[44,45] These oligomeric species are extremely toxic and may be responsible for the severe toxic side-effects invivo.[3,34] After interaction with the DNA, the degradation products are excreted via the liver and kidneys.

$$[PtCl_2(NH_3)_2] \underset{+Cl^-}{\overset{-Cl^-}{\rightleftharpoons}} [Pt(NH_3)_2Cl(H_2O)]^+ \underset{+Cl^-}{\overset{-Cl^-}{\rightleftharpoons}} [Pt(NH_3)_2(H_2O)_2]^{2+}$$

$$[Pt(NH_3)_2Cl(H_2O)]^+ \underset{+H^+}{\overset{-H^+}{\rightleftharpoons}} [Pt(NH_3)_2Cl(OH)] \qquad [Pt(NH_3)_2(H_2O)_2]^{2+} \underset{+H^+}{\overset{-H^+}{\rightleftharpoons}} [Pt(NH_3)_2(H_2O)(OH)]^+$$

$$[Pt(NH_3)_2Cl(OH)] \underset{+Cl^-}{\overset{-Cl^-}{\rightleftharpoons}} [Pt(NH_3)_2(H_2O)(OH)]^+ \underset{+H^+}{\overset{-H^+}{\rightleftharpoons}} [Pt(NH_3)_2(OH)_2]$$

Diagram 1.9: Hydrolysis reactions of cisplatin.

1.11 INTERACTIONS WITH DNA

It is now widely accepted that cisplatin mediates its anti-neoplastic effects by binding to DNA and inhibiting replication in the cancer cell.[3,7] When cisplatin reacts with DNA, there are several binding modes, including intrastrand, interstrand and DNA-protein crosslinking.[26] Exactly which one of these binding modes is primarily responsible for the displayed anti-cancer activity is unknown. An attractive explaination can be made by comparing the major differences in the binding of cis- and transplatin. The geometric isomer transplatin can bind to DNA and block replication, but it is ineffective as an anti-cancer agent.[46,47] Stereochemical differences in the adducts formed by the two isomers imply that the anti-cancer activity of cisplatin arises from the formation of a specific platinum-DNA adduct.

Intrastrand Crosslinks

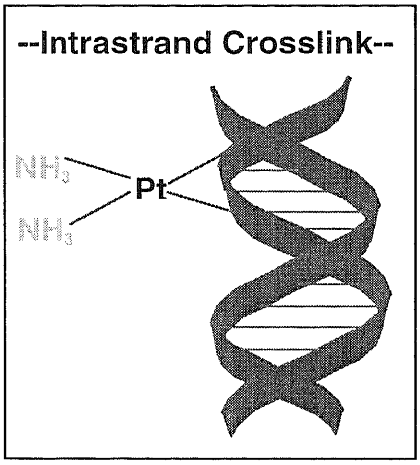

Several types of intrastrand interactions are possible. Cisplatin prefers to form 1,2-intrastrand crosslinks between adjacent bases.[3] Approximately 65% of these intrastrand products involve platinum coordination to the N(7) position of two guanine bases.[3,48] Adenine-Guanine intrastrand crosslinks occur less frequently.[42] The greater propensity to form guanine-guanine crosslinks results principally from kinetic effects.[49,50]

1,2-Intrastrand crosslinks are a stereochemically unique mode of binding for cisplatin. This type of adduct cannot be formed by clinically ineffective transplatin due to geometric constraints, instead it forms 1,3- and 1,4-adducts.[51,52] It has been suggested that the inactivity of transplatin may be related to this inability to form 1,2-intrastrand adducts.[46]

Electrophoresis and two-dimensional nuclear magnetic resonance (2D-NMR) studies have shown that guanine-guanine intrastrand crosslinks result in an unwinding of 13° and bending of the duplex by an angle of 40°.[16,47] Although this kink is clearly visible in models, the stacking and base pairing are only slightly distrupted.[53] Consensus is appearing that this kinked DNA is recognised by damage recognition proteins known as high-mobility group proteins (HMG). These HMG proteins bind only to DNA containing 1,2-intrastrand crosslinks.[54] Binding of HMG proteins increases the duplex bending creating a structure that mimics natural substrates.[51] This shields the adducts from repair reactions, thereby inhibiting replication and eventually leading to cell death.[54,55]

Interstrand Crosslinks

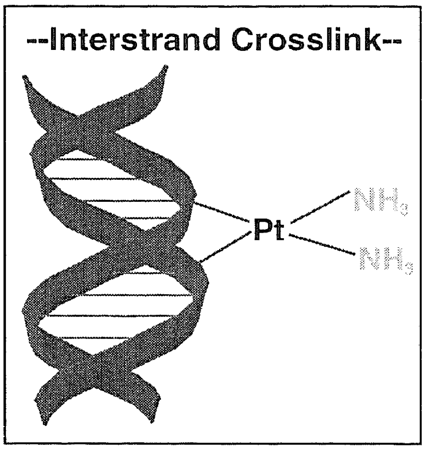

Interstrand crosslinks were the first adducts recognised in early biological studies. Cisplatin preferentially forms interstrand crosslinks between guanine residues in the 5'-CG-3' sequence,[3] however this mode of binding represents only a minor portion(<5%) of the total cisplatin adducts induced.[21]

In contrast, the most prominant adduct of transplatin is the crosslink between guanine and complementary cytosine residues.[46] The fact that transplatin also forms interstrand crosslinks makes it unlikely that such adducts are responsible for the anti-tumour activity of cisplatin.[52]

Protein Crosslinks

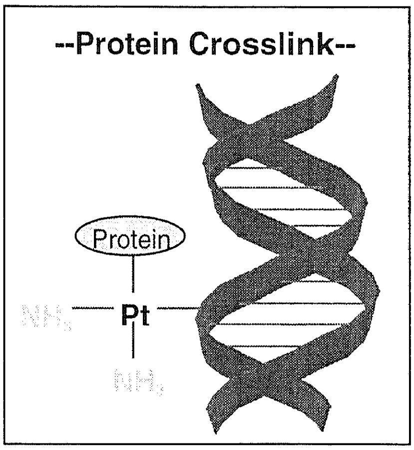

The formation of protein crosslinks by cisplatin has been reported. However, these events occur at such a low frequency in comparison to the other adducts that their contribution is assumed to be minimal.

Intercalators

Intercalators are of particular importance because of their pharmalogical utility as mutagens, antibacterials, antifungicides, antibiotics and anti-cancer agents.[52] In the clinic, cisplatin is usually administered in combination with other intercalative drugs.[3] It is thought that the simultaneous administration of the two classes of drugs affects the individual interactions with DNA, thereby increasing the therapeutic effects. For example, before the use of combination therapy, the survival rate for patients with testicular cancer was about only 5%. Today, treatment regimes have dramatically increased the survival rate to 80-90%.[12] Intercalators can be broken up into two general classes, classical and non-classical.

1.12 CLASSICAL INTERCALATORS

Classical intercalators are flat, planar, aromatic molecules which bind by insertion of the fused aromatic ring system between the base pairs along the DNA backbone.[56,57] As seen in Diagram 1.10, the planar molecule is orientated roughly perpendicular to the DNA helix and is in very close contact to the DNA bases.

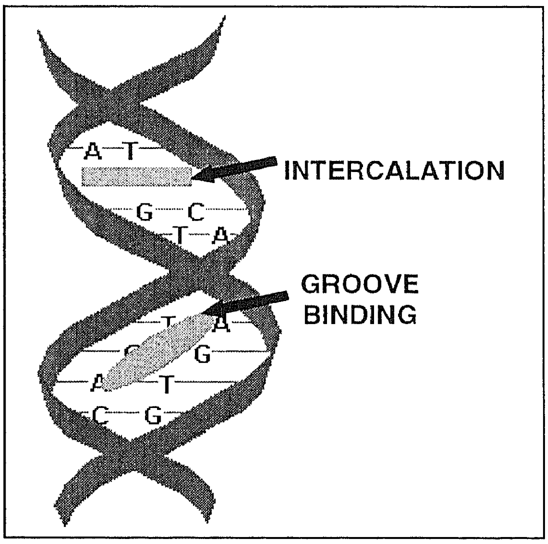

Diagram 1.10: Schematic representation of intercalation and groove binding.

Groove binding involving direct interactions of the bound molecule with the edges of base pairs in either the minor or major grooves of DNA[61] often completes with intercalation. Many drugs fit snugly into the minor groove to form a tight complex without intercalating. Whilst others do not fall into a single category and may bind to DNA using a combination of intercalation and groove binding interactions.

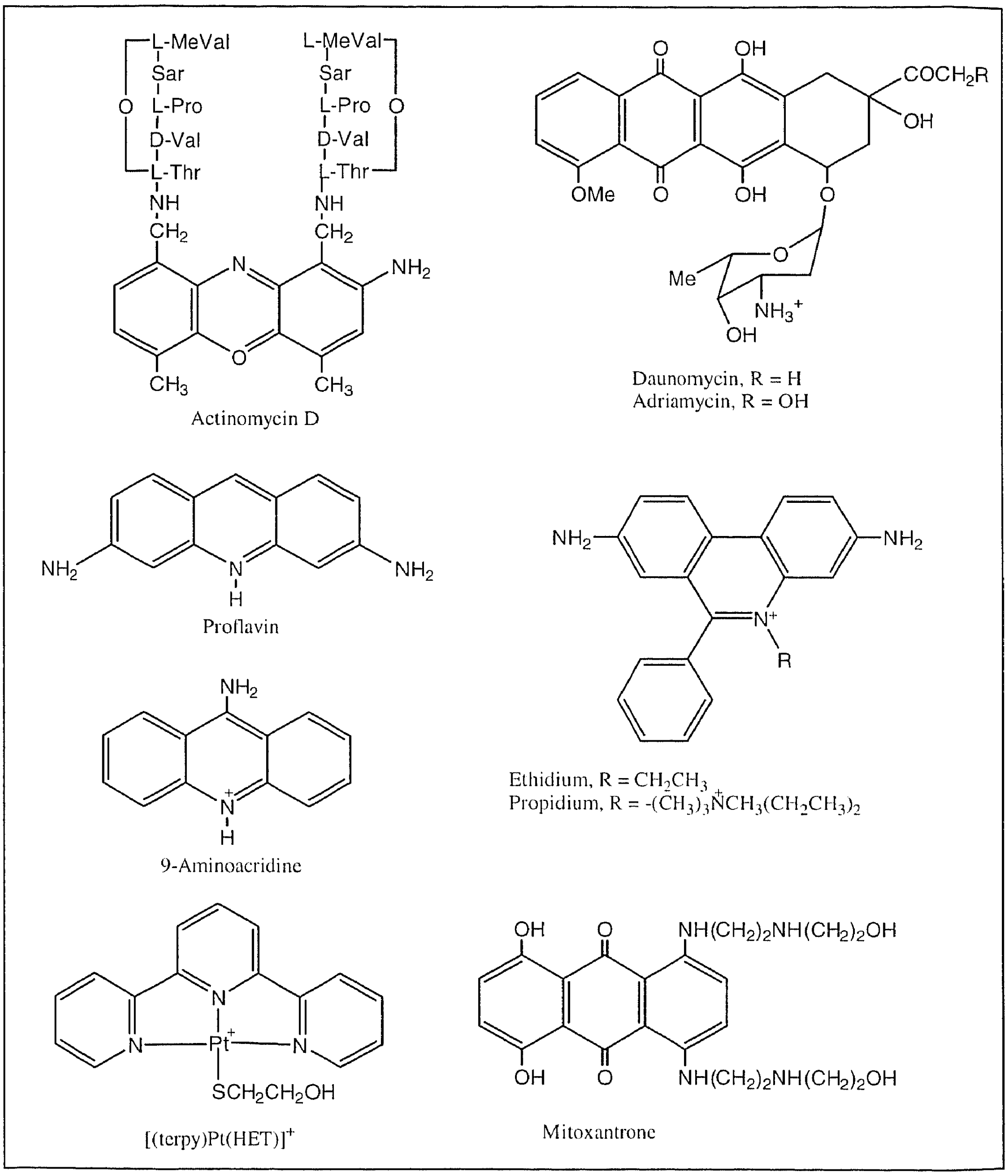

Diagram 1.11: Some intercalating agents.

Intercalating agents come in many guises. The drugs with an established place in the clinic include actinomycin, daunomycin, Adriamycin and mitoxantrone. The structures of some intercalators are given in Diagram 1.11. Also shown in Diagram 1.11 is the complex 2-hydroxyethanethiolato-2,2',2''-terepyridineplatinum(II) ($[(terpy)\text{-}Pt(HET)]^+$). This was the first metallointercalation reagent to display the capacity for intercalative binding.[58]

Intercalation of planar chromophores between stacked duplex bases in DNA and RNA was first recognised by Lerman in 1961.[59] Intercalation results in substantial changes in the DNA structure. Firstly, there is a separation of base pairs and a lengthening of the double helix.[57] This can be detected experimentally by hydrodynamic methods such as viscosity and sedimentation measurements.[60] The distance between adjacent base pairs (contour length) in DNA is typically near 3.4 Å.[58] This contour length can be increased by as much as 3.0 Å, depending on the type of intercalating ring system that is to be inserted. The increases in contour length for some common intercalating agents are shown in Table 1.2. To compensate for the structural distortions, the helix also unwinds and the usual 36° helical twist of one base to the next is decreased. The amount of unwinding ranges from 12 to 26° depending on the drug type. The unwinding angles of a number of intercalating drugs have been determined by closed circular supercoiled DNA experiments,[61] and are shown in Table 1.2.

Table 1.2: The unwinding angles and increases in contour length for several intercalating drugs.

Intercalator	Unwinding Angle (°)	Contour Length (Å)
Ethidium and Propidium	26	2.7
Proflavin and 9-Aminoacridine	17	3.0
Adriamycin and Daunomycin	11	1.7

1.13 NON-CLASSICAL INTERCALATORS

Compounds with bulky substituents on opposite sides of the ring system make up the class of non-classical intercalators. Porphyrins are an example of this type.[61] The nature of the porphyrin-DNA interaction is sensitive to the porphyrin structure.[62] Those porphyrins possessing bulky substituents on the porphyrin framework exhibit external groove binding, whilst simpler porphyrins intercalate between the base pairs of DNA.[61,62]

Porphyrins are of particular interest because they tend to be located preferentially in tumour tissue as compared with normal tissue.[63] This concept originated from the observation of a characteristic red fluorescence, attributable to the porphyrin, in the tumour.[63] The exact processes by which tumour localisation occurs are not known. Based upon the characteristics of tumours and the chemical properties of porphyrins the following hypotheses are generally accepted in the scientific community.

(a) It has been shown that, once injected, porphyrins penetrate the vascular compartment to reach the interstitial fluid compartment (Diagram 1.12). In normal cells the porphyrins are cleared by vascular and lymphatic drainage. In tumours, a number of factors contribute to the apparent localisation of the porphyrin. These factors include high vascular permeability, the lack of lymphatic drainage and sluggish venous flow.[63]

(b) The concentration of collagen is significantly high in the tumour interstitial compartment.[63] Tumour localising porphyrins show a high affinity for collagen, a property not shared by non-localising porphyrins.

(c) The cellular uptake of porphyrins depend upon binding to low density lipoproteins (LDL). Thus specific enrichment occurs in tumour tissue because tumour cells show a higher LDL receptor activity than normal cells.[64,65]

(d) Accumulation of porphyrins in the large interstitial water space in tumours is favoured owing largely to their size and potential for aggregation.[63]

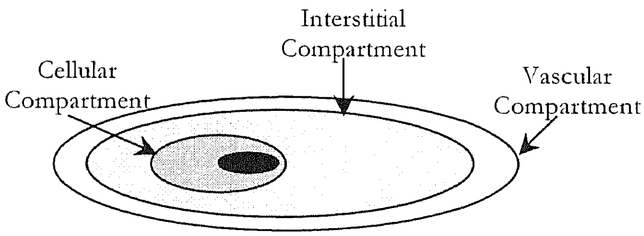

Diagram 1.12: Cancer tissue is presented schematically as a three-compartment system.

It is the tumour localising ability that is exploited by diagnostic and clinical oncologists who use porphyrins as photosensitisers in phototherapy. Phototherapy originated in the 1890s when *lupus vulgaris*, a tubercular condition of the skin, was treated with heat-filtered light from a carbon arc lamp.[66] Phototherapy now plays a significant role in the treatment of cancer, where it is better known as photodynamic therapy (PDT).

PDT uses the interaction between light and a non-toxic photosensitising agent to destroy cancerous cells.[65,67] The patient is injected intravenously with 100-400mg/kg of the sensitising agent. This is followed by a short period of time (48-72 hours) whereby the photosensitising agent is absorbed into the cell.[68] Although it is taken up by both normal and cancer cells, it is eliminated from cancer cells at a much slower rate. As a consequence, cancer cells treated with the agent remain sensitive to photodynamic effects for longer periods of time.[69] The tumour area is then exposed to light from a laser. The interval between injection and light exposure is carefully timed to give the maximum differential concentration of agent in the tumour.[66] At present, the most effective results are achieved using red light from an argon pumped dye laser tuned to a wavelength of 630nm.[64]

Once the photosensitiser has been activated by absorbing the light, one of three processes can occur (Diagram 1.13).[70]

(a) The activated photosensitiser can react with tissue oxygen to produce singlet oxygen. This very reactive free radical diffuses into the surrounding cancer tissue causing irreversible oxidation of some essential cellular components and leads to tumour destruction. This activated state is short-lived and the photosensitised molecule returns back to the ground state whereupon it can be activated again.

(b) A portion of the activated photosensitiser molecules may emit light (fluoresce) and decay back to the ground state. These molecules can the be activated again.

(c) The activated photosensitiser may undergo photodegradation whereby they are destroyed by the activating light.

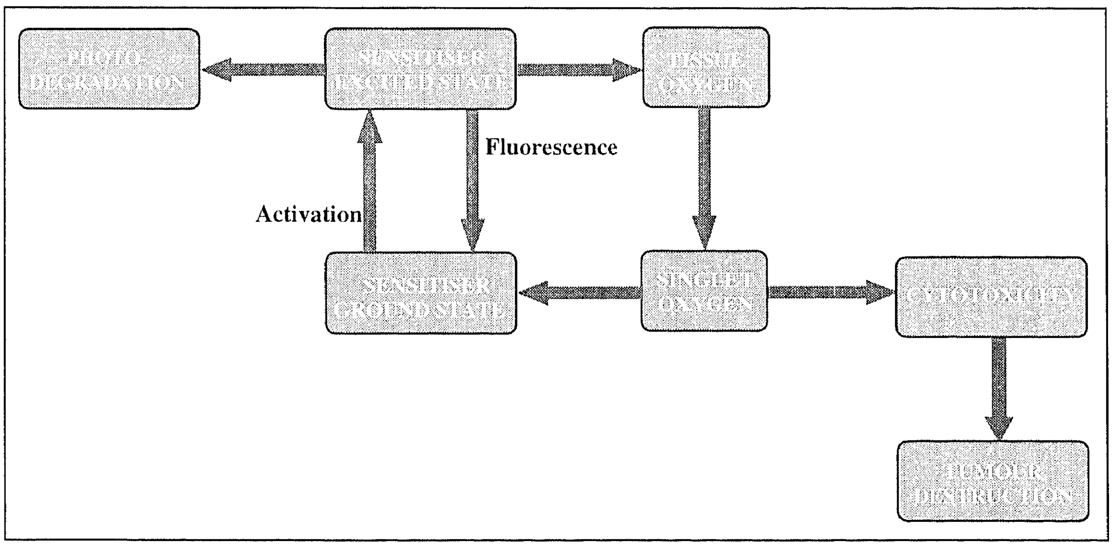

Diagram 1.13: Outline mechanism of photodynamic action.

Hematoporphyrin derivative (HPD) was the first photosensitiser used in clinical trials. HPD is a complex mixture of products whose composition varies in different preparations and with time of storage. The active components that produce the desired photosensitising properties have been described as a dihematoporphyrin ether/ester (DHE).[71] Over the ensuing years a number of improved sensitisers have been developed. These show a 50-fold increase in localisation, and include tetra(3-hydroxyphenyl)porphyrin (3THPP) and tetraphenylporphyrin tetrasulfonate ($TPPS_4$).[72] The structures of HPD, 3THPP and $TPPS_4$ are shown in Diagram 1.14.

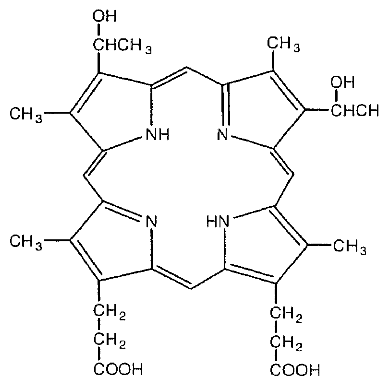

Hematoporphyrin

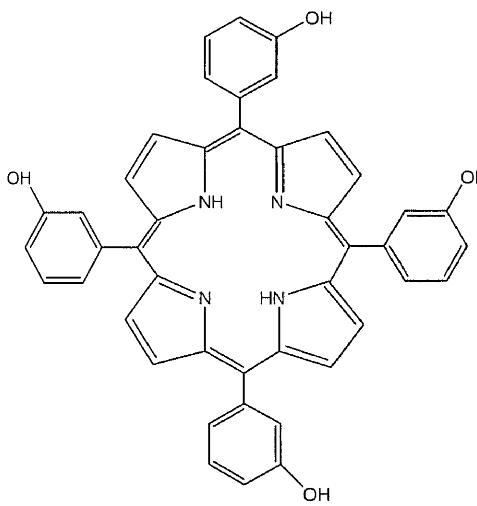

3THHP

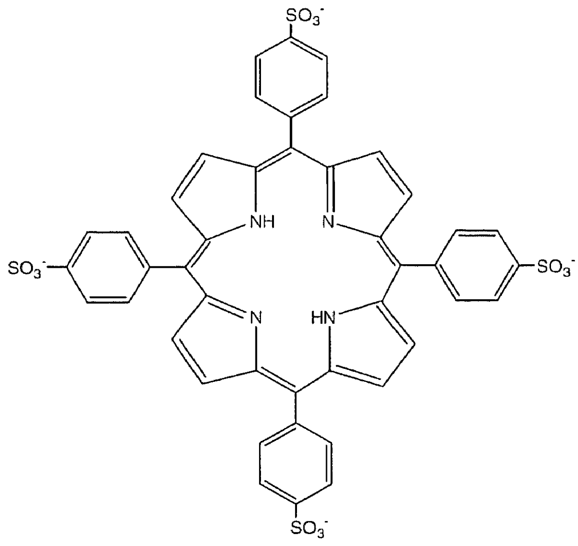

$TPPS_4$

Diagram 1.14: Structural diagram of selected photosensitisers.

The major side-effect of these drugs is skin sensitivity. The skin in the treated area remains sensitive to light for up to six weeks after treatment. Other side-effects include nausea, vomiting, a metallic taste in the mouth and eye sensitivity to light.

Overall PDT has several advantages. Firstly, cancer cells can be selectively destroyed with relatively little damage to the surrounding normal tissue. Secondly, the damaging effect of the photosensitising agent occurs only when the treated area is exposed to light. In turn, these features reduce the side-effects. In spite of the utility of the technique, PDT is restricted to the treatment of surface tumours such as those on or just under the skin or on the lining of internal organs such as the lung or bladder. This is due to the fact that laser light cannot pass through more than 1cm of tissue.

Linked Platinum-Intercalator Complexes

As mentioned in section 2, the major limitations of the platinum-based drugs that are used today is the occurrence of toxic side effects produced by the lack of selectivity. Attempts to limit this problem have incorporated strategies which include the tethering of carrier molecules to a chemically reactive platinum functionality. It is believed that the incorporation of the two different drugs into a single compound may lead to a conjugate with the essential characteristics contributed from both precursors.

The first bifunctional molecule to be synthesised was $[Pt\{AO(CH_2)_6en\}Cl_2]$; it comprised of the DNA intercalator acridine orange (AO) linked to the platinum complex, $[Pt(en)Cl_2]$ via a hexamethylene chain.[56] Mapping studies revealed that the platinum portion binds independently to DNA and that the acridine orange moiety intercalates one or two bases away.[73] $[Pt\{AO(CH_2)_6en\}Cl_2]$ has been reported to be slightly active against cisplatin-resistant tumours.[32]

A series of bifunctional drugs have also been made by binding the active platinum components directly to an intercalator. One such complex is [Pt(tba)(adria)Cl_2], where tba is tert-butylamine and adria is the intercalator adriamycin.[32] This compound binds intercalatively, but no covalent binding of the platinum is observed. It is thought that the simultaneous intercalation and covalent binding in the major groove may be steroechemically difficult for the [Pt(tba)(adria)Cl_2] complex.[56] Another directly bound Pt-intercalator complex is cis-[Pt$(NH_3)_2$(N(9)-9-AA)Cl]$^+$, in which a cisplatin moiety is bound to 9-aminoacridine orange (9-AA) through the N(9) position of the imino tautomer. Platinum complexes of ethidium and anthraquinone (AQ) have also been synthesised (Diagram 1.15).[56]

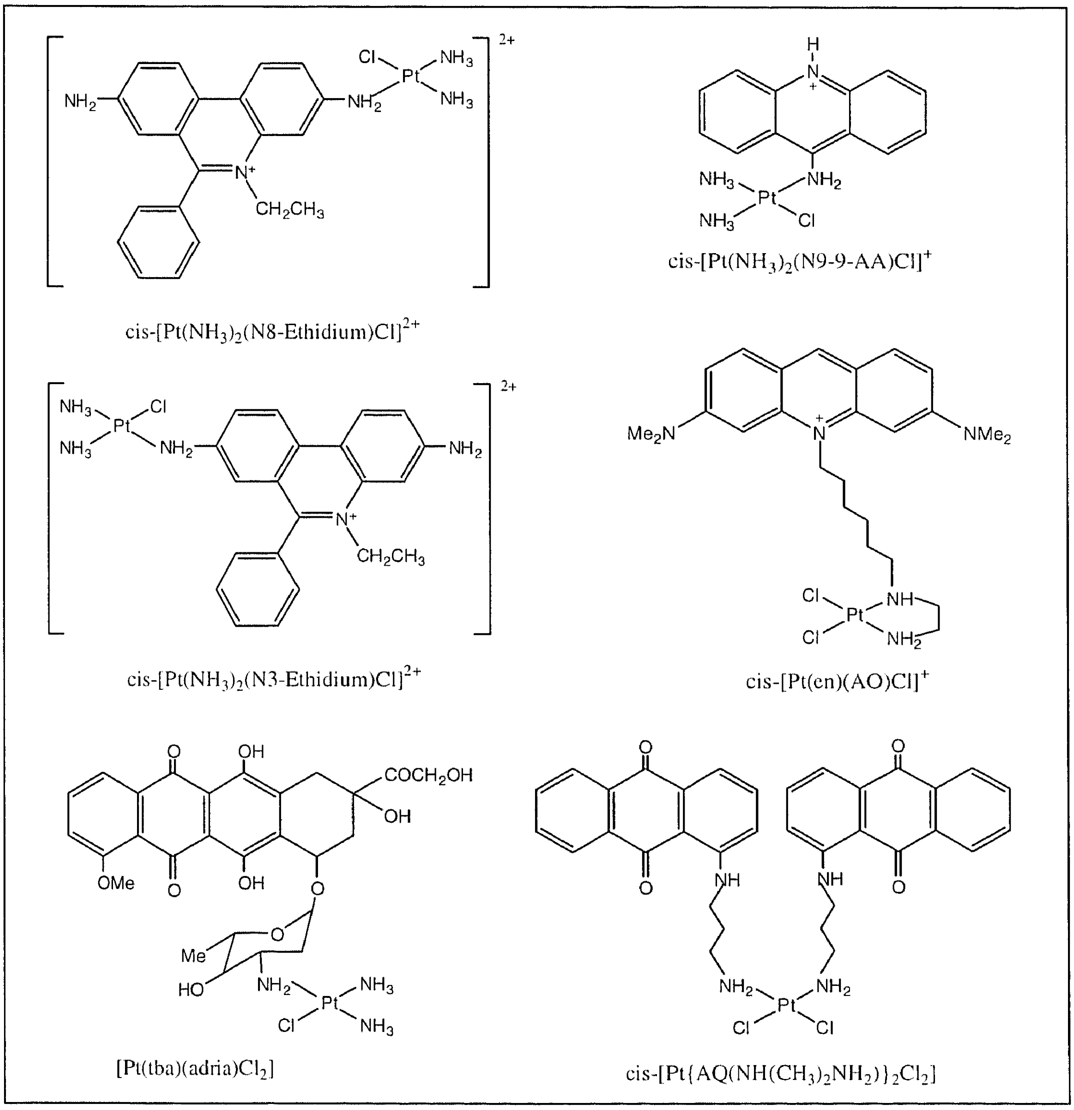

Diagram 1.15: Structures of some platinum complexes linked to DNA intercalators.

The majority of the Pt-Intercalator complexes incorporate classical intercalators. There have been very few reports on the use of porphyrins as carrier molecules.[74,75] The demonstrated localisation property of porphyrins was an incentive for using porphyrins as carrier ligands. In order to mitigate unwanted distribution and increase the tumour uptake of platinum anti-cancer drugs, our efforts have focused on linking porphyrins to various platinum derivatives. Our objective was to develop novel bifunctional drugs that take advantage of the tumour selectivity of porphyrins and the inherent cytotoxicity of platinum based drugs. Hence, the platinum-porphyrin conjugates represent a class of fourth generation compounds that use the tumour selectivity of porphyrins to convey the active platinum components to tumour tissue sparing normal tissue.

References

1 W. McLennan, Causes of Death Australia 1998, Australian Bureau of Statistics, Canberra, 1999, p. 1-32.

2 L. Benjamin, Genes V, Oxford University Press, New York, 1994, p. 1181-1229.

3 P. Umpathy, Coord. Chem. Rev., 1989, **95**,129-181.

4 J. Marx, Science, 1994, **266**,1942-1944.

5 J. Marx, Science, 1994, **266**,1321-1322.

6 G. Felsenfeld, Scientific American, 1995, October,44-51.

7 S. E. Sherman and S. J. Lippard, Chem. Rev., 1987, **87**, 1153-1181.

8 J. Marx, Science, 1994, **266**, 728-730.

9 P. Modrich, Science, 1994, **266**,1959-1960.

10 P. C. Hanawalt, Science, 1994, **266**,1957-1958.

11 A. Sancer, Science, 1994, **266**, 1954-1956.

12 V. A. Bohr, Carcinogenesis, 1991, **12**, 1983-1992.

13 B. Rosenberg, L. VanCamp, and T. Krigas, Nature, 1965, **205**, 698.

14 M. J. Abrams and B. A. Murrer, Science, 1993, **261**, 725-730.

15 N. Farrel, Transition metal complexes as drugs and chemotherapeutic agents, Klewer Academic Publishers, Dordrecht, 1989, p. 3.

16 J. Reedijk, J. Chem. Soc., Chem. Comm., 1996, 801-806.

17 S. Cascinu, L. Cordella, E. Delferro, M. Fronzoni and G. Cantalano, Journal of Clinical Oncology, 1995, **13**, 26-32.

18 M. J. McKeage, Drug Safety, 1995, **13**, 228-244.

19 Y. Sumiyoshi, K. Hashine, K. Kasahara and T. Karashima, Japanese Journal of Cancer Chemotherapy, 1996, **23**, 1506-1508.

20 M. Treskes, W. J. F. Vandervijgh, Cancer Chemother. Pharmacol., 1993, **33**, 93-106.

21 K. M. Comess, J. N. Burstyn, J. M. Essigmann and S. J. Lippard, Biochemistry, 1992, **31**,3975-3990.

22 R. M. Bukowski, European J. of Cancer, 1996, **32A** (Suppl 4), S2-4.

23 J. A. Fosternora and R. Siden, American Journal of Health-System Pharmacy, 1997, **54**, 787-800.

24 K. S. Wyatt, K. N. Harrison and C. M. Jensen, Inorg. Chem., 1991, **31**, 3867-3868.

25 F. A. Blommaert, H. C. Van Dijk-Knijnenburg, F. J. Dijt, L. D. Engelse, R. A. Baan, F. Berends and M. J. Fichtinger-Schepman, Biochemistry, 1995, **34**, 8474-8480.

26 W. Kaim and B. Schwederski, Bioinorganic Chemistry:Inorganic Elements in the Chemistry of Life, John Wiley and Sons Ltd, Chinchester,1994, p363-378.

27 M. Gosland, B. Lum, J. Schimmelpfennig, J. Baker and M. Doukas, Pharmacotherapy, 1996, **16**, 16-39.

28 L. R. Kelland and M. J. McKeage, Drugs and Aging, 1994, **5**, 85-95.

29 N. Motlet-Auselo, F. BansRosset, P. Costa, J. F. Louis and H. Nauratil, Oncology, 1993, **50** (Suppl 2), 28-36.

30 S. J. Harland, D. R. Newell, Z. H. Siddik, R. Chadwick, A. H. Calvert and K. R. Harrap, Cancer Res., 1984, **44**, 1693-1697.

31 U. Frey, J. D. Ranford and P. J. Sadler, Inorg. Chem., 1993, **32**, 1333-1340.

32 R. B. Weiss and M. C. Christian, Drugs, 1993, **46**, 360-377.

33 D. B. Brown, A. R. Khokhar, M. P. Hacker, J. J. McCormack and R. A Newman, in Platinum, gold and other metal chemtherapeutic agents, ed. S. J. Lippard, American Chemical Society, Washington D.C, 1983, p. 265.

34 A. Pasini and F. Zunino, Angew. Chem. Int. Ed. Engl.,1987, **26**, 615-624.

35 R. E. Cramer, P. L. Dahlstrom, M. J. T. Seu, T. Norton and M. Kashiwagi, Inorg. Chem., 1980, **19**, 148-154.

36 E. Bersanetti, A. Pasini, G. Pezzoni, G. Pratesi, G. Sau, R. Supino and F. Zunino, Inorg. Chim. Acta., 1984, **93**, 167.

37 Merck Index

38 B. Rosenberg, V. Camp, J. E. Trosko and V. H. Mansour, Nature, 1969, **222**, 385-386.

39 K. Inagaki, H. Nakahara, M. Alink and Y. Kidani, Inorg. Chem., 1990, **48**, 793-806.

40 K. J. Barnham, M. L. Djuran, P. Murdoch, J. D. Ranford and P. J. Sadler, J. Chem. Soc. Dalton Trans., 1995, 3721-3726.

41 K. J. Barnham, M. L. Djuran, P. Murdoch, J. D. Ranford and P. J. Sadler, Inorg. Chem., 1996, **35**, 1065-1072.

42 J. Reedijk, Inorganica Chimica Acta., 1992,**198**, 873-881.

43 S. J. Lippard, Science, 1982, **218**, 1075-1082.

44 M. Noji, S. Motoyama, T. Tashiro and Y. Kidani, Chem. Pharm. Bull., 1983, **31**,1469-1473.

45 L. E. Erickson, M. Godfrey and R. G. Larsen, Inorg. Chem., 1987, **26**, 992-997.

46 J. Kasparkova and V. Brabec, Biochemistry,1995, **34**, 12379-12387.

47 S. E. Sherman, D. Gibson, A. H. J Wang and S. J. Lippard, J. Am. Chem. Soc., 1988, **110**, 7368-7381.

48 S. F. Bellon, J. H. Coleman and S. J. Lippard, Biochemistry, 1991, **30**, 8026-8035.

49 S. Mansy, G. Y. H. Chu, R. E. Duncan and R. S. Tobias, J. Am. Chem. Soc., 1978, **100**, 607-616.

50 J. P. Caradonna and S. J. Lippard, Inorg. Chem., 1988, **27**, 1454-1466.

51 S. A. Kane and S. J. Lippard, Biochemistry, 1996, **35**, 2180-2188.

52 M. Gniazdowski and C. Cera, Chem. Rev., 1996, **96**, 619-634.

53 W. I. Sunquist and S. J. Lippard, Biochemistry, 1986, **25**,1520-1524.

54 P. M. Phil and S. J. Lippard, Science, 1992, **256**, 234-237.

55 B. Lambert, J. L. Jestin, P. Brehin, C. Oseykowski, A. T. Yeung, P. Mailliet, C. Pretot, J. B. Le-Pecq, A. Jacquemin-Sablon and J. C. Chottard, J. Biol. Chem., 1995, **270**, 21251-21257.

56 W. I. Sunquist and S. J. Lippard, Coord. Chem. Rev., 1990, **100**, 293-322.

57 U. Pindur, M. Haber and K. Sattler, J. Chem. Ed., 1993. **70**, 263-272.

58 J. Barton, Comments on Inorg. Chem., 1985, **3**, 321-348.

59 H. M. Sobell, in Nucleic Acid Geometry and Dynamics. (Ed. R. H. Sarma), Pergamon Press, Oxford, England,pp. 289-323 (1980).

60 L. P. G. Wakelin and M. J. Waring, DNA intercalating agents. In Agents acting on nucleic acids. p703-724.

61 G. M. Blackburn and M. J. Gait, Nucleic Acids in Chemistry and Biology, IRL press at Oxford University Press, Oxford, 1995, p. 297-336.

62 N. E. Mukundan, G. Petho, D. W. Dixon, M. S. Kim and L. G. Marzilli, Inorg. Chem., 1994, **33**, 4676-4687.

63 R. J. Fiel, E. Mark, T. Button, S. Gilant and D. Musser, Cancer Lett., 1988, **40**, 23-32.

64 H. Brunner and H. Obermeier, Angew. Chem. Int. Ed. Engl., 1994, **33**, 2214-2215.

65 K. Berg, J. C. Bommer, J. W. Winkelman and J. Moan, Photochem. Photobiol., 1990, **52**, 775-781.

66 R. Bonnett, Chem. Soc. Rev., 1995, **24**, 19-33.

67 D. Kessel, Biochemical Pharmacology, 1984, **33**, 1389-1393.

68 J. D. Spikes, Photochem. Photobiol., 1986, **43**, 691-699.

69 I. Cozzani, G. Jori, E. Reddi, L. Tomio, P. L. Zorat, T. Sicuro and G. Malvaldi, 1984. In porphyrins in tumour phototherapy, ed. A. Andreoni and R. Cudeddu, Plenum, New York, 1984, p. 156-165.

70 A. J. Pope and S. G. Bown, Br. J. Urol, 1991, **68**, 1-9.

71 J. Moan, Photochem. Photobiol., 1986, **43**, 681-690.

72 J. Moan, Q. Peng, J. F. Evenson, K. Berg, A. Western and C. Rimington, Photochem. Photobiol., 1987, **46**, 713-721.

73 B. E. Bowler and S. J. Lippard, Biochemistry, 1986, **25**, 3031-3038.

74 H. Brunner, H. Obermeier and R. M. Szeimies, Chem. Ber., 1995, **128**, 173-181.

75 H. Brunner, F. Maiterth and B. Treittinger, Chem. Ber., 1994, **127**, 2141-2149.

CHAPTER

2

PLATINUM(II) COMPLEXES OF AMINO ACIDS

Introduction

In an effort to overcome the drawbacks of cisplatin, many platinum(II) complexes have been synthesised and screened for anti-cancer activity. Many of these studies have been devoted to the coordination compounds of platinum with amino acids.[1,2] The use of amino acids is attractive for two main reasons. Firstly, amino acids are used for the growth of cells, and secondly their complexes with platinum generally display favourable solubility properties. These factors open up the possibility that the active moiety may be easily transported through cell membranes into the interior of the cancerous tissue.

Amino acids are interesting ligands, not only because of their biological importance, but also for their versatility in forming a large variety of complexes with metals. Consider aspartic acid, for example. It is capable of binding to the metal in three different bonding modes. These include O,O-, N,αO- or N,βO-chelation, as shown in Diagram 2.1.

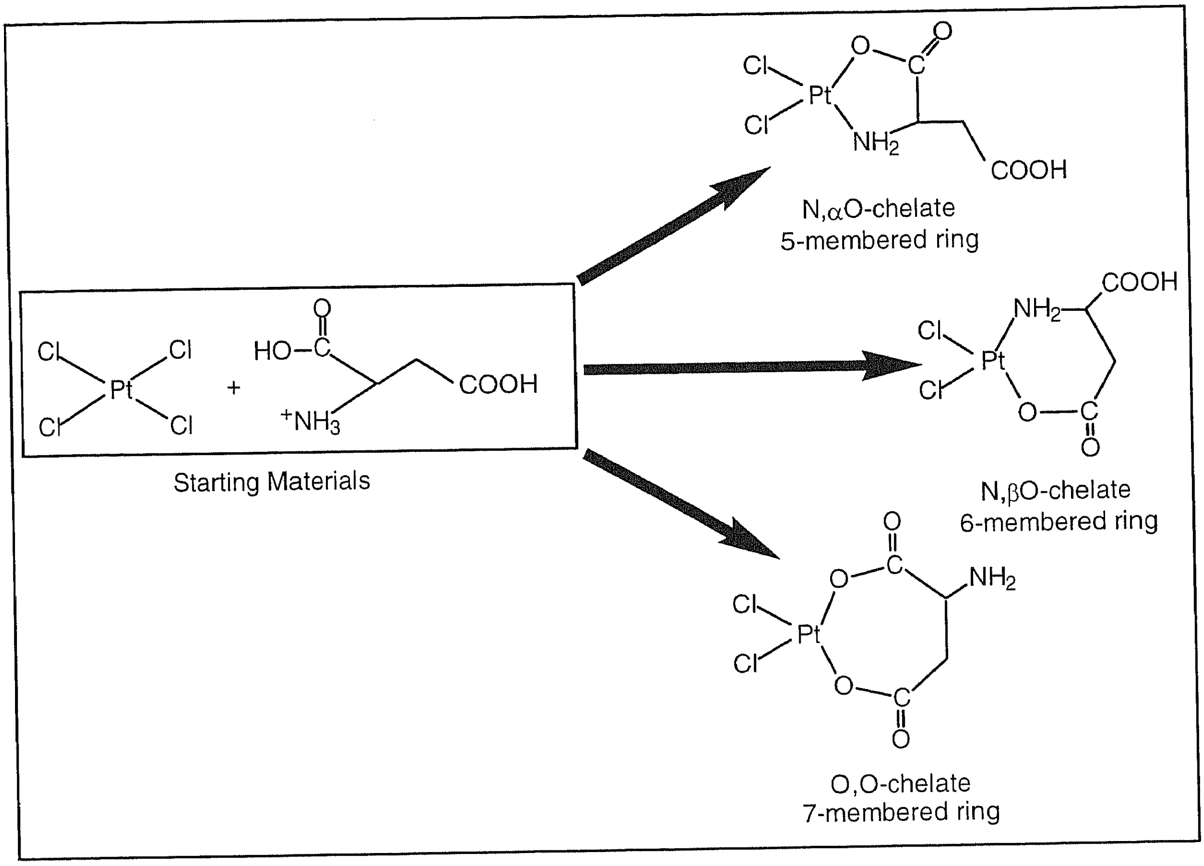

Diagram 2.1: Three possible modes of chelation for aspartic acid.

Although O,O-chelation is a well-known mode of binding for metals such as cobalt(II), for platinum(II), which is generally accepted as a 'soft' metal, bonds to nitrogen will be much more thermodynamically stable than bonds to oxygen.[3] In addition, five-membered rings are also preferred.[4] Thus N,O chelation through the α-carboxylate is the most commonly encountered species.

Structural formulas of the neutral forms of the amino acids whose platinum(II) complexes are described in this chapter are given in Diagram 2.3. These particular compounds represent a series of simple amino acids capable of N,O-chelation under controlled conditions, each containing a terminal R-group through which a suitable carrier group will be bound.

Experimental

2.1 MATERIALS

L-Aspartic acid (L-asp), L-glutamic acid (L-glu), L-glutamic acid-methyl ester (L-glu.OMe), L-serine and L-lysine were obtained from Aldrich Chemical Company. Potassium tetrachloroplatinate(II) ($K_2[PtCl_4]$, 98%) was purchased from Johnson Matthey and used without further purification. All other reagents were purchased from Ajax Chemicals.

2.2 MEASUREMENTS

Elemental analysis of carbon, hydrogen and nitrogen for the platinum complexes were performed by the Microchemical Unit of the Australian National University, Canberra, ACT. Infrared spectra (IR) were recorded as nujol mulls on sodium chloride plates in the range of 4000-500 cm^{-1} using a BioRad FTS-7 Fourier Transform spectrometer.

Electrospray ionisation (ESI) mass spectra were recorded at 50eV on a VG-Quattro mass spectrometer at the University of Wollongong (Department of Chemistry). Both positive and negative ion spectra were obtained. Samples were analysed by direct injection of sample prepared in acetonitrile.

The ^{1}H (300 MHz) and ^{13}C (75 MHz) nuclear magnetic resonance (NMR) spectral data were acquired on a Varian Unity-Plus 300 spectrometer at room temperature. The NMR samples were freshly prepared in deuterium oxide (D_2O). Chemical shifts are referenced to an internal standard, sodium 2,2,3,3-tetradeutero-3-(trimethylsily)propionate (TMSP) and are expressed in parts per million (ppm). The Heteronuclear Correlation through Multiple Quantum Coherence (HMQC) experiment on $[Pt(L\text{-}asp)Cl_2]$ was recorded at 30°C. For the HMQC experiment, data sets with 1024 x 1024 complex points were acquired with sweep width of 1800 Hz in the proton dimension and 20000 Hz in the carbon dimension. A total of 512 scans were collected per t_1 increment. Computer simulations were performed on a LC475 Macintosh using the computer program gNMR.

The pH measurements were made using a Hanna H18519 pH meter with a combination glass electrode calibrated with T.P.S pH 4.0 and pH 6.88 standard buffer solutions. Readings from the pH meter in D_2O were converted to pD values by addition of 0.4 to the reading.[5]

2.3 X-RAY STRUCTURE DETERMINATION

X-ray quality crystals of $[Pt(L\text{-lysine})Cl_2]^-$ were obtained by slow evaporation of a concentrated aqueous solution over P_2O_5. X-ray data was collected at 173K on a Siemans P4 diffractometer using graphite monochromated Mo Kα radiation. The structure was solved by direct methods and refined by full-matrix least-squares methods using the SHELXTL PLUS (VMS) program package. Hydrogen atoms were included using a riding model.

2.4 SYNTHESIS OF PLATINUM COMPLEXES

Dichloro(L-aspartic acid)platinum(II). $K[Pt(L\text{-asp-N,O})Cl_2]$.

$K_2[PtCl_4]$ (1.00 g, 2.41 mmol) was dissolved in water (30 mL). The solution was filtered and L-aspartic acid (0.318 g, 2.41 mmol) in water (20 mL) was added. The reaction mixture was heated at 40-50°C on a water bath. The pH of the solution was kept constant at 3.0 with KOH (0.1 M). The reaction reached completion when a total of 24 mL of KOH had been added. The final yellow solution was evaporated to dryness on a water bath to give a yellow-orange solid consisting of the product mixed with $K_2[PtCl_4]$ and potassium chloride. The solid was transferred into a small glass sinter and washed with small volumes of water, leaving the product as a bright yellow precipitate on the sinter. The yellow residue was air-dried, and placed in a desiccator over silica gel.

Yield: 0.55 g (52%).
Anal. Calcd for $C_4H_6NO_4PtCl_2K$ (437): C, 10.99; H, 1.38; N, 3.20. Found: C, 11.04; H, 1.34; N, 2.91. ^1H NMR (D_2O, ppm): δ = 3.93 (q, 1H, H^1), 2.84, 2.92 (2 x m, J_{21} = 4.8 Hz, J_{31} = 5.7 Hz and J_{23} = 18 Hz, H^2, H^3). ^{13}C NMR (D_2O, ppm): δ = 40.6 (s, β-CH_2), 58.5 (s, α-CH), 179.6 (s, β-COOH), 191.4 (s, α-COO^-). ESI-MS: m/e = 398.0 (100%, M^+), 362.0 (65, $C_4H_6NO_4PtCl$), 318.0 (38, $C_3H_6NO_2PtCl$). IR (Nujol, cm^{-1}): 3600-3400 (br, νOH), 3260-3200 (br, ν(N-H)), 1716, 1609 (2 x s, C=O).

Dichloro(L-serine)platinum(II). K[Pt(L-serine)Cl_2].

An aqueous solution of $K_2[PtCl_4]$ (1.00 g, 2.41 mmol) and L-serine (0.25 g, 2.41 mmol) was heated on a water bath preheated to 35-40°C. After 30 minutes, KOH (0.1 M) was added to raise the pH to 2.5. Periodic adjustments were performed until the pH remained constant. Overall the reaction required a total of 19 mL of KOH. The solution was concentrated to approximately 2.5 mL on the water bath and then placed in a desiccator over phosphorus pentoxide. After 12 hours, yellow needles were afforded.

Yield: 0.158 g (16%)
Anal. Calcd for $C_3H_6NO_3PtCl_2K$ (409): C, 8.80; H, 1.48; N, 3.42. Found: C, 8.54; H, 1.33; N, 3.50. ^1H NMR (D_2O, ppm): δ = 3.73 (q, 1H, H^1), 3.84, 3.94 (2 x m, J_{12} = 3.7 Hz, J_{13} = 5.3 Hz and J_{23} = 12.1 Hz, H^2, H^3). ^{13}C NMR (D_2O, ppm) δ = 64.4 (s, β-CH_2), 62.9 (s, α-CH), 190.4 (s, α-COO^-). ESI-MS: m/e = 370 (100%, M^+), 333 (8, $C_3H_6NO_3PtCl$). IR (Nujol, cm^{-1}): 3507-3300 (br, νOH), 3240-3100 (br, ν(N-H)), 1649 (s, C=O), 1581 (s, δ_s(N-H)).

Dichloro(L-glutamic acid)platinum(II). K[Pt(L-glu-N,O)Cl_2].

A solution containing $K_2[PtCl_4]$ (1.00 g, 2.41 mmol) and L-glutamic acid (0.35 g, 2.41 mmol) was prepared in water (40 mL). It was heated on a water bath for 15 minutes. The pH was then carefully adjusted to 4.0 using KOH (0.1 M) and placed back onto the water bath for further heating. Similar adjustments were made periodically until a total of 24 mL of KOH had been added, during which time the solution colour changed from a deep red to yellow. The solution was concentrated on a water bath, to give the product as a yellow powder, which was filtered and air-dried.

Yield: 0.52 g (46%).
Anal. Calcd for $C_5H_8NO_4PtCl_2K.H_2O$ (469): C, 12.80; H, 2.13; N, 2.99. Found: C, 12.83; H, 2.12; N, 3.31. ^{1}H NMR (D_2O, ppm): δ = 3.53 (q, 1H, H^1), 2.10, 1.95 (2 x m, J_{12} = 4.8 Hz, J_{13} = 6.7 Hz and J_{23} = 15 Hz, H^2, H^3), 2.46, 2.36 (2 x m, J_{24} = 7.1 Hz, J_{25} = J_{34} = 8.7 Hz, J_{35} = 6.7 Hz and J_{45} = 15 Hz, H^4, H^5). ^{13}C NMR (D_2O, ppm): δ = 31.5 (s, β-CH_2), 35.6 (s, γ-CH_2), 58.9 (s, α-CH), 183.7 (s, β-COOH), 192.7 (s, α-COO^-). ESI-MS: m/e = 411.8 (80%, M^+), 376.6 (19, $C_5H_8NO_4Cl$), 112 (100, $C_5H_6NO_2$). IR (Nujol, cm^{-1}): 3600-3400 (br, νOH), 3253-3105 (br, ν(N-H)), 1710, 1633 (2 x s, C=O), 1594 (s, δ_s(N-H)).

Dichloro(L-glutamic acid-methyl ester)platinum(II). K[Pt(L-glu.OMe)Cl_2].

To a hot saturated aqueous solution (15 mL) of L-glutamic acid-methyl ester (0.3882 g, 2.41 mmol) was added $K_2[PtCl_4]$ (1.00 g, 2.41 mmol). The resulting solution was heated on a water bath for 15 minutes after which time the pH fell to 2.5. KOH solution (0.1 M) was then added to increase the pH to 3.4. The solution was continually heated at 50°C on a water bath with parallel monitoring of the pH. The pH was kept at 3.4 with 0.1 M KOH. After 24 mL of KOH had been added a small amount of unreacted ligand was removed by filtration, and the filtrate was evaporated to dryness. The yellow product was extracted from other solid products with hot 90% ethanol (3 x 15 mL). The suspension was filtered, to give a fine yellow powder. This was air-dried and placed in a desiccator over silica gel.

Yield: 0.35 g (31%)
Anal. Calcd for $C_6H_{10}NO_4PtCl_2K.3KCl$ (689): C, 10.46; H, 1.45; N, 2.03. Found: C, 10.48; H, 1.41; N, 2.21. ^{1}H NMR (D_2O, ppm): δ = 3.72 (s, 3H, -OCH_3), 3.66 (q, 1H, H^1), 2.27, 2.10 (2 x m, J_{12} = 5.4 Hz, J_{13} = 7.2 Hz and J_{23} = 14.4 Hz, H^2, H^3), 2.72, 2.65 (2 x m, J_{24} = J_{35} = 6.8 Hz, J_{25} = 7.3

Hz, J_{34} = 7.5 Hz and J_{45} = 14.4 Hz, H^4, H^5). ^{13}C NMR (D_2O, ppm): δ = 30.0 (s, β-CH_2), 32.3 (s, γ-CH_2), 55.4 (s, -OCH_3), 60.4 (s, α-CH), 178.4 (s, β-$COOCH_3$), 191.5 (s, α-COO^-). ESI-MS: m/e = 426 (100%, M^+), 390 (48, $C_6H_{10}NO_4PtCl$). IR (Nujol, cm^{-1}): 3500-3400 (br, νOH), 3260-3100 (br, ν(N-H)), 1738, 1682 (2 x s, C=O), 1657 (s, δ_s(N-H)).

Dichloro(L-lysine)platinum(II). H[Pt(L-lysine)Cl_2].

Method A.

An aqueous solution (10 mL) of L-lysine (0.440 g, 2.41 mmol) was added to a freshly prepared solution of $K_2[PtCl_4]$ (1.00 g, 2.41 mmol) in water (30 mL). The reaction mixture was heated on a water bath at 40°C for approximately 2.5 hours. During this time the pH of the solution was constantly adjusted to 6.0 by the addition of KOH (0.1 M). When the temperature and pH were carefully controlled, a colour change from red to yellow was observed. On occasions, platinum metal was deposited. In such cases the solution was cooled and filtered through a fine glass sinter. After a total of 24 mL had been added, the solution was allowed to evaporate at room temperature in a desiccator until a yellow solid deposited.

Yield: 0.16 g (15%)

Anal. Calcd for $C_6H_{14}N_2O_2PtCl_2$.1.5H_2O (439): C, 16.40; H, 3.87; N, 6.38. Found: C, 16.22; H, 3.57; N, 6.36. ^1H NMR (D_2O, ppm): δ = 3.58 (q, 1H, H^1), 1.73, 1.89 (2 x m, J_{12} = 5.31 Hz, J_{13} = 6.8 Hz and J_{23} = 19.2 Hz, H^2, H^3), 1.51, 1.68 (2 x m, J_{24} = J_{25} = J_{34} = J_{35} = 7.1 Hz and J_{45} = 15.0 Hz, H^4, H^5), 1.68, 1.69 (2 x m, J_{46} = J_{47} = J_{56} = J_{57} = 6.0 Hz and J_{67} = 15.2 Hz, H^6, H^7), 3.1 (t, J_{68} = $J_{68'}$ = J_{78} = $J_{78'}$ = 7.0 Hz, H^8, $H^{8'}$). ^{13}C NMR (D_2O, ppm): δ = 24.7 (s, γ-CH_2), 29.7 (s, β-CH_2), 34.1 (s, δ-CH_2), 42.0 (s, ε-CH_2), 61.0 (s, α-CH), 193.6 (s, α-COO^-). ESI-MS: m/e = 411 (75%, M^+), 375 (7, $C_6H_{13}N_2O_2PtCl$), 145 (12, $C_6H_{13}N_2O_2$), 89 (100, fragmentation of lysine). IR (Nujol, cm^{-1}): 3615-3400, 3245-3000 (2 x br, ν(N-H)), 1642 (s, C=O), 1599 (s, δ_s(N-H)).

Method B.

The same product was also obtained by carrying out the reaction at room temperature over a period of 3 days, with occasional additions of 0.1 M KOH to maintain the pH at 6.0. After a total of 24 mL of KOH had been added, the solution was filtered, and the filtrate was placed in a refrigerator for several weeks until large yellow crystals formed.

Yield: 0.38 g (38%)

Anal. Calcd for $C_6H_{14}N_2O_2PtCl_2.H_2O$ (430): C, 16.74; H, 3.72; N, 6.51. Found: C, 16.90; H, 3.95; N, 6.52. ^{1}H NMR (D_2O, ppm): δ = 3.59 (q, 1H, H^1), 1.72, 1.89 (2 x m, J_{12} = 5.3 Hz, J_{13} = 6.8 Hz and J_{23} = 19.0 Hz, H^2, H^3), 1.50, 1.67 (2 x m, $J_{24} = J_{25} = J_{34} = J_{35}$ = 7.1 Hz and J_{45} = 15.0 Hz, H^4, H^5), 1.67, 1.68 (2 x m, $J_{46} = J_{47} = J_{56} = J_{57}$ = 6.0 Hz and J_{67} = 15.2 Hz, H^6, H^7), 3.0 (t, $J_{68} = J_{68'} = J_{78} = J_{78'}$ = 7.0 Hz, H^8, $H^{8'}$). ^{13}C NMR (D_2O, ppm): δ = 24.4 (s, γ-CH_2), 29.3 (s, β-CH_2), 34.5 (s, δ-CH_2), 42.1 (s, ε-CH_2), 61.0 (s, α-CH), 192.8 (s, α-COO^-). ESI-MS: m/e = 411 (100%, M^+), 374 (11, $C_6H_{13}N_2O_2PtCl$), 145 (10, $C_6H_{13}N_2O_2$), 90 (50, fragmentation of lysine). IR (Nujol, cm^{-1}): 3615-3400, 3245-3000 (2 x br, ν(N-H)), 1642 (s, C=O), 1599, 1502 (2 x s, δ_s(N-H)).

Results and Discussion

The five amino acid complexes of platinum, of the general formula, $[Pt(amino\ acid)Cl_2]^-$, were prepared by reacting $K_2[PtCl_4]$ with the amino acid in water at 40-50°C. The amino acids used were L-aspartic acid, L-glutamic acid, L-glutamic acid-methyl ester, L-serine and L-lysine.

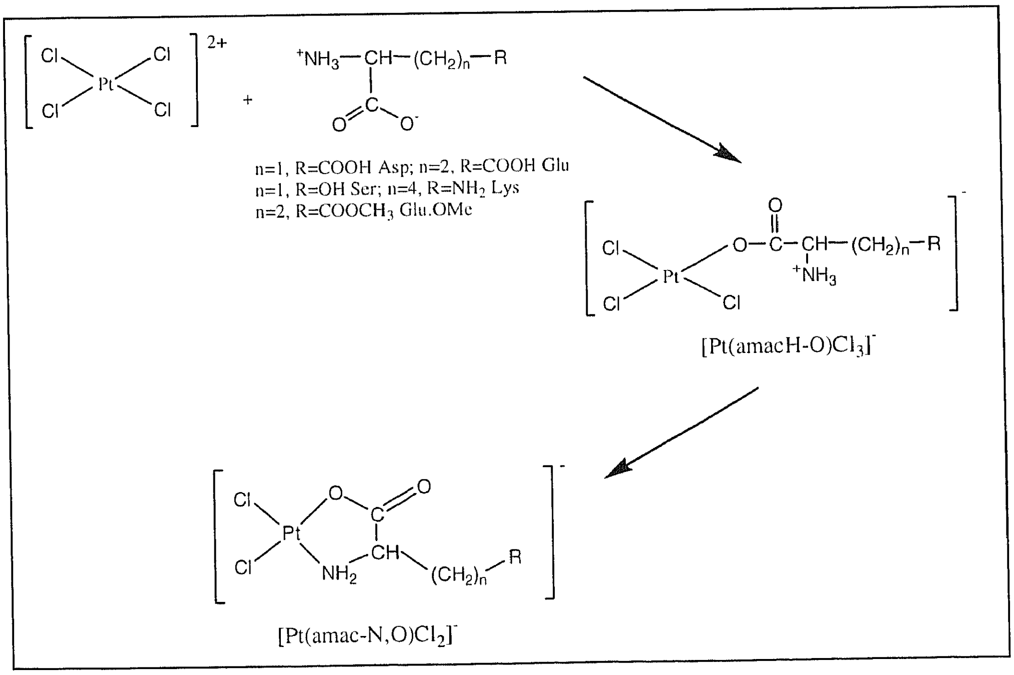

Diagram 2.2: Formation of five-membered ring chelate through facile ring closure.

The likely modes of binding of the amino acids are governed primarily by the pH of the solutions. In strong acidic solutions the amino acids will be present as a cation because the amino group(s) will be protonated. The first proton to be lost as the pH is raised is a proton on the α-carboxyl group. Careful maintenance at a specific pH will ensure that only the α-carboxyl group remains deprotonated and available for binding.

Based on studies done on similar systems[6] and by consideration of the experimental pH conditions used, it is likely that $K_2[PtCl_4]$ reacts with amino acids to give initially [Pt(amacH-O)Cl_3] in which the amino acid (amac) is an oxygen bound unidentate ligand. Subsequent ring closure to the [Pt(amac-N,O)$Cl_2]^-$ chelate occurs upon heating. In each of our compounds, the N,O-chelate ring which is formed by facile ring closure is five-membered (Diagram 2.2). Therefore, shorthand references made to a compound, for example [Pt(L-asp-N,O)$Cl_2]^-$ refer to the N,αO-chelate unless otherwise stated.

Reaction of $K_2[PtCl_4]$ with L-lysine at 40°C (method A) often resulted in precipitation of platinum metal. In order to prevent this deposition of platinum metal, the same reaction was carried out at room temperature over a three-day period (method B). Apart from a small difference in the yields obtained (c. f. method A; 15% with method B; 38%) both methods gave essentially the desired product. By consideration of the yields and the observed heat-sensitivity of the reaction, method B was considered to be the most effective method for the preparation of [Pt(L-lysine)$Cl_2]^-$. The following discussion therefore only applies to the product obtained by method B. For specific data relating to the results of method A refer to the Experimental section.

For the description of individual protons and carbons in the amino acids, a nomenclature has been adopted. This nomenclature involves allocating numbers to the protons and Greek symbols to the carbon atoms. This has been illustrated in Diagram 2.3.

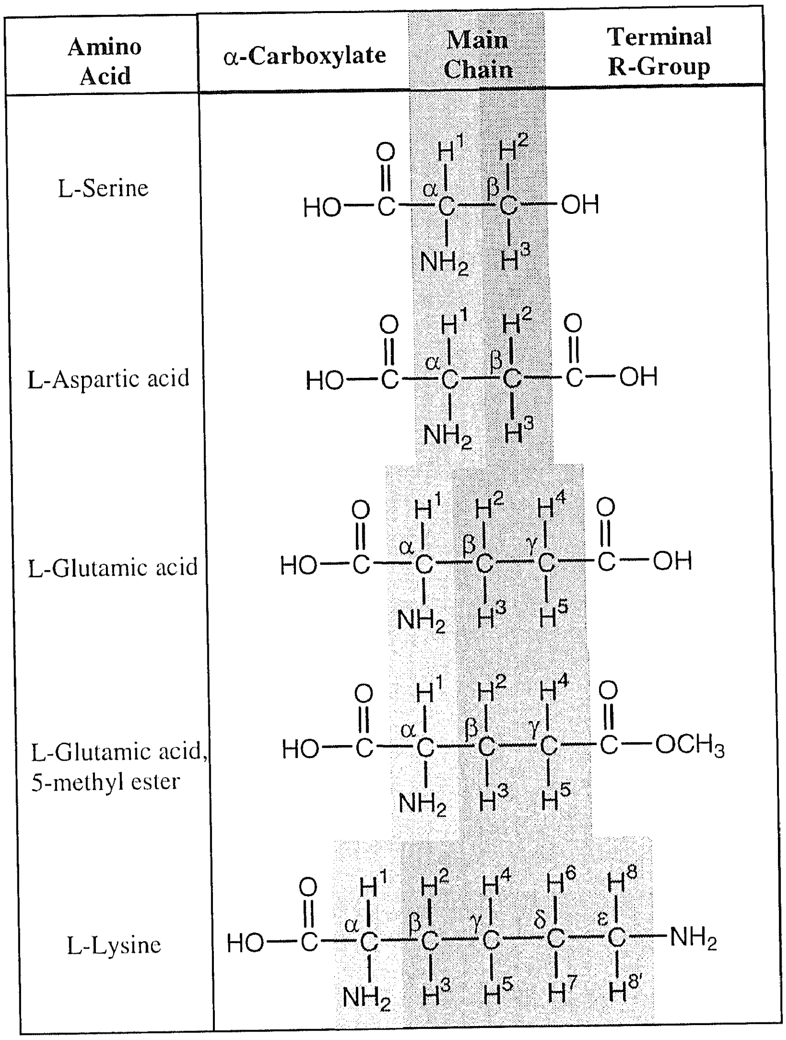

Diagram 2.3: Chemical structures of the amino acids.

The elemental analyses for K[Pt(L-asp-N,O)Cl_2], K[Pt(L-glu-N,O)Cl_2], K[Pt(L-glu-OMe)Cl_2], K[Pt(L-serine)Cl_2] and H[Pt(L-lysine)Cl_2] are in good agreement with the suggested empirical formulas, given in Table 2.1. The elemental analyses results for K[Pt(L-glu-OMe)Cl_2] indicate a small amount of KCl impurity. $[Pt(L\text{-glu-OMe})Cl_2]^-$, however, was pure in its ^1H NMR and Mass

Spectra. The structures and conformation of the complexes in this series are mainly deduced from the NMR studies, infrared and mass spectra, which are discussed below.

Table 2.1: Elemental analysis of amino acid platinum complexes.

Compound	% Carbon		% Hydrogen		% Nitrogen	
	Calc	Found	Calc	Found	Calc	Found
$K[Pt(L\text{-}asp\text{-}N,O)Cl_2]$	10.99	11.04	1.38	1.34	3.20	2.91
$K[Pt(L\text{-}glu\text{-}N,O)Cl_2].H_2O$	12.80	12.83	2.13	2.12	2.99	3.31
$K[Pt(L\text{-}glu.OMe)Cl_2].3KCl$	10.45	10.48	1.45	1.41	2.03	2.21
$K[Pt(L\text{-}serine)Cl_2]$	8.80	8.54	1.48	1.33	3.42	3.50
$H[Pt(L\text{-}lysine)Cl_2].\ 1.5H_2O$	16.46	16.22	3.88	3.57	6.40	6.36
$H[Pt(L\text{-}lysine)Cl_2]$	17.48	17.43	3.30	2.86	6.80	6.75

2.5 INFRARED SPECTRA

The (NH_2, COO^-) bidentate chelation of the amino acids with Pt(II) can be ascertained readily from their infrared spectra.[7] Of the various modes in the infrared spectra, particular attention is focused on the stretching vibrations of the NH_2 group(s), and the OH and C=O of the carboxylic acid group(s) of the complex. It is these groups which are most likely to change as a consequence of complexation. Table 2.2 gives the wavenumbers of the absorption bands in the infrared spectra of the compounds in the 4000-1000 cm^{-1} region.

Amino acid complexes of L-serine, L-aspartic and L-glutamic acid display very broad, intense OH stretching absorptions covering the region of 3600-3400 cm^{-1}. The OH stretching band disappeared in the spectrum of $[Pt(L\text{-}glu.OMe)Cl_2]^-$. This disappearance can serve as confirmation of coordination through the α-carboxylate.

The N-H stretching region (ν(N-H) = 3300-3000 cm^{-1}) of all amino acid complexes contains two distinct, sharp peaks corresponding to the asymmetric and symmetric stretching in the amine groups. In the spectra of $[Pt(L\text{-serine})Cl_2]^-$, $[Pt(L\text{-glu-N,O})Cl_2]^-$ and $[Pt(L\text{-glu-OMe})Cl_2]^-$ a shoulder appears on the low-frequency side of the N-H stretching band. This shoulder arises from the overtone of the N-H bending band (δ_s(N-H)) intensified by Fermi resonances.[8] The infrared spectrum of $[Pt(L\text{-lysine})Cl_2]^-$ displays an additional strong, broad absorption in the 3615-3400 cm^{-1} region because of the N-H stretching vibrations of the uncoordinated amine group.

Table 2.2: Characteristic infrared frequencies of the amino acid compounds.

Compound	νOH	ν(N-H)	δ_s(N-H)	Coord. COO-	Uncoord. COOR[a]
$K[Pt(L\text{-asp-N,O})Cl_2]$	3600-3400	3260-3200	-	1609	1716
$K[Pt(L\text{-glu-N,O})Cl_2].H_2O$	3600-3400	3253-3105	1594	1633	1710
$K[Pt(L\text{-glu.OMe})Cl_2]$	3500-3400	3260-3100	1657	1689	1738
$K[Pt(L\text{-serine})Cl_2]$	3507-3300	3240-3100	1581	1649	N/A
$H[Pt(L\text{-lysine})Cl_2]$	N/A	3615-3400[b]	1599	1642	N/A
		3245-3000[c]			

[a] R = H for L-aspartic and L-glutamic acid, R = CH_3 for L-glutamic acid, 5-methyl ester.
[b] Refers to the terminal NH_2 group. [c] Refers to the coordinated NH_2 group.

In the complex $[Pt(L\text{-asp-N,O})Cl_2]^-$, the broad band at 1609 cm^{-1} is assigned to the overlapping of the coordinated carboxylate motion and the N-H bending band. This N-H motion can be seen as a shoulder at the lower frequency. In other amino acids, the N-H bending band and the carboxylate band of the coordinated complex are shown as two different bands. For example, in the IR spectra of $[Pt(L\text{-glu-N,O})Cl_2]^-$, the N-H bending motion occurs at 1594 cm^{-1} and the carboxylate at 1633 cm^{-1}. In $[Pt(L\text{-lysine})Cl_2]^-$, the band at 1502 cm^{-1} results from the N-H bending of the free amine group.

As expected, the IR spectrum of $[Pt(L\text{-asp-N,O})Cl_2]^-$ and $[Pt(L\text{-glu-N,O})Cl_2]^-$ also exhibits an uncoordinated carboxyl group. These bands occur near 1716 cm^{-1} and 1710 cm^{-1}, respectively.. In the $[Pt(L\text{-glu-OMe})Cl_2]^-$ complex, a free methyl ester group is seen at 1738 cm^{-1}.

2.6 ^1H NMR

The ^1H NMR spectra of the platinum complexes and free ligands have been recorded in D_2O referenced to TMSP. A summary of the chemical shifts and coupling constant data are presented at the end of this section in Tables 2.4 and 2.5.

The ^1H NMR spectra of aspartic acid and its Pt(II) chelate were recorded in aqueous solution at different pH values. The spectra are that of a three-spin ABX type system. An example is shown in Diagram 2.4. The eight-line portion assignable to the methylene protons is made up of two AB sub-spectra due to the magnetic non-equivalence of protons H^2 and H^3. Two factors could contribute to this non-equivalence. The first is an incomplete averaging out of the electronic environment at the α-carbon atom,[9] even in the presence of free rotation. The second is restricted rotation leading to the existence of preferred rotamers. The X part (or methine resonances) consists of four detectable lines. This resonance always appears downfield due to the deshielding produced by the amino and carboxylate group. Most spectra exhibit sharp peaks, however some broadening of the methine resonance occurs in the Pt(II) chelates at low pH. Selective broadening of the methine peak may be attributed to decreased motional freedom of that particular part of the aspartic acid ligand.

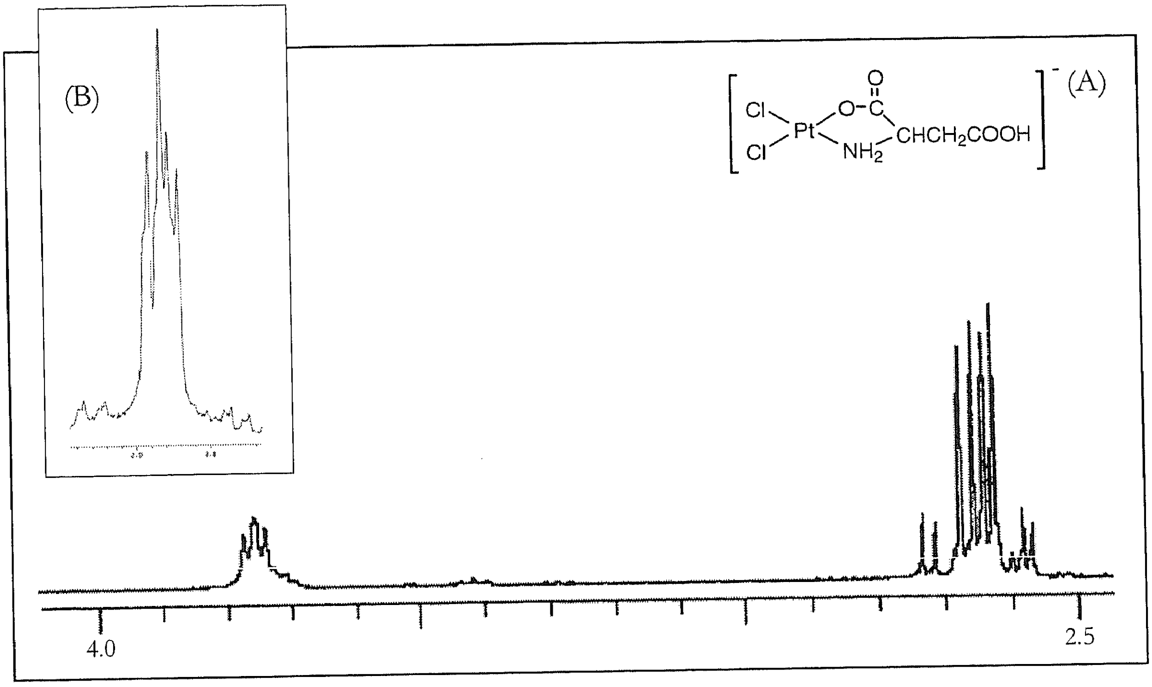

Diagram 2.4: The [1]H NMR spectrum of $[Pt(L\text{-}asp\text{-}N,O)Cl_2]^-$ at 300 MHz (A) and the AB-portion at 200MHz (B).

It is of interest to note that a first-order analysis of the 200 MHz [1]H NMR spectra of the series of pH solutions was difficult because the H^2 and H^3 resonances overlap producing completely distorted spectra. However, at 300 MHz, a well-defined ABX pattern is observed, making analysis much easier. Selected chemical shifts and coupling constants obtained from these analyses are given in Table 2.3.

In aspartic acid, as the molecule goes from pH 2.8 to pH 12, the following changes are noted:

(a) All protons experience an upfield shift

(b) The chemical shift distance between the methylene protons increases. The major factor in effecting a large chemical shift difference between the methylene protons is due to the asymmetric amino group.

(c) The geminal coupling constant J_{23} decreases. The significant change in the geminal coupling constant between pH 8-12 is due to the change in electronegativity of the amino and carboxylate group.

Table 2.3: ^{1}H NMR[a] Data for [Pt(L-asp-N,O)Cl_2]$^-$ and the free aspartic acid ligand at various pD values.

Species	pD	-CH- proton			-CH_2- protons		
		δH^1	J_{21}	J_{31}	δH^2	δH^3	J_{23}
[Pt(L-asp-N,O)Cl_2]	3.2	3.93	4.8	5.7	2.84	2.92	18.0
	4.4	3.87	4.0	5.6	2.77	2.83	17.7
	6.4	3.77	4.0	5.6	2.62	2.69	17.2
	8.5	3.77	4.0	5.8	2.61	2.69	17.4
	12.4	3.77	4.0	5.8	2.61	2.69	17.4
H_3asp^+	3.2	4.03	4.2	6.9	3.00	2.90	18.0
	4.4	3.94	4.2	8.1	2.88	2.76	17.7
	6.4	3.89	3.9	8.4	2.81	2.67	17.4
	8.5	3.88	3.9	8.7	2.80	2.66	17.4
	12.4	3.53	3.6	9.9	2.63	2.23	15.3

[a] Chemical shifts in ppm and coupling constants in Hz

Platinum binding to amino acids invariably produces a downfield shift of their proton resonances.[10] In our pH experiments on [Pt(L-asp-N,O)Cl_2]$^-$, only the H^3 methylene proton shifts downfield as a consequence of coordination. The chemical shifts of the remaining aspartic acid protons appear to be the average of downfield shifts due to platinum(II) chelation and upfield shifts due to hydrophobic interaction of the side-chain of the aspartic acid with the five-membered chelate ring. The result is an upfield shift ranging from 0.07 to 0.24 ppm.

When the pH of a aqueous solution of [Pt(L-asp-N,O)Cl_2]$^-$was increased to 12, the ^{1}H NMR spectrum of the solution shows two quartets in the α-proton region with an intensity ratio of 1:2. The two methine quartets were assigned to the isomers [Pt(L-asp-N,O)Cl_2]$^-$ and [Pt(L-asp-O,O)Cl_2] with that at 3.77 ppm corresponding to the N,O-chelate and that at 3.63 ppm to the O,O-chelate. Several hours later, the methine quartet belonging to [Pt(L-asp-O,O)Cl_2] disappeared from the spectrum. This suggests that upon standing [Pt(L-asp-O,O)Cl_2] slowly isomerises to give the thermodynamically more stable five-membered N,O-chelate.

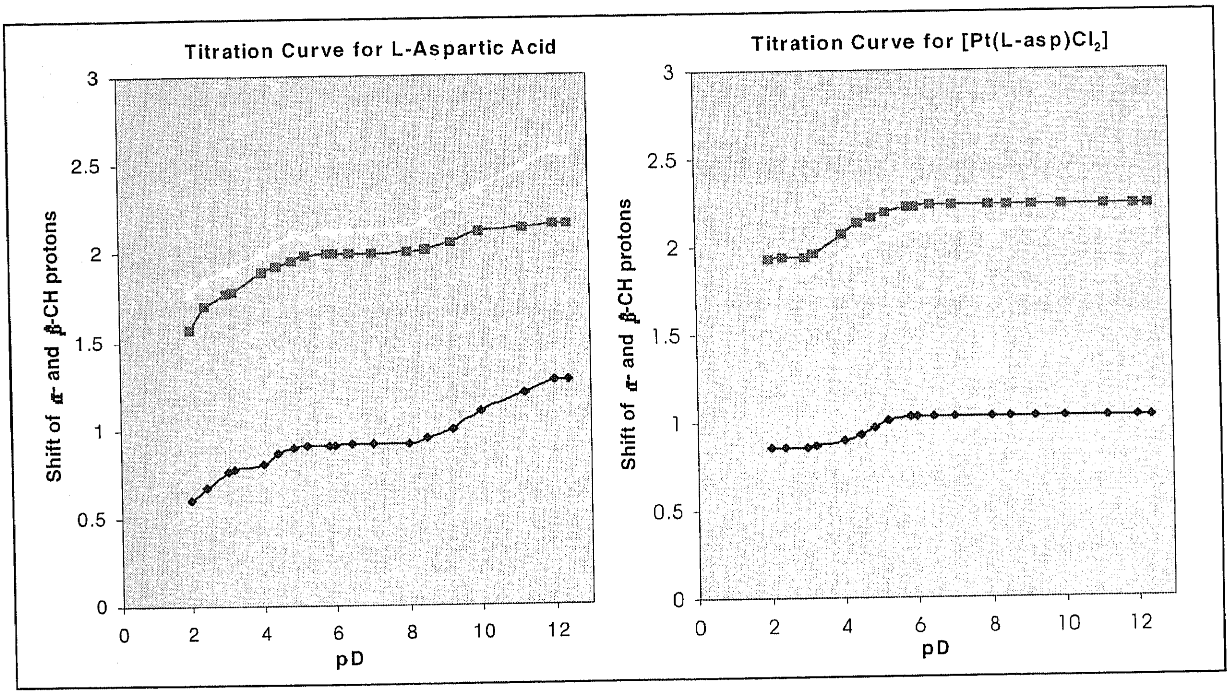

Diagram 2.5: Titration curves for aspartic acid and [Pt(L-asp-N,O)Cl_2]$^-$. The chemical shifts of the H^1 ( ), H^2 ( ) and H^3 ( ) resonances are all relative to D_2O.

The pH dependence of the chemical shifts is shown in Diagram 2.5. These chemical shifts were found to vary with pH in a manner that reflects a titration curve. The free aspartic acid ligand shows three steps in the graph. The pH at the midpoint of a step corresponds to the pKa value of the group. The first step is due to the ionisation of the α-carboxyl group, the next from the β-carboxyl and the last from the NH_3^+ group. In Diagram 2.5, the midpoints for aspartic acid occur at pH values 2.0, 3.9 and 10.0. These values are in agreement with dissociation constants given in the literature.[11] Only a single pK_a value was obtained for $[Pt(L\text{-}asp\text{-}N,O)Cl_2]^-$. Obtaining a single pK_a value of 3.9 for the Pt(II) chelate is consistent with the idea that the complex is an N,O-chelate in which the second carboxylate is unbound.

Like $[Pt(L\text{-}asp\text{-}N,O)Cl_2]^-$, the ^1H NMR spectra of $[Pt(L\text{-}serine)Cl_2]^-$ display a pronounced ABX character. This is not surprising, for serine differs from aspartic acid only in the replacement of the terminal carboxylate of the latter with a hydroxy group. It is the presence of this hydroxy moiety which causes the methylene protons to appear furthermost downfield. Comparison of the protons in the free ligand and their complex shows only a slight upfield shift due to complexation. The resonances in the ^1H NMR of $[Pt(L\text{-}serine)Cl_2]^-$ are somewhat broader than that of the free ligand particularly the methine quartet. Broad ^1H NMR signals for the methine and methylene protons indicate that the complex may exhibit a pronounce degree of conformational flexibility. The proton chemical shifts and coupling constants are given in Tables 2.4 and 2.5.

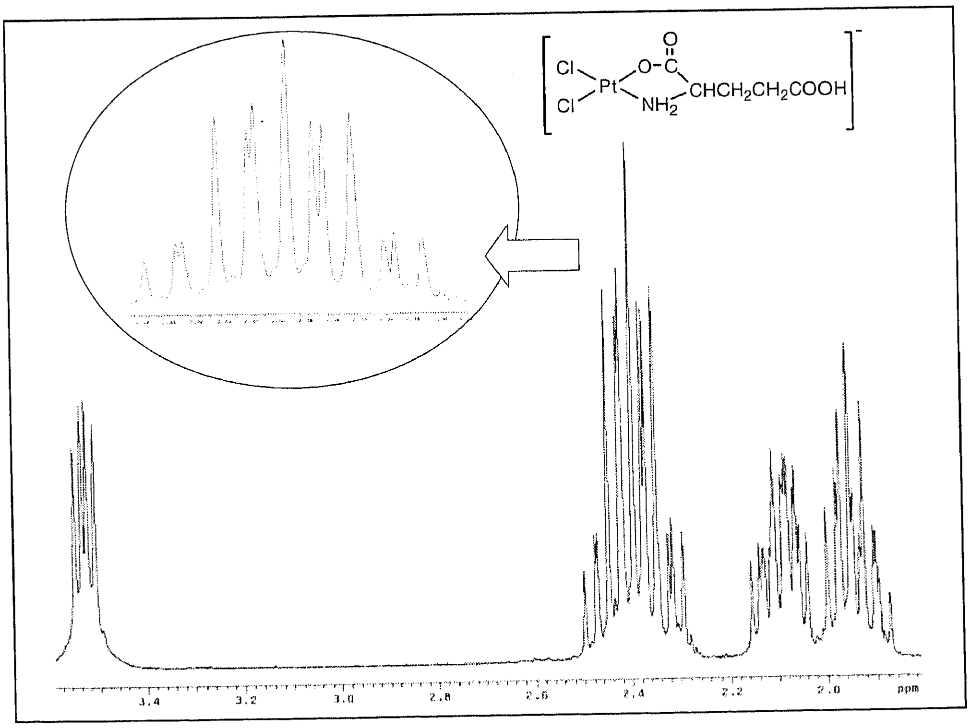

Diagram 2.6: ^1H NMR of $[Pt(L\text{-}glu\text{-}N,O)Cl_2]^-$.

Diagram 2.6 shows the ^{1}H NMR spectrum of $[Pt(L\text{-}glu\text{-}N,O)Cl_2]^-$. The spectrum clearly consists of four groups of lines for the five magnetically non-equivalent protons. Closer inspection of the splitting shows that the thirteen-line portion centred around 2.4 ppm is made up of two sub-spectra, thus all five interacting nuclei have different chemical shifts. Following the normal nomenclature, the spectrum can be described as a five spin ABXYR type system.[12, 13] Each of the γCH_2 protons will couple to the βCH_2 protons to give 16 lines (resembles two ABX type patterns), and similarly the βCH_2 protons couple to the αCH and γCH_2 protons to give a complex splitting pattern consisting of 32 lines (resembles two ABXR patterns). This simplification to two sets of ABX and ABXR type patterns enable a complete analysis to be performed. The spin coupling constants obtained from these analyses are:

(a) For the ABXR type systems

$J_{gem} = J_{23} = 15$ Hz

$J_{trans} = J_{13} = 8.4$ Hz

$J_{cis} = J_{12} = 4.8$ Hz

(b) For the ABX type systems

$J_{gem} = J_{45} = 15$ Hz

$J_{trans} = J_{25} = J_{34} = 8.7$ Hz

$J_{cis} = J_{24} = 7.1$ Hz

$J_{cis} = J_{35} = 6.7$ Hz

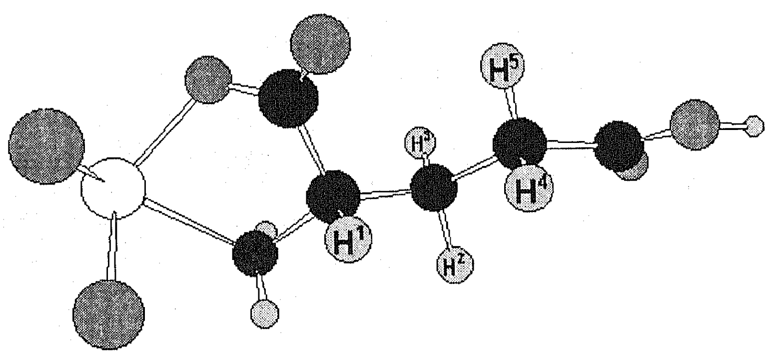

The complex splitting pattern originating from all five non-equivalent protons in the ^{1}H NMR of $[Pt(L\text{-}glu\text{-}N,O)Cl_2]^-$ is not seen in the spectrum of the free glutamic acid ligand. The spectrum can easily be mistaken as an AA'BB'X type system because the pairs of protons on the β- and γ-carbon are so close in chemical shift. On closer inspection of the fine splitting, what appeared to be only an average signal is actually a crossover of the splitting patterns. In addition, Table 2.5 shows that the $^3J(\beta CH_2\text{-}\gamma CH_2)$ proton coupling constants of L-glutamic acid do not change on coordination. This indicates equally populated rotamer distribution, due to free rotation around the β- and γ-carbon bond.[14]

With $[Pt(L\text{-}glu.OMe)Cl_2]^-$ and the corresponding free methyl ester, determination of the proton coupling constants was complicated due to the extensive overlapping of resonances. In view of the difficulty of locating the necessary signals, all values were confirmed by computer simulation. The simulated spectra were remarkably similar to those observed. The observed and computer-simulated ^1H NMR spectra of $[Pt(L\text{-}glu.OMe)Cl_2]^-$ are presented in Diagram 2.7. Tables 2.4 and 2.5 contain the refined chemical shift and coupling constant data.

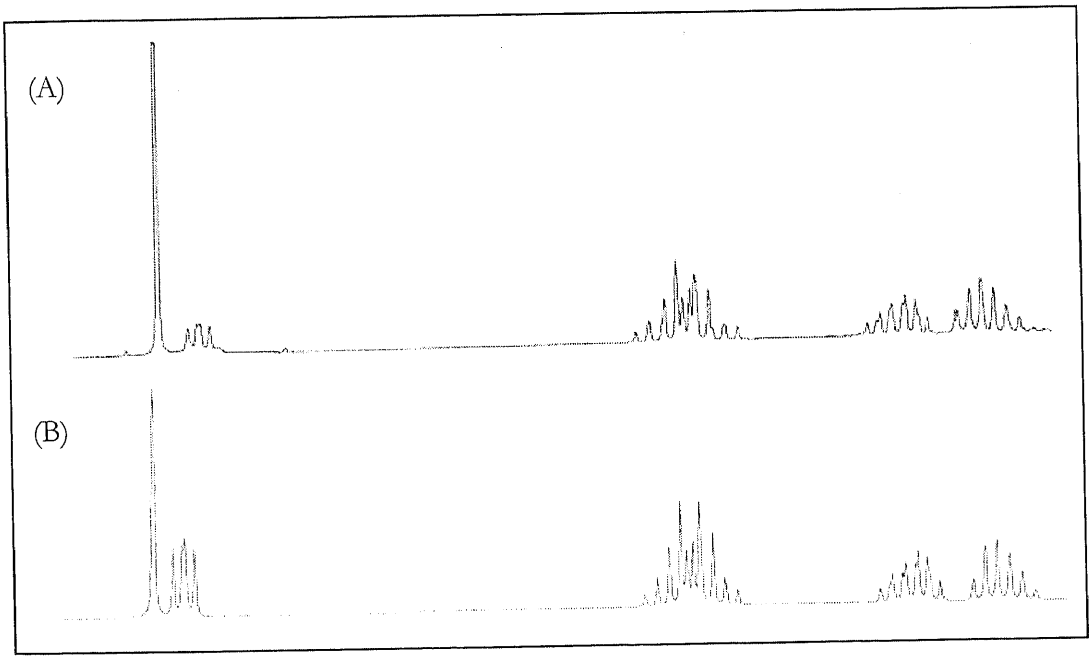

Diagram 2.7: ^1H NMR of the observed spectrum (A) and the simulated spectrum (B) of $[Pt(L\text{-}glu.OMe)Cl_2]^-$ at 300 MHz.

The general appearance of the ^1H NMR spectrum of $[Pt(L\text{-}glu.OMe)Cl_2]^-$ is very similar to that of $[Pt(L\text{-}glu\text{-}N,O)Cl_2]^-$ with the additional resonance at 3.72 ppm corresponding to the methyl ester moiety. This methyl resonance does not shift significantly on coordination due to the considerable distance away from the binding site. In contrast, the methine proton adjacent to the Pt(II) binding site undergoes a pronounced upfield shift of 0.12 ppm on coordination.

When comparing the ^1H NMR of $[Pt(L\text{-glu.OMe})Cl_2]^-$ and its corresponding free methyl ester, two major differences are clearly evident. Firstly, in the ^1H NMR of $[Pt(L\text{-glu.OMe})Cl_2]^-$ the methine resonance is a quartet indicating unequal coupling between the methine and the two methylene protons (H^2 and H^3). This methine is also expected to appear as a doublet of doublets in the ^1H NMR of the free methyl ester due the non-equivalence of the methylene protons. In actuality, the methine resonance resembles a 1:2:1 triplet, which indicates that the couplings between the α-CH proton and β-CH_2 protons are approximately equal ($J_{21} = J_{31} = 6.3$ Hz). Secondly, the AB region of $[Pt(L\text{-glu.OMe})Cl_2]^-$ clearly shows splittings due to each of the methylene protons on the β-carbon. In the spectrum of the free methyl ester, the chemical shift difference between the methylene protons on the β-carbon is so small that the splittings crossover causing the spectrum to appear deceptively simple.

The ^1H NMR of $[Pt(L\text{-lysine})Cl_2]^-$ and the free ligand show five major resonances due to the methine and the four methylene protons. As indicated by the splitting patterns the ε-CH_2 protons appear to be equivalent. All other methylene protons appear to be non-equivalent. Despite the complexity brought about by an eight-spin system a total analysis of the spectra was achieved with the aid of the simulation program gNMR. Coupling constants and proton chemical shifts for $[Pt(L\text{-lysine})Cl_2]^-$ are presented in Tables 2.4 and 2.5, together with that of free lysine for comparison.

When comparing the ^{1}H NMR of $[Pt(L\text{-lysine})Cl_2]^-$ with free lysine, the following aspects are noted.

(a) The resonances in the ^{1}H NMR of $[Pt(L\text{-lysine})Cl_2]^-$ are somewhat broader than that of the free ligand, suggesting the there is some degree of flexibility in the complex.

(b) The methine resonance experiences a substantial shift to lower field on formation of the complex. As already observed with $[Pt(L\text{-glu.OMe})Cl_2]^-$, this methine resonance is seen as a quartet (i.e $J_{21} \neq J_{31}$) in the spectrum of $[Pt(L\text{-lysine})Cl_2]^-$. However, a ^{1}H NMR spectrum showing a 1:2:1 methine triplet (i.e $J_{21} = J_{31}$) was obtained for free lysine.

(c) An effectively unchanged position around 3.0 ppm for the ε-CH_2 protons rule out coordination through the terminal amine. The complex may therefore be formulated as containing a N,O-chelate ring.

(d) In the methylene region (1.5 -1.9 ppm) of the complex there is a small degree of overlapping. For example, the resonances due to H^3 and H^5 are located directly beneath the broad δ-CH_2 peak.

Table 2.4: ^{1}H NMR chemical shifts.[a]

	-CH-	-CH$_2$-								-OCH$_3$
Compound	δH^1	δH^2	δH^3	δH^4	δH^5	δH^6	δH^7	δH^8	δH$^{8'}$	
L-asp	4.03	3.00	2.90							
[Pt(L-asp-N,O)Cl$_2$]	3.93	2.84	2.92							
L-serine	3.84	3.98	3.94							
[Pt(L-serine)Cl$_2$]	3.73	3.84	3.94							
L-glu	3.77	2.14	2.10	2.45	2.47					
[Pt(L-glu-N,O)Cl$_2$]	3.53	2.10	1.95	2.46	2.36					
L-glu.OMe	3.78	2.18	2.15	2.56	2.60					3.72
[Pt(L-glu.OMe)Cl$_2$]	3.66	2.27	2.10	2.72	2.65					3.72
L-lysine	3.76	1.91	1.90	1.50	1.49	1.72	1.70	3.0	3.0	
[Pt(L-lysine)Cl$_2$]	3.59	1.72	1.89	1.50	1.67	1.67	1.68	3.0	3.0	

[a] Chemical Shifts in ppm, spectra run in D_2O referenced to TMSP. [b] The spectra of [Pt(L-serine)(NH_3)$_2$Cl] and [Pt(L-lysine)(NH_3)$_2$Cl]were recorded after the NH_3 protons had exchanged with deuterium in order to observe other resonances.

Table 2.5: ^{1}H NMR coupling constants.[a]

Compound	^{3}J Coupling Constants														^{2}J Coupling Constants		
	$^3J_{12}$	$^3J_{13}$	$^3J_{24}$	$^3J_{25}$	$^3J_{34}$	$^3J_{35}$	$^3J_{46}$	$^3J_{47}$	$^3J_{56}$	$^3J_{57}$	$^3J_{68}$	$^3J_{68'}$	$^3J_{78}$	$^3J_{78'}$	$^2J_{23}$	$^2J_{45}$	$^3J_{67}$
L-asp	4.2	6.9													18		
[Pt(L-asp-N,O)Cl$_2$]	4.8	5.7													18		
L-serine	4.2	5.3													12.3		
[Pt(L-serine)Cl$_2$]	3.7	5.3													12.1		
L-glu	5.4	5.4	6.7	8.7	8.7	7.1									14.6	14.6	
[Pt(L-glu-N,O)Cl$_2$]	4.8	6.7	7.1	8.7	8.7	6.7									15	15	
L-glu.OMe	6.3	6.3	7.2	7.8	7.8	7.2									14.7	14.7	
[Pt(L-glu.OMe)Cl$_2$]	5.4	7.2	6.8	7.3	7.5	6.8									14.4	14.4	
L-lysine	6.2	6.2	7.7	7.7	7.7	7.7	7.5	7.3	7.3	7.5	7.7	7.7	7.7	7.7	15.2	15.2	15.0
[Pt(L-lysine)Cl$_2$]	5.3	6.8	7.1	7.1	7.1	7.1	6.0	6.0	6.0	6.0	7.0	7.0	7.0	7.0	19.0	15.0	15.2

[a] Coupling constants in Hz, recorded at 300 MHz.

2.7 CONFORMATIONAL STUDIES

The determination of the conformations of amino acids in solution using ^1H NMR spectra is now well recognised. It is based on the use of the Karplus equation,[15,16] which relates the proton coupling constants in a fragment to the dihedral angle, ϕ, between relevant C-H bonds. The originally proposed relationship is of the form:

$$J_{HH} = J_o \cos^2 \phi - B \qquad (1)$$

where J_o = 8.5 Hz ($0<\phi<90$), J_o = 9.5 Hz ($90<\phi<180$) and B = 0.28 Hz. A modified yet equivalent three-parameter equation[17,18] is commonly used. It is valid for the entire range $0<\phi<180$, and written in the following form:

$$J = A \cos^2\phi - B \cos\phi + C \qquad (2)$$

The theoretical Karplus constants adjusted to equation (2) now become: A = 9.0, B = 0.5 and C = - 0.3 Hz. It appears that, whilst equation (2) gives the form of the angular dependence of coupling constants, the parameters A, B, and C are regarded as empirically adjustable parameters, to be extracted from geometrical data on the system to be investigated.[19] Different systems require different parameters to yield consistent and reasonable results. Thus, the significance of the equation is difficult to assess, causing some uncertainty in the conclusions deduced from its use. The results of these Karplus calculations for aspartic acid and its Pt(II) chelate using the modified form of the equation are shown in Tables 2.6. An example is also represented as a 3D-illustration in Diagram 2.8. The observed deviations of the dihedral angles from the ideal trans (180°) and gauche (60°) conformations may in fact be due to the uncertainty in the value of the constants used in the Karplus equation.

Tables 2.6: Dihedral angles[a] for $[Pt(L\text{-}asp\text{-}N,O)Cl_2]^-$ and the free aspartic acid ligand.

Species	J21	J31	Dihedral angle, ϕ	
			H²	H³
$[Pt(L\text{-}asp\text{-}N,O)Cl_2]^-$	4.8	5.7	43.0	37.9
	4.0	5.6	48.4	37.9
	4.0	5.8	48.4	37.3
H_3asp^+	4.8	6.9	43.5	157.3
	4.2	8.1	47.2	159.8
	3.9	8.4	49.0	162.9
	3.9	8.7	49.0	166.6
	3.6	9.9	50.9	-

[a]Dihedral angles calculated form the modified Karplus equation.

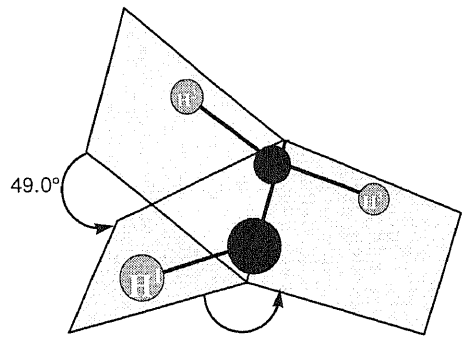

Diagram 2.8: 3D-Illustration showing the orientation of H¹, H² and H³ in aspartic acid at pD 6.4.

A simplified procedure for the conformational analysis of aspartic acid can also be used. The coupling constants displayed in Table 2.3 are considered to be the weighed average of three rotational isomers.[20] If the population of these three rotational isomers were equal, the two methylene protons would be magnetically equivalent since each of them spends the same time in the same environment. The pronounced ABX character in the ¹H NMR clearly demonstrates that this is not the case for aspartic acid and its Pt(II) chelate. The methylene protons are non-equivalent, with each appearing at a different chemical shift with individual vicinal coupling constants. This indicates that in solution an unequal population of rotational isomers exists. The three predominant staggered rotamers of aspartic acid, designated for the purpose of labelling and expressing mole fractions as t, g, and h are shown in Diagram 2.9. The disposition of the side-chain is trans to the carboxyl group in the t rotamer, trans to nitrogen in rotamer g, and trans to the α-hydrogen in rotamer h.

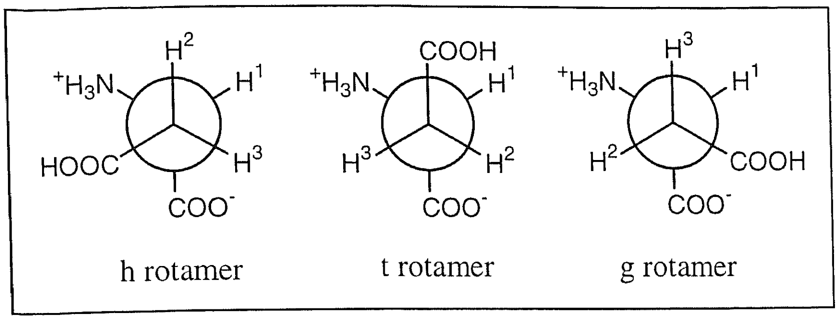

Diagram 2.9: Three staggered rotamers of α-amino acid with two β-hydrogens (H^2 and H^3).

The population of each of the three rotamers of amino acids is related to the vicinal coupling constants J_G and J_T for the gauche and trans positions of proton H^1 with respect to H^2 and H^3, by means of the equations[20,21,22]

$$J_{21} = t\,J_G + g\,J_T + h\,J_G \qquad (3)$$

$$J_{31} = t\,J_T + g\,J_G + h\,J_G \qquad (4)$$

Solutions of equations (3) and (4) with t + g + h =1 gives

$$t = (J_{31} - J_G) / (J_T - J_G) \qquad (5)$$

$$g = (J_{21} - J_G) / (J_T - J_G) \qquad (6)$$

$$h = 1 - t - g \qquad (7)$$

These expressions allow rotamer populations to be deduced from the observed vicinial coupling constants J_{21} and J_{31}, provided one has reliable values for J_G and J_T. Values of J_G = 2.5 Hz and J_T = 12.8 Hz have been recommended for L-aspartic acid.[23]

Using the data in Table 2.3, the relative populations of the different conformers in solution were calculated. Tables 2.7 tabulates vicinal coupling constants and rotamer mole percentages. The data indicate that across the pH range examined, unbound aspartic acid displays a strong preference for the trans conformation in which the proton H^1 is gauche to H^2 and trans to H^3 (Diagram 2.9). It may also be noted that raising the pH results in a dramatic increase in rotamer t, with percentages increasing from 46% to 72%. The greater thermodynamic stability of rotamer t over g and h in basic solutions is expected for spacial and electrostatic repulsions between the α-carboxylate and the terminal carboxylate on the β-carbon are at a minimum. Inspection of the chemical shift data illustrates that as the pH is increased the H^3 proton experiences a greater upfield shift than H^2, suggesting that H^3 is closer to the amino group. This gives further support to the assignment of the preferred conformation as the t isomer.

Tables 2.7: Vicinial coupling constants (Hz) and rotamer mole populations for $[Pt(L\text{-}asp\text{-}N,O)Cl_2]^-$ and the free aspartic acid ligand at various pH values.

Species	pH	J_{21}	J_{31}	t	g	h
$[Pt(L\text{-}asp\text{-}N,O)Cl_2]^-$	2.8	4.8	5.7	0.31	0.22	0.46
	4.0	4.0	5.6	0.30	0.15	0.55
	6.0	4.0	5.6	0.30	0.15	0.55
	8.1	4.0	5.8	0.32	0.15	0.49
	12.0	4.0	5.8	0.34	0.15	0.49
H_3asp^+	2.8	4.8	6.9	0.42	0.22	0.36
	4.0	4.2	8.1	0.54	0.17	0.29
	6.0	3.9	8.4	0.57	0.14	0.29
	8.1	3.9	8.7	0.60	0.14	0.26
	12.0	3.6	9.9	0.72	0.11	0.17

It should be emphasised that the conclusion that rotamer t is the predominant rotameric form for free aspartic acid is a direct consequence of the assignments of the H^2 and H^3 hydrogens. Reversal of these assignments results in a reversal of the population of rotamers t and g. Many researchers simply state that the highest field proton is taken as the H^3 proton.[20,23,24,25] Rather than assign the H^2 and H^3 protons exclusively on the basis of chemical shifts, this labelling of H^2 and H^3 involves a commitment to the designation of H^3 as the proton more strongly coupled to H^1. Assignments were made by analogy with coupling data on cysteine and histidine derivatives.[24] Cysteine is a good comparative model for it differs from aspartic acid only in the replacement of the terminal carboxylate function of the latter by a sulfhydryl group.

The platinum complex of aspartic acid displays relatively low coupling constants, and a preponderance of the structure with a conformation about the α- and β-carbons similar to the hindered gauche appears to prevail. This implies that the aliphatic side-chain is directed toward the platinum metal-ion chelated between the amino and carboxylate groups (Diagram 2.10). This conclusion is corroborated by the observation that the methine and one of the methylene protons undergoes an upfield shift on coordination. Similar side-chain-metal interactions have been observed elsewhere.[14]

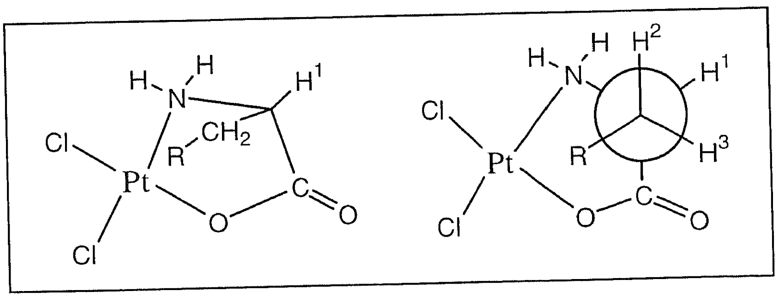

Diagram 2.10: The most stable rotamer of $[Pt(L\text{-}asp\text{-}N,O)Cl_2]^-$.

2.8 ^{13}C NMR

The ^{13}C NMR of the platinum complexes and free ligands were run with the instrument internally locked on D_2O and with ^1H decoupling. The shifts were measured relative to TMSP. ^{13}C NMR data are listed in Table 2.8.

Table 2.8: ^{13}C NMR data.[a]

Compound	Carboxylate		Methylene				$-OCH_3$
	α-COO$^-$	Terminal COOR[b]	α-CH	β-CH_2	γ-CH_2	Others	
L-asp	176.8	179.6	54.7	38.8			
[Pt(L-asp-N,O)Cl$_2$]	191.4	179.6	58.5	40.6			
L-serine	175.3	-	59.2	63.0			
[Pt(L-serine)Cl$_2$]	190.4	-	62.9	64.4			
L-glu	187.2	183.9	63.9	40.2	35.6		
[Pt(L-glu-N,O)Cl$_2$]	192.7	183.7	58.9	31.5	35.6		
L-glu.OMe	176.2	177.9	56.7	36.7	32.6		55.0
[Pt(L-glu.OMe)Cl$_2$]	191.5	178.4	60.4	30.0	32.3		55.4
L-lysine	177.53	-	57.4	29.2	24.3	41.9[c] 32.8[d]	-
[Pt(L-lysine)Cl$_2$]	192.8	-	61.0	29.3	24.4	42.1[c] 34.5[d]	-

[a] Chemical shifts in ppm relative to TMSP, spectra run in D_2O.
[b] R = H for L-aspartic and L-glutamic acid, R = CH_3 for L-glutamic acid, 5-methyl ester.
[c] ε-CH [d] δ-CH

The ^{13}C NMR spectrum of [Pt(L-asp-N,O)Cl$_2$]$^-$ shows the expected four peaks. Two of these peaks that occur at lower frequency (58.5 and 40.6 ppm) may be confidently assigned to the methine and methylene carbon atoms respectively. Assignments of these resonances were confirmed by the HMQC spectrum. The remaining two peaks at higher frequency (191.4 and 179.6 ppm) correspond to the carboxylate carbon atoms. The peak at 191.4 ppm, shifted significantly from the peak for the free ligand (176.8 ppm), is assigned to the coordinated carboxylate. Such high frequency is characteristic of a carboxylate group being incorporated into a five-membered chelate ring.[26,27] In six-membered chelate ring complexes, the carboxylate resonances are more shielded. For example, in β-alanine analogues the carboxylate carbon nucleus occurs at 181 ppm.[28,29] The peak at 179.6 ppm is only shifted slightly from that of the free ligand (179.4 ppm), providing additional evidence that the β-carboxylate is not coordinated in this complex.

Similarly, the ^{13}C NMR spectrum of $[Pt(L\text{-serine})Cl_2]^-$ is consistent with the formation of an N,αO-chelate complex. In the carboxlyate region the spectrum shows a peak at 190.4 ppm. This peak is shifted significantly from the carboxyl resonance of the free ligand (175.3 ppm) and is characteristic of a carboxylate group that is part of a five-membered chelate ring. The spectrum also shows a methine and a methylene carbon. The methine carbon, 62.9 ppm, was deshielded by 3.7 ppm relative to the free ligand, and the methylene carbon, 64.4 ppm, by 1.4 ppm.

The ^{13}C NMR spectrum of $[Pt(L\text{-glu-N,O})Cl_2]^-$ shows a singlet at 58.9 ppm from the methine carbon, two singlets from the methylene carbon atoms at 35.6 ppm and 31.5 ppm, and two singlets at 192.7 ppm and 183.7 ppm. Especially notable was the presence of a carboxylate peak at relatively high frequency (192.7 ppm), confirming the presence of a five-membered chelate ring. The methine and methylene carbon resonances were assigned by comparison with $[Pt(L\text{-asp-N,O})Cl_2]^-$.

The ^{13}C NMR spectrum of $[Pt(L\text{-glu.OMe})Cl_2]^-$ shows six singlets, one signal corresponding to a methyl group (55.4 ppm), two methylene signals (30.0 and 32.3 ppm), two carboxylate signals (178.4 and 191.5 ppm) and a methine signal (60.4 ppm). The presence of both the methyl resonance and a carboxylate peak at high frequency (191.5 ppm) gives a good indication of the N,αO- bidentate nature of platinum chelation.

The ^{13}C NMR spectrum of $[Pt(L\text{-lysine})Cl_2]^-$ shows the expected six peaks. The most significant features include the carboxyl resonance at 192.7 ppm and the methine carbon at 61 ppm. Each peak is further downfield relative to the free ligand (177.5 and 57.4 ppm respectively). Such a strong downfield progression indicates the formation of a five-membered N,αO-chelate. The methylene resonances do not shift as significantly as the carboxyl and methine resonances on coordination due to their considerable distances from the binding site. Shifts for the four methylene carbons are given in Table 2.8.

2.9 MASS SPECTRA

The mass spectra of all platinum complexes were scanned from 0 to 1000 amu. An example of a typical mass spectrum is depicted in Diagram 2.11. The spectrum of $[Pt(L\text{-asp-N,O})Cl_2]^-$ shows the intense molecular ion peak as a base peak at m/e= 398, along with appreciable peaks. This molecular ion base peak highlights that the molecular ion of the N,O-isomer is very stable. Diagram 2.11 also shows that the isotopic peak cluster ratio of this molecular ion was consistent with a dichloro species, since a dichloroplatinum fragment ion should give rise to a cluster of 7 peaks separated by 1 mass unit in the approximate ratio (70:73:100:46:57:8:16).

The molecular ion also emerged as a base peak in the mass spectra of $[Pt(L\text{-glu.OMe})Cl_2]^-$, $[Pt(L\text{-serine})Cl_2]^-$ and $[Pt(L\text{-lysine})Cl_2]^-$. For $[Pt(L\text{-glu-N,O})Cl_2]^-$, the mass spectrum of showed a prominent molecular ion peak at m/e = 411.8, and is consistent with the expected mass. The base peak at m/e= 112 is probably due to the cleavage and fragmentation of the glutamic acid ligand. The mass spectrum of $[Pt(L\text{-lysine})Cl_2]^-$ also show some additional peaks at m/e = 145 and 90, presumably due to the cleavage and fragmentation of the lysine ligand.

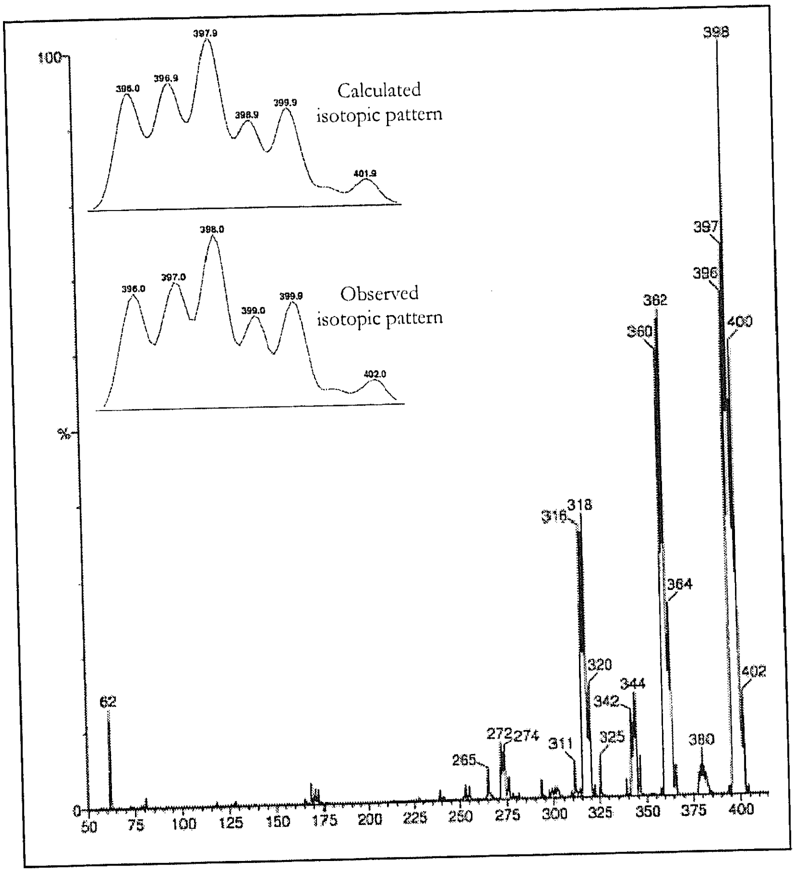

Diagram 2.11: Mass spectra of [Pt(L-asp-N,O)Cl_2]$^-$

It is worth noting that in addition to a molecular ion peak consistent with the expected mass, all mass spectra show a prominent peak corresponding to the loss of chlorine. A summary of the mass spectral data is listed in Table 2.9.

Table 2.9: Summary of mass spectral data.

Compound	Base Peak [M^+]	[M^+- Cl]	Others
[Pt(L-asp-N,O)Cl_2]$^-$	398.0	362.0	318.0
[Pt(L-serine)Cl_2]$^-$	370.0	333.0	-
[Pt(L-glu-N,O)Cl_2]$^-$	411.8	376.6	112.0
[Pt(L-glu.OMe)Cl_2]$^-$	426.0	390.0	-
[Pt(L-lysine)Cl_2]$^-$	411.0	374.0	145.0
			50

2.10 X-RAY STRUCTURAL ANALYSIS

The solid state structure of $[Pt(L\text{-lysine})Cl_2]^-$ was determined by single-crystal X-ray diffraction. $[Pt(L\text{-lysine})Cl_2]^-$ crystallised as yellow needles in the monoclinic space group P2(1) with two independent molecules in the asymmetric unit and unit dimensions a = 9.634(8) Å, b = 11.113(11) Å, c = 11.057(9) Å and β = 102.02(6)°. The space group P2(1) is non-centrosymmetric therefore the molecules are chiral. The crystal data and selected experimental parameters used are summarised in Table 2.10. Selected bond lengths and bond angles are listed Table 2.11. Additional crystallographic details are provided in the Appendix.

Table 2.10: Crystallographic data and experimental parameters for the crystal structure analysis of $[Pt(L\text{-lysine})Cl_2]^-$.

Empirical Formula C12 H32 Cl4 N4 O6 Pt2	Radiation MoK alpha (0.71073 Å)
Color; Habit yellow needle	Temperature 173 K
Crystal Size (mm)0.2 x 0.2 x 0.6	2 theta Range 3.0 to 49.0°
Crystal System Monoclinic	Index Ranges 0 < H < 11;
Space Group P 2(1)	-12 < K < 12 ;
Unit Cell Dimensions:	-12 < L < 12
a = 9.634(8) Å	Reflections Collected 4089
b = 11.113(11) Å	Independent Reflections 3833 (Rint = 3.62%)
c = 11.057(9) Å	Observed Reflections 3573 (F obs> 4.0 sigma(F))
beta = 102.02(6)°	Number of Parameters refined 252
Volume 1157.9(17) Å ^{3}	Final R indices (obs. data) = 4.85 %, wR = 7.59 %
Z = 4	Indices (all data) = 5.23 %, wR = 7.84 %
Formula weight 426.7	Goodness-of-Fit 1.24
Density(calc.) 2.447 g/cm^3	Largest Difference Peak 4.48 e^{-3}
Absorption Coefficient 12.695 mm^{-1}	
F(000)794	

An ORTEP drawing of the crystal structure is presented in Diagram 2.12. The structure shows that in each discrete molecule the lysine ligand is coordinated to the central platinum atom via the α-carboxylate and NH_2 group to form a five-membered chelate ring. The absolute configurations of the two molecules in the unit cell are the same, as expected. The square planar entities are "stacked" above each other in such a way that the carbonyl oxygen of each lysine interacts in a pseudo-axial fashion with the platinum atom of the other molecule in the unit cell. These Pt-O distances are between 3.2 to 3.3 Å.

Angles of Cl-Pt-Cl, Cl-Pt-N, Cl-Pt-O and N-Pt-O all deviate from 90° indicating that the platinum atoms are in a slightly distorted square-planar environment. Geometrical parameters worthy of note include the Pt-N distances from the primary amine nitrogen to the platinum center (2.061 and 1.984 Å), the Pt-O distances from the carboxylate and the platinum center (2.006 Å) and the Pt-Cl bond lengths which vary between 2.316 to 2.297 Å. The N-Pt-O angles in the two molecules (82.3(6)° and 83.2(6)°) agree well with the value of 83°, predicted for a mean metal-donor bond distance of 2.0 Å.[30]

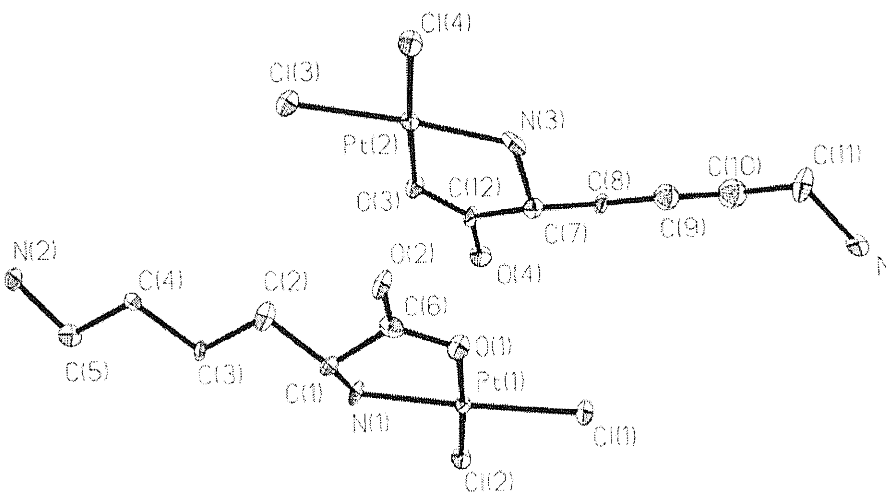

Diagram 2.12: ORTEP drawing of [Pt(L-lysine)Cl_2]$^-$.

The H_3O^+ counterions are not shown.

Table 2.11: Selected bond lengths (Å) and angles (deg).

Bond lengths			
Pt(1)-Cl(1)	2.316 (6)	Pt(2)-Cl(3)	2.321 (6)
Pt(1)-Cl(2)	2.297 (5)	Pt(2)-Cl(4)	2.288 (5)
Pt(1)-N(1)	2.061 (18)	Pt(2)-O(3)	2.007 (14)
Pt(1)-O(1)	2.006 (14)	Pt(2)-N(3)	1.984 (23)
Bond angles			
Cl(1)-Pt(1)-Cl(2)	92.9(2)	Cl(3)-Pt(2)-Cl(4)	92.7(2)
Cl(1)-Pt(1)-N(1)	173.5(4)	Cl(3)-Pt(2)-O(3)	90.9(4)
Cl(2)-Pt(1)-N(1)	93.6(4)	Cl(4)-Pt(2)-O(3)	175.8(4)
Cl(1)-Pt(1)-O(1)	91.2(5)	Cl(3)-Pt(2)-N(3)	174.1(5)
Cl(2)-Pt(1)-O(1)	175.2(5)	Cl(4)-Pt(2)-N(3)	93.2(5)
N(1)-Pt(1)-O(1)	82.3(6)	O(3)-Pt(2)-N(3)	83.2(6)
Pt(1)-N(1)-C(1)	109.8(11)	Pt(2)-O(3)-C(12)	115.6(11)
Pt(1)-O(1)-C(6)	117.6(12)	Pt(2)-N(3)-C(7)	112.7(12)

References

1 L. M. Volshtein, Sov. J. Coord. Chem., 1975, **1**, 483-509.

2 F. R. Hartley, The Chemistry of Platinum and Palladium, Applied Science, London, 1973, pp. 205-209.

3 T. G. Appleton, J. R. Hall, and S. F. Ralph, Inorg. Chem., 1985, **24**, 673-677.

4 J. Altman, M. Wilchek and A. Warshawsky, Inorg. Chim. Acta., 1985, **107**, 165.

5 T. G. Appleton and F. B. Ross, Inorg. Chim. Acta., 1996, **252**, 79-89.

6 T. G. Appleton, J. R. Hall, W. N. Donald and C. S. M. Thompson., Inorg. Chem., 1990, 29, 3985-3990.

7 K. Nakamoto, Infrared and Raman Spectra of Inorganic and Coordination Compounds 4th ed., Wiley, New York, 1986, pp. 237.

8 R. M. Silverstein, G. C. Bassler and T. C. Morrill, Spectrometric Identification of Organic Compounds 4th ed.,Wiley, New York, 1981, pp. 95-180.

9 W. Kemp, NMR in Chemisry: A Multinuclear Introduction, Macmillan Education LTD, London, 1986, pp. 51-52.

10 L. E. Erickson, J. W. McDonald, J. K. Howie and R. P. Clow, J. Am. Chem. Soc., 1968, **90**, 6371-6382.

11 G. Aylward and T. Findlay, SI Chemical Data, John Wiley and Sons, Brisbane, 1994, pp. 106.

12 J. A. Pople and T. Schaeffer, Mol. Phys., 1960, **3**, 547.

13 R. J. Abraham and K. A. McLauchlan, Mol. Phys., 1962, **5**, 195.

14 A. Iakovidis, N. Hadjiliadis, H. Schollhorn, U. Thewart and G. Trotscher, Inorg. Chim. Acta., 1989, **164**, 221-229.

15 M. Karplus, J. Chem. Phys., 1959, **30**, 11.

16 L. M. Jackman and S. Sternhell, Application of Nuclear Magnetic Resonance Spectroscopy in Organic Chemistry 2nd ed., Pergamon Press, Oxford, 1969.

17 C. Altona, H. R. Buys, H. J. Hageman and E. Havinga, Tetrahedron, 1967, **23**, 2265-2279.

18 B. J. Blackburn, R. D. Lapper and I. C. P. Smith, J. Am. Chem. Soc., 1973, **95**, 2873-2878.

19 R. J. Abraham and J. S. E. Holker, J. Am. Chem. Soc., 1963, 806-811.

20 J. J. M. Rowe, J. Hilton and K. L. Rowe, Chem. Rev., 1970, **70**, 1-57.

21 R. B. Martin, J. Phys. Chem., 1979, **83**, 2404-2407.

22 S. Kim and R. B. Martin, J. Am. Chem. Soc., 1984, **106**, 1707-1712.

23 W. G. Espersen and R. B. Martin, J. Phys. Chem., 1976, **80**, 741-745.

24 R. B. Martin and R. Mathur, J. Am. Chem. Soc., 1965, **87**, 1065-1070.

25 J. P. Casey and R. B. Martin, J. Am. Chem. Soc., 1972, **94**, 6141-6151.

26 O. W. Howarth, P. Moore and N. Winterton, J. Chem. Soc., Dalton Trans., 1974, 2271-2276.

27 T. G. Appleton, J. R. Hall, T. W. Hambley and P. D. Prezler, Inorg. Chem., 1990, **29**, 3562-3569.

28 T. G. Appleton, A. J. Bailey, D. R. Bedgood and J. R. Hall, Inorg. Chem. 1994, **33**, 216-226.

29 T. G. Appleton, J. R. Hall and S. F. Ralph, Aust. J. Chem., 1986, **39**, 1347-1362.

30 H. C. Freeman, Adv. Protein Chem., 1967, **22**, 257.

CHAPTER

3

DICHLORO DIAMINE PLATINUM(II) COMPLEXES

Introduction

It is now widely accepted that the anti-cancer properties of cisplatin are the result of specific interactions of the *cis*-$[Pt(NH_3)_2]^{2+}$ fragment with DNA. The possible binding sites on DNA include the N(7) atom of guanine and adenine, the N(1) atom of adenine and the N(3) atom of cytosine (Diagram 3.1).[1] Out of these four possible sites, cisplatin shows a strong preference for the N(7) site of guanine.[2,3] This preference seems to be related to the stronger basicity of guanine-N(7) atom and hydrogen bonding.[1,4] Secondary interactions between the hydrogens on the amine and the nearby O(6) atom may influence the kinetics of the reaction and thermodynamic stabilisation after binding to the N(7) atom.

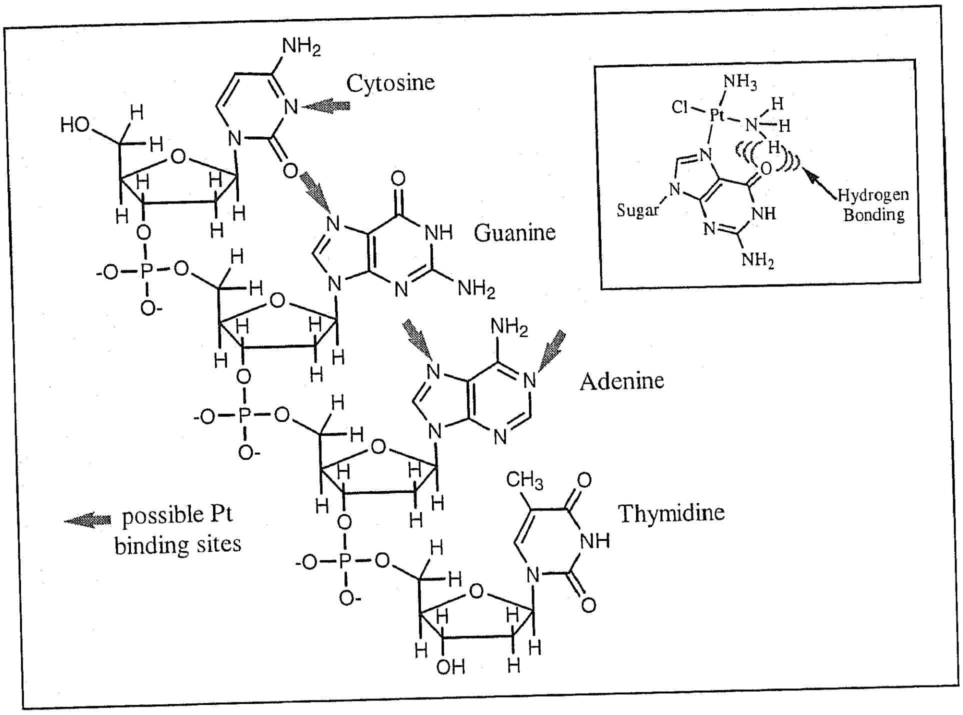

Diagram 3.1: Schematic diagram showing the possible platinum binding sites on DNA. Inset shows the hydrogen bonding interactions upon binding to guanine.

From these observations on cisplatin, it appears that having at least one hydrogen attached to each of the amines is an important feature that may influence the overall activity of the platinum analogue.[5] A panoply of Pt(II) complexes containing a variety of amine ligands have been studied. From these structure-activity relationship studies the anti-cancer activity has been reported to decrease following the order $NH_3 \geq RNH_2 \geq R_2NH \geq R_3N$.[6]

The most promising analogues are platinum(II) complexes containing a 1,2-diaminocyclohexane (dach) substituent in the non-leaving position. The dach-Pt complexes have been the focus of considerable research, primarily due to their potential activity against cisplatin-resistant cells[7] and their reduced nephrotoxicity and myelotoxicity compared to cisplatin and carboplatin. Structurally, the dach ligand has two asymmetric carbon centres. Thus, it can exist as three isomers, the *trans*-R,R, *trans*-S,S or *cis* isomers. An intriguing observation is that each of the platinum(II) complexes containing the different chiral structures exhibits markedly different anti-cancer activities. The *trans* isomers are generally considered to be more effective than the *cis* isomer, with the *trans*-R,R isomer being somewhat more effective than the *trans*-S,S isomer.[8,9] However, these differences are small and moderately dependent on both the *in vivo* tumour models employed and the leaving groups attached. For example, anti-tumour tests revealed that [Pt(*trans*-R,R-dach)Cl_2] was more active against Leukemia L1210 tumour cells implanted in mice. However, against an *in vivo* Sarcoma-180 murine tumour, [Pt(*cis*-R,S-dach)Cl_2] [9,10,11,12] is more active. Similarly, anti-tumour activity studies using isomers bearing either sulfate or cyclobutanedicarboxylate (CBDCA) as the leaving group show that the *trans*-R,R form of [Pt(dach)(SO_4)(H_2O)] was more effective against an L1210 tumour model than [Pt(*trans*-R,R-dach)(CBDCA)].[12]

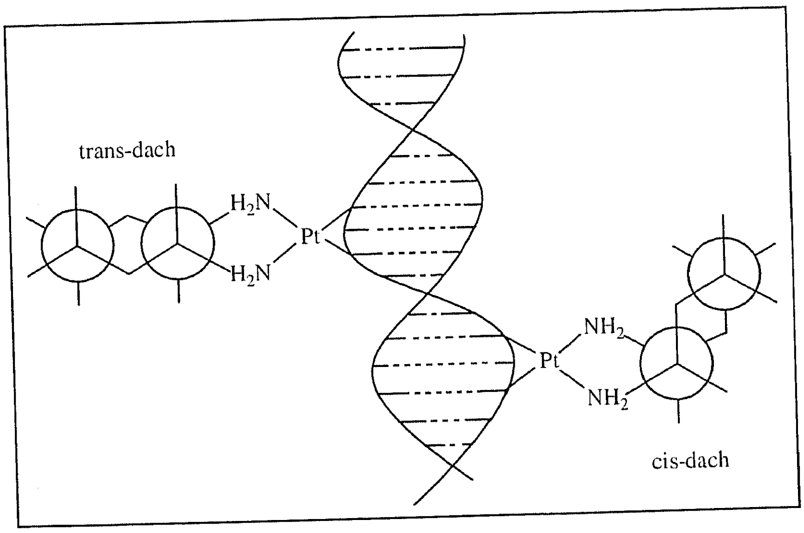

Diagram 3.2: Schematic diagram showing the orientation of the *cis*- and *trans*-dach ligand upon binding to DNA.[13]

The differences in biological activity between *trans* and *cis* isomers has been explained of in terms of the stability of the Pt-DNA adduct and/or the degree of distortion of the DNA. On formation of the most common type of adduct (ie binding at the N(7) position of two adjacent guanines) the cyclohexane ring is orientated perpendicular to the DNA helical axis in both the *trans* diastereomers and one of the *cis* diastereomers. In this arrangement there is only minor steric hindrance as the coplanarity of the dach-Pt complexes gives them easy access to the major grooves of the DNA allowing them to interact readily with the DNA bases. On the other hand, for one of the *cis* diastereomers, the cyclohexane ring is aligned almost parallel with the DNA axis (Diagram 3.2). In this conformation, the *cis*-R,S-dach-Pt adduct is not easily accommodated in the major groove due to steric hinderance and as a result would produce a significantly larger distortion of the DNA strand.[7,13]

Differences in anti-tumour activity also exist between the *trans*-dach-Pt isomers, and this isomeric difference may be modulated moderately by secondary hydrogen bonding interactions. Like cisplatin, for the *trans*-R,R-dach-Pt adduct, the axial amino proton is closer to the O(6) atom on the 5'-guanine. However, for the *trans*-S,S-dach-Pt adduct, the axial amino proton is closer to the O(6) on the 3'-guanine. Both hydrogen bonding interactions would stabilise the Pt-DNA adduct, but the degree of stabilisation is slightly different for the two diastereomeric forms.[7]

Oxaliplatin and ormaplatin (formerly called tetraplatin) are two examples of this dach-structural class that have been under clinical evaluation. Oxaliplatin is currently in phase II and III clinical trials.[14] Clinical data have shown that it is active against a variety of tumour models and is more potent *in vivo* than cisplatin.[15,16] The agent is less nephrotoxic than cisplatin and lacks auditory toxic effects.[14] The dose-limiting toxicity is peripheral neuropathy, however this neurologic toxicity is highly reversible, with the majority of patients experiencing a complete recovery within 4-8 months on cessation of oxaliplatin. Other toxicities are myelosuppression, nausea, vomiting and fever.[15,16] Ormaplatin, a structurally related complex, was also introduced to circumvent cisplatin tumour resistance. It is a platinum(IV) analogue that has reactive leaving groups on the Z axis. Cisplatin and carboplatin are platinum(II) analogues, with reactive leaving groups in the X and Y planes, not the Z axis. Clinically used ormaplatin is a mixture of the two *trans* stereoisomers. This racemic mixture was used because of only minor differences between the *trans*-R,R and *trans*-S,S isomers in relation to their solubility, stability and biological activity.

Unfortunately, it had to be withdrawn from clinical trials due to severe and dose-limiting peripheral neurotoxicty.[17,18]

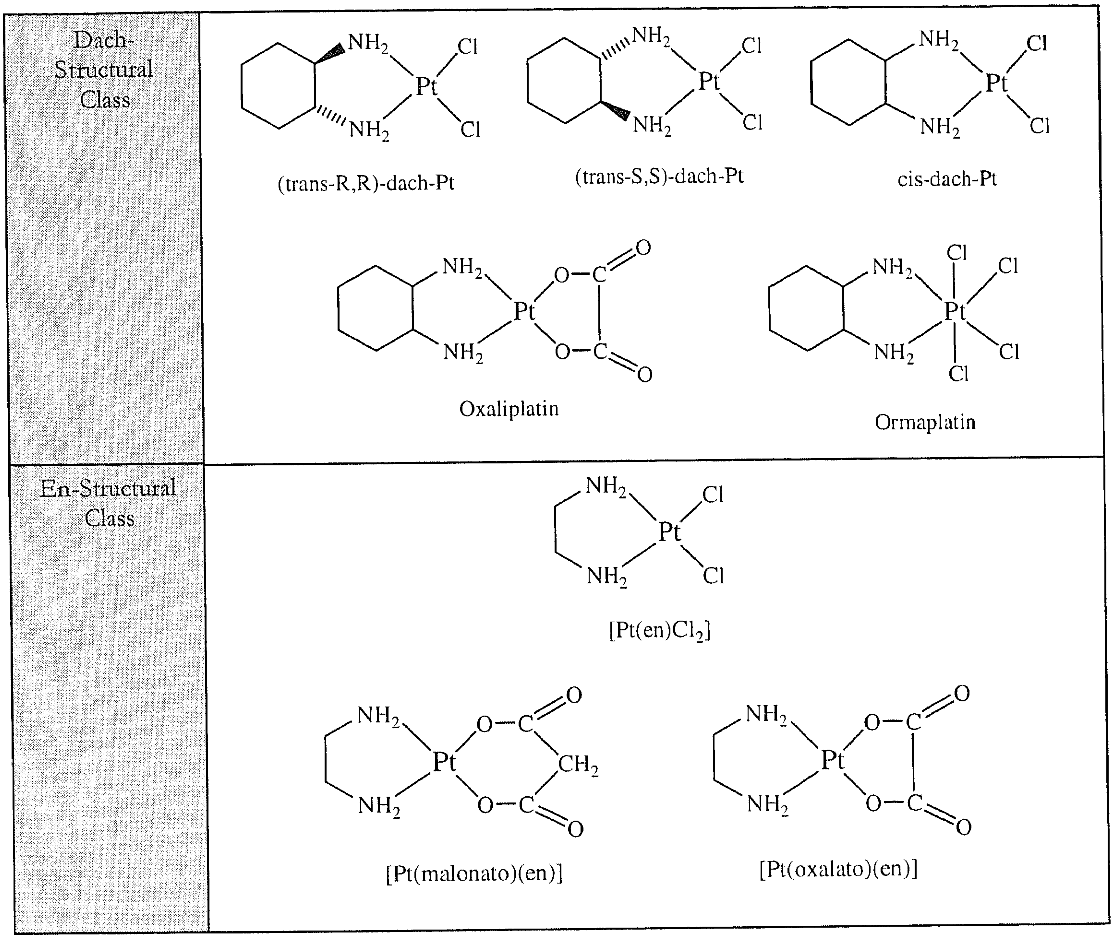

Diagram 3.3: Chemical structures of the common platinum compounds containing dach or en.

In addition to the dach-platinum complexes, agents containing ethylenediamine (en) also display favourable anti-tumour activity. Dichloro(ethylenediamine)platinum(II) ([Pt(en)Cl_2]) is one of the most famous examples. Following the success of [Pt(en)Cl_2] various derivatives were developed. [Pt(malonato)(en)] (JM-40, Diagram 3.3) showed higher activity than [Pt(en)Cl_2] and was introduced into clinical studies due to its favourable preclinical toxicity in dogs, being less emetic and less nephrotoxic than cisplatin.[19] However, in humans, where the maximum tolerated dose is much higher than for animals (c. f. Humans 1200 mg/m^2 with mouse 276 mg/m^2), the dose limiting toxicities were found to be nausea, vomiting and nephrotoxicity.[19] Nephrotoxicity is reversible in 4 weeks up to a dose level of 1200 mg/m^2. JM-40 did not exhibit any other dose related side-effects. Another compound is [Pt(oxalato)(en)], which unfortunately has extremely high neurological damage as the chief limiting toxicity.

Diamineplatinum(II) complexes with active dach or en non-leaving groups are required for subsequent experiments. For this reason effort was invested determining the best procedure for synthesising [Pt(en)Cl_2]. Ethylenediamine was the ligand of choice for these trials for it is relatively inexpensive compared to the dach isomers. Based on these experimental results the selected method will then be employed in the synthesis of the three different dach-Pt complexes. In selecting the synthesis of diamine complexes, three considerations were important. A method is desirable in which the sequence involves a small number of steps, the product is produced in a reasonably high yield and of high purity, preferably without the need of lengthy recrystallisation steps. Guided by these considerations, a number of experimental methods have been explored. The methods used to obtain [Pt(en)Cl_2] are outlined in Diagram 3.4.

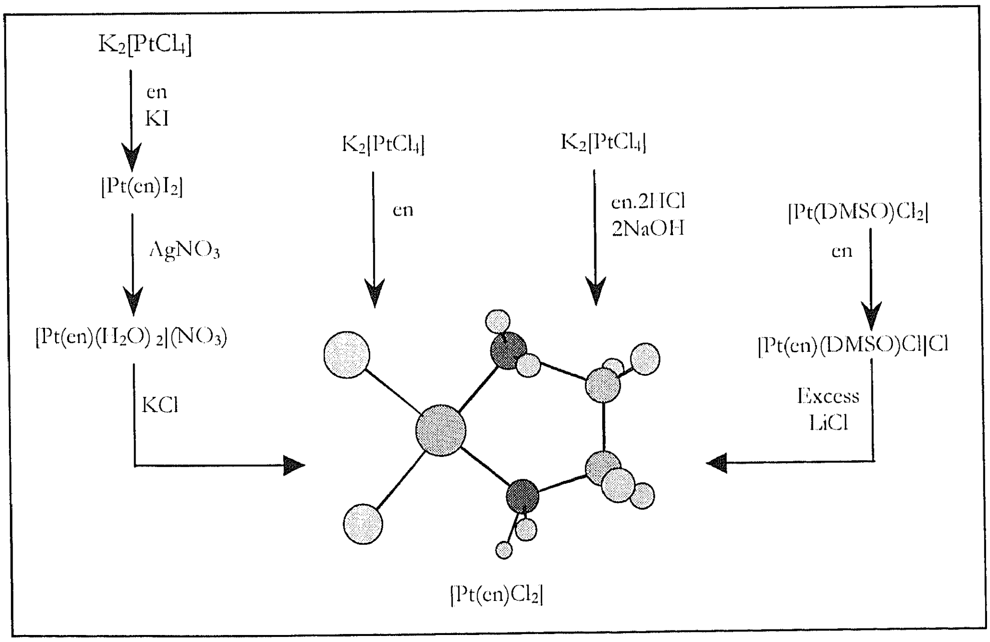

Diagram 3.4: The four different synthetic methods for the preparation of [Pt(en)Cl_2].

In this chapter, the synthetic details and characterisation of [Pt(en)Cl_2] and [Pt(dach)Cl_2] are presented. Two additional dach-related complexes, [Pt(diaminobenzoic acid)Cl_2] and [Pt(o-nitro-phenylenediamine)Cl_2] have also been synthesised and characterised.

Experimental

3.4 MATERIALS

o-Nitro-phenylenediamine (o-nitro-phen), 3,4-diaminobenzoic acid (dbn), ethylenediamine and its dihydrochloride were supplied by Aldrich and used without further purification. R,R, S,S and the *cis* forms of dach were also purchased from Aldrich. Potassium tetrachloroplatinate(II) (98%) was obtained from Johnson Matthey. All other reagents and solvents were purchased for Ajax Chemicals. [Pt(DMSO)$_2$$Cl_2$] was prepared by previously reported procedures.[20]

3.4 MEASUREMENTS

Elemental analyses of the platinum complexes were performed by the Microanalytical Unit, Australian National University (Canberra, ACT). Infrared spectra were obtained as nujol mulls on NaCl plates using a Biorad FTS-7 Fourier Transform spectrometer. NMR spectra were recorded on solutions in d_6-dimethylsulfoxide (d_6-DMSO) on a Varian Unity-Plus 300 spectrometer.

ESI mass spectra of [Pt(o-nitro-phen)Cl_2] and [Pt(dbn)Cl_2] were performed at the University of Wollongong on a VG-Quattro mass spectrometer. Each listed m/e value for the platinum-containing ions (which has more than one isotope) is the most intense peak of a cluster with an isotopic pattern in good agreement with the calculated pattern. Diagram 3.5 shows the expected isotopic pattern for an R-PtCl_2 and R-PtCl fragment where R is the diamine. Ethylenediamine and diaminocyclohexane complexes had insufficient solubility properties in appropriate solvents, thus no ESI mass spectra were obtained.

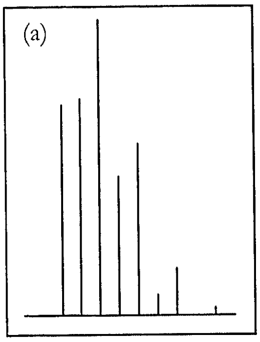

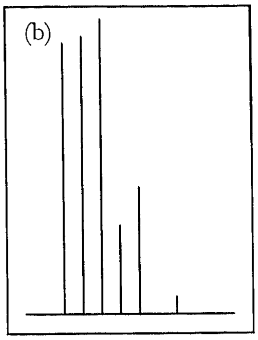

Diagram 3.5: Calculated isotopic pattern for (a) R-$PtCl_2$ and (b) R-PtCl where R is a diamine.

3.3 NOMENCLATURE

The nomenclature used to describe the various protons on the dach ligand has been adopted. This system is illustrated in Diagram below. In some cases axial and equatorial protons are indistinguishable and references are made simply to H^3, for example.

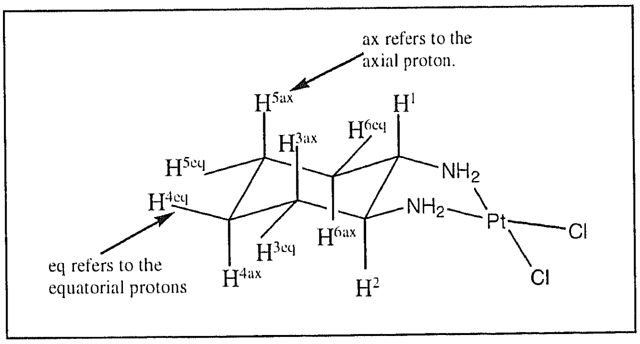

Diagram 3.6: Nomenclature used to describe the protons on dach.

3.4 SYNTHESIS OF PLATINUM COMPLEXES

Dichloro(ethylenediamine)platinum(II). [Pt(en)Cl_2].

Method A. [Pt(en)Cl_2] was initially synthesised by a slight modification of a published method.[21] A slight excess of ethylenediamine (93.8 mg, 1.57 mmol) was added to an aqueous solution of K_2[PtCl_4] (500 mg, 1.21 mmol). Precipitation of the desired [Pt(en)Cl_2] occurred on standing at room temperature. This precipitate was collected every 10-15 minutes to prevent further reaction. As the reaction progressed the period between collections was extended to 30-40 minutes. Whenever the product ceased to separate more ethylenediamine was added to the solution. Collection was continued until the solution becomes clear. The combined precipitates were washed with water, ethanol and ether, and suction dried for 10-15 minutes to give a yellow product.

Yield: 210 mg (53%)
Anal. Calcd for $C_2H_8N_2PtCl_2$ (326): C, 7.37; H, 2.47; N, 8.59. Found: C, 7.43; H, 2.49; N, 8.53. ^{1}H NMR (d_6-DMSO, ppm): δ = 2.56 (s, 2H). ^{13}C NMR (d_6-DMSO, ppm): δ = 47.6 (s, CH_2). IR (Nujol, cm^{-1}): 3273-3188 (br, ν(N-H)), 1557 (s, δ_s(N-H)).

Method B.

[Pt(en)Cl_2] was prepared by the method of Johnson[22], with the liquid ammonia recrystallisation step omitted. An aqueous solution (7 mL) of K_2[PtCl_4] (503 mg, 1.21 mmol) was mixed with a solution of ethylenediamine dihydrochloride (167 mg, 1.26 mmol) and heated on a water bath for 1 hour 45 minutes. During this time, the solution was kept constant at pH 6 by the dropwise addition of a solution of sodium hydroxide (113 mg, 2.75 mmol in 4 mL H_2O). It is worth noting that the addition of sodium hydroxide causes the pH to rise as free ethylenediamine is liberated from its hydrochloride and then slowly decreases as the ligand reacts with tetrachloroplatinum(II) ion. Care must be taken not to allow the solution to become more alkaline than pH 7, otherwise metallic platinum black forms. Mechanical stirring of the solution helped prevent the precipitation of platinum during the addition of base.

Yellow [Pt(en)Cl_2] precipitated out of solution before the addition of base was complete. The reaction was considered to be complete when the solution remained constant at pH 6. After cooling in ice water, the solid was filtered off, washed with cold water, ethanol and ether, and air-dried.

Yield: 268 mg (68%)
Anal. Calcd for $C_2H_8N_2PtCl_2$ (326): C, 7.37; H, 2.47; N, 8.59. Found: C, 7.27; H, 2.41; N, 8.63. ^{1}H NMR (d_6-DMSO, ppm): δ = 2.56 (s, 2H). ^{13}C NMR (d_6-DMSO, ppm): δ = 47.7 (s, CH_2). IR (Nujol, cm^{-1}): 3268-3194 (br, ν(N-H)), 1557 (s, δ_s(N-H)).

Method C.

[Pt(en)Cl_2] was synthesised by using an adaption of the Dhara method[23] for the preparation of cisplatin in which NH_3 is replaced by ethylendiamine. An aqueous solution (10 mL) of $K_2[PtCl_4]$ (500 mg, 1.21 mmol) was allowed to react with potassium iodide (1.63 g, 9.84 mmol) for 15 minutes at 25°C to yield $K_2[PtI_4]$. Ethylenediamine (70 mg, 1.21 mmol) was added and the dark yellow [Pt(en)I_2] was collected after 2 hours, washed with water and ethanol, and air-dried under vacuum. Typical yields are in excess of 74%.

The [Pt(en)I_2] (460 mg, 0.9 mmol) was suspended in water (20 mL) and added to a solution of silver nitrate (310 g, 1.7 mmol) in water (30 mL). The mixture was protected from light and heated on a water bath at 60°C for 10-15 minutes. The solution was taken off the water bath and stirred for an additional 2 hours. Insoluble AgI was removed by filtration and the filtrate was treated with an 10% excess of potassium chloride (relative to [Pt(en)$(H_2O)_2$]$(NO_3)_2$). The solution was heated on a water bath and within 5 minutes [Pt(en)Cl_2] began to precipitate out of solution. The heating was continued for 10 minutes for completion of the reaction. The mixture was cooled in an ice-bath for 24 hours, and the resulting yellow needles were filtered off, washed with water, ethanol and ether, and dried in air.

Yield: 655 mg (22.3% relative to [Pt(en)I_2])
Anal. Calcd for $C_2H_8N_2PtCl_2$ (326): C, 7.37; H, 2.47; N, 8.59. Found: C, 7.30; H, 2.33; N, 8.52. ^{1}H NMR (d_6-DMSO, ppm): δ = 2.54 (s, 2H). ^{13}C NMR (d_6-DMSO, ppm): δ = 47.7 (s, CH_2). IR (Nujol, cm^{-1}): 3279-3198 (br, ν(N-H)), 1556 (s, δ_s(N-H)).

Method D.

[Pt(en)Cl_2] was prepared by thermal decomposition of the ionic species [Pt(en)(DMSO)Cl]Cl as described in the literature.[24] A solution of ethylendiamine (60 mg, 1 mmol) in 10 mL of methanol was added to a suspension of [Pt(DMSO)$_2Cl_2$] (422 mg, 1 mmol) in 40 mL of methanol. The yellow mixture was stirred at room temperature until a clear solution was formed. The solution was cooled and filtered to remove a small amount of unreacted [Pt(DMSO)$_2Cl_2$]. The filtrate was reduced to 5 mL volume and diethyl ether was added to precipitate [Pt(en)(DMSO)Cl]Cl. This fine cream powder was filtered, washed with ether and air-dried. Typical yields were in excess of 90%.

A solution of [Pt(en)(DMSO)Cl]Cl (362 mg, 0.9 mmol) and lithium chloride (190 mg, 4.5 mmol) in water (16 mL) was placed in a small flask fitted with a reflux condenser. The mixture was heated at 70°C with stirring for 2 hours. The yellow solid that precipitated was filtered off, washed with water and dried in a vacuum desiccator over silica gel.

Yield: 60 mg (22%)
Anal. Calcd for $C_2H_8N_2PtCl_2$ (326): C, 7.37; H, 2.47; N, 8.59. Found: C, 7.46; H, 2.41; N, 8.52. ^{1}H NMR (d_6-DMSO, ppm): δ = 2.54 (s, 2H). ^{13}C NMR (d_6-DMSO, ppm): δ = 47.7 (s, CH_2). IR (Nujol, cm^{-1}): 3278-3199 (br, ν(N-H)), 1565 (s, δ_s(N-H)).

A second crop of product was gained by evaporating the filtrate. The yellow needles were filtered and recrystallised twice from hydrochloric acid (0.1 M).

Yield: 100 mg (36%)

Anal. Calcd for $C_2H_8N_2PtCl_2$ (326): C, 7.37; H, 2.47; N, 8.59. Found: C, 7.59; H, 2.52; N, 8.66. ^{1}H NMR (d_6-DMSO, ppm): $\delta = 2.55$ (s, 2H). ^{13}C NMR (d_6-DMSO, ppm): $\delta = 47.8$ (s, CH_2). IR (Nujol, cm^{-1}): 3275-3198 (br, ν(N-H), 1566 (s, δ_s(N-H)).

Dichloro(*cis*-R,S-1,2-diaminocyclohexane)platinum(II). [Pt(*cis*-R,S-dach)Cl_2].

An excess of *cis*-R,S-1,2-diaminocyclohexane (0.826 g, 7.233 mmol) was added to an aqueous solution of $K_2[PtCl_4]$ (0.5 g, 1.21 mmol). Precipitation of the desired [Pt(*cis*-R,S-dach)Cl_2] occurred on standing at room temperature. This precipitate was collected every 2-3 minutes to prevent any further reaction with the free ligand. As the reaction progressed the time interval between collections was increased to 12-15 minutes. Collection was continued until the solution was clear and the product ceased to separate. The combined precipitates were then washed with water, ethanol, ether and suction dried for 15 minutes to give fine cream coloured needles.

Yield: 250 mg (57%)

Anal. Calcd for $C_6H_{14}N_2PtCl_2$ (380): C, 18.95; H, 3.68; N, 7.37. Found: C, 18.74; H, 3.67; N, 7.21. ^{1}H NMR (d_6-DMSO, ppm): $\delta = 2.9, 2.57$ (2 x s, 2 x ($H^1 + H^2$)), 1.77, 1.66 (2 x s, 2 x ($H^3 + H^6$)), 1.30, 1.14 (2 x s, 2 x ($H^4 + H^5$)). ^{13}C NMR (d_6-DMSO, ppm): $\delta = 58.18, 57.84$ (2 x s, 2 x α-CH), 58.97, 57.26 (2 x s, 2 x β-CH), 25.77, 25.64 (2 x s, 2 x (γ-CH_2 + ζ-CH_2)), 21.14, 19.77 (2 x s, 2 x (δ-CH_2 + ε-CH_2)). IR (Nujol, cm^{-1}): 3250-3180 (br, ν(N-H)), 1566 (s, δ_s(N-H)).

Dichloro(*trans*-R,R-1,2-diaminocyclohexane)platinum(II). [Pt(*trans*-R,R-dach)Cl_2].

Trans-R,R-1,2-diaminocyclohexane (0.275 g, 2.41 mmol) dissolved in water (15 mL) was added dropwise to an aqueous solution of $K_2[PtCl_4]$ (1.0 g, 2.41 mmol). After 1 hour, the yellow solid that had precipitated out of solution was filtered, washed with water, ethanol, ether and air-dried.

Yield: 518 mg (57%)

Anal. Calcd for $C_6H_{14}N_2PtCl_2$ (380): C, 18.95; H, 3.68; N, 7.37. Found: C, 18.90; H, 3.64; N, 7.48. ^{1}H NMR (d_6-DMSO, ppm): $\delta = 2.11$ (m, $H^1 + H^2$), 1.83 (m, $H^{3eq} + H^{6eq}$), 1.42 (m, $H^{3ax} + H^{6ax}$), 1.20 (m, H^{4eq} + H^{5eq}), 0.94 (m, H^{4ax} + H^{5ax}). ^{13}C NMR (d_6-DMSO, ppm): δ = 62.8 (s, α-CH + β-CH), 31.5 (s, γ-CH_2 + ζ-CH_2), 24.3 (s, δ-CH_2 + ε-CH_2). IR (Nujol, cm^{-1}): 3254-3174 (br, ν(N-H)), 1564 (s, δ_s(N-H)).

Dichloro(*trans*-S,S-1,2-diaminocyclohexane)platinum(II). [Pt(*trans*-S,S-dach)Cl_2].

Pt(*trans*-S,S-dach)Cl_2] was synthesised in a manner identical to that described for [Pt(*trans*-R,R-dach)Cl_2], using 0.275 g (2.41 mmol) of *trans*-S,S-1,2-diaminocyclohexane and 1.0 g (2.41 mmol) of $K_2[PtCl_4]$.

Yield: 370 mg (40%)

Anal. Calcd for $C_6H_{14}N_2PtCl_2$ (380): C, 18.95; H, 3.68; N, 7.37. Found: C, 18.76; H, 3.80; N, 7.36. ^{1}H NMR (d_6-DMSO, ppm): δ = 2.11 (m, H^1 + H^2), 1.83 (m, H^{3eq} + H^{6eq}), 1.42 (m, H^{3ax} + H^{6ax}), 1.20 (m, H^{4eq} + H^{5eq}), 0.94 (m, H^{4ax} + H^{5ax}). ^{13}C NMR (d_6-DMSO, ppm): δ = 62.8 (s, α-CH + β-CH), 31.5 (s, γ-CH_2 + ζ-CH_2), 24.3 (s, δ-CH_2 + ε-CH_2). IR (Nujol, cm^{-1}): 3254-3174 (br, ν(N-H)), 1564 (s, δ_s(N-H)).

Dichloro(3,4-diaminobenzoic acid)platinum(II). [Pt(dbn)Cl_2]

An aqueous solution (10 mL) of $K_2[PtCl_4]$ (500 mg, 1.21 mmol) in was allowed to react with potassium iodide (1.63 g, 9.84 mmol) for 15 minutes at 25°C to yield $K_2[PtI_4]$. 3,4-Diaminobenzoic acid (184 mg, 1.21 mmol) was added and the dark brown [Pt(dbn)I_2] was collected after 24 hours.

The [Pt(dbn)I_2] (652 mg, 1.09 mmol) was suspended in water (25 mL) and added to a solution of silver nitrate (327 mg, 2.2 mmol) in water (25 mL). The mixture was protected from light and heated on a water bath at 60°C for 10-15 minutes. The solution was taken off the water bath and stirred for an additional 24 hours. Insoluble AgI was filtered off and the filtrate was treated with an 10% excess of potassium chloride (relative to [Pt(dbn)$(H_2O)_2](NO_3)_2$). The solution was heated on a water bath for 15 minutes. The mixture was cooled in an ice-bath for 24 hours, and then evaporated to about 2 mL in a vacuum desiccator over P_2O_5. The dark precipitate was filtered and air-dried.

Yield: 160 mg (35% relative to [Pt(dbn)I_2])

Anal. Calcd for $C_7H_8N_2O_2PtCl_2$ (418): C, 20.10; H, 1.91; N, 6.70. Found: C, 20.14; H, 1.98; N, 6.63. ^1H NMR (d_6-DMSO, ppm): δ = 7.26 (d, J_{23} = 7.9 Hz, H^3), 7.74 (s, H^1), 7.83 (d, H^2). ^{13}C NMR (d_6-DMSO, ppm): δ = 126.3 (s, ε-CH), 127.0 (s, γ-CH), 128.2 (s, ε-CH), 130.0 (s, δ-C), 143.9 (s, β-C), 148.0 (s, α-C), 166.0 (s, COOH). ESI-MS: m/e = 417 (100%, $C_7H_7N_2O_2PtCl_2$), 382 (14, $C_7H_7N_2O_2PtCl$). IR (Nujol, cm^{-1}): 3318-3074 (br, ν(N-H)), 1625 (s, C=O).

Dichloro(o-nitro-phenylenediamine)platinum(II). [Pt(o-nitro-phen)Cl_2]

K_2PtCl_4 (415 mg, 1 mmol) was dissolved in a 1:1 mixture of DMF/H_2O (200 mL) and a suspension of o-nitro-phenylenediamine (153 mg, 1 mmol) in DMF/H_2O (200 mL) was added. The mixture was protected from light and stirred at room temperature for 3 days. After this period, the brown precipitate that formed was removed by filtration and air-dried.

Yield: 59 mg (12%)

Anal. Calcd for $C_6H_7N_3O_2PtCl_2$ .HCON$(CH_3)_2$ (492): C, 21.95; H, 2.85; N, 11.38. Found: C, 22.38; H, 2.68; N, 11.95. ^1H NMR (d_6-DMSO, ppm): δ = 7.39 (d, J_{23} = 13.2 Hz, H^3), 7.88 (d, J_{12} = 3.6 Hz, H^1), 8.08 (q, H^2). ^{13}C NMR (d_6-DMSO, ppm): δ = 112.5 (s, γ-CH), 117.9 (s, ε-CH), 122.8 (s, ζ-CH), 146.2 (s, β-C), 148.1 (s, δ-C), 150.3 (s, α-C). ESI-MS: m/e = 418 (100%, $C_6H_6N_3O_2PtCl_2$), 382 (14, $C_6H_6N_3O_2PtCl$), 301 (6, $C_6H_6N_2PtCl$). IR (Nujol, cm^{-1}): 3391-3329 (br, ν(N-H)), 1607 (s, δ_s(N-H)), 1515 (s, ν_{as}(NO)), 1333 (s, ν_s(NO)).

Results and Discussion

3.5 DICHLORO(ETHYLENEDIAMINE)PLATIMUN(II) COMPLEXES

Synthetic Strategies

[Pt(en)Cl_2] was prepared and described as early as 1950 by Basolo, Bailar and Tarr[21] who synthesised the compound by slow addition of a 5% solution of ethylenediamine to a cold aqueous solution of potassium tetrachloroplatinate. This method is very time-consuming and only produces yields of up to 45-55%. Contrary to some published opinion,[22] the product obtained is of high purity, provided the precipitated $[Pt(en)Cl_2]$ is filtered at short intervals to prevent any further reaction.

In an alternative approach, Johnson[22] has produced $[Pt(en)Cl_2]$ in yields of up to 68%. The preparation involves the liberation of free ethylenediamine from its dihydrochloride by the addition of sodium hydroxide. The ligand then reacts with tetrachloroplatinate(II) to give $[Pt(en)Cl_2]$ and the chief by-product of the reaction, $[Pt(en)_2][PtCl_4]$ (Magnus salt). The author then describes the purification of the crude $[Pt(en)Cl_2]$ by recrystallisation in liquid ammonia. However, purification in liquid ammonia proved problematic for ammonia could exchange with the chloro ligands during evaporation of the solvent to produce a bisammine species (namely $[Pt(en)(NH_3)_2]^{2+}$). The ammonia recrystallisation step was eliminated from subsequent preparations using this method. Microanalysis results of the yellow product gained from the modified preparation were within the acceptable limits.

In a later paper,[23] the authors suggest that the formation of a Magnus salt by-product could be completely avoided by controlling the chloride ion concentration. By a modification of the preparation for the synthesis of $[Pt(NH_3)_2Cl_2]$, the equivalent en complex can be prepared according to the following reaction sequence.

$$K_2[PtCl_4] + 4KI + en \longrightarrow [Pt(en)I_2] + 2KI + 4KCl$$

$$[Pt(en)I_2] + 2AgNO_3 \xrightarrow{H_2O} [Pt(en)(H_2O)_2](NO_3)_2 + 2AgI$$

$$[Pt(en)(H_2O)_2](NO_3)_2 + 2KCl \longrightarrow [Pt(en)Cl_2] + 2KNO_3 + 2H_2O$$

This preparation only produces $[Pt(en)Cl_2]$ in yields of up to 20%. Together with the fact that this approach requires a large number of steps compared to the other experimental procedures, this method is not considered as a viable method for the synthesis of large amounts of [Pt(en)Cl_2].

Table 3.1: Yields and Microanalytical results for [Pt(en)Cl_2]

Synthetic Method[a]	Yield (%)	Microanalytical Results [b]		
		Carbon	Hydrogen	Nitrogen
Method A	53	7.43	2.49	8.53
Method B	68	7.27	2.41	8.63
Method C	22	7.30	2.33	8.52
Method D[c]	22	7.46	2.41	8.36
	36	7.29	2.43	8.11

[a] Synthetic methods A, B, C and D: refer to experimental section
[b] Calculated Values: C, 7.37; H, 2.47; N, 8.59.
[c] Two crops of product were obtained from this method.

Finally the method of Coluccia, Giordano, Loseto, Intini, Maresca and Natile[24] was used to prepare [Pt(en)Cl_2]. Unlike the previous synthetic methods, the starting material is [Pt(DMSO)$_2$$Cl_2$] not K_2[PtCl_4]. The procedure is based on two key steps; an initial reaction between [Pt(DMSO)$_2$$Cl_2$] and en to give [Pt(DMSO)(en)Cl]. Secondly the intermediate species undergoes thermal decomposition with lithium chloride producing the desired product in yields of up to a total of 58%. Despite this reasonably high yield, the second precipitate needed recrystallising twice to reach a suitable level of purity.

The purity of the products gained by each of the different methods cannot be measured solely by the microanalytical results. This is because the [Pt(en)$_2$][PtCl_4] salt will analyse the same as [Pt(en)Cl_2]. However, a major physical difference between the two compounds is their colouration. [Pt(en)$_2$][PtCl_4] salts are violet in colour indicating some cation-anion electronic interactions[25] whilst [Pt(en)Cl_2] is yellow. Since no violet coloured contaminant was visable in any of the products the microanalytical results listed in Table 3.1 can be regarded as [Pt(en)Cl_2]. In addition, conductivity measurements were performed in order to verify the neutrality of the compounds. Molar conductivities were recorded for 1mM aqueous solutions of the products immediately after the solutions were prepared. All products were found to have molar conductivities ranging from 18-21 cm^{-1} mol^{-1} Ω^{-1}. These results fall well below the 118-131 cm^{-1} mol^{-1} Ω^{-1} range expected for a 1:1 electrolyte.[26] Thus, the products are neutral in solution. The NMR and IR spectra of all the products are also in accord with the formation of the desired $[Pt(en)Cl_2]$ complexes. These spectral studies are discussed below.

Overall, the simple one-step method of Basolo et al. and the alternative method of Johnson were recognised as the most effective methods for the formation of analytically pure $[Pt(en)Cl_2]$. Yields and the microanalytical results for each of the methods evaluated are summarised in Table 3.1.

Spectral Studies

All methods produced the desired $[Pt(en)Cl_2]$ complex. Characterisation by infrared was very simple, for ethylenediamine complexes have strong absorptions in the region of 3300-3100 cm^{-1}, which can be assigned to the N-H stretching vibrations (ν(N-H)). This occured at a lower frequency than the corresponding vibrations in the free ligand and is consistent with the formation of the platinum-nitrogen bond. These N-H vibrations are relatively sharp and rather complex in terms of splitting. Instead of displaying the two bands expected from asymmetrical and symmetrical stretching in the amine groups, the infrared showed three peaks with an additional shoulder on the low frequency side (Diagram 3.7). The presence of the third band may be influenced by intramolecular hydrogen bonding, whilst the shoulder arises from Fermi interactions between the stretching modes and the overtones of the N-H bending modes (δ_s(N-H)).[27] The N-H bending (scissoring) vibrations were observed in the 1570-1550 cm^{-1} region of the spectra. IR data is summarised in Table 3.2.

Since $[Pt(en)Cl_2]$ is only sparingly soluble in water, the NMR spectra of the ethylenediamine platinum(II) complexes were obtained in d_6-DMSO. The NMR spectra were also straightforward in that there is the usual single resonance around 2.56 ppm in the ^1H NMR and at 47.6 ppm in the ^{13}C NMR, due to the equivalent methine protons.

Table 3.2: Infrared data.

Complex	Infrared Band (cm^{-1})		
	ν(N-H)	Fermi Resonance Band	δ_s(N-H)
$[Pt(en)Cl_2]$			
Method A	3273-3188	3112	1557
B	3268-3194	3107	1557
C	3279-3198	3112	1556
D	3278-3199	3108	1565
	3275-3198	3115	1566
$[Pt(trans\text{-}R,R\text{-}dach)Cl_2]$	3254-3174	3106	1564
$[Pt(trans\text{-}S,S\text{-}dach)Cl_2]$	3254-3174	3106	1564
Isomeric mixture	3250-3180	3109	1566

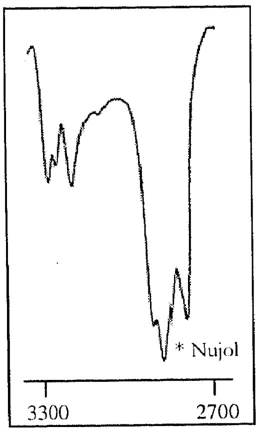

Diagram 3.7: IR spectrum of $[Pt(en)Cl_2]$ as a nujol mull.

3.6 DICHLORO(DIAMINOCYCLOHEXANE)PLATINUM(II) COMPLEXES

NMR Data

Examination of the ^{13}C NMR spectrum of $Pt(\textit{cis}\text{-}R,S\text{-}dach)Cl_2$ shows that the number of ^{13}C resonances observed is twice that expected for a single dach complex. This indicates the coexistence of two conformers. When the same reaction is carried out with *trans*-R,R-dach or *trans*-S,S-dach, the ^{13}C NMR spectra disclose that only one conformer is present. This result is consistent with the fact that the five-membered chelate ring in the R,S-configured dach complex can adopt λ or δ conformations, which can easily interconvert. A schematic drawing of these conformations is depicted in Diagram 3.8. This structural property sharply contrasts with that of the enantiomeric pair $Pt(\textit{trans}\text{-}R,R\text{-}dach)Cl_2$ and $Pt(\textit{trans}\text{-}S,S\text{-}dach)Cl_2$, where the dach, on complexation, yields rigid structures that do not allow facile interconversion between λ and δ conformations. Instead the *trans*-R,R and *trans*-S,S-configured chelates exist exclusively in the energetically favoured λ and δ conformations, respectively.

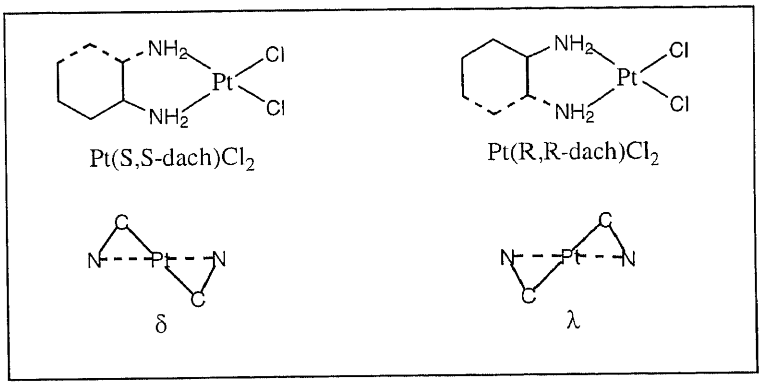

Diagram 3.8: The λ and δ conformations of *trans*-dach complexes.

The [1]H NMR of Pt(*trans*-R,R-dach)Cl_2 and Pt(*trans*-S,S-dach)Cl_2 were essentially the same, each giving five broad peaks corresponding to the ten protons of the cyclohexane ring. This similarity was to be expected, for Pt(*trans*-R,R-dach)Cl_2 and Pt(*trans*-S,S-dach)Cl_2 are optical isomers and the NMR technique cannot discriminate between the isomers. Table 3.3 shows the chemical shift data for the Pt(*trans*-R,R/S,S-dach)Cl_2 compounds. The H^1 and H^2 protons of the dach ring are equivalent because both the isomers have a C_2 axis through the platinum and the middle of the two-chloro groups. Furthermore, the presence of the fixed cyclohexane and chelate rings means that the axial and equatorial protons of the cyclohexane ring are non-equivalent, thus displaying different chemical shifts.

In the spectrum of Pt(*cis*-R,S-dach)Cl_2, six broad resonance peaks are observed, three of which are at a considerably lower intensity. Like the ^{13}C NMR spectrum, the ^1H NMR spectrum of Pt(*cis*-R,S-dach)Cl_2 is expected to display resonances due to both to λ and δ conformations. Inversion between the two λ and δ conformations alone does not result in the observed resonances. It is most likely that the observed peaks are the result of the inversion of the 5-

membered chelate ring (λ and δ) coupled to the inversion of the cyclohexane ring into a chair or boat-type arrangement. Structures of the four possible conformations are shown in Diagram 3.9.

Table 3.3: ^{1}H and ^{13}C NMR data for the dach complexes.[a]

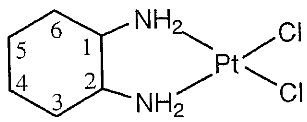

Position	^{13}C NMR			^{1}H NMR		
	2a or 2b[b]	1a or 1b[b]	R,R and S,S[c]	2a or 2b	1a or 1b	R,R and S,S[c]
1,2	58.18, 58.97	57.84, 57.26	62.8	2.90	2.57	2.10
3, 6	25.77	25.64	31.5	1.77	1.66	1.83 ($H^{3eq} + H^{6eq}$) 1.42 ($H^{3ax} + H^{6ax}$)
4, 5	21.14	19.77	24.3	1.31	1.14	1.20 ($H^{4eq} + H^{5eq}$) 0.94 ($H^{4ax} + H^{5ax}$)

[a] Values in ppm. [b] Refer to Diagram 3.6 for schematic structures of 1a, 1b, 2a and 2b.
[c] Refers to [Pt(*trans*-R,R-dach)Cl_2] and [Pt(*trans*-S,S-dach)Cl_2]

It is unknown as to which peaks in the ^{1}H NMR spectrum correspond to which conformation. The spectrum does however, reveal that the three resonance peaks at 2.90, 1.77 and 1.31 ppm have half-height widths larger than the remaining peaks, suggesting that the rate of inversion between λ and δ conformations is relatively slow. Inspection of molecular models reveal that the structures containing a boat arrangement (2a and 2b) seem to be more sterically crowded compared to the other conformations. This is likely to slow the inversion rate and may lead to an increase of the half-height width of the cyclohexane ring protons. By contrast the conformations featuring the cyclohexane ring in a chair-type arrangement (1a and 1b) have no unfavourable interactions between the chelate ring and the H^5 proton on the cyclohexane ring. Thus making them the more thermodynamically stable and in turn may lead to an increase in the rate of interconversion between λ and δ conformations. On the basis of this consideration, it is reasonable to assign the peaks at 2.90, 1.77 and 1.31 ppm to conformation 2a and/or 2b, thus the peaks at 2.57, 1.66, and 1.31 ppm are due to conformation 1a and/or 1b. Further support for the existence of two distereomers comes from the appearance of four NH_2 resonances at 6.23, 5.66, 5.30 and 4.90 ppm in the spectrum of Pt(*cis*-R,S-dach)Cl_2. In contrast, the spectra of Pt(*trans*-R,R-dach)Cl_2 and Pt(*trans*-S,S-dach)Cl_2 show only two peaks due to the NH_2 groups. Selected chemical shift data appear in Table 3.3. Coupling constants can be found in the Experimental Section under the individual complexes.

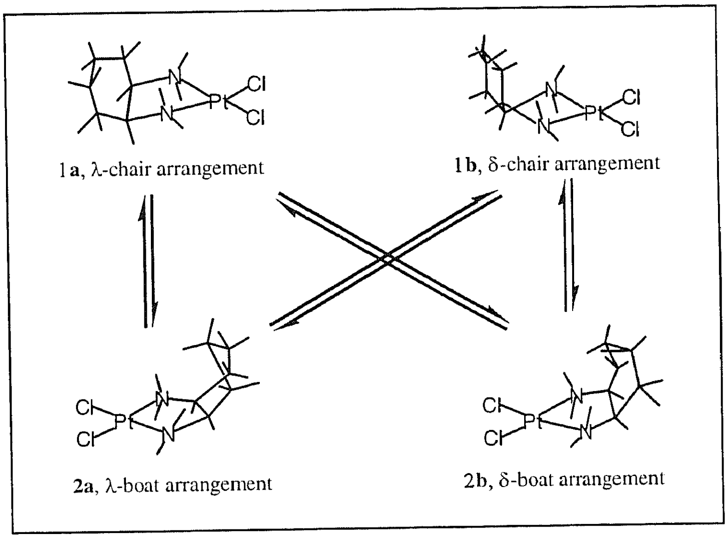

Diagram 3.9: Schematic drawings of the conformations of coordinated *cis*-dach.

Infrared Data

Infrared measurements made on the three distereomers show the characteristic bands around 3246 cm^{-1} and 3182 cm^{-1} assigned to asymmetric and symmetric N-H stretching vibrations respectively. The N-H bending vibrations of the products appear around 1566 cm^{-1}. This band is moved to slightly higher frequencies compared to the free ligand. The shoulder on the low frequency side of the N-H stretching band seems to be due to Fermi resonance with the overtone of band at 1566 cm^{-1}. Infrared data for the optically active and meso forms of the compounds is displayed in Table 3.2.

3.6 OTHER RELATED PLATINUM COMPLEXES

$[Pt(dbn)Cl_2]$ and $[Pt(o\text{-nitro-phen})Cl_2]$ which are structurally related to the previously mentioned dach complexes were prepared and characterised by mass spectrometry and NMR spectral studies. Diagram 3.10 illustrates the nomenclature used to describe the individual protons and carbons in the two substituted benzenes.

$[Pt(o\text{-nitro-phen})Cl_2]$ was prepared by a simple reaction between $K_2[PtCl_4]$ and o-nitro-phenylenediamine. Surprisingly, attempted synthesis of $[Pt(dbn)Cl_2]$ by a similar reaction with $K_2[PtCl_4]$ was unsuccessful. Instead an adaptation of the Dhara method was used to give $[Pt(dbn)Cl_2]$ in 35% yield.

NMR Spectral Studies

Coupling interactions among nuclei are transmitted via the spins of electrons in the intervening bonds. Four or five bond couplings are rare in saturated compounds but they do arise in π-bonded systems such as aromatic rings.[28] This long range coupling is observed in the ^1H NMR spectra of 3,4-diaminobenzoic acid, o-nitro-phenylenediamine and its corresponding platinum complex.

Table 3.4: ^1H NMR data for $[Pt(dbn)Cl_2]$ and $[Pt(o\text{-nitro-phen})Cl_2]$

	Chemical Shifts (ppm)			Coupling Constants (Hz)	
Compound	H^1	H^2	H^3	$^3J_{23}$	$^4J_{12}$
dbn	7.13	7.06	6.49	8.1	2.0
$[Pt(dbn)Cl_2]$	7.74	7.83	7.26	7.9	-
o-nitro-phen	7.40	7.38	6.52	8.4	2.7
$[Pt(o\text{-nitro-phen})Cl_2]$	7.88	8.08	7.39	13.2	3.6

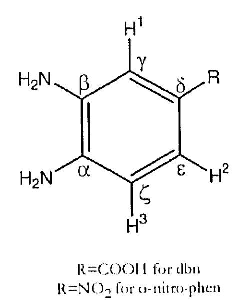

Diagram 3.10: Proton and carbon labelling scheme.

The ^{1}H NMR spectrum of o-nitro-phenylenediamine shows a doublet of doublets at 7.38 ppm due to H^{2} and two doublets at 7.40 and 6.52 ppm due to H^{1} and H^{3} respectively. In addition, the signals for the amine protons are found at 6.0 and 5.0 ppm. The splitting patterns reveal a $^{4}J_{12}$ coupling constant of 2.7 Hz, which was verified by simulation. In substituted benzenes, the meta coupling constant is listed as being between 2-3 Hz.[28] Thus a $^{4}J_{12}$ coupling constant of 2.7 Hz lies within the characteristic range.

As expected the ^{1}H NMR of [Pt(o-nitro-phen)Cl_2] was similar to that of the free ligand. Assignments are given in Table 3.4. It should be pointed out that all three resonances have moved considerably downfield on complexation and the $^{4}J_{12}$ coupling constant is larger than 3 Hz.

In similar experiments with diaminobenzoic acid, the ^{1}H NMR shows a doublet of doublets at 7.06 ppm due to H^{2} and two doublets at 7.13 and 6.49 ppm due to H^{1} and H^{3} respectively with a $^{4}J_{12}$ coupling constant of 2.0 Hz. Although, in principle, the long range coupling observed in the ^{1}H NMR of diaminobenzoic acid might be expected to occur in the NMR of [Pt(dbn)Cl_2], no measurable splitting was observed. This is probably due to line broadening of the proton signals. The absence of measurable long range coupling in the ^{1}H NMR spectrum of [Pt(dbn)Cl_2] simply reduces the spectrum to a singlet at 7.74 ppm due to H^{1} and two doublets at 7.83 and 7.26 ppm due to H^{2} and H^{3} respectively. The ^{1}H NMR chemical shifts of both [Pt(dbn)Cl_2] and its metal free ligand are summarised in Table 3.4. A comparison of the spectral data revealed downfield shifts of around 0.6-0.9 ppm when platinum coordination occurs.

[Pt(o-nitro-phen)Cl_2] and [Pt(dbn)Cl_2] were also characterised using ^{13}C NMR spectroscopy. The ^{13}C-assignments were straightforward and do not merit special comment. Details can be found in the Experimental Section.

Mass Spectra

The proposed structures were confirmed by ESI-mass spectroscopy. The mass spectrum of [Pt(o-nitro-phen)Cl_2] shows a molecular ion peak of $[C_6H_7N_3O_2PtCl_2 - H]^+$ at m/e=418 and a signal at m/e = 382 due to the loss of one chlorine. The spectrum also shows a very small signal at 6% base height at 301 probably due to the fragment $[M^+ - Cl_2NO_2]$.

The mass spectrum of [Pt(dbn)Cl_2] shows a molecular ion peak of $[C_7H_8N_2O_2PtCl_2 - H]^+$ at m/e=417 and a signal at m/e = 382 due to the loss of one chlorine. All isotopic pattern clusters are in agreement with the calculated pattern (Refer to Experimental Section).

References

1 J. Reedijk, Inorganica Chimica Acta, 1992, **198-200**, 873-881

2 D. Kiser, F. P. Intini, Y. Xu, G. Natile and L. G. Marzilli, Inorg. Chem., 1994, **33**, 4149-4158.

3 A. Eastman, Biochemistry, 1986, **25**, 3912.

4 A. Pasini and F. Zunino, Angew. Chem. Int. Ed. Engl., 1987, **26**, 615-624.

5 S. J. Berners-Price, J. Amer. Chem. Soc., 1993, **115**, 8649-8659 and references within.

6 M. Alink, H. Nakahara, K. Inagaki, M. Nakanshi, Y. Kidani and J. Reedijk, Inorg. Chem., 1991, **30**, 1236-1241.

7 S. G. Chaney, International Journal of Oncology, 1995, **6**, 1291-1305.

8 M. M. Jennerwein, A. Eastman and A. R. Khokhar, Mutation Research, 1991, **254**, 89-96.

9 J. F. Vollano, S. Al-Baker, J. C. Dabrowaik and J. E. Schurig, J. Med. Chem., 1987, **30**, 716-719.

10 Y. Kidani, K. Inagaki, R. Saito and S. Tsukagoshi, J. Clin. Hem. Oncol., 1977, **7**, 197.

11 Y. Kidani, K. Inagaki, M. Ligo, A. Hoshi and K. Kuretani, J. Med. Chem., 1978, **21**, 1315.

12 Z. H. Siddik, S. Al-Baker, T. L. Burditt and A. R. Khokhar, J. Cancer Res. Clin. Oncol., 1993, **120**, 12-16.

13 M. Noji, K. Okamoto and Y. Kidani, J. Med. Chem., 1981, **24**, 508-515.

14 P. Challet, M. A. Bensmaire, S. Brienza, C. Deloche, H. Cure, H. Caillet and E. Cvitkovic, Annals of Oncology, 1996, **7**, 1065-1070.

15 R. B. Weiss and M. C. Christian, Drugs, 1993, **46**, 360-377.

16 M. Gosland, B. Lum, J. Schimelpfennig, J. Baker and M. Doukas, Pharmacotherapy, 1996, **16**, 17-39.

17 D. Screnci, H. M. Er, T. W. Hambley, P. Galettis, W. Brouwer and M. J. McKeage, Br. J. Cancer, 1997, **76**, 502-510.

18 M. J. McKeage, Drug Safety, 1995, 1995, **13**, 228-244.

19 B. Winograd, J. B. Vermorken, W. W. ten Bokkel Huinink, G. Simonetti, H. E. Gall, M. K. Tish Knobf, W. J. F. van der Vijgh, J. G. McVie and H. M. Pinedo, Cancer Research, 1986, **46**, 2148-2151.

20 J. H. Price, A. N. Williamson, R. F. Schramm and B. B. Wayland, Inorg. Chem., 1972, **11**, 1280.

21 F. Basolo, J. C. Bailar and B. R. Tarr, J. Amer. Chem. Soc., 1950, **72**, 2433.

22 G. L. Johnson, Inorg. Synth, 1963, **7**, 242.

23 S. C. Dhara, Indian J. Chem., 1970, **8**, 193.

24 M. Coluccia, D. Giordano, F. Loseto, F. P. Intini, L. Maresca and G. Natile, Anticancer Research, 1989, **9**, 795-798.

25 T. G. Appleton and Hall, J. R. Inorg. Chem., 1972, **11**, 112-117.

26 Z. Szafran, R. M. Pike and M. M. Singh, Microscale Inorganic Chemistry-A Comprehensive Laboratory Experience, John Wiley and Sons, New York, 1991, pp. 102-105.

27 R. M. Silverstein, G. C. Bassler and T. C. Morrill, Spectroscopic Identification of Organic Compounds 4th ed., Wiley, New York, 1981, pp. 95-180.

28 W. Kemp, NMR in Chemistry: A Multinuclear Introduction, Macmillan Education LTD, London, 1986, pp. 65-70.

CHAPTER

4

AMMINE/DIAMINE PLATINUM(II) COMPLEXES WITH AMINO ACIDS AS LEAVING GROUPS

Introduction

Cisplatin and carboplatin are the most commonly used drugs in cancer chemotherapy. Their therapeutic efficacy, however, is limited by the emergence of drug resistance. Thus, one of the key selection criterion for the clinical development of a third generation platinum complex is based upon the ability of an agent to overcome cisplatin and/or carboplatin resistance.

As described in the previous chapter, it was the potential ability of platinum(1,2-diaminocyclohexane)complexes to overcome cisplatin-resistance in tumour cells that led to their clinical development. With the exception of oxaliplatin and ormaplatin, many complexes incorporating the various forms of the dach ligand were impeded by low aqueous solubility and molecular instability. In an attempt to redress these problems, work is now directed toward the synthesis of a series of derivatives incorporating amino acids with the aim of improving both the anti-tumour and solubility properties of the original diamine complexes. This class of chelate complexes are mainly of the type [Pt(amac)(A)]Cl where amac represents one of the selected amino acids and A signifies a 1,2-dach ligand (*cis*-, *trans*-R,R- or *trans*-*S*,*S*-), ethylenediamine or two ammonia groups.

Experimental

4.1 MATERIALS

All reagents were purchased from Aldrich. The $[Pt(amac\text{-}N,O)Cl_2]^-$ starting materials were prepared by reaction of the free amino acids with $K_2[PtCl_4]$ in a 1:1 mole ratio as described earlier in Chapter 2.

4.2 MEASUREMENTS

The 75 MHz ^{13}C and 300 MHz ^{1}H NMR spectra were run on a Varian Unity-Plus 300 spectrometer in D_2O using TMSP as internal reference. Typically, 20-30 mg of compound was dissolved in 1 mL of D_2O. Infrared data (4000-500 cm^{-1}) were obtained for nujol mulls between NaCl plates with a Biorad FTS-7 Fourier Transform spectrometer.

Elemental Analyses were performed by the Microchemical Unit, Australian National University, Canberra. ESI mass spectra were measured using a VG-Quattro mass spectrometer at the University of Wollongong (Department of Chemistry).

4.3 NOMENCLATURE

A modified version of the nomenclature used to describe the amino acid and dach protons in Chapters 2 and 3 has been adopted. Since the new compounds contain each of these groups, it is necessary to use a system that differentiates between the protons in the amino acid from the protons in the dach component. An example of this system is illustrated below.

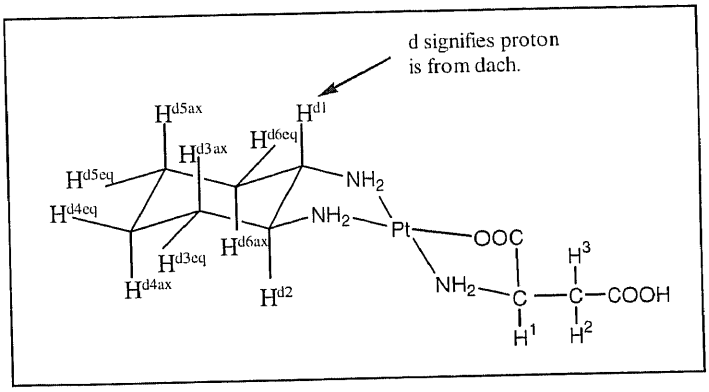

Diagram 4.1: Nomenclature used to describe the protons of the amino acid and dach components.

4.4 SYNTHESIS OF PLATINUM COMPLEXES

Bis(ammine)(L-aspartic acid)platinum(II) chloride. [Pt(L-asp-N,O)(NH_3)$_2$]Cl.

Ammonia solution (4 mL, 28%) was added to a heated, stirrred suspension of [Pt(L-asp-N,O)Cl_2]$^-$ (437 mg, 1 mmol) in water (1 mL). After 10 minutes, the solution lost its initial yellow colour. Evaporation to dryness yielded a colourless, glassy solid. Trituration under acetone produced a white solid. This solid was quickly collected and immediately placed in a desiccator over P_2O_5 due to its hygroscopic nature.

Yield: 0.274 g (69%).
^{1}H NMR (D_2O, ppm): δ = 3.97 (br s, 6H, NH_3), 3.56 (m, 1H, H^1), 2.63, 2.40 (m, J_{12} = 9.0 Hz, J_{13} = 9.6 Hz and J_{23} = 17.2 Hz, 2H, H^2, H^3). ESI-MS: m/e = 361 (30%, M^+), 344 (18, $C_4H_{11}N_3O_3Pt$), 245 (44, H_8N_3Pt). IR (Nujol, cm^{-1}): 3500-3250 (br, νOH and ν(N-H)), 1717, 1615 (2 x s, C=O), 1574 (s, δ_s(N-H)).

Bis(ammine)(L-serine)platinum(II) chloride. [Pt(L-serine)$(NH_3)_2$]Cl.

This complex was prepared from [Pt(L-serine)Cl_2]$^-$ (100 mg, 0.3 mmol), and an excess of ammonia solution by the general method described for [Pt(L-asp-N,O)$(NH_3)_2$]Cl. In some cases, trituration under acetone was not required as evaporation to dryness produced a white powder.

Yield: 64 mg (58%)
^{1}H NMR (D_2O, ppm): δ = 3.49 (q, 1H, H^1), 3.88, 4.09 (2 x m, $J_{12} = J_{13}$ = 6.0 Hz and J_{23} = 12.0 Hz, 2H, H^2, H^3). ESI-MS: m/e = 333 (30%, M^+), 316 (25, $C_3H_{11}N_3O_2Pt$), 261 (18, H_8N_3OPt), 245 (18, H_8N_3Pt). IR (Nujol, cm^{-1}): 3507-3270 (br, νOH and ν(N-H)), 1644 (s, C=O), 1598 (s, δ_s(N-H)).

Bis(ammine)(L-glutamic acid)platinum(II) chloride. [Pt(L-glu-N,O)$(NH_3)_2$]Cl.

Ammonia solution (3 mL, 28%) was added to a heated, stirrred suspension of [Pt(L-glu-N,O)Cl_2]$^-$ (226 mg, 0.5 mmol) in water (1 mL). After 10 minutes, the solution lost its initial yellow colour. Evaporation to dryness yielded a colourless, glassy solid. Trituration under acetone produced a white solid. This solid was quickly collected and dried (P_2O_5).

Yield: 110 mg (54%).
^{1}H NMR (D_2O, ppm): δ = 3.93 (br s, 6H, NH_3), 3.25 (m, 1H, H^1), 2.31, 2.32 (2 x m, $J_{12} = J_{13}$ = 7.5 Hz and J_{23} = 13.5 Hz, 2H, H^2, H^3) 1.95, 1.83 (2 x m, $J_{24} = J_{35}$ = 7.4 Hz, $J_{25} = J_{34}$ = 7.5 Hz and J_{45} = 13.5 Hz, 2H, H^4, H^5). ESI-MS: m/e = 375 (40%, M^+), 358 (18, $C_5H_{13}N_3O_3Pt$), 245 (44, H_8N_3Pt). IR (Nujol, cm^{-1}): 3500-3250 (br, νOH and ν(N-H)), 1716, 1615 (2 x s, C=O), 1578 (s, δ_s(N-H)).

Bis(ammine)(L-lysine)platinum(II) chloride. [Pt(L-lysine)$(NH_3)_2$]Cl.

This complex was prepared by mixing [Pt(L-lysine)Cl_2]$^-$ (220 mg, 0.53 mmol) with ammonia solution (5 mL, 28%). The mixture was evaporated to dryness and triturated under acetone. The white solid was filtered and placed in a desiccator.

Yield: 0.176 g (80%)
^{1}H NMR (D_2O, ppm): δ = 3.37(q, 1H, H^1), 1.77, 1.91 (2 x m, J_{12} = 5.1 Hz, J_{13} = 8.1 Hz and J_{23} = 19.0 Hz, 2H, H^2, H^3), 1.44, 1.43 (2 x m, $J_{24} = J_{25} = J_{34} = J_{35}$ = 7.8 Hz and J_{45} = 15.6 Hz, 2H, H^4,

H^5), 1.69, 1.74 (2 x m, $J_{46} = J_{47} = J_{56} = J_{57}$ = 7.8 Hz and J_{67} = 15.5 Hz, 2H, H^6, H^7), 2.98, 3.03 (2 x m, $J_{68} = J_{69} = J_{78} = J_{79}$ = 7.0 Hz and J_{45} = 15.5 Hz, 2H, H^8, H^9). ESI-MS: m/e = 374 (20%, M^+), 357 (13, $C_6H_{16}N_3O_2Pt$), 340 (21, $C_6H_{13}N_2O_2Pt$), 323 (8, $C_6H_{12}NO_2Pt$), 58 (100, fragmentation of lysine). IR (Nujol, cm^{-1}): 3245-3000 (br, ν(N-H)), 1649 (s, C=O), 1592 (s, δ_s(N-H)).

(L-Aspartic acid)(ethylenediamine)platinum(II) chloride. [Pt(L-asp-N,O)(en)]Cl.

Method 1.

An aqueous solution containing $[Pt(L\text{-}asp\text{-}N,O)Cl_2]^-$ (437 mg, 1 mmol) and ethylenediamine (60 mg, 1 mmol) was heated gently on a water bath for approximately 40 minutes. The completion of the reaction was indicated by the loss of yellow colour. Addition of excess ethanol to the solution yielded a white solid. This solid was filtered, washed with acetone and dried.

Yield: 20 mg (13%).

Anal. Calcd for $C_6H_{14}N_3O_4PtCl$ (423): C, 17.05; H, 3.34; N, 9.94. Found: C, 16.81; H, 3.35; N, 9.78. ^1H NMR (D_2O, ppm): δ = 3.93 (q, 1H, H^1), 2.84, 2.92 (2 x m, J_{12} = 4.8 Hz, J_{13} = 5.7 Hz and J_{23} = 18.0 Hz, 2H, H^2, H^3), 2.61 (s, 4H, $CH_{2(en)}$). ESI-MS: m/e = 387 (100%, M^+). IR (Nujol, cm^{-1}): 3420 (br, OH), 3106 (br, ν(N-H)), 1635 (C=O), 1583 (br, δ_s(N-H)).

Method 2.

An aqueous solution containing $[Pt(L\text{-}asp\text{-}N,O)Cl_2]^-$ (437 mg, 1 mmol) and ethylenediamine dihydrochloride (133 mg, 1 mmol) was brought to the boil on a water bath. After 15 minutes, NaOH (1M) was added to increase the pH to 6, and the solution was heated gently at 50°C. The pH was continually adjusted until the pH value became constant, signifying the end of the reaction. This reaction required 4 mL NaOH and took about 45 minutes. The completion of the reaction was also indicated by the loss of yellow colour. The reaction mixture was cooled, filtered and evaporated to dryness.

Yield: 0.327 g (77%).

Anal. Calcd for $C_{12}H_{26}N_6O_8Pt_2$ (772): C, 18.65; H, 3.37; N, 10.88. Found: C, 18.39; H, 3.36; N, 10.72. ^1H NMR (D_2O, ppm): δ = 3.77 (q, 1H, H^1), 3.90 (q, 1H, $H^{1'}$), 2.61, 2.70 (2 x m, J_{12} = 3.9 Hz, J_{13} = 6.3 Hz and J_{23} = 17.0 Hz, 2H, H^2, H^3), 2.63, 2.72 (2 x m, J_{12} = 3.9 Hz, J_{13} = 6.3 Hz and

J_{23} = 17.0 Hz, 2H, $H^{2'}$, $H^{3'}$), 2.61 (s, 4H, $CH_{2(en)}$), 2.67 (s, 4H, $CH_{2(en')}$). ^{13}C NMR (D_2O, ppm): δ = 48.9 (s, $CH_{2(en')}$), 49.8 (s, $CH_{2(en)}$), 50.4 (s, β-CH_2'), 51.2 (s, β-CH_2), 56.9 (s, α-CH + α-CH'), 57.2 (s, $CH_{2(en')}$), 188.6, 187.8, 187.1, 185.0 (4 x s, COO^-). ESI-MS: m/e = 387 (100%, $C_6H_{14}N_3O_4Pt$), 773 (2.5, M^+ + 1). IR (Nujol, cm^{-1}): 3209-3106 (br, *ν*(N-H)), 1639 (C=O), 1573 (br, δ_s(N-H)).

(Ethylenediamine)(L-serine)platinum(II) chloride. [Pt(L-serine)(en)]Cl.

This compound was prepared by the a procedure similar to that of [Pt(L-asp-N,O)(en)]Cl. The reactant concentrations were [Pt(L-serine)Cl_2]$^-$ (100 mg, 0.24 mmol) and ethylenediamine dihydrochloride (32 mg, 0.24 mmol). About 1.5 mL of NaOH (1M) was added over a period of 1 hour.

Yield: 0.76 g (80%)
Anal. Calcd for $C_5H_{14}N_3O_3PtCl$ (395): C, 15.21; H, 3.55; N, 10.65. Found: C, 15.42; H, 3.72; N, 10.55. ^1H NMR (D_2O, ppm): δ = 3.84 (q, 1H, H^1), 3.94, 4.00 (2 x m, J_{12} = 4.2 Hz, J_{13} = 5.1 Hz and J_{23} = 12.0 Hz, 2H, H^2, H^3). ESI-MS: m/e = 360 (30%, M^+), 314 (100, $C_3H_9N_3O_2Pt$), 255 (40, $C_2H_8N_2Pt$). IR (Nujol, cm^{-1}): 3507-3340 (br, νOH) 3251-3110 (br, ν(N-H)), 1645 (s, C=O), 1584 (s, δ_s(N-H)).

(L-Aspartic acid)(*trans*-R,R-diaminocyclohexane)platinum(II).
[Pt(L-asp-N,O)(*trans*-R,R-dach)].

trans-R,R-Diaminocyclohexane (79.3 mg, 0.63 mmol) was added to an aqueous solution of [Pt(L-asp-N,O)Cl_2]$^-$ (275 mg, 0.63 mmol) in water. The combined solution was heated on a water bath until the solution became colourless. The solution was placed in a refrigerator for 24 hours and then evaporated to dryness. The residual solid was washed with cold water and dried (silica gel).

Yield: 129 mg (43%).
Anal. Calcd for $C_{10}H_{19}N_3O_4Pt.0.5H_2O$ (450): C, 26.72; H, 4.23; N, 9.35. Found: C, 26.71; H, 4.28; N, 8.98. ^1H NMR (D_2O, ppm): δ = 3.66 (q, 1H, H^1), 2.53, 2.62 (2 x m, J_{12} = 3.9 Hz, J_{13} = 6.3 Hz and J_{23} = 17.0 Hz, 2H, H^2, H^3), 2.54 (m, 2H, H^{d1} + H^{d2}), 1.93 (m, 2H, H^{d3eq} + H^{d6eq}), 1.45 (m, 2H, H^{d3ax} + H^{d6ax}), 1.15 (m, 2H, H^{d4eq} + H^{d5eq}), 1.02 (m, 2H, H^{d4ax} + H^{d5ax}). IR (Nujol, cm^{-1}): 3558-3110 (br, νOH), 3209-3048 (br, ν(N-H)), 1654, 1630 (2 x s, C=O), 1546 (s, δ_s(N-H)).

(L-Aspartic acid)(*cis*-R,S-1,2-diaminocyclohexane)platinum(II).
[Pt(L-asp-N,O)(*cis*-R,S-dach)].

cis-R,S-1,2-Diaminocyclohexane (79.3 mg, 0.63 mmol) was added to an aqueous solution of $[Pt(L\text{-}asp\text{-}N,O)Cl_2]^-$ (275 mg, 0.63 mmol) in water. The solution was heated on a water bath until it became colourless. The solution was placed in a refrigerator for 48 hours. The white solid that precipitated was filtered, washed with cold water and dried (silica gel). Occasionally, evaporation was required to isolate the white product.

Yield: 211 mg (83%).
Anal. Calcd for $C_{10}H_{19}N_3O_4Pt.H_2O$ (458): C, 26.20; H, 4.58; N, 9.16. Found: C, 26.40; H, 4.38; N, 8.99. ^1H NMR (D_2O, ppm): δ = 3.89 (q, 1H, H^1), 2.87 (m, 2H, H^{d1} + H^{d2}), 2.67, 2.84 (2 x m, J_{12} = 3.6 Hz, J_{13} = 5.4 Hz and J_{23} = 14.1 Hz, 2H, H^2, H^3), 1.68 (m, 4H, H^{d3eq} + H^{d6eq} + H^{d3eq} + H^{d6eq}), 1.44 (m, 2H, H^{d4eq} + H^{d5eq}), 1.32 (m, 2H, H^{d4ax} + H^{d5ax}). IR (Nujol, cm^{-1}): 3558-3109 (br, νOH), 3249-3108 (br, ν(N-H)), 1668, 1613 (2 x s, C=O), 1568 (s, δ_s(N-H)).

Results and Discussion

4.5 BIS(AMMINE) COMPLEXES

A series of bis(ammine) derivatives were prepared using a standard method.[1,2] The procedure was found by repetition to give variable yields which were sometimes low. It involved heating an aqueous solution of $[Pt(amac\text{-}N,O)Cl_2]^-$ and ammonia at 50-60°C for 10-15 minutes. Displacement of the two-chloro groups was indicated by the loss of yellow colour. Evaporation of the aqueous solutions always yielded 'glasses', which by trituration under acetone were converted into fine powders. These powders were very hygroscopic and tended to lose ammonia on heating or long standing in solution to reform the respective $[Pt(amac\text{-}N,O)Cl_2]^-$ starting material. These factors made characterisation in the solid state (i.e microanalysis) very difficult. However, ^1H NMR and mass spectra of solutions of these solids are consistent with the presence of $[Pt(amac\text{-}N,O)(NH_3)_2]^+$.

Spectral Data

Because of the relatively long time required to obtain suitable ^{13}C NMR spectra, and the instability of the bis(ammine) complexes in solution, it was not practicable to obtain ^{13}C NMR spectra for this series of complexes. However, with the much shorter time required to obtain a ^{1}H NMR spectrum, it was possible to get well-resolved proton spectra for the series. These spectra provide sufficient structural information concerning the formation of bis(ammines). The formation of bis(ammine) derivatives is manifested in the ^{1}H NMR spectra both by the slight changes in chemical shifts (as compared to the dichloro complexes) and by the appearance of a very broad signal around 3.9 ppm in freshly prepared solutions due to the coordinated ammine ligands. This ammine peak is lost through deuterium exchange on standing in D_2O solutions.

The NMR spectra of the bis(ammine) derivatives resemble those of their dichloro counterparts with respect to splitting patterns and require no detailed description. Diagnostic ^{1}H NMR data for the bis(ammine) series are summarized in Tables 4.1 and 4.2. When compared to data on the dichloro complexes (cf. Table 2.4), all signals have shifted upfield upon exchange of the labile chloro ligands with ammonia.

Table 4.2: ^{1}H NMR chemical shifts.[a]

Compound	Amino Acid Protons[b]									Others
	-CH-	-CH$_2$-								
	δH^1	δH^2	δH^3	δH^4	δH^5	δH^6	δH^7	δH^8	δH^9	
[Pt(L-asp-N,O)(NH$_3$)$_2$]Cl	3.56	2.63	2.40							3.97
[Pt(L-serine)(NH$_3$)$_2$]Cl	3.49	3.88	4.09							-
[Pt(L-glu-N,O)(NH$_3$)$_2$]Cl	3.25	2.31	2.32	1.95	1.83					3.93
[Pt(L-lysine)(NH$_3$)$_2$]Cl	3.59	1.77	1.91	1.44	1.43	1.69	1.74	2.98	3.03	-
[Pt(L-asp-N,O)(en)]Cl	3.93	2.84	2.92							2.61

[a] Chemical Shifts in ppm, spectra run in D_2O referenced to TMSP. [b] The spectra of [Pt(L-serine)(NH$_3$)$_2$]Cl and [Pt(L-lysine)(NH$_3$)$_2$]Cl were recorded after the NH_3 protons had exchanged with deuterium in order to observe other resonances.

Table 4.3: ^{1}H NMR coupling constants.[a]

Compound	^{3}J Coupling Constants														^{2}J Coupling Constants			
	$^3J_{12}$	$^3J_{13}$	$^3J_{24}$	$^3J_{25}$	$^3J_{34}$	$^3J_{35}$	$^3J_{46}$	$^3J_{47}$	$^3J_{56}$	$^3J_{57}$	$^3J_{68}$	$^3J_{69}$	$^3J_{78}$	$^3J_{79}$	$^2J_{23}$	$^2J_{45}$	$^3J_{67}$	$^3J_{89}$
[Pt(L-asp-N,O)(NH_3)$_2$]Cl	9.0	9.6													17.2			
[Pt(L-serine)(NH_3)$_2$]Cl	6.0	6.0													12.0			
[Pt(L-glu-N,O)(NH_3)$_2$]Cl	7.5	7.5	7.4	7.5	7.5	7.4									13.5	13.5		
[Pt(L-lysine)(NH_3)$_2$]Cl	5.1	8.1	7.8	7.8	7.8	7.8	7.8	7.8	7.8	7.8	7.0	7.0	7.0	7.0	19.0	15.6	15.5	15.5
[Pt(L-asp-N,O)(en)]Cl	4.8	5.7													18.0			

[a] Coupling constants in Hz, recorded at 300 MHz.

4.6 ETHYLENEDIAMINE COMPLEXES

The two synthetic routes adopted for the preparation of [Pt(L-asp-N,O)(en)]Cl were based on similar procedures used for the synthesis of [Pt(en)Cl_2].[3,4] In these cases the K_2[PtCl_4] starting material was replaced by [Pt(L-asp-N,O)Cl_2]$^-$ and the products were isolated either by addition of ethanol or by evaporation.

The ^{1}H NMR spectrum of [Pt(L-asp-N,O)(en)]Cl prepared from ethylenediamine, [Pt(L-asp-N,O)Cl_2]$^-$ and precipitated with ethanol (method 1) is very straightforward. It displays the expected eight-line portion assignable to the methylene protons of the aspartic acid ligand in the 2.58-2.78 ppm region, along with a quartet downfield at 3.74 ppm due to the methine protons of aspartic acid. These methylene and methine resonances have shifted upfield as compared to the dichloro complex. The presence of coordinated ethylendiamine was readily apparent by the appearance of a strong singlet at 2.61 ppm. ^{1}H NMR data on this compound have been included in Tables 4.1 and 4.2.

From the reaction of ethylenediamine dihydrochloride with $[Pt(L\text{-}asp\text{-}N,O)Cl_2]^-$ and sodium hydroxide to generate free ethylendiamine (method 2), a mixture of two slightly spectroscopically different species was detected. The ^1H NMR spectrum shows two methine peaks in the downfield region and two strong singlets attributable to the methylene protons of coordinated ethylenediamine. A series of other peaks, which are obviously the superposition of two or more methylene resonances from the aspartic acid components, are also evident. In the ^{13}C NMR, four distinct carbonyl resonances at 188.6, 187.8, 187.1 and 185 ppm were observed. As previously mentioned in Chapter 2, aspartic acid belongs to a class of compounds that are capable of binding to the metal in three different ways; O,O-, N,βO- and N,αO-chelation. Under the conditions used in method 2 (i.e. pH 6) and despite the preference platinum has for nitrogens, it is concievable that the coordinated aspartic acid has become bound to a second platinum atom via the terminal carboxyl to produce a bis(platinum) complex. The proposed structure along with the ^1H NMR chemical shift data are shown in Diagram 4.2. The fact that the signals for the carbonyl carbons showed high field shifts are strong evidence for the bis(platinum) structure shown in Diagram 4.2. The microanalysis and mass spectrum (with its molecular ion at m/e 773) are in complete harmony with the proposed structure.

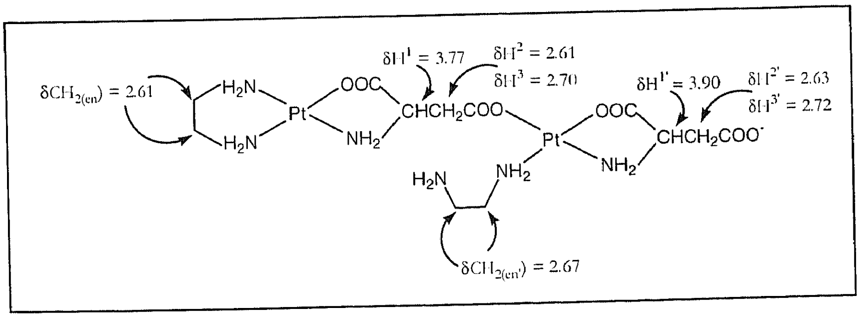

Diagram 4.2: Proposed structure for the product prepared by method 2.

The infrared spectrum for the N,αO-chelate (method 1) and the proposed bis(platinum) species (method 2) is shown in Diagram 4.3. Comparison of the two spectra show that the bands of the N,αO-chelate are relatively strong and clear whereas those of the bis(platinum) species are blunt and unresolved. Despite this difference, both spectra show the characteristic band near 1630 cm^{-1} assigned to the asymmetric stretching frequencies of the carboxyl group. The bands at 1573 and 1583 cm^{-1} seem to be the N-H bending vibrations of the amines.

The ^{1}H NMR of [Pt(L-serine)(en)]Cl also consists of an eight-line pattern due to the non-equivalent methylene protons in the 3.9-4.0 ppm region, a methine quartet at 3.8 ppm and a very strong singlet at 3.2 ppm due to the methylene protons of ethylenediamine. Chemical shifts and coupling constants are listed in Tables 4.1 and 4.2. All other data are consistent with the proposed structure and can be found in the Experimental Section.

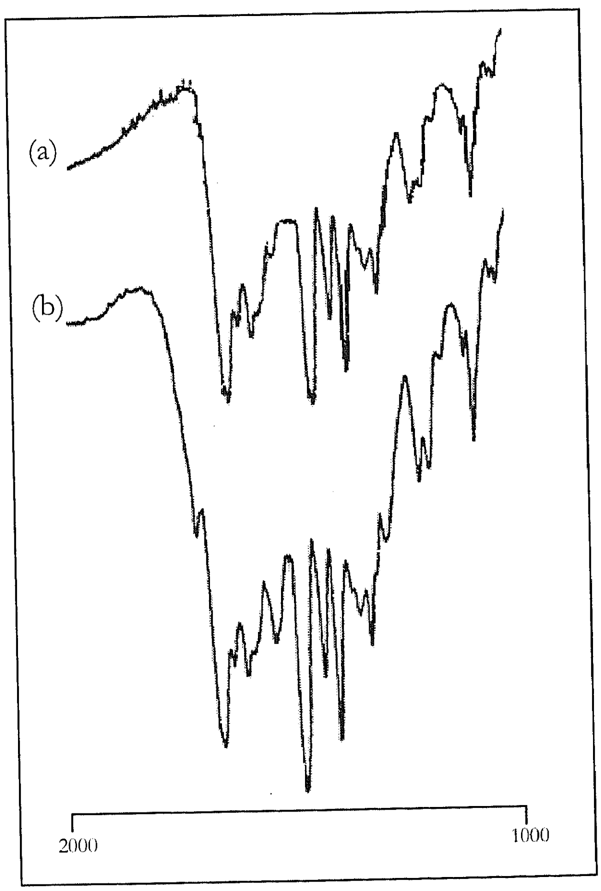

Diagram 4.3: Infrared spectra of the proposed bis(platinum) species (a) and the N,αO-chelate [Pt(L-asp-N,O)(en)]Cl (b).

4.7 DIAMINOCYCLOHEXANE COMPLEXES

For the synthesis of the diaminocyclohexane platinum complexes, [Pt(L-asp-N,O)(*trans*-R,R-dach)] and [Pt(L-asp-N,O)(*cis*-R,S-dach)], 1:1 mixtures of the appropriate dach ligand and [Pt(L-asp-N,O)Cl_2]$^-$ were heated until the intense yellow colour of the solutions faded. The platinum complexes either precipitated out of solution (e.g [Pt(L-asp-N,O)(*cis*-R,S-dach)]) or were isolated by evaporation (e.g [Pt(L-asp-N,O)(*trans*-R,R-dach)]). The structures of the complexes were mainly deduced from the ^{1}H NMR and infrared spectra, and microanalytical data.

Infrared Data.

The infrared spectra of both complexes are dominated by strong ν(N-H) stretching bands between 3250-3040 cm^{-1}. Uncoordinated carboxyl groups usually show a strong infrared peak above 1700 cm^{-1}.[5] No such peak was seen in the infrared of either of the complexes. However two strong bands at 1654 and 1630 cm^{-1} for [Pt(L-asp-N,O)(*trans*-R,R-dach)] and at 1668 and 1613 cm^{-1} for [Pt(L-asp-N,O)(*cis*-R,S-dach)] were observed. These bands are consistent with a coordinated carboxylate motion and a free ionised carboxylate.[5] This is supported by the microanalysis which also suggest that the complexes have a deprotonated terminal carboxylate group.

^{1}H NMR Data

The most revealing structural information of the reaction of dach with [Pt(L-asp-N,O)Cl_2]$^-$ was gained from the ^{1}H NMR spectra. The assignments for resonances were made based on the integrated intensity of the resonances and by analogy to spectra in Chapters 2 and 3.

The ^{1}H NMR spectrum of [Pt(L-asp-N,O)(*trans*-R,R-dach)] shows eight main peaks. Of these, the methine proton of the aspartic acid ligand is found at 3.66 ppm, while the methylene protons diplay a typical ABX-type splitting pattern in which the H^2 protons lie at 2.53 ppm and the H^3 protons at 2.62 ppm. The *trans*-R,R-dach component shows a series of complicated multiplets in the 1.03-1.93 ppm region integrated for eight protons, and an additional peak at 2.54 ppm integrated for two protons. A summary of the ^1H NMR data for [Pt(L-asp-N,O)(*trans*-R,R-dach)] is presented in Table 4.4.

Table 4.4: ^1H NMR[a] Data for [Pt(L-asp-N,O)(*trans*-R,R-dach)] and [Pt(L-asp-N,O)(*cis*-R,S-dach)].

Protons	[Pt(L-asp-N,O)-(*trans*-R,R-dach)]	[Pt(L-asp-N,O)-(*cis*-R,S-dach)]
Dach		
$H^{d1} + H^{d2}$	2.54	2.87
$H^{d3eq} + H^{d6eq}$	1.93	1.68
$H^{d3ax} + H^{d3ax}$	1.45	1.68
$H^{d4eq} + H^{d5eq}$	1.15	1.44
$H^{d4ax} + H^{d5ax}$	1.02	1.32
Aspartic Acid		
H^1	3.66	3.89
H^2	2.53 $J_{12} = 3.9$	2.67 $J_{12} = 3.6$
H^3	2.63 $J_{13} = 6.3$	2.84 $J_{13} = 5.4$
	$J_{23} = 17.0$	$J_{23} = 14.0$

[a]Chemical Shifts in ppm and coupling constants in Hz

It is worth noting that in the ^1H NMR spectrum of [Pt(L-asp-N,O)(*trans*-R,R-dach)], the (H^{d1} + H^{d2}) and (H^{d3eq} + H^{d6eq}) protons were shifted downfield by 0.43 and 0.10 ppm respectively, relative to the same protons in the [Pt(*trans*-R,R-dach)Cl_2] compound. Similarly, the methine and methylene protons of the aspartic acid component have shifted upfield by about 0.30 ppm relative to [Pt(L-asp-N,O)Cl_2]$^-$.

Table 4.4 gives the ^1H NMR data for the [Pt(L-asp-N,O)(*cis*-R,S-dach)] derivative. The spectrum shows a peak at 2.87 ppm attributable to the (H^{d1} + H^{d2}) protons of the *cis*-R,S-dach moiety. These protons are equivalent on the NMR time scale between the limiting conformations of λ and δ. The four protons at H^{d4} and H^{d5} gave two splitting peaks even under rapid interconversion because the axial and equatorial protons are inequivalent. This should have also been the case for the four protons at H^{d3} and H^{d6}, however coincidental overlap or averaging out prevented the two individual resonances from being observed. Instead one broad resonance, integrated for four protons was observed at 1.68 ppm.

The spectrum of [Pt(L-asp-N,O)(*cis*-R,S-dach)] also shows the expected eight-line pattern in the 2.6-2.9 ppm region assignable to the methylene protons of the aspartic acid ligand. In addition, the methine quartet of aspartic acid is seen at 3.89 ppm. Like [Pt(L-asp-N,O)(*trans*-R,R-dach)], these protons also exhibit a pronounced upfield shift relative to $[Pt(L\text{-}asp\text{-}N,O)Cl_2]^-$. The proton chemical shifts and coupling constants are given in Table 4.4.

References

1 T. G. Appleton and J. R. Hall, Inorg. Chem., 1970, **9**, 1800.

2 L. E. Erickson, M. D. Erickson and B. L. Smith, Inorg. Chem., 1973, **12**, 412.

3 F. Basolo, J. C. Bailar and B. R. Tarr, J. Amer. Chem. Soc., 1950, **72**, 2433.

4 G. L. Johnson, Inorg. Synth., 1970, **8**, 193.

5 K. Nakamoto, Infrared and Raman Spectra of Inorganic and Coordination Compounds 4th ed., Wiley, New York, 1981, pp. 95-180.

CHAPTER

5

SYNTHESIS OF TETRASUBSTITUTED PORPHYRINS FOR LINKING WITH PLATINUM(II) COMPLEXES

Introduction

As the knowledge about both natural and synthetic porphyrins expands, so does the number of applications. Initial interest in porphyrins arose primarily due to their use as photosensitisers in photodynamic therapy,[1,2] however, in the early 90's interest stemmed from the exhibited antiviral activity against HIV-1- the virus responsible for AIDS.[3] Other fields of research which have received significant attention include solar energy conversion,[4,5] catalysis,[6] photo-induced energy and electron transfer particularly in relation to photosynthesis,[7] and the cleavage of double-stranded DNA by their metallo derivatives.[8]

The word porphyrin originated from the Greek word *porphura* which was used to describe the colour purple. This immediately highlights one of the most characteristic features of porphyrins: their intense purple colour. Chemically porphyrins are complex macrocyclic ring products composed of four pyrrole units joined at the α position by four methine bridging groups. The basic ring structure is called porphin (Diagram 5.1). The numbering of ring positions including nitrogen is also shown in Diagram 5.1. The porphin nucleus is planar and contains a conjugating system of 18 delocalisable π-electrons. It is the presence of such a large number of conjugated double bonds which make porphyrin compounds absorb light strongly and are therefore highly coloured. Porphyrins form complexes (Diagram 5.1) with suitable metal ions. In these complexes, the insertion of the metal ion occurs by displacement of a proton from each of two opposing nitrogen atoms to generate a square planar complex.

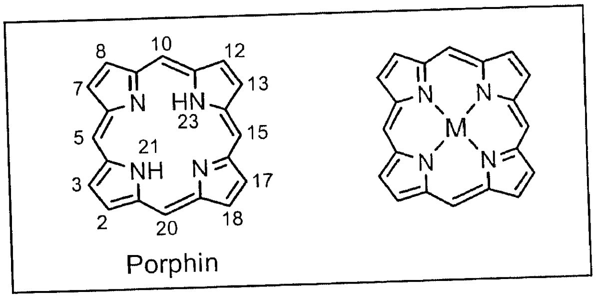

Diagram 5.1: Porphin and a metal chelate.

Porphin itself does not occur in nature, but several analogous compounds with various side-chains on the pyrrole rings are of great biological importance. The best known examples are heme, an iron complex present in the red blood pigment hemoglobin and chlorophyll, the green plant pigment essential to photosynthesis (Diagram 5.2). It was the discovery of naturally occurring pigments which motivated researchers to create a variety of porphyrin derivatives carrying functional groups attached to the periphery of the macrocycle. One famous example is 5,10,15,20-tetraphenylporphyrin (TPP).

TPP was first reported in 1935 by Rothemund, who prepared it by heating a mixture of pyrrole and benzaldehyde at 220°C under nitrogen for 48 hours.[9,10,11] The Rothemund reaction was carried out anaerobically in a sealed tube in pyridine solution. The yield of porphyrin is generally less than 5% [12] and the conditions are so severe that few substituted benzaldehydes can be converted to the corresponding porphyrins. Adler and Longo later developed an improved synthesis of TPP. Adler and Longo obtained a 20% yield of TPP from the reaction of equimolar amounts of benzaldehyde and pyrrole in refluxing propionic acid for 30 minutes at 141°C, open to the air.[13] These comparatively milder reaction conditions allow a wider range of substituted benzaldehydes to be converted into porphyrins, however problems still occur with benzaldehydes bearing sensitive functional groups. The Adler and Longo method is also beset with purification problems especially with those porphyrins that do not precipitate out at the end of the reaction.[14] In addition, the batch-to-batch reproducibility of the reaction is often rather poor.

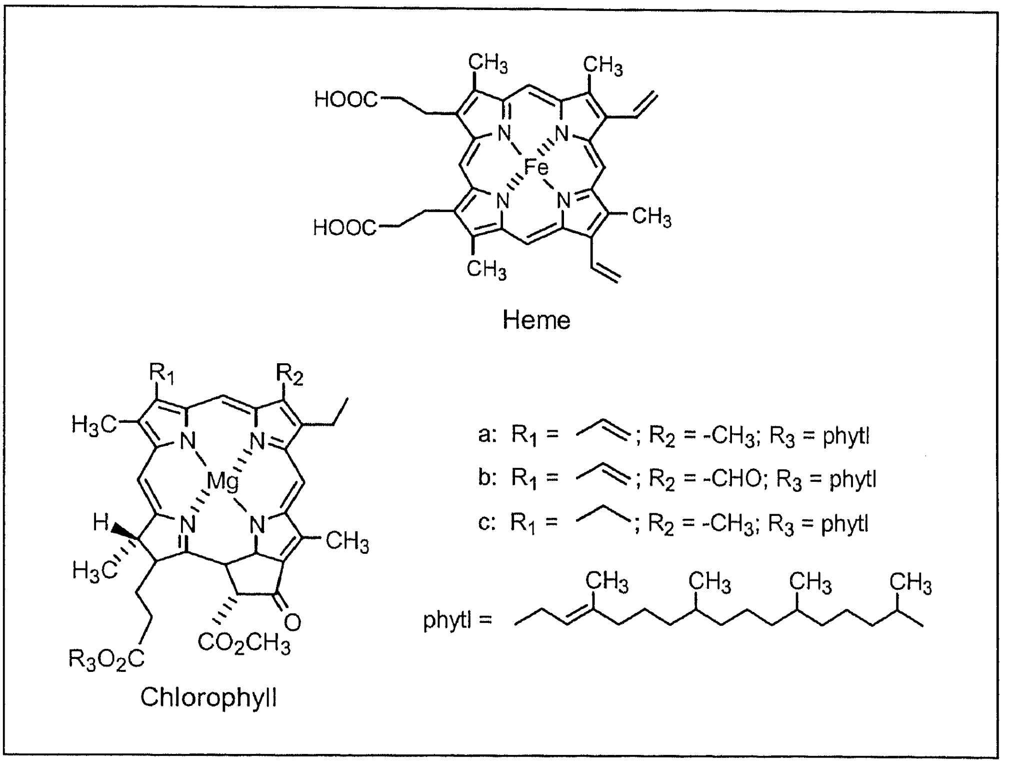

Diagram 5.2: Heme and some chlorophylls.

Due to the problems involved with the Rothemund and Adler and Longo methods, milder, cleaner and more convenient synthetic procedures were developed.[14,15] With the new synthetic strategy pyrrole and the desired benzaldehyde were reacted at room temperature with trace amounts of an acid catalyst to form tetraphenylporphyrinogens, which in turn oxidise to porphyrins. The mechanism of the reaction is thought to involve formation of a carbonium ion (Equation 1).[12]

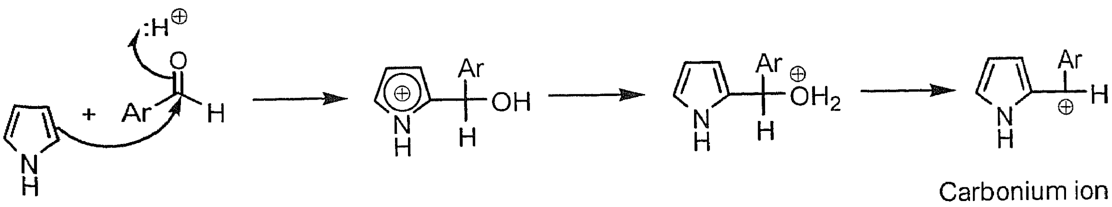

(1)

This carbonium ion then attacks the free α-position of another pyrrole to give a dipyrrylmethane. Chain building continues until tetrapyrrylcarbinols are formed. Ring closure follows to give porphyrinogens which are oxidised to give the porphyrin (Diagram 5.3).[8]

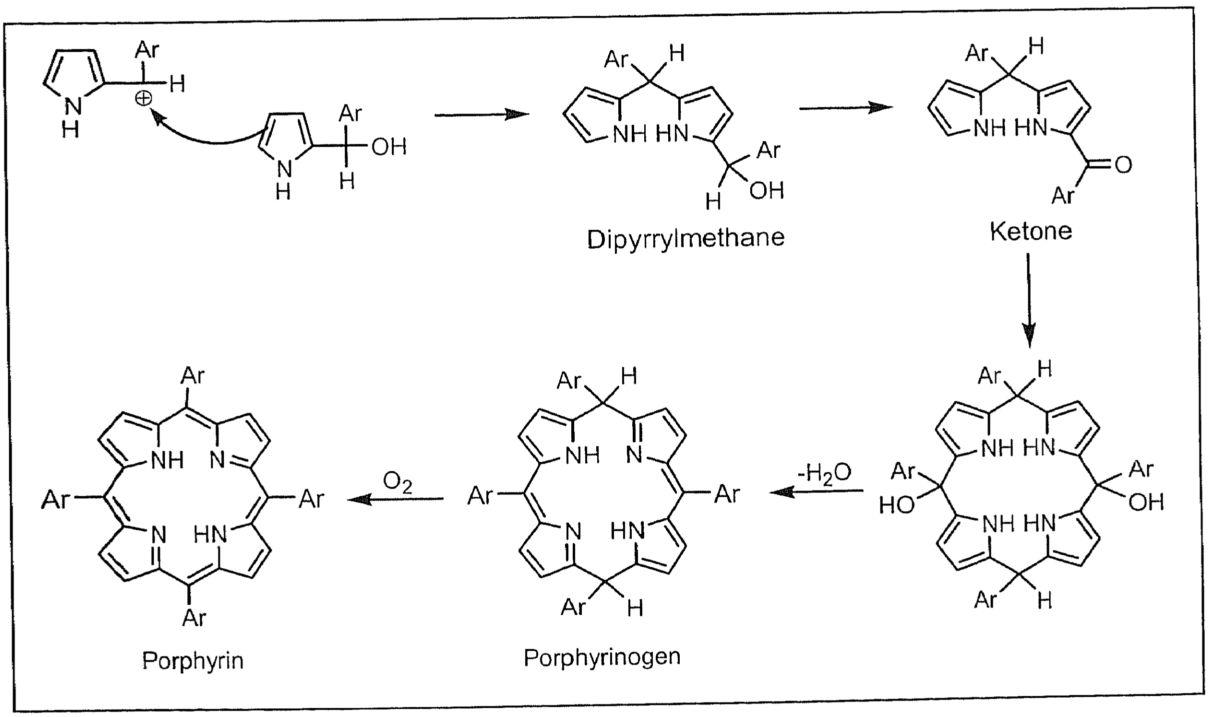

Diagram 5.3: Mechanism of TPP synthesis

Several acid catalysts can be used. These include boron trifluoride diethyl etherate (BF_3-etherate), trifluoroacetic acid (TFA) and boron trichloride (BCl_3). The rate of porphyrinogen formation is proportional to the concentration of the acid catalyst and although the rate of reaction is different for each of the catalysts the yields are only slightly altered. The oxidation of porphyrinogen to porphyrin can be performed with either p-chloranil or 2,3-dichloro-5,6-dicyanobenzoquinone (DDQ). p-Chloranil is a much milder oxidant requiring an exposure time of one-hour for complete reaction. On the other hand, instantaneous conversion of porphyrinogen to porphyrin occurs upon addition of DDQ at room temperature. Generally, higher yields can be obtained using p-chloranil. DDQ is more useful for rapid quenching when monitoring the progress of the reaction.[14]

Our long-term goals are to build better, more specific anticancer drugs. A step towards this goal is to prepare a set of porphyrins with each porphyrin bearing one or more peripheral functional groups. These groups can be used as handles for joining the porphyrin with a platinum containing drug. This chapter describes the synthesis and characterisation of tetra-substituted porphyrins featuring various para-substituents for linking with platinum complexes.

Our approach to porphyrin synthesis makes use of mild reaction conditions, which convert the aldehyde and pyrrole to the corresponding porphyrin. The use of pre-functionalised benzaldehydes wherever possible minimises the synthetic manipulations of the porphyrin structure, which in turn minimises the by-products. The three functional groups selected are those that can be used in direct-coupling reactions. These functional groups include an amine, a carboxylic acid and a methyl ester.

Experimental

5.1 MATERIALS

4-Methoxybenzaldehyde dimethyl acetal was purchased from Lancaster. All solvents employed were Ajax Chemicals analytical grade materials, which were used without further purification unless noted otherwise. All references to chloroform ($CHCl_3$) contain ethanol (1-2%) as the stabiliser. Pyrrole was freshly distilled directly before use. All other chemicals were of reagent grade and obtained from Aldrich. Stock solutions (2.5 M) of BF_3 etherate were prepared in $CHCl_3$ and were used for approximately one week. Column chromatography was performed on silica gel (Kieselgel 60G, Merck) using $CHCl_3$, CH_2Cl_2, or CH_2Cl_2/hexane (2:1) as the eluent. A column size of 180 mm by 12 mm in diameter or 360 mm by 50 mm in diameter was used under gravity. Merck precoated plates (silica gel 60, 2 mm) were used for thin layer chromatography (TLC).

5.2 MEASUREMENTS

ESI mass spectra were measured with a VG-Quattro mass spectrometer at the University of Wollongong (Department of Chemistry). UV-visible spectra were taken on a Shimadzu 160 UV-Visible recording spectrophotometer. ^{1}H and ^{13}C NMR spectra were obtained in $CDCl_3$ and recorded with a Varian Unity-Plus 300 spectrometer. ^{1}H NMR spectra were recorded from -3 to 10 ppm. The NMR samples were prepared by dissolving 7 mg in 1.0 mL of $CDCl_3$. Higher concentrations were not recommended owing to the potential for porphyrins to aggregate in solution. Chemical shift values are given in ppm relative to TMS. Coupling constants are expressed in Hz.

5.3 NOMENCLATURE

For the description of individual protons and carbons in the porphyrins, a nomenclature has been adopted. The protons and carbons (ortho, meta and para) on the phenyl rings are identified with respect to their positions relative to the porphyrin ring system. This nomenclature is illustrated in the diagram below.

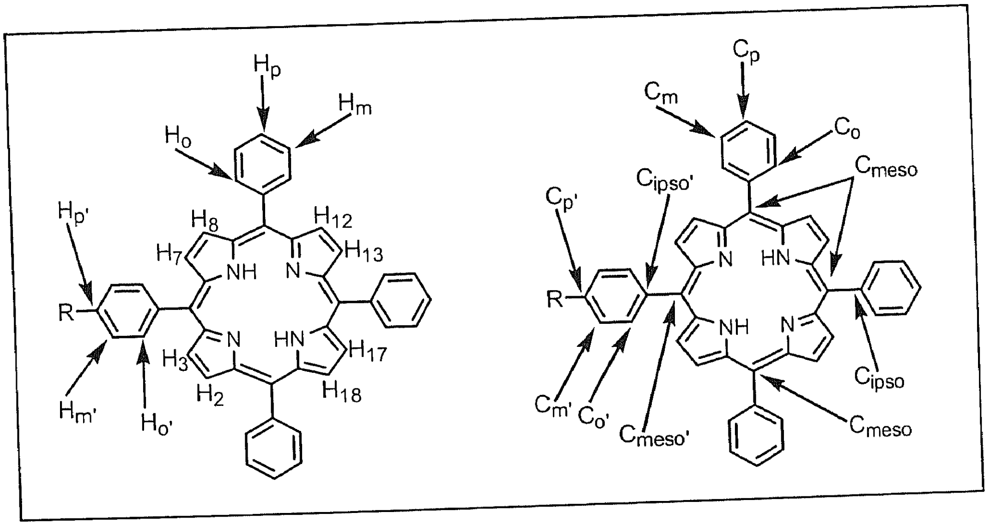

Diagram 5.4: Nomenclature adopted to describe protons and carbons in the porphyrins.

5.4 SYNTHESIS OF PORPHYRINS

5,10-15,20-tetraphenylporphyrin. TPP

Benzaldehyde (11.3 g, 107 mmol) and pyrrole (7.2 g, 107 mmol) were added to refluxing propionic acid (400 mL). The mixture was heated under reflux for 30 minutes. The dark brown reaction mixture was then cooled to room temperature. The purple lustrous precipitate was filtered, washed with methanol (2 x 50 mL) and dried under vacuum.

Yield: 2.8 g (18%)
^{1}H NMR ($CDCl_3$, ppm):δ = -2.74 (br s, 2H, pyrrole NH), 7.77 (m, 12H, H_m + H_p), 8.24 (m, 8H, H_o), 8.87 (s, 8H, β-pyrrole). ^{13}C NMR ($CDCl_3$, ppm): δ = 120.1 (s, C_{meso}), 126.7 (s, C_m), 127.7 (s, C_p), 131.1 (br s, β-pyrrole), 134.6 (s, C_o), 142.2 (s, C_{ipso}). ESI-MS: m/e = 615 (45%, M^+ + 1). UV-Vis ($CHCl_3$, nm): λ = 417, 514, 550, 590, 646.

5-(4-Nitrophenyl)-10,15,20-triphenylporphyrin. TPP-NO_2

Tetraphenylporphyrin (2.0 g, 3.25 mmol) was dissolved in CH_2Cl_2 (300 mL) under nitrogen. Red fuming nitric acid (3.4 g, 54 mmol) was added carefully to the stirred solution of the porphyrin at 0-5°C through a pressure-equalising dropping funnel over a period of 2 hours. The reaction was monitored at intervals by TLC (silica, $CHCl_3$) to insure total conversion of the starting material (R_f = 0.88) to product (R_f = 0.78). The dark green solution was extracted with water (5 x 300 mL) and dried over magnesium sulfate ($MgSO_4$) and sodium carbonate (Na_2CO_3). The solution was then evaporated to about 70 mL and chromatographed on silica with $CHCl_3$ as the eluent. Fractions containing only the mono-nitro derivative were combined. Evaporation of the solvent afforded the desired product as a dark purple powder.

Yield: 1.09 g (50%)

^{1}H NMR ($CDCl_3$, ppm): δ = -2.71 (br s, 2H, pyrrole NH), 7.72 (m, 9H, H_m + H_p), 8.22 (m, 6H, H_o), 8.33 (d, 2H, J = 8.7 Hz, $H_{o'}$), 8.54 (d, 2H, J = 8.7 Hz, $H_{m'}$), 8.72 (d, 2H, J = 4.8 Hz, β-pyrrole (H^2 + H^8)), 8.88 (d, 2H, J = 4.8 Hz, β-pyrrole (H^3 + H^7)), 8.90 (s, 4H, β-pyrrole (H^{12} + H^{13} + H^{17} + H^{18})). ^{13}C NMR ($CDCl_3$, ppm): δ = 120.3 (s, C_{meso}), 121.7 (s, $C_{m'}$), 126.7 (s, C_m), 127.7 (s, C_p), 131.9 (br s, β-pyrrole), 134.6 (s, C_o), 135.6 (s, $C_{o'}$), 142.2 (s, C_{ipso}), 147.7 (s, $C_{p'}$), 148.2 (s, $C_{ipso'}$). ESI-MS: m/e = 660 (48%, M^+ + 1). UV-Vis (CH_2Cl_2, nm): λ = 418, 515, 550, 592, 646.

5-(p-Aminophenyl)-10,15,20-triphenylporphyrin. TPP-NH_2

5-(4-Nitrophenyl)-10,15,20-triphenylporphyrin (1.0 g, 1.52 mmol) was dissolved in concentrated hydrochloric acid (32 mL) under nitrogen. Tin(II) chloride dihydrate (1.04 g, 4.6 mmol) was added to the solution, and the reaction was heated to 65°C for 1 hour. The porphyrin mixture was cooled to room temperature and poured into cold water (120 mL). The pH was adjusted to pH 8 with concentrated ammonia. The aqueous phase was extracted with $CHCl_3$ (6 x 120 mL). The combined organic layers were dried ($MgSO_4$), filtered and evaporated to 100 mL. The desired product was isolated by column chromatography on silica, with CH_2Cl_2 as the eluent.

Yield: 671 mg (71%)

^1H NMR ($CDCl_3$, ppm):δ = -2.70 (br s, 2H, pyrrole NH), 3.97 (br s, 2H, amino), 7.00 (d, 2H, J = 8.4 Hz, $H_{m'}$), 7.77 (m, 9H, H_m + H_p), 8.00 (d, 2H, J = 8.4 Hz, $H_{o'}$), 8.25 (m, 6H, H_o), 8.87 (d, 2H, J = 4.8 Hz, β-pyrrole (H^3 + H^7)), 8.88 (s, 4H, β-pyrrole ((H^{12} + H^{13} + H^{17} + H^{18})), 8.97 (d, 2H, J = 4.8 Hz, β-pyrrole (H^2 + H^8)). ^{13}C NMR ($CDCl_3$, ppm):δ = 113.4 (s, $C_{m'}$), 119.7, 120.0, 120.9 (3 x s, C_{meso}+ $C_{meso'}$), 126.7 (s, C_m), 127.7 (s, C_p), 131.1 (br s, β-pyrrole), 132.3 (s, $C_{ipso'}$), 134.6 (s, C_o), 135.7 (s, $C_{o'}$), 142.2 (s, C_{ipso}), 146.0 (s, $C_{p'}$). ESI-MS: m/e = 630 (13%, M^+ + 1). UV-Vis (CH_2Cl_2, nm): λ = 407, 422, 521, 557, 651.

5-(p-Methoxycarbonylphenyl)-10,15,20-tri(p-methylphenyl)porphyrin. TMePP-COOMe

Methyl 4-formylbenzoate (0.970 g, 5.91 mmol) and 4-tolualdehyde (3.56 g, 29.6 mmol) in propionic acid (70 mL) were added to a solution of pyrrole (2.38 g, 35.5 mmol) in propionic acid (370 mL) preheated to 130°C. The reaction mixture was refluxed for 1 hour and then propionic acid (300 mL) was removed by distillation. The solution was refrigerated for 36 hours, after which a purple precipitate formed. This precipitate was filtered, rinsed with methanol (150 mL) and dried at the pump for 15 minutes. Purification was achieved by chromatography on silica with CH_2Cl_2/hexane (2:1) as the eluent.

Yield: 590 mg (14%)

^1H NMR ($CDCl_3$, ppm):δ = -2.79 (br s, 2H, NH), 2.69 (s, $ArCH_3$), 4.09 (s, -OCH_3), 7.53 (d, 6H, J = 7.8 Hz, H_m), 8.08 (d, 6H, J = 7.8 Hz, H_o), 8.28 (d, 2H, J = 8.3 Hz, $H_{o'}$), 8.42 (d, 2H, J = 8.3 Hz, $H_{m'}$), 8.75 (d, 2H, J = 4.8 Hz, β-pyrrole (H^3 + H^7)), 8.84 (s, 4H, β-pyrrole ((H^{12} + H^{13} + H^{17} + H^{18})), 8.86 (d, 2H, J = 4.8 Hz, β-pyrrole (H^2 + H^8)). ^{13}C NMR ($CDCl_3$, ppm):δ = 21.7 (s, $ArCH_3$), 52.5 (s, $COOCH_3$), 118.2, 120.1, 120.4 (3 x s, C_{meso}), 120.5 (s, $C_{meso'}$), 127.4 (s, C_m), 127.9 (s, $C_{m'}$), 129.5 (s, $C_{p'}$), 131.1 (br s, β-pyrrole), 134.5 (s, C_o + $C_{o'}$), 137.3 (s, C_p), 139.3 (s, C_{ipso}), 147.3 (s, $C_{ipso'}$), 167.4 (s, COO^-). ESI-MS: m/e = 715 (20%, M^+). UV-Vis (CH_2Cl_2, nm): λ = 418, 516, 553, 591, 648.

5,10,15-Trimesityl-20-(4-methoxycarbonylphenyl)porphyrin. TMesPP-COOMe

A 1L three-neck round bottom flask fitted with a reflux condenser, septum seal and nitrogen inlet port was charged with $CHCl_3$ (800 mL), mesitaldehyde (0.89 g, 6 mmol), methyl 4-formyl-benzoate (328 mg, 2 mmol) and pyrrole (1.61 g, 24 mmol). After the solution was purged for 5 minutes with nitrogen, 2.5 M BF_3-etherate (0.340 g, 2.4 mmol) was added via syringe. The reaction vessel was shielded from ambient light and the reaction was allowed to proceed at room temperature. After 1 hour, oxidation was initiated by addition of p-chloranil (1.35 g, 5.5 mmol, in 50 mL toluene) and the solution was refluxed (60-65°C) for a further 1 hour.

The solution was cooled to room temperature and triethylamine (0.243 g, 2.4 mmol) was added to liberate the free porphyrin base. The crude reaction mixture was then evaporated to dryness by rotary evaporation. The crude product was purified by column chromatography on silica with CH_2Cl_2/hexane (2:1) as the eluent.

Yield: 188 mg (12%)
^{1}H NMR ($CDCl_3$, ppm):δ = -2.5 (br s, 2H, NH), 1.8 (s, o-CH_3), 2.6 (s, p-CH_3), 4.1 (s, -OCH_3), 7.25 (s, H_m), 8.26 (d, 2H, J = 8.1 Hz, $H_{m'}$), 8.40 (d, 2H, J = 8.1 Hz, $H_{o'}$), 8.61, 8.68 (m, 8H, β-pyrrole). ^{13}C NMR ($CDCl_3$, ppm):δ = 21.7 (s, ArCH_3), 52.5 (s, -OCH_3), 118.1, 117.6 (2 x s, C_{meso}), 127.7 (s, C_m), 128.1 (s, $C_{m'}$), 130.1 (br s, β-pyrrole), 132.4 (s, $C_{p'}$), 134.4 (s, $C_{o'}$), 137.6 (s, C_p), 139.4 (s, C_{ipso}), 140.8 (s, C_o), 147.1 (s, $C_{ipso'}$), 167.7 (s, COO^-). ESI-MS: m/e = 799 (48%, M^+ + 1). UV-Vis (CH_2Cl_2, nm): λ = 418, 516, 548, 591, 644.

5-(p-Methoxyphenyl)-10,15,20-tri(p-methylphenyl)porphyrin. TMePP-OMe

Pyrrole (2.38 g, 35.5 mmol) was added to a solution of 4-methoxybenzaldehyde dimethyl acetal (1.24 g, 5.91 mmol) and 4-tolualdehyde (3.56 g, 29.6 mmol) in propionic acid (370 mL). The reaction mixture was refluxed for 1 hour at 130°C. After standing for 24 hours, propionic acid (300 mL) was removed by distillation. The solution was left to stand for a further 3 days, after which a purple precipitate formed. This precipitate was filtered and dried at the pump for 15 minutes. Purification was achieved by chromatography on silica with CH_2Cl_2/hexane (2:1) as the eluent.

Yield: 239 mg (5.8%)
^{1}H NMR ($CDCl_3$, ppm):δ = -2.8 (br s, 2H, NH), 2.69 (s, ArCH_3), 4.07 (s, -OCH_3), 7.27 (d, 2H, J = 8.4 Hz, $H_{m'}$), 7.54 (d, 6H, J = 7.8 Hz, H_m), 8.09 (d, 6H, J = 7.8 Hz, H_o), 8.12 (d, 2H, J = 8.4

Hz, $H_{o'}$), 8.86 (br s, β-pyrrole). ^{13}C NMR ($CDCl_3$, ppm):δ = 21.5 (s, $ArCH_3$), 55.5 (s, $-OCH_3$), 112.2 (s, $C_{m'}$), 120.1 (s, C_{meso} + $C_{meso'}$), 127.4 (s, C_m), 131.1 (br s, β-pyrrole), 134.5 (s, C_o), 134.6 (s, $C_{ipso'}$), 135.6 (s, $C_{o'}$), 137.3 (s, C_p), 139.3 (s, C_{ipso}), 159.3 (s, $C_{p'}$). ESI-MS: m/e = 687 (83%, $M^+ + 1$). UV-Vis (CH_2Cl_2, nm): λ = 420, 517, 553, 592, 652.

5-(p-Carboxylphenyl)-10,15,20-tri(p-methylphenyl)porphyrin. TMePP-COOH

4-Carboxybenzaldehyde (0.900 g, 6 mmol) and 4-tolualdehyde (2.16 g, 18 mmol) in propionic acid (250 mL) were added to a solution of pyrrole (1.61 g, 24 mmol) in propionic acid (50 mL) preheated to 130°C. The reaction mixture was refluxed for 1 hour and then propionic acid (200 mL) was removed by distillation. The solution was refrigerated for 36 hours, after which a purple precipitate formed. This precipitate was filtered, rinsed with methanol (250 mL) and dried at the pump for 15 minutes. The precipitate was then chromatographed on silica with CH_2Cl_2 as the eluent.

Yield: 644 mg (15%)

^1H NMR ($CDCl_3$, ppm):δ = -2.80 (br s, 2H, NH), 2.69 (s, $ArCH_3$), 7.53 (d, 2H, J = 7.8 Hz, H_m), 8.07 (d, 6H, J = 7.8 Hz, H_o), 8.32 (d, 2H, J = 8.4 Hz, $H_{o'}$), 8.47 (d, 2H, J = 8.4 Hz, $H_{m'}$), 8.76(d, 2H, J = 4.8 Hz, β-pyrrole ($H^3 + H^7$)), 8.83 (s, 4H, β-pyrrole (($H^{12} + H^{13} + H^{17} + H^{18}$)), 8.87 (d, 2H, J = 4.8 Hz, β-pyrrole ($H^2 + H^8$)). ^{13}C NMR ($CDCl_3$, ppm):δ = 21.5 (s, $ArCH_3$), 118.0, 120.1, 120.5 (3 x s, C_{meso}), 127.4 (s, C_m), 128.5 (s, $C_{m'}$), 130.8 (s, $C_{p'}$), 131.1 (br s, β-pyrrole), 134.5 (s, C_o), 134.7 (s, $C_{o'}$), 137.3 (s, C_p), 139.3 (s, C_{ipso}), 147.3 (s, $C_{ipso'}$), 167.4 (s, COOH). ESI-MS: m/e = 701 (10%, $M^+ + 1$). UV-Vis (CH_2Cl_2, nm): λ = 418, 514, 548, 592, 648.

Results and Discussion

A selection of seven porphyrins were synthesised and characterised. Of these porphyrins 5,10,15,20-tetraphenylporphyrin (TPP) and 5-(4-nitrophenyl)-10,15,20-triphenyl-porphyrin (TPP-NO_2) served as synthetic intermediates for the preparation of an amino substituted porphyrin. Originally, 5,10,15-trimesityl-20-(4-methyoxycarbonylphenyl)porphyrin (TMesPP-COOMe) was also going to be used to prepare other derivatives, however, yields were too low to warrant use as a synthetic intermediate. 5-(p-Methoxycarbonylphenyl)-10,15,20-tri(p-methylphenyl)porphyrin (TMePP-COOMe) can be produced in slightly higher yields and was prepared as an alternative to TMesPP-COOMe. 5-(p-Methoxyphenyl)-10,15,20-tri(p-methylphenyl)porphyrin (TMePP-OMe) was also synthesised mainly for comparative purposes, however TMePP-OMe may undergo demethylation with boron tribromide to produce an alcohol[5] which in turn may also be used for linking. This is, however, beyond the scope of this thesis and efforts were focused mainly on producing porphyrins containing an amine, a carboxylic acid and a methyl ester.

The structure determination of all the synthesised porphyrins is based mainly on ^{1}H and ^{13}C NMR data. The UV-visible and mass spectral data also support the proposed structures. The general aspects of the NMR spectra are discussed below. For a more detailed assignment of the individual porphyrins refer to the Experimental Section.

5.5 TPP AND OTHER RELATED DERIVATIVES

TPP is the simplest porphyrin structurally. It was synthesised using the universal method of Adler and Longo by refluxing pyrrole with benzaldehyde in propionic acid for 30 minutes.[13] The purple solid was filtered after cooling and washed free from soluble poly-pyrrolic impurities with methanol. The yield was not high, about 18-20%, but the synthesis was simple and direct.

When TPP reacted with fuming nitric acid in $CHCl_3$ selective and stepwise nitration of the aryl groups at the para position occured.[16] The reaction progress was monitored closely by TLC to insure total conversion of TPP to the mono-nitro derivative, TPP-NO_2. Tin chloride reduction of TPP-NO_2 in concentrated hydrochloric acid gave the known amino derivative, 5-(p-aminophenyl)-10,15,20-triphenylporphyrin (TPP-NH_2) in 70% overall yield after column chromatography (Diagram 5.5).[16]

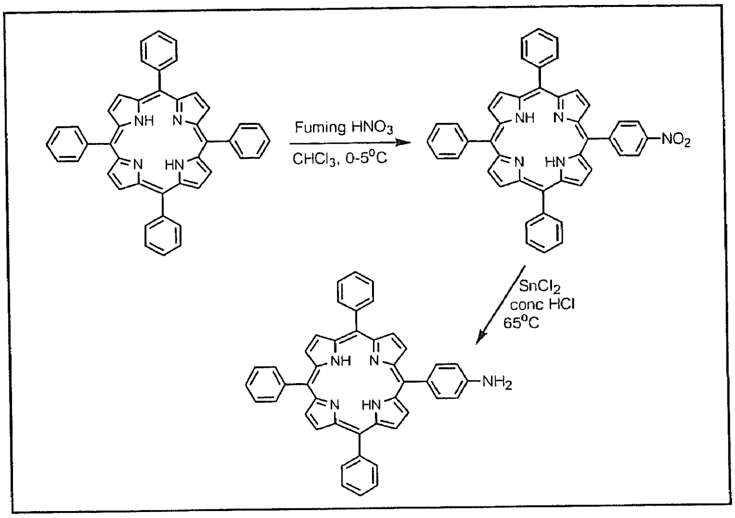

Diagram 5.5: Aryl nitration of TPP followed by reduction to the amino derivative.

^{1}H NMR spectroscopy was used for the characterisation of the three porphyrins. The NMR spectral properties are governed by the symmetry of the molecules. At room temperature, TPP possesses four-fold symmetry (D_{4h} symmetry), due to the rapid exchange of the inner two N-H protons about the four-pyrrole nitrogens.[17] This property is reflected in the ^{1}H NMR of TPP, whereby the eight equivalent β-pyrrole protons, which are deshielded by virtue of their location on the outskirts of the porphyrin π system, appear as a singlet at 8.87 ppm. In comparison, TPP-NO_2 possesses a symmetry plane defined by the nitro substituent (i.e C_2 symmetry). Thus, the β-pyrrole protons appear as a doublet (H^2 + H^8) at 8.72 ppm, as a doublet (H^3 + H^7) at 8.88 ppm and as a singlet (H^{12} + H^{13} + H^{17} + H^{18}) at 8.90 ppm. A similar β-pyrrole pattern is also observed in the spectrum of TPP-NH_2.

In addition to showing changes in the β-pyrrolic region, mono-substitution in the para position also causes changes in the phenyl region. For example, the ^{1}H NMR spectrum of TPP-NO_2 showed two new signals corresponding the phenyl protons meta and ortho to the nitro substituent at 8.54 and 8.25 ppm, whilst the ^{1}H NMR spectrum of TPP-NH_2 showed two new signals at 7.00 and 8.00 ppm. The ^{1}H NMR chemical shifts of the three related porphyrins are summarised in Table 5.1.

Table 5.1: ^{1}H NMR chemical shifts for TPP, TPP-NO_2 and TPP-NH_2.

Porphyrin	Pyrrole N-H	Aromatic Region				β-Pyrrole Region		
		$H_m + H_p$	H_o	$H_{m'}$[b]	$H_{o'}$[b]	H_2+H_8	H_3+H_7	$H_{12}+H_{13},H_{17}+H_{18}$
TPP	-2.74	7.77	8.87	-	-	8.87[a]		
TPP-NO_2	-2.71	7.72	8.22	8.54	8.33	8.72	8.88	8.90
TPP-NH_2	-2.70	7.77	825	7.00	8.00	8.97	8.87	8.88

[a] All β-pyrrole protons are equivalent in TPP. [b] Substituted phenyl ring.

The effects due to electron-donating and electron-withdrawing groups are readily apparent within this set of para-substituted porphyrins. An overlay of all the porphyrin spectra in the aromatic region are presented in Diagram 5.6. The NMR spectra show that the electron-donating properties of the NH_2 group in TPP-NH_2 causes the protons in the phenyl ring to be more shielded (upfield chemical shift), whereas electron-withdrawing groups at the para site (ie NO_2) result in decreased shielding (downfield chemical shift). Shielding-deshielding effects are more pronounced in the meta protons on the substituted phenyl ring (labelled as $H_{m'}$) than in the ortho protons (labelled as $H_{o'}$) owing to the greater electron attracting inductive effects at the position in which the effects are minimal.

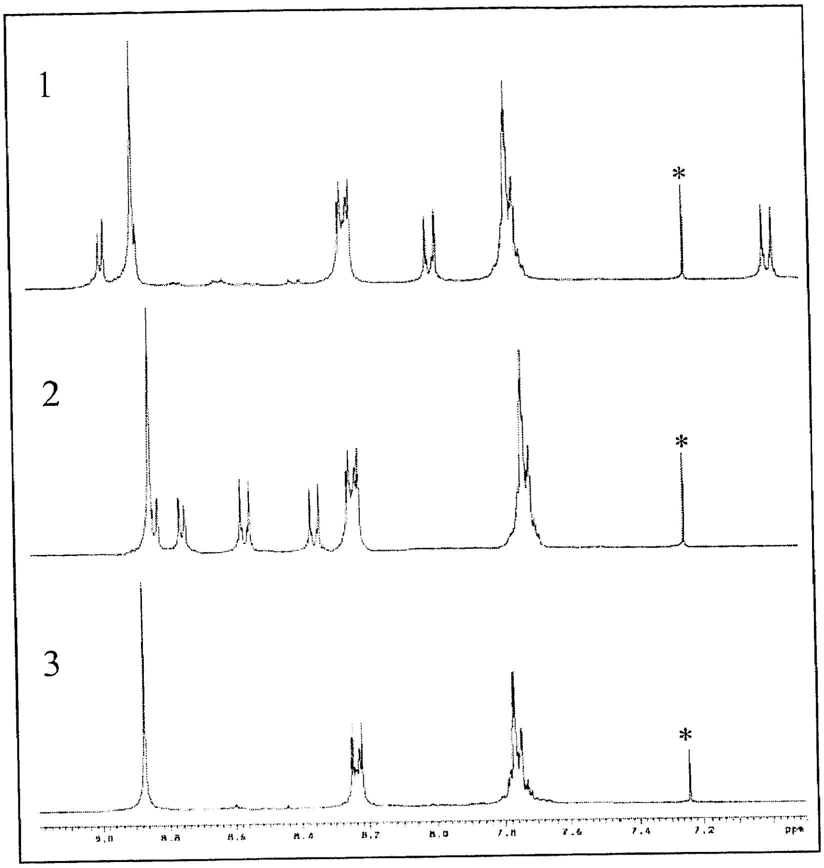

Diagram 5.6: An overlay of the aromatic region of TPP-NH_2 (1), TPP-NO_2 (2) and TPP (3). *$CHCl_3$

5.6 A_3B-PORPHYRINS

Synthesis

For the A_3B-porphyrins, TMePP-COOMe, TMePP-OMe, TMePP-COOH and TMesPP-COOMe the introduction of only one functional group on the porphyrin can be achieved by a mixed aldehyde condensation. Aldehyde B provides the reactive para substituent whilst aldehyde A serves to complete the construction of the porphyrin (Table 5.2).

Like TPP, the synthesis of TMePP-COOMe was achieved using the classical Adler condensation, from methyl 4-formylbenzoate, 4-tolualdehyde and pyrrole.[18] No purification problems with respect to poly-pyrrolic impurities were encountered since the product readily precipitated out of solution at the end of the reaction. It was however, necessary to isolate the desired methyl ester from a mixture of porphyrin products via chromatography. Similarly, TMePP-OMe was prepared by an Adler condensation of 4-methoxybenzaldehyde dimethyl acetal, 4-tolualdehyde and pyrrole. In this reaction the dimethyl acetal group is removed to give the corresponding aldehyde which is then incorporated into the porphyrin ring via the usual mechanism (refer to Diagram 5.3). It is worth noting that in the synthesis of TMePP-COOMe and TMePP-OMe, the reactant concentrations were 29.6 mmol aldehyde A, 5.91 mmol aldehyde B and 35.5 mmol pyrrole. These reactant concentrations produce the best yields of the desired mono-substituted porphyrins. Deviations from these concentrations result in a larger amount of di-substituted porphyrin products.[19]

Table 5.2: A,B-Porphyrins bearing one functional group.

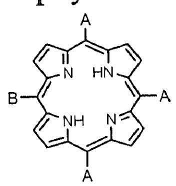

Porphyrins	A	B
TMePP-COOMe	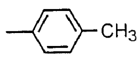	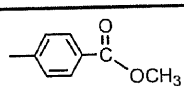
TMePP-OMe	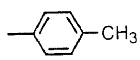	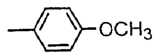
TMePP-COOH	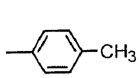	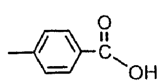
TMesPP-COOMe	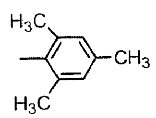	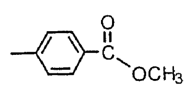

Unlike TMePP-COOMe, the porphyrinic carboxylic ester TMesPP-COOMe was not obtained by an Adler condensation of the appropriate aldehydes. When prepared by the Adler method, the porphyrin did not precipitate out at the end of the reaction. TLC showed numerous products and despite testing various solvent systems no definitive separation of the complex reaction mixture could be achieved. Consequently, TMesPP-COOMe was made by the Lindsey method.[20]

With the Lindsey method, the yield of the porphyrin is not contingent on the precipitation of the product at the end of the reaction. This method involved treating a mixture of mesitaldehyde, methyl 4-formylbenzoate and pyrrole with a BF_3-etherate catalyst followed by slow oxidation of the intermediate porphyrinogens with p-chloranil. $CHCl_3$ containing at least 0.75% ethanol was the solvent of choice because porphyrins formed by mixed aldehyde condensations with substituted benzaldehydes require BF_3-ethanol co-catalysis.[20,21] Chromatographic purification delivered the desired porphyrin in 12% yield.

Originally TMesPP-COOMe was to be hydrolysed to form a carboxylic acid for linking. Instead, the carboxyl porphyrin, 5-(p-carboxylphenyl)-10,15,20-tri(p-methylphenyl)porphyrin (TMePP-COOH) was prepared directly by an Adler condensation of 4-formylbenzoic acid, 4-tolualdehyde and pyrrole. TMePP-COOH could have been prepared by the Lindsey method, however this method requires the carboxylic acid group to be protected due to the limited solubility of 4-formylbenzoic acid in CH_2Cl_2 and $CHCl_3$. One of the simplest methods of protecting the carboxyl group uses 2-(trimethylsilyl)ethanol in the presence of DCC and DMAP. The resulting benzaldehyde bearing an ester may be deprotected under gentle conditions to give the desired carboxy-substituted porphyrin (Diagram 5.7).[20] 4-Formylbenzoic acid was, however, found to be soluble in propionic acid with the aid of sonication. Thus, rather than follow the multi-step Lindsey method, an Adler condensation was considered to be the better method for synthesising TMePP-COOH. In addition, 4-tolualdehyde was chosen over mesitaldehyde because introduction of methyl groups into the ortho-phenyl positions enhances solubility and the porphyrin does not precipitate out of solution at the end of the reaction. This in turn makes it more difficult to wash poly-pyrrolic impurities from the desired porphyrin (as experienced with the synthesis of TMePP-COOMe via an Adler condensation).

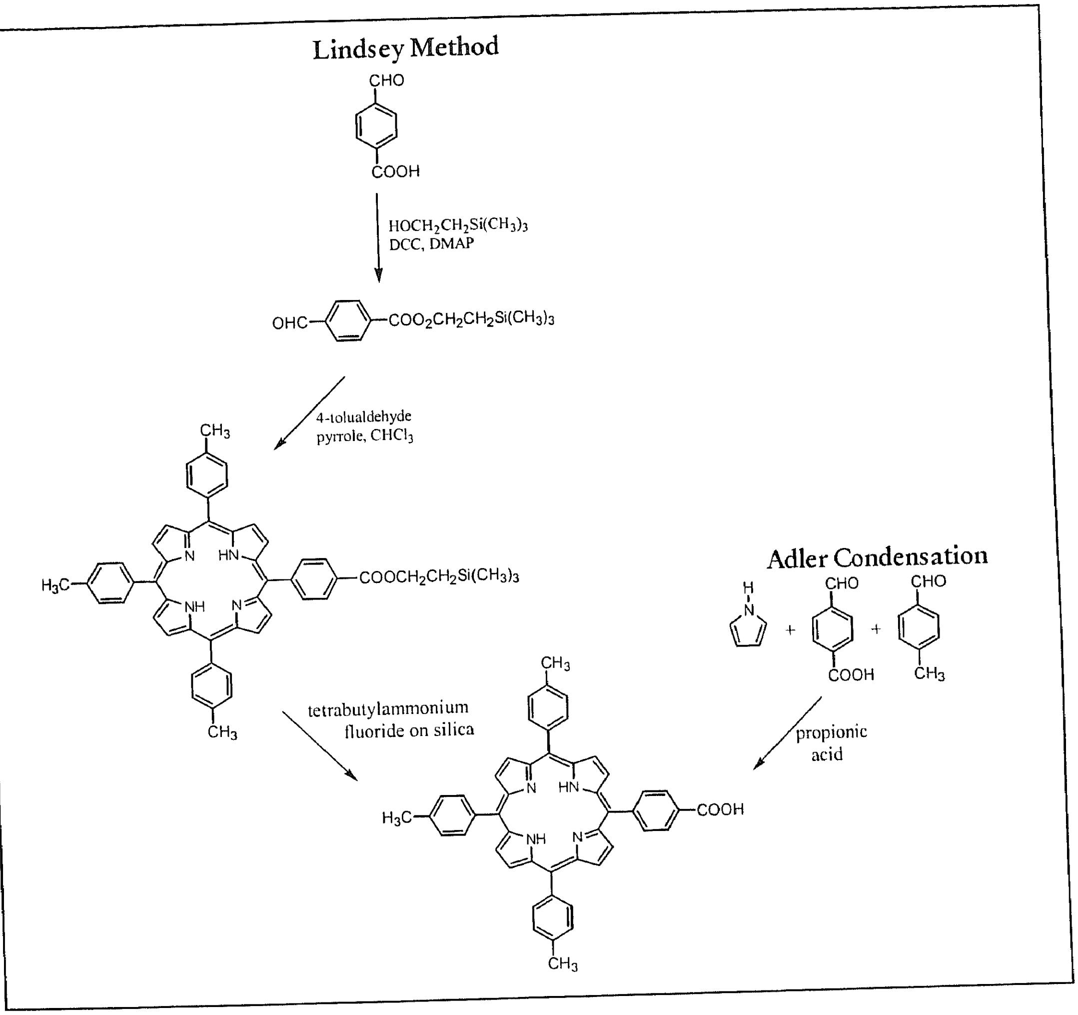

Diagram 5.7: Schematic diagram outlining the synthesis of TMePP-COOH via the Lindsey method and an Adler condensation.

Characterisation

A mixture of six porphyrins is possible from a mixed aldehyde condensation. These are depicted in Diagram 5.8. The mixture can usually be separated by column chromatography and the products are sufficiently dissimilar in the β-pyrrole region to allow identification by ^1H NMR spectroscopy.

The best separation of a porphyrin mixture was observed during the purification of TMePP-COOMe, where four out of the six possible porphyrins were isolated. TMePP-COOMe was chromatographed on silica gel with CH_2Cl_2/hexane (2:1) as the eluent. The first porphyrinic fraction was identified as tetratolyporphyrin (TTP). The ^{1}H NMR of TTP is relatively simple owing to its high symmetry. It shows the para-substituted methyl group as a singlet at 2.70 ppm, two doublets at 7.53 and 8.08 ppm (J=7.8 Hz) due to the meta and ortho-phenyl protons and a broad singlet due to the β-pyrrole protons at 8.86 ppm.

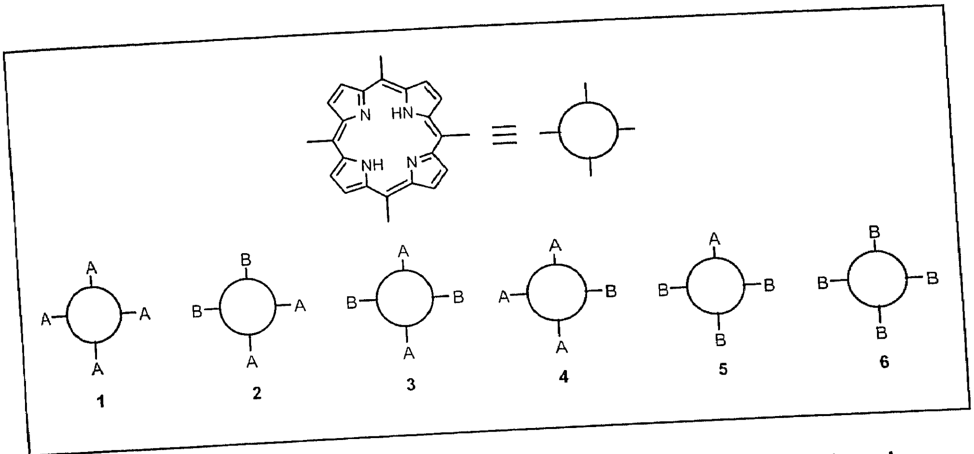

Diagram 5.8: Possible six porphyrins from a mixed aldehyde condesation.

Porphyrins 2 and 3 are the *cis*- and *trans*- di-substituted porphyrins respectively.

The second fraction was the desired methyl ester, TMePP-COOMe. The most characteristic feature of the ^{1}H NMR spectrum of TMePP-COOMe is the singlet at 4.09 ppm, which arises from the methyl ester moiety. The ^{1}H NMR spectrum of TMePP-COOMe in the aromatic region is presented in Diagram 5.8 (spectrum 2). The diagram shows the β-pyrrole protons as a doublet at 8.75 ppm (H^{3} + H^{7}), a singlet at 8.84 ppm ((H^{12} + H^{13}) and (H^{17} + H^{18})) and a doublet at 8.86 ppm (H^{3} + H^{7}). It is interesting to note that the protons (H^{12} + H^{13}) and (H^{17} + H^{18}) which possessed a quasi-equivalent environment, are incidentally equivalent. The spectrum also features two AB-type splitting patterns belonging to the two different ortho and meta phenyl protons.

Finally, the third porphyrin fraction was a mixture of di-substituted porphyrins. These porphyrins were later separated on a second silica gel column and identified as 5,10-di(p-methoxycarbonyl)-15,20-di(p-methylphenyl)porphyrin (DMePP-cisCOOMe) and the 5,15-di(p-methoxycarbonyl)-10,20-di(p-methylphenyl)porphyrin (DMePP-transCOOMe). These products are the *cis* and *trans* isomers respectively. *Cis* and *trans* isomers are readily distinguished by their ^1H NMR spectra. For the cis isomer, the β-pyrrole region shows a doublet at 8.76 ppm ($H^3 + H^{12}$, J=6.4 Hz), two singlets at 8.78 and 8.86 ppm ($H^7 + H^8$ and $H^{17} + H^{18}$) and another doublet at 8.87 ppm ($H^2 + H^{13}$, J=5.3 Hz). Such a pattern is indicative of four different β-hydrogen environments, only possible with a *cis* configuration of the meso substituents. In contrast, the *trans*-configured product shows an AB-type spin system, indicative of only two different β-hydrogen environments. An overlay of the aromatic region for each of the different porphyrins isolated during the synthesis of TMePP-COOMe is presented in Diagram 5.9.

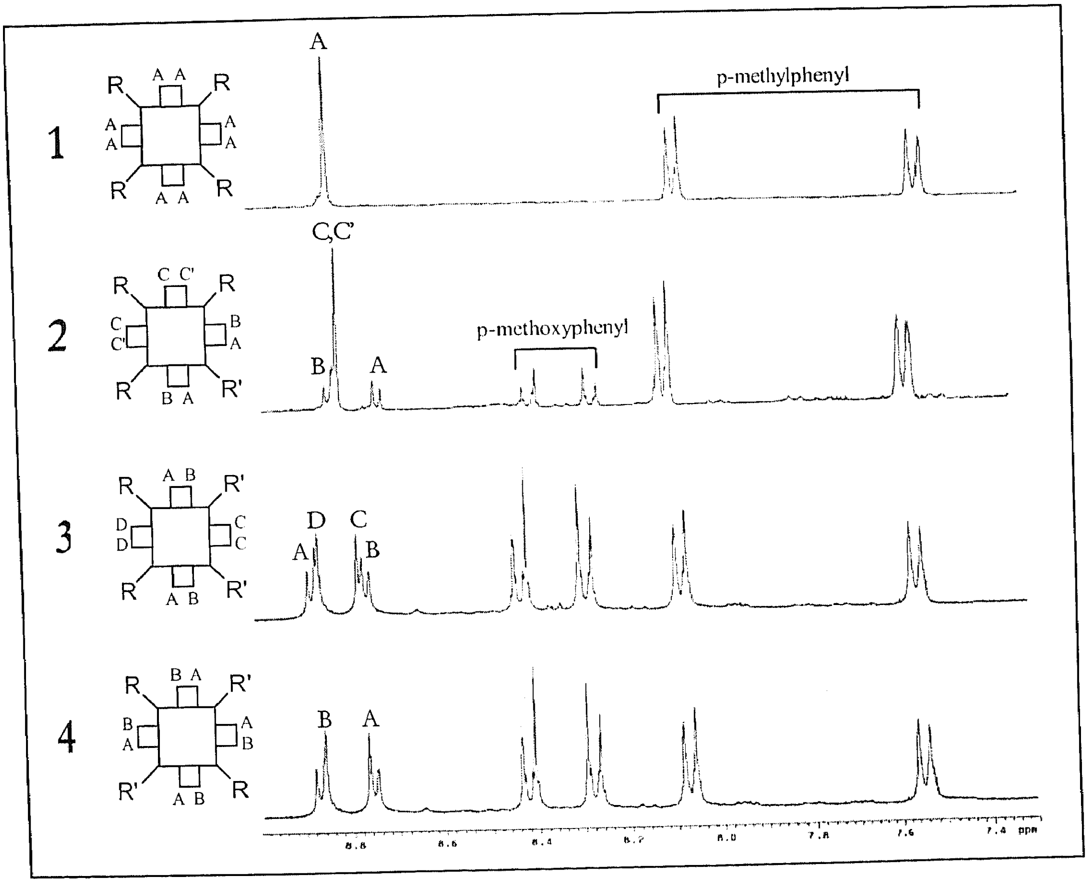

Diagram 5.9: Aromatic region of the ^1H NMR spectra of TTP (1), TMePP-COOMe (2), DMePP-cisCOOMe (3) and DMePP-transCOOMe (4). A-D, β-pyrrole protons; R, p-methylphenyl; R', p-methoxyphenyl.

The main purpose for this reaction was to isolate relatively pure TMePP-COOMe. The spectroscopic data for TMePP-COOMe was identical in all respects with that found in the literature.[18]

The structure of TMePP-OMe is evident from the ^{1}H NMR spectrum. In the aliphatic region, it showed a singlet at 2.70 ppm due to the para-substituted methyl groups and a singlet at 4.07 ppm due to the methyoxy group. In the aromatic region, the protons ortho and meta to the methyl substituents (labelled H_m and H_o) appear as a typical AB-type pattern at 7.5 and 8.0 ppm. Similarly, the protons ortho and meta to the methoxy substituent (labelled $H_{m'}$ and $H_{o'}$) also produce a well defined AB-type pattern at 7.3 and 8.1 ppm. These resonances lie further upfield compared to that of TMePP-COOMe due to the presence of the methoxy substituent as opposed to a methyl ester moiety. It is worth noting that the doublet due to the protons next to the methoxy group ($H_{o'}$) are slightly obscured by the doublet due to the protons next to the methyl group (H_o). In addition the ^{1}H NMR spectrum displays a very broad singlet at 8.86 ppm due to the β-pyrrole protons. This indicates that the methoxy substituent does not appear to induce important electronic and/or steric contributions to modify the chemical shifts of the adjacent β-pyrrole protons. Thus, no differentiation between the eight β-pyrrole protons is observed.

Supporting evidence for the formation of TMePP-OMe has been obtained by ^{13}C NMR studies. The ^{13}C NMR spectrum of TMePP-OMe showed 12 carbon signals, which were resolved through a DEPT experiment into two methyl, five methine and five quaternary carbons. The key carbon signals include the methine signal at 112 ppm attributable to the carbons ortho to the methoxy substituent ($C_{m'}$) and the quaternary carbon signal at 159 ppm assigned to the carbon bearing the methoxy substituent ($C_{p'}$).

As expected, the ^{1}H NMR of TMePP-COOH is remarkably similar to that of TMePP-COOMe, it differs merely by the absence of the methyl signal of the ester group at 4.07 ppm. The ^{13}C NMR spectrum recorded for TMePP-COOH is in complete harmony with the proposed constitution. Assignments do not merit special comment and can be found listed in the Experimental Section.

For TMesPP-COOMe, the introduction of methyl groups into the ortho-phenyl positions not only affects the solubility of the porphyrin but it also significantly changes the appearance of the ^{1}H NMR spectrum. The spectrum exhibits two singlets for the ortho and para-substituted methyl groups at 1.8 and 2.6 ppm, a singlet at 4.1 ppm attributable to the methyl ester moiety and another singlet at 7.25 ppm due to the protons on the meta position of the mesityl rings (H_m). Even though the H_m protons lie very close to the $CDCl_3$ signal they are still visible. The protons on the methyoxycarbonyl substituted phenyl ring ($H_{m'}$ and $H_{o'}$) are seen as two doublets at 8.3 and 8.4 ppm. In addition the β-pyrrole protons give a series of multiplets centred around 8.6 and 8.7 ppm. In the ^{13}C NMR spectrum of TMesPP-COOMe, 12 signals were observed. The observed chemical shifts compare well with that of TMePP-COOMe. All ^{13}C NMR data can be found in the Experimental Section.

One characteristic feature of all the porphyrin ^{1}H NMR spectra described above is the broad signal at very high field (around -2.6 ppm). This signal arises from the inner N-H protons located in the shielded core of the porphyrin ring.

References

1 A. J Pope and S. G Brown, British Journal of Urology, 1991, **68**, 1-9.

2 T. J. Dougherty, Seminars in Surgical Oncology, 1986, **2**, 24-37.

3 L. G. Marzilli, G. Petho, M. Lin, M. S. Kim and D. W. Dixon, J. Amer. Chem. Soc., 1992, 114, 7575-7577.

4 L. R. Milgrom, J. Chem. Soc., Perkin Trans. 1,1983, 2535-2539.

5 L. R. Milgrom, J. Chem. Soc., Perkin Trans. 1,1984, 1483-1487.

6 B. Meunier, Chem. Rev., 1992, 1411.

7 M. R. Wasielewski, Chem Rev., 1992, 435.

8 L. R. Milgrom, *The Colours of Life: An Introduction to the Chemistry of Porphyrins and Related Compounds*, Oxford University Press, New York, 1997.

9 P. J. Rothemund, J. Amer. Chem. Soc., 1935, **57**, 2010.

10 P. J. Rothemund, J. Amer. Chem. Soc., 1936, **58**, 625.

11 P. J. Rothemund, J. Amer. Chem. Soc., 1941, **63**, 267.

12 J. B. Kim, A. D. Adler, F. R. Longo, In *The Porphyrins*. (Ed. D. Dolphin), Academic Press, New York, 1978, Vol I, pp. 85-100.

13 A. D. Adler, F. R. Longo, J. D. Finarelli, J. Goldmacher, J. Assour and L. J. Korsakoff, J. Org. Chem., 1967, **32**, 476.

14 J. S. Lindsey, I. C. Schreiman, H. C. Hsu, P. C. Kearney and A. M. Marguueretta, J. Org. Chem., 1987, **52**, 827-836.

15 J. S. Lindsey, I. C. Schreiman and H. C. Hsu, Tetrahedron Lett., 1986, 27, 4969.

16 W. J. Kruper, T. A. Chamerlin and M. Kochanny, J. Org. Chem., 1989, **54**, 2753-2756.

17 T. R. Janson and J. J. Kratz, In *The Porphyrins*. (Ed. D. Dolphin), Academic Press, New York, 1979, Vol IV, pp. 1.

18 H. K. Hombrecher and S. Ohm, Tetrahedron, 1993, 49, 2447-2456.

19 Personnel Communications with Prof. H. K. Hombrecher of Institut fur Chemie der Medizinischen Universitat zu Lubeck, Germany and Dr M. Antolovich of Charles Sturt University, Wagga Wagga.

20 J. S. Lindsey, S. Prathapan, T. E. Johnson and R. W. Wagner, Tetrahedron, 1994, 50, 8941-8968.

21 J. S. Lindsey and R. W. Wagner, J. Org. Chem., 1989, **54**, 828-836.

CHAPTER 6

SYNTHESIS OF NEW AMINO ACID PLATINUM-PORPHYRIN CONJUGATES

Introduction

The design and construction of new anti-cancer drugs with tailor made structural and functional properties is a goal that is currently being vigorously pursued. A promising approach toward this goal would be to take advantage of the existing chemotherapeutic/photosensitising agents by incorporating selective components into one structural ensemble. Our research has taken on this approach by coupling porphyrins to platinum-based derivatives. It is hoped that the new platinum-porphyrin conjugates would display enhanced tumor selectivity due to the porphyrin, whilst inheriting the cytotoxicity from the active platinum component.

Ideal chemistry would allow coupling to be carried out rapidly and quantitatively under mild conditions, avoiding side-reactions without challenging the integrity of other components and generating only easily removed by-products. With this in mind, there are a number of coupling chemistries to explore. The vast majority of these involve conjugation by formation of an amide bond, however linking may also be achieved through transesterification.

6.1 TRANSESTERIFICATION

Transesterification is the process by which one ester is converted into another (equation (1)). Transesterification is catalysed by either acids (H_2SO_4 or dry HCl) or bases (alkoxide ion).[1]

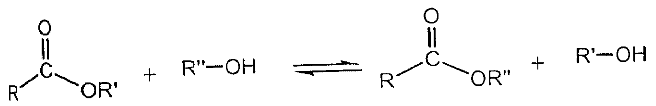

(1)

Since transesterification requires the presence of acid catalysts, severe problems are usually encountered with acid-sensitive compounds. Furthermore, this reaction is reversible, often exhibiting an unfavourable equilibrium constant. As a consequence, it is necessary to remove water and/or use a large excess of alcohol in order to achieve reasonable yields of product. Finally, transesterification of tertiary or sterically hindered alcohols is generally ineffective because of the increased steric interaction in the tetrahedral intermediate. One method that claims to overcome these limitations uses lithium alkoxides in tetrahydrofuran (THF) for effecting transesterification (equation (2)).[2]

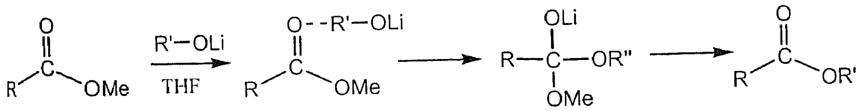

(2)

6.2 AMIDE BOND FORMATION

Amides are of great biological importance. The linkages that join individual amino acids to form proteins are primarily amide linkages. As a consequence, much research has been done on amide bond formation.

Ordinary carboxylic acids form salts with amines at ambient temperatures, and transformation of these dry salts directly into amides requires severe heating. This is generally a poor method for preparing amides and such harsh conditions are quite incompatible with structural subtleties of the molecule. Consequently, activation or attachment of a leaving group to the acyl carbon of the carbonyl component to enable attack by an amino group is necessary. The most common methods of activation and coupling are briefly described below.[1,3,4,5]

Acyl chlorides

Conversion of a carbonyl group into an acyl chloride is one of the most classical methods of activating carboxylic acids for amide synthesis. Acyl chlorides are easily prepared from carboxylic acids and react rapidly with amines at low temperatures to produce amides in high yields (equation (3)).

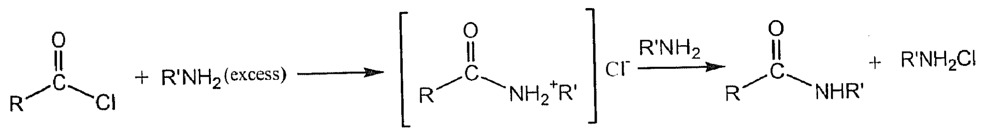

(3)

The reagents traditionally used for acyl chloride formation include thionyl chloride ($SOCl_2$), oxalyl chloride ($(COCl)_2$), phosphorus trichloride (PCl_3) and phosphorus pentachloride (PCl_5). Thionyl chloride is particularly useful for the by-products formed are gases and thus easily separated from the acyl chloride. In addition, thionyl chloride has low boiling point of 79°C so excess thionyl chloride is easily removed by distillation. Oxalyl chloride is quickly gaining popularity due to the milder reaction conditions allowed by the reagent.[6] Aprotic solvents such as $CHCl_3$, DMF and pyridine must be applied in the chlorination.

Acyl Azides

Another widely used method for amide bond formation involves activation of the carboxyl group by conversion to an acyl azide. Conversion to the azide can be achieved by treating the ester with hydrazine to give the acyl hydrazide. Then the hydrazide is treated with nitrous acid to give the acyl azide. Acyl Azides are less reactive than acyl chlorides and more reactive than esters.

When acyl azides are mixed with an amine, typical nucleophilic substitution occurs. The essential chemistry of the approach is summarised in equation (4).

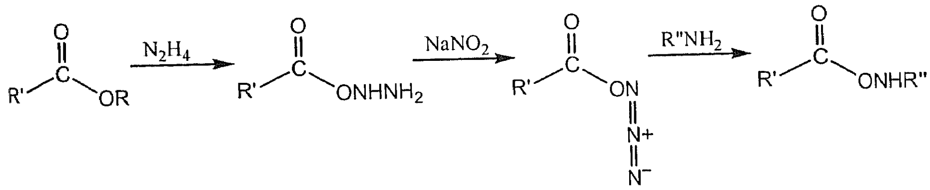

(4)

Anhydrides

The reaction of ammonia and amines with anhydrides is analogous to that of acyl chlorides. The reaction yields an amide and one equivalent of carboxylic acid. Since the liberated acid reacts to form a salt with the ammonia or the amine, it is necessary to employ an excess of that reagent (equations (5) and (6)). Anhydrides are generally more reactive than esters in their reactions with ammonia and amines but less reactive than acyl chlorides.

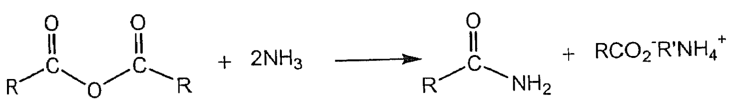

(5)

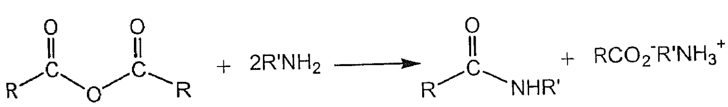

(6)

Active Esters

Esters also react with ammonia and amines to yield the corresponding amide and the alcohol of the ester (equation (7)). This reaction takes place more slowly than those of acyl chlorides and anhydrides, but they are synthetically useful in cases where the corresponding acyl chloride or anhydride is unstable or not easily available. An example of such a case is when the molecule contains a hydroxyl group. Since the hydroxyl group reacts rapidly with an acyl chloride, all attempts to prepare the acyl chloride would lead to a polymer.

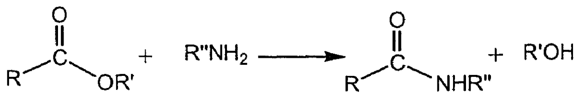

(7)

The reaction between esters and ammonia or amines is facilitated by the leaving ability of the ester group. A large number of active esters have been investigated. From these, the esters of phenols and other acidic functionalities are considered to be especially reactive. A selection of active esters is shown in Diagram 6.1.

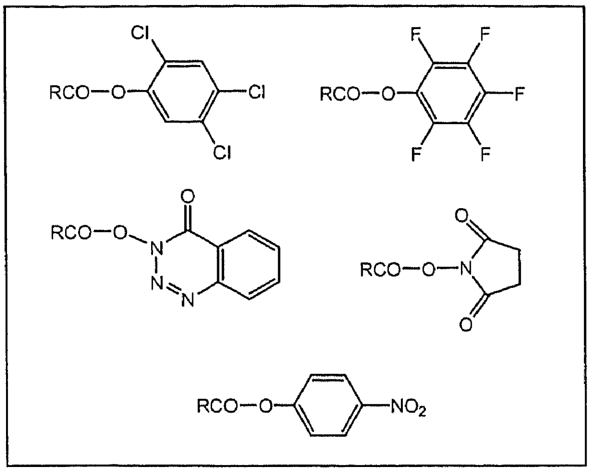

Diagram 6.1: Active esters.

When deciding on which active ester to use, as well as reactivity, the ease of co-product removal is also an important consideration. For example, in the synthesis of a water-insoluble product, a succinimido ester coupling is especially convenient, since N-hydrosuccinimide is very water-soluble. If on the other hand, the product is water-soluble, a halophenyl ester is the best choice, for halophenyls are ether soluble.

Carbodiimide reagents

One especially useful coupling reagent for amide synthesis is N,N-dicyclohexylcarbodiimide (DCC). DCC is commercially available and is prepared from cyclohexylamine and carbondisulfide. DCC is an effective catalyst for the condensation of carboxylic acids with alcohols and amines. The reagent promotes amide formation by reacting with the carboxyl group of an acid and activating it toward nucleophilic substitution.

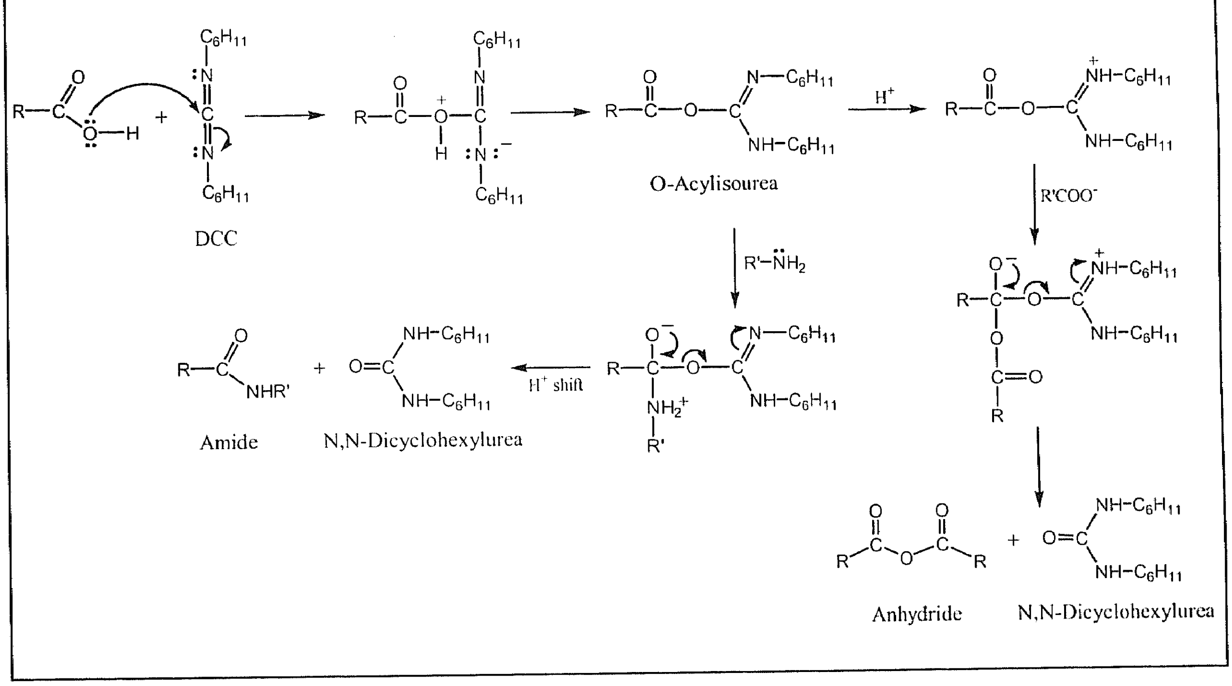

Diagram 6.2: Reactions of DCC with carboxylic acids.

The probable mechanism for the DCC coupling reaction was first suggested in 1953[7] and is schematically outlined in Diagram 6.2. The initial reaction takes place between the free carboxyl group and the carbodiimide to give an O-acylisourea. The intermediate O-acylisourea is an activated carboxylic acid derivative that is similar in reactivity to an anhydride or an acyl chloride. The amine then attacks at the carbonyl group of the O-acylisourea, generating the product with concomitant formation of an N,N-dicyclohexylurea. Since N,N-dicyclohexylurea is highly insoluble in most solvents, its separation from the desired product is very easy. Alternatively, the

O-acylisourea can be attacked by a second carboxylate to give the anhydride, which can then be attacked by the amine, giving the amide and regenerating one of the carboxylates.[7]

DCC activation is very dependent on the solvent. In solvents such as $CHCl_3$ and CH_2Cl_2 activation is rapid, however activation is sluggish in dipolar solvents such as DMF. In aqueous solutions, the water-soluble carbodiimide, 1-ethyl-3-(3-dimethylaminopropyl)carbodiimide hydrochloride (EDAC) may be used as an alternative to DCC.

The intermediate O-acylisourea species shown in Diagram 6.2 is highly reactive and significant side-reactions may occur. One of the most disturbing side-reactions in DCC-mediated coupling is the formation of N-acylurea (Diagram 6.3). N-acylurea results from extensive racemisation of the carboxyl components or by collapse of the O-acylisourea by intramolecular acyl transfer.

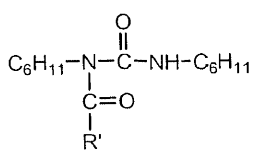

Diagram 6.3: N-Acylurea.

N-acylurea formation not only severely limits the yield but it may also give rise to purification problems. These difficulties may be greatly reduced by performing the coupling in the presence of a suitable α-nucleophile that is able to react rapidly with the O-acylisourea before any side-reactions take place. An acylating agent of lower potency is formed. These are still reactive with respect to aminolysis but do not lead to racemisation or other side reactions. Two of the most commonly used additives, which in effect generate an active ester *in situ*, include N-hydrosuccinimide (NHS) and 1-hydroxybenzotriazole hydrate (HOBT). The reaction of O-acylisourea with HOBT has been illustrated in Diagram 6.4.

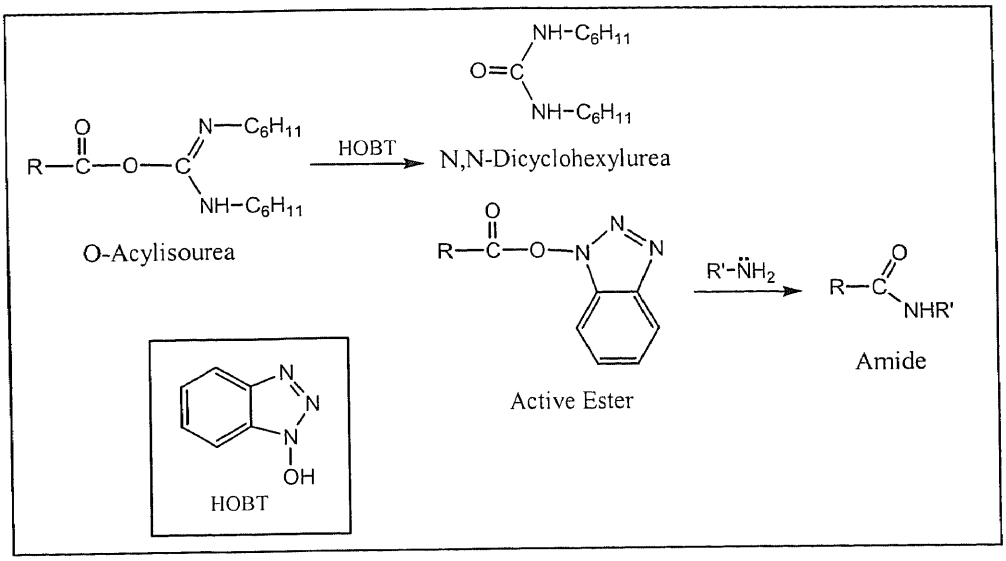

Diagram 6.4: Reaction of O-acylisourea with HOBT.

Out of the many different coupling chemistries described above, our research has focused on creating a platinum-porphyrin conjugate through ester aminolysis, transesterification, and by standard carbodiimide-mediated coupling. From these, the procedures utilising coupling reagents were the most successful. The great advantage to these procedures is that the sensitive platinum complex is not exposed to harsh reaction conditions.

Experimental

6.3 MATERIALS

The porphyrins, TMePP-COOMe and TPP-NH_2 were prepared according to the procedures described in Chapter 5. The platinum derivatives, $[Pt(L\text{-asp-N,O})(NH_3)_2]^+$ and $[Pt(L\text{-serine})(NH_3)_2]^+$ used in the coupling reactions were synthesised according to the procedures described in Chapter 4. 5-(4-Aminophenyl)-10,15,20-tris(4-sulfonatophenyl)porphyrin ($TPPS_3$-NH_2) was kindly donated by Dr Michael Antolovich at Charles Sturt University, Wagga Wagga.

All solvents and reagents were of reagent grade quality and were purchased from Aldrich and Ajax Chemicals. Dry THF (sodium and benzophenone) was employed. A commercially available solution of n-butyllithium (n-BuLi) in hexane (1.6 M) was used without further purification.

Column chromatography was performed on silica gel (Kieselgel 60G, Merck) using $CHCl_3$, or CH_2Cl_2 as the eluent. A column size of 180 mm by 12 mm in diameter or 360 mm by 50 mm in diameter was used under gravity. Merck precoated plates (silica gel 60, 2 mm) were used for TLC. For the water-soluble products, column chromatography was performed on Sephadex-G10 column purchased from Pharmacia.

6.4 MEASUREMENTS

^1H and ^{13}C NMR spectra were obtained in the indicated deuteriated solvents with a Varian Unity-Plus 300 spectrometer. Chemical shifts are reported in ppm relative to TMSP or TMS. Coupling constants are expressed in Hz.

6.5 PREPARATION OF A TETRAPHENYLBORATE SALT

A tetraphenylborate salt was prepared by adding an equimolar aqueous solution of sodium tetraphenylborate ($(C_6H_5)_4BNa$) to a concentrated solution of $[Pt(L\text{-}asp\text{-}N,O)(NH_3)_2]^+$ in water. The fine white precipitate, which separated out immediately, was filtered, protected from ambient light and dried over P_2O_5.

6.6 SYNTHESIS OF PLATINUM-PORPHYRIN CONJUGATES

Conjugation of [Pt(L-asp-N,O)(NH_3)$_2$](C_6H_5)$_4$B to TPP-NH_2 using the carbodiimide, N,N-Dicyclohexylcarbodiimide (DCC). Conjugate 1.

[Pt(L-asp-N,O)(NH_3)$_2$](C_6H_5)$_4$B (142 mg, 220 μmol) was added to a solution of HOBT (29.7 mg in 220 μL of DMF) and DCC (220 μL, 1 M in CH_2Cl_2). The combined mixture was stirred vigorously for 15 minutes. The reaction mixture was centrifuged to remove a small amount of dicyclohexylurea and the supernatant was added dropwise to a solution of TPP-NH_2 (69.3 mg, 110 μmol) in CH_2Cl_2 (30 mL). The solution was protected from ambient light and stirred overnight at room temperature.

Unreacted [Pt(L-asp-N,O)(NH_3)$_2$](C_6H_5)$_4$B was removed by filtration and the red filtrate was evaporated to dryness. The residue was chromatographed on silica using $CHCl_3$ as the eluent.

Yield: 63.5 mg (45%)

^{1}H NMR ($CDCl_3$, ppm):δ = -2.80 (br s, 2H, pyrrole NH), 3.73 (br s, 6H, NH_3), 4.00 (m, 1H, H^1), 3.43 (m, 2H, H^2, H^3), 7.00-7.20 (m, 12H, (C_6H_5)$_4$B), 7.38 (d, 2H, J = 8.1 Hz, $H_{m'}$), 7.61 (m, 8H, (C_6H_5)$_4$B), 7.76 (m, 9H, H_m + H_p), 8.08 (s, 1H, amide NH), 8.13 (d, 2H, J = 8.1 Hz, $H_{o'}$), 8.20 (m, 6H, H_o), 8.72 (d, 2H, J = 4.8 Hz, β-pyrrole (H^3 + H^7)), 8.84 (s, 4H, β-pyrrole ((H^{12} + H^{13} + H^{17} + H^{18})), 8.85 (d, 2H, J = 4.8 Hz, β-pyrrole (H^2 + H^8)). ^{13}C NMR ($CDCl_3$, ppm):δ = 49.2 (s, β-CH_2), 53.3 (α-CH), 120.3 (s, $C_{m'}$), 121.8 (s, C_{meso}+ $C_{meso'}$), 126.7 (s, C_m), 127.7 (s, C_p), 131.1 (br s, β-pyrrole), 133.6 (s, $C_{o'}$), 134.6 (s, C_o), 138.2 (s, $C_{ipso'}$ + $C_{p'}$), 142.2 (s, C_{ipso}), 193.3 (s, α-COO^-), 222.5 (s, CONH). IR (Nujol, cm^{-1}): 3467-3250 (br, ν(N-H)), 1637 (s, C=O), 1576 (s, δ_s(N-H)).

Conjugation of [Pt(L-asp-N,O)(NH_3)$_2$]Cl to TPPS$_3$-NH_2 using the water-soluble carbodiimide, 1-ethyl-3-(3-dimethylaminopropyl)carbodiimide hydrochloride (EDAC). Conjugate 2.

A solution containing [Pt(L-asp-N,O)(NH_3)$_2$]Cl (36.2 mg, 91.4 μmol) and EDAC (17.5 mg, 91.4 μL) in water (5 mL) was stirred vigorously for 15-20 minutes. This was then added dropwise to an aqueous solution (20 mL) of $TPPS_3$-NH_2 (70.7 mg, 91.4 μmol). The combined mixture was stirred overnight at room temperature before being evaporated. The crude product was purified by column chromatography on sephadex-G10 with water as the eluent.

Yield:59.2 mg (52%)

^{1}H NMR (D_2O, ppm):δ = 3.57 (q, 1H, H^1), 2.54, 2.29 (2 x m, J_{12} = 3 Hz, J_{13} = 10.2 Hz and J_{23} = 17.1 Hz, 2H, H^2, H^3), 6.93 (br m, 2H, β-pyrrole (H^3 + H^7)), 7.08 (br m, 2H, β-pyrrole (H^2 + H^8)) 7.20 (br s, 4H, β-pyrrole ((H^{12} + H^{13} + H^{17} + H^{18})), 7.69 (br m, 2H, $H_{o'}$), 7.91 (br m, 8H, $H_{m'}$ + H_m), 8.11 (br m, 6H, H_o). ^{13}C NMR (D_2O, ppm):δ = 49.8 (s, β-CH_2), 52.6 (α-CH), 120.7 (s, $C_{m'}$), 122.4 (s, C_{meso}+ $C_{meso'}$), 126.6 (s, C_m), 131.1 (br s, β-pyrrole), 133.6 (s, $C_{o'}$), 134.6 (s, C_o), 137.7 (s, C_p+ $C_{p'}$), 138.4 (s, $C_{ipso'}$), 146.2 (s, C_{ipso}), 191.3 (s, α-COO^-), 220.1 (s, CONH). IR (Nujol, cm^{-1}): 3513-3260 (br, ν(N-H)), 1642 (s, C=O), 1577 (s, δ_s(N-H)).

Attempted Transesterification of TMePP-COOMe with [Pt(L-serine)(NH_3)$_2$](C_6H_5)$_4$B.

[Pt(L-serine)(NH_3)$_2$](C_6H_5)$_4$B (48.9 mg, 750 μmol) in THF (1 mL) was placed in a dried 10 mL round bottom flask. Then n-BuLi (24.8 mg, 240 μmol of a 1.6 M hexane solution) was added at 3-5°C. The reaction mixture was gently warmed up to room temperature, then a solution of TMePP-COOMe (53.5 mg, 750 μmol) in THF (3 mL) was added. The combined mixture was stirred at room temperature overnight. Then CH_2Cl_2 (25 mL) and NH_4Cl (50 mL of a 2 M solution) were added. The organic layer was separated and dried over sodium sulfate (Na_2SO_4). The solvent was evaporated and the residue chromatographed on silica with CH_2Cl_2/hexane (2:1) as the eluent.

Yield: No detectable amount of a linked platinum-porphyrin conjugate.

Results and Discussion

Attempts to use ester aminolysis for amide bond formation was first made in the infancy of the project with very little success (equations (8) and (9)). It was envisaged that the methyl esters employed were not of sufficient reactivity. If this approach were to be successful more reactive esters would have to be made. Attempts to synthesise platinum derivatives containing a benzyl ester moiety were fruitless. The limitation of making porphyrins with more reactive esters (e.g. pentafluorophenyl esters or succinimidyl esters, Diagram 6.1) relates to their laborious preparation, usually involving numerous clean-up steps plagued with low yields. Therefore alternative procedures which utilised the range of porphyrins and platinum derivatives already synthesised were adopted.

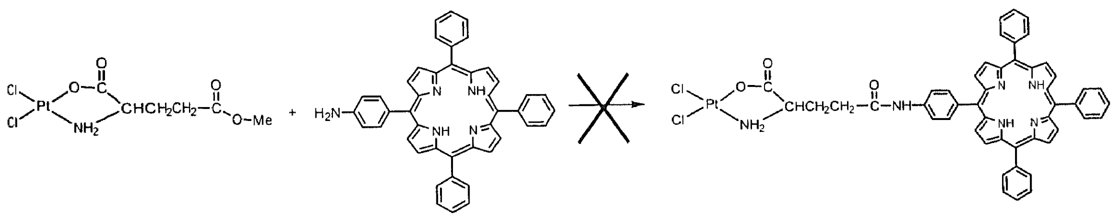

(8)

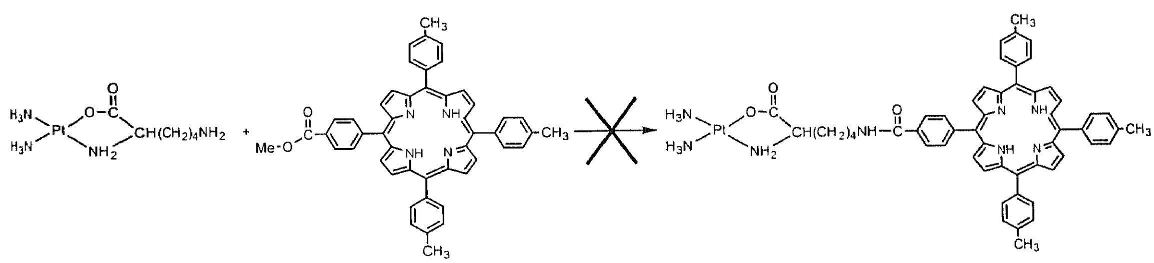

(9)

6.7 TRANSESTERIFICATION

The second coupling strategy that has been explored involved the reaction of TMePP-COOMe with $[Pt(L\text{-serine})(NH_3)_2]^+$ through transesterification. The literature method[2,8] that was employed claimed that methyl esters undergo efficient transesterification with alcohols in the presence of butyllithium in THF. However, even after considerable experimentation, no detectable yields of a linked platinum-porphyrin conjugate were afforded. Although inclusion of this method in the Experimental section is unconventional, details have been given for easy reference.

The lack of success with the transesterification reaction may be due to a number of factors. Firstly the extreme basicity of the butyllithium may adversely affect the integrity of the platinum complex. Secondly, a major limitation of transesterification with lithium alkoxides involves alcohols that strongly complex to the lithium, thus preventing further reaction of the lithium alcoholate (refer to equation (2)) with the ester. It is possible that the $[Pt(L\text{-serine})(NH_3)_2]^+$ complex has become strongly bound to the lithium and has subsequently passed through the column undetected.

6.8 CARBODIIMIDE-MEDIATED COUPLING

Over the years carbodiimides have proven to be useful reagents and are frequently employed in coupling reactions. The great advantages of carbodiimide-mediated coupling are that the procedures are extremely convenient and mild. For example, DCC-mediated coupling is effected by stirring a CH_2Cl_2/DMF solution of the carboxylic acid, HOBT and DCC for 15 minutes. The dicyclohexylurea by-product is easily removed by centrifugation and the supernatant is allowed to react with an amine for 18 hours. Evaporation of the solvent and purification by simple column chromatography provides the amide in reasonable yields. Similar reactions can be carried out in aqueous solutions using a water-soluble carbodiimide such as EDAC. Coupling procedures which use both DCC and EDAC in the conjugation of $[Pt(L\text{-asp-N,O})(NH_3)_2]^+$ and an amino-porphyrin have been explored. Both reactions have proven to be successful and are briefly discussed below.

DCC-Mediated Coupling

TPP-NH_2 and [Pt(L-asp-N,O)$(NH_3)_2$]$(C_6H_5)_4$B were subjected to standard DCC-mediated coupling conditions to apparently give a single compound as demonstrated by TLC. Chromatography on silica, however, indicated inhomogenity; a dark brown leading band followed by a second band that streaked. The ^{1}H NMR of the leading band revealed that it was simply unreacted porphyrin.

The ^{1}H NMR of conjugate 1 (band 2) can be divided into three regions: the β-pyrrole region, aromatic region and the aliphatic region. The β-pyrrole region showed a doublet at 8.85 ppm (H^2 + H^8, J = 8.1 Hz), a strong singlet at 8.84 ppm (H^{12} + H^{13} + H^{17} + H^{18}) and another doublet at 8.74 ppm (H^3 + H^7, J = 8.1 Hz). In the aromatic region, the protons ortho and meta to the amide bond (labelled $H_{m'}$ and $H_{o'}$) produced a well-defined AB-type pattern at 7.4 and 8.1 ppm. These resonances lie further downfield compared to that of TPP-NH_2 due to the deshielding effects of the amide carbonyl. The aromatic protons on the unsubstituted phenyl rings (i.e. those in positions 10, 15 and 20 on the porphyrin ring) remained essentially constant. This is not surprising for they are a considerable distance away from the amide bond. Outlined in Diagram 6.5 is a schematic representation of the resonances in the β-pyrrole and aromatic region that undergo significant changes as a result of the amide linkage.

In the aliphatic region, the methine and methylene protons of the aspartic acid appeared as multiplets around 4.0 and 3.4 ppm respectively. A more detailed inspection of the structural parameters is impeded by the poor resolution. The ^{1}H NMR spectrum also featured a broad signal at -2.8 ppm due to the pyrrole N-H protons, a series of multiplets in the 7.0-7.6 ppm region due to the tetraphenlyborate counterion and a singlet at 8.1 ppm due to the amide N-H proton.

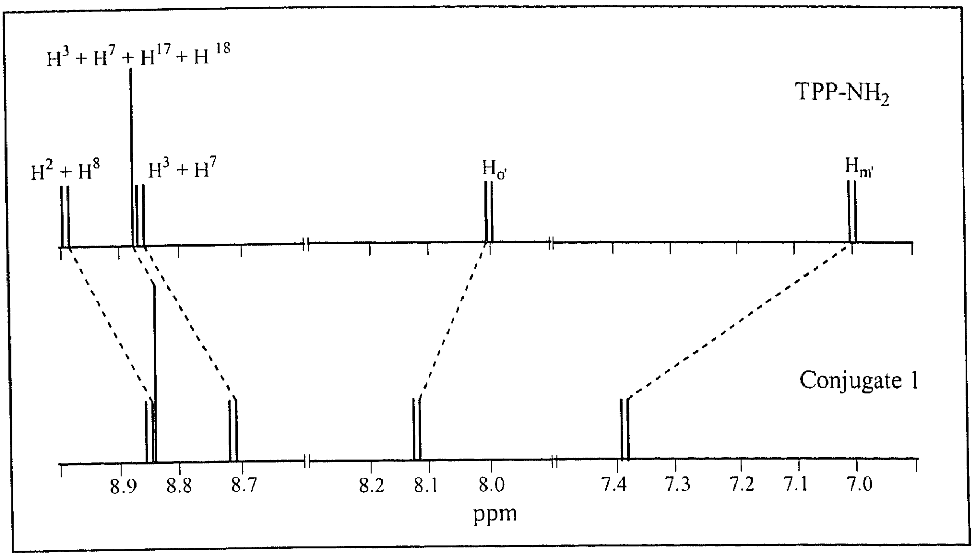

Diagram 6.5: Schematic representation of selected changes in the ^{1}H NMR of TPP-NH_2 on formation of conjugate 1.

The infrared spectrum of conjugate 1 completely lacked the absorption band of the free carboxylic acid of the parent platinum complex at 1717 cm^{-1} and showed a very strong band at 1637 cm^{-1} which may be associated with a mixture of the coordinated carboxylate group and the amide bond carboxylate.

Water-Soluble Carbodiimide Coupling

Many of the platinum derivatives synthesised to date make poor anticancer drugs largely because of water insolubility. Thus, if the new platinum-porphyrin conjugates are to be effective as anticancer agents, it is of interest to synthesise conjugates with favourable water-solubility properties. This was achieved by linking a water-soluble porphyrin, $TPPS_3$-NH_2 to the platinum derivative, [Pt(L-asp-N,O)$(NH_3)_2$]Cl, using EDAC.

The ^{1}H NMR spectrum of conjugate 2 in D_2O exhibits signals at 6.9 ppm (H^3 + H^7), 7.1 ppm (H^2 + H^8) and 7.2 ppm (H^{12} + H^{13} + H^{17} + H^{18}). These β-pyrrole protons remained essentially constant upon linking. The porphyrin aromatic protons appear at 7.7 ppm ($H_{o'}$), 7.9 ppm (H_m +

$H_{m'}$) and 8.1 ppm (H_o). It is worth noting that the peak at 7.9 ppm integrates to eight protons supporting the conclusion that the protons ortho to the amide bond (labelled $H_{m'}$) overlap with the protons ortho to the SO_3H groups (labelled $H_{m'}$). The most dramatic effect arising from coupling TPPS$_3$-NH$_2$ with [Pt(L-asp-N,O)(NH_3)$_2$]Cl is the shift of the protons ortho to the amide link. Like conjugate 1, this signal has shifted significantly downfield (~1.2 ppm) due to the deshielding effect of the amide carbonyl. Unfortunately, it was difficult to calculate reliable coupling constants due to line broadening.

In the aliphatic region, the ^{1}H NMR of conjugate 2, showed the expected eight-line portion assignable to the methylene protons of the aspartic acid ligand in the 2.24-2.58 ppm region, along with a quartet downfield at 3.57 ppm due to the methine protons of aspartic acid. These methylene resonances have shifted slightly upfield when compared to the bis(ammine) complex. The peaks assignable to the ammine, amide and pyrrole N-H protons are all absent due to proton exchange with deuterium.

References

1 T. W. G. Solomons, *Organic Chemistry*, 4th ed., Wiley, New York, 1988.

2 O. Meth-Cohn, J. Chem. Soc., Chem. Commun., 1986, 695.

3 R. T. Morrison and R. N. Boyd, *Organic Chemistry*, 4th ed., Allyn and Bacon Inc, Boston, 1983.

4 A. Streitwieser and C. H. Heathcock, *Indroduction to Organic Chemistry*, 2th ed., Macmillan Publishing Co. Inc, New York, 1981.

5 S. J. Weininger and F. R. Stermitz, *Organic Chemistry*, Academic Press, Orlando, 1984.

6 A. Jackson, Chim. Oggi., 1994, **12**, 33.

7 H. G. Khorana, Chem. Rev., 1953, **53**, 145.

8 H. K. Hombrecher and S. Ohm, Tetrahedron, 1993, 49, 2447-2456.

CHAPTER

7

SUMMARY AND CONCLUSIONS

Many platinum anticancer drugs developed to date lack the ability to distinguish between healthy and unhealthy tissue. As a result they have often created dangerous side-effects. Future drugs of will need to be more specific. One method to achieve this specificity is to attach the cytotoxic drug to a carrier molecule. Such molecules can seek out cancer cells in the body and integrate the active components to the DNA of these cells. Specificity of the drug would limit the needless side-effects caused by the use of ineffective drugs. This thesis describes a direct contribution to this goal. The project can summarily be categorised into three stages:

(1) The Synthesis of a Series of Platinum(II) Complexes

(2) The Synthesis of Porphyrins Containing Suitable Linker Groups

(3) The Coupling of Platinum and Porphyrin Components to Produce a Superior Drug

<u>Stage 1</u>: The Synthesis of a Series of Platinum(II) Complexes

The first stage involved the isolation of a series of 1:1 dichloro platinum(II) complexes using a variety of amino acids. These amino acid form part of the leaving group, and their primary roles are to firstly provide a terminal linker group through which a carrier molecule can be attached, and secondly, to aid with the water solubility of the platinum complex. The range of amino acids selected includes L-serine, L-lysine, L-glutamic acid-methyl ester, aspartic and glutamic acid.

These amino acids provide a carboxyl, a methyl ester, a hydroxyl and an amine linker group, all of which can be used in direct-coupling reactions.

Overall, six [Pt(amac-N,O)Cl_2] derivatives were successfully synthesised and characterised. These complexes were prepared by simply reacting $K_2[PtCl_4]$ with the amino acid at 40-50°C whilst controlling the pH with KOH in order to deprotonate the α-carboxylate. The reaction of $K_2[PtCl_4]$ with L-lysine was found to be particularly heat-sensitive so the reaction was carried out at room temperature to avoid precipitation of platinum metal. The crystal structure of [Pt(L-lysine)$Cl_2]^-$ has been determined by X-ray diffraction. [Pt(L-lysine)$Cl_2]^-$ crystallised as yellow needles in the monoclinic spacer group P2(1) with two independent molecules in the asymmetric unit and lattice parameters a = 9.63(8) Å, b = 11.11(11) Å, c = 11.05(9) Å and β = 102.02(6)°. Crystals of [Pt(L-serine)Cl_2] were also obtained by slow evaporation of aqueous solutions over P_2O_5 and X-ray structure determination is in progress. A hallmark of these experimentally simple reactions is the marked increase in complexity in the ^1H NMR spectra on formation of [Pt(amac-N,O)Cl_2]. Despite this complexity, a total analysis of the structural parameters was achieved with the aid of the simulation program gNMR.

Once fully characterised, a number of these dichloro platinum(II) complexes were modified to include an active component. This active component is the non-leaving group and is mainly responsible for the cytotoxicity of the complex. Modification was achieved by exchanging the labile chloride ions with ammonia, ethylenediamine or diaminocyclohexane. In this series, eight new [Pt(amac-N,O)(A)] complexes have been prepared. Of these four contain an active bis(ammine) component, two contain ethylenediamine, one contains *cis*-R,S-diaminocyclohexane and the last contains *trans*-R,R-diaminocyclohexane. Refer to Table 7.1 for specific details. It is worth noting that a complete examination of the spectroscopic features displayed by the dichloro diamine platinum(II) complexes of ethylenediamine and diaminocyclohexane was carried out prior to the synthesis of the [Pt(amac-N,O)(A)] complexes.

Table 7.1: Platinum(II) derivatives developed for linking

Ligand 1	Ligand 2				
	2 x Cl	2 x NH_3	en	cis-R,S-dach	trans-R,R-dach
L-asp	✔	✔	✔	✔	✔
L-serine	✔	✔	✔		
L-glu	✔	✔			
L-glu.OMe	✔				
L-lysine	✔	✔			

Stage 2: The Synthesis of Porphyrins Containing Suitable Linker Groups

Porphyrins are very versatile molecules that are well known due to their use as photosensitisers in photodynamic therapy. In this project, porphyrins were used as carrier molecules. The primary interest in porphyrins as carrier ligands derives from the findings that a number of porphyrins possessed tumour-localising properties. In this new generation of compounds, the porphyrin is anticipated to play a key role in directing the cytotoxic agent toward the tumour site.

A series of tetra-substituted porphyrins of basically the same shape but with a range of linker groups were created. The three linker groups selected were those that can be used in direct coupling reactions. These linker groups include an amine, a carboxylic acid and a methyl ester.

It was of interest to prepare porphyrins in gram quantities for use in coupling reactions. Unfortunately, most of the commonly used synthetic routes give porphyrins in only small yield, moreover many routes even lead to very complicated mixtures which are difficult to separate. The most successful synthesis was that of TPP-NH_2. This porphyrin was synthesised in three successive steps. Firstly, TPP was prepared by heating a mixture of pyrrole with benzaldehyde in propionic acid. TPP was then reacted with fuming nitric acid in $CHCl_3$ to give the mono-nitro derivative, TPP-NO_2 which after tin chloride reduction in hydrochloric acid gave TPP-NH_2 in 70% overall yield.

Three additional A_3B-porphryins were also synthesised and characterised. Two of these contain a methyl ester moiety (TMePP-COOMe and TMesPP-COOMe) and the third a carboxyl group (TMePP-COOH). TMePP-COOMe and TMePP-COOH were prepared using the classical Adler condensation whilst TMesPP-COOMe was made by the Lindsey's method.[1] All three porphyrins were produced in yields ranging from 12-15%. In the A_3B-porphyrins the tolualdehyde group (serving as A) is superior in terms of ease of isolation.

Stage 3: The Coupling of Platinum and Porphyrin Components to Produce a Superior Drug

The final stage involved coupling the porphyrins to the platinum-based derivatives. It is proposed that the tethering of a molecule with an independent affinity for cancer cells such as a porphyrin would enhance the efficacy of the agent by delivering a much larger concentration of the cytotoxic platinum component to cancer infected cells. In the linkage of porphyrin and platinum components three different coupling strategies were explored. From these, the procedures utilising coupling reagents were the most successful.

Standard carbodiimide-mediated coupling has been applied successfully to the synthesis of two conjugates (Diagram 7.1). Conjugate 1 was prepared by stirring $[Pt(L\text{-}asp\text{-}N,O)(NH_3)_2]^+$, DC and HOBT in $CHCl_2$/DMF for 15 minutes. The dicyclohexylurea by-product was removed b centrifugation and the resulting HOBT ester was allowed to react with TPP-NH_2 for 18 hour Evaporation of the solvent followed by column chromatography provided the conjugate in 45 yield.

Conjugate 2, a water-soluble version, was also prepared by carbodiimide-mediated coupling using $[Pt(L\text{-}asp\text{-}N,O)(NH_3)_2]^+$, EDAC and $TPPS_3\text{-}NH_2$ in 52% yield. $[Pt(L\text{-}asp\text{-}N,O)(NH_3)_2]^+$ was used in both preparations primarily because the active ligands (2 x NH_3) are the same as the parent compound cisplatin-a known potent anticancer agent.

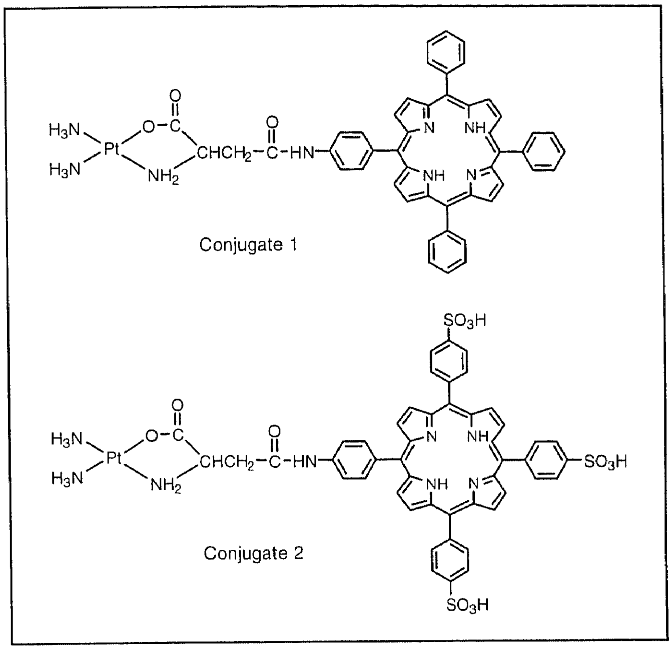

Diagram 7.1: Structural diagram of Conjugate 1 and Conjugate 2.

Attempts to link $[Pt(L\text{-}serine)(NH_3)_2]^+$ and TMePP-COOMe through transesterification were fruitless. Also a number of ester aminolysis reactions proved unsuccessful.

Although the carbodiimide-mediated experiments have been specifically demonstrated with $[Pt(L\text{-}asp\text{-}N,O)(NH_3)_2]^+$, TPP-$NH_2$ and $TPPS_3\text{-}NH_2$, it is undoubtedly not limited to these reagents. This approach lends itself to the synthesis of a larger range of conjugates by:

(a) Alternating the porphyrin and platinum derivatives featured in this thesis. For example, TMePP-COOH can be reacted with $[Pt(L\text{-}lysine)(NH_3)_2]^+$.

(b) Using A_3B porphyrins containing different types of meso-substituents (A). A number of different meso-groups are shown in Diagram 7.2. The selection of meso-substituents is important, for the porphryin must maintain a high level of solubility. In general, the pentyl, methyl and methoxy substituents impart much greater solubility in non-polar solvents than does the phenyl group. The para-glycosylated porphyrins are appealing because they would have relatively good solubility in aqueous solutions. Aqueous solubility being a pertinent physical property to the use of platinum-porphyrin conjugates as agents in cancer therapy.

(c) Inserting different metal centres such as copper and zinc into free base porphyrins. Metalation would increase the charge of the platinum-porphyrin conjugates.

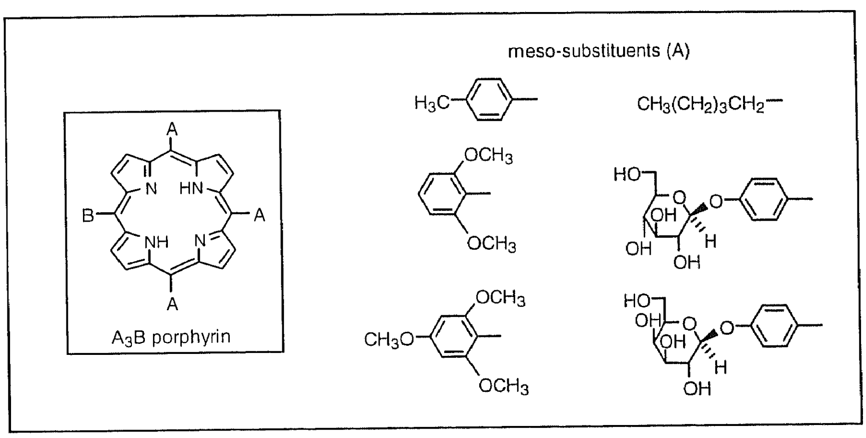

Diagram 7.2: A selection of various meso-substituents.

Although the parent porphyrins are known to localise, the two newly designed platinum-porphyrin conjugates may not mimic this behaviour. By screening the two conjugates for DNA binding, ability to sensitise formation of singlet oxygen, ability to cleave plasmid DNA and cytotoxic activity against various tumour cell lines, valuable information on their biological activity would be provided and thus identify their potential therapeutic value. Such studies are beyond the scope of this thesis but represent a crucial step toward the development of these conjugates. Overall, with respect to the structural components, the two new platinum-porphyrin conjugates have the potential to be more specific, safer drugs.

References

1 J. S. Lindsey, S. Prathapan, T. E. Johnson and R. W. Wagner, Tetrahedron, 1994, **50**, 8941-8968.

APPENDIX

I

SUPPLEMENTARY X-RAY CRYSTAL DATA

Table I.1: Atomic coordinates (x 10^4) and equivalent isotropic displacement coefficients.

Pt(1)	709(1)	0	8915(1)	16(1)
Cl(1)	1569(5)	-1905(5)	9499(5)	27(1)
Cl(2)	-1588(5)	-671(5)	8326(5)	28(2)
N(1)	177(15)	1762(16)	8455(13)	20(5)
N(2)	-591(16)	7429(21)	6182(12)	25(6)
O(1)	2676(14)	689(15)	9314(13)	29(5)
O(2)	3920(15)	2314(14)	9234(13)	30(5)
C(1)	1427(21)	2565(18)	8928(18)	29(7)
C(2)	1486(22)	3586(22)	8117(21)	34(7)
C(3)	171(24)	4414(19)	7862(22)	28(7)
C(4)	450(22)	5608(22)	7225(19)	33(7)
C(5)	-897(18)	6417(20)	7012(16)	23(6)
C(6)	2818(21)	1852(19)	9131(18)	24(6)
Pt(2)	4406(1)	1630(1)	6187(1)	19(1)
Cl(3)	3612(5)	3496(5)	5387(5)	30(2)
Cl(4)	6700(5)	2284(6)	6774(5)	32(2)
O(3)	2422(14)	974(14)	5777(12)	27(5)
O(4)	1106(13)	-600(14)	5987(14)	33(5)
N(3)	4883(16)	-27(21)	6803(15)	30(5)
N(4)	5556(14)	-5725(19)	8689(15)	24(6)
C(7)	3610(20)	-726(16)	6956(16)	22(6)
C(8)	3623(22)	-2069(18)	6697(18)	24(6)
C(9)	4824(28)	-2704(24)	7522(27)	48(9)
C(10)	4781(28)	-4054(22)	7229(31)	61(11)
C(11)	5905(23)	-4775(24)	7873(22)	45(8)
C(12)	2274(18)	-69(24)	6151(17)	26(6)
O(5)	-672(14)	1374(17)	5717(14)	40(5)
O(6)	4093(15)	5456(16)	432(15)	44(6)

Equivalent isotropic U defined as one third of the trace of the orthogonalized Uij tensor

Table I.2: Anisotropic displacement coefficients.

Pt(1)	14(1)	18(1)	17(1)	0(1)	2(1)	1(1)
Cl(1)	24(2)	20(3)	35(2)	3(2)	4(2)	2(2)
Cl(2)	17(2)	25(3)	43(3)	-1(2)	7(2)	2(2)
N(1)	14(7)	13(9)	28(8)	5(7)	-8(6)	13(7)
N(2)	36(11)	19(11)	20(9)	2(7)	2(8)	6(6)
O(1)	15(7)	26(9)	44(9)	0(6)	3(6)	-1(7)
O(2)	30(8)	22(8)	33(8)	-9(7)	-4(6)	9(6)
C(1)	26(10)	32(12)	31(11)	-6(9)	9(8)	4(9)
C(2)	33(11)	19(11)	49(12)	-5(9)	9(9)	0(9)
C(3)	34(12)	7(10)	46(13)	-5(8)	12(10)	-4(9)
C(4)	30(11)	47(14)	22(10)	7(10)	2(8)	-7(9)
C(5)	21(9)	21(13)	26(9)	6(8)	0(7)	2(8)
C(6)	30(10)	16(12)	26(10)	-3(9)	9(8)	-7(8)
Pt(2)	13(1)	20(1)	23(1)	-1(1)	1(1)	-1(1)
Cl(3)	24(2)	28(3)	37(2)	-8(2)	0(2)	4(2)
Cl(4)	15(2)	37(3)	41(3)	-1(2)	-1(2)	2(2)
O(3)	25(7)	23(9)	32(8)	-7(6)	3(6)	9(6)
O(4)	16(7)	34(9)	53(9)	-6(6)	18(7)	1(7)
N(3)	20(8)	24(9)	47(9)	-3(8)	9(7)	-13(9)
N(4)	6(7)	25(12)	42(10)	-9(6)	9(7)	-2(8)
C(7)	27(9)	20(9)	18(9)	-7(7)	6(7)	0(7)
C(8)	32(10)	2(9)	34(10)	1(7)	-3(9)	1(7)
C(9)	40(14)	29(13)	67(18)	9(11)	-8(13)	4(12)
C(10)	36(15)	23(13)	106(24)	-8(10)	-30(15)	19(14)
C(11)	35(12)	34(17)	54(13)	-23(11)	-19(10)	7(11)
C(12)	16(8)	31(12)	29(9)	6(9)	0(7)	6(10)
O(5)	25(7)	60(11)	31(7)	-4(7)	-4(6)	-5(8)
O(6)	29(8)	56(12)	48(9)	-5(7)	10(7)	-13(7)

Table I.3. H-Atom coordinates (x 10^4) and isotropic displacement coefficients.

H(1A)	-557	1984	8793	80
H(1B)	-93	1835	7628	80
H(2A)	236	7464	5926	80
H(2B)	-1248	8007	5957	80
H(1C)	1325	2871	9717	80
H(2A)	1647	3297	7340	80
H(2B)	2287	4073	8481	80
H(3A)	-107	4593	8627	80
H(3B)	-596	3990	7344	80
H(4A)	691	5433	6443	80
H(4B)	1237	6022	7728	80
H(5A)	-1723	5977	6612	80
H(5B)	-1054	6715	7788	80
H(3C)	5767	-332	6966	80
H(4C)	4652	-5781	8783	80
H(4D)	6217	-6236	9095	80
H(7A)	3529	-634	7802	80
H(8A)	3581	-2178	5829	80
H(8B)	2783	-2421	6886	80
H(9A)	4941	-2520	8386	80
H(9B)	5658	-2435	7253	80
H(10A)	4583	-4212	6356	80
H(10B)	3968	-4309	7537	80
H(11A)	6294	-5159	7240	80
H(11B)	6629	-4270	8345	80

Table I.4: Observed and calculated structure factors for $[Pt(L\text{-}lysine)Cl_2]^-$ in P2(1).

H	K	L	10FO	10FC	10S
0	-12	0	1103	1192	12
1	-12	0	121	133	-54
2	-12	0	828	735	12
3	-12	0	52	133	-52
4	-12	0	149	26	-44
1	-11	0	706	725	12
2	-11	0	535	474	12
3	-11	0	957	900	12
4	-11	0	807	711	13
5	-11	0	621	542	13
0	-10	0	209	250	22
1	-10	0	1112	1099	11
2	-10	0	376	363	15
3	-10	0	258	226	21
4	-10	0	338	238	18
5	-10	0	533	506	13
6	-10	0	464	483	15
7	-10	0	926	846	13
1	-9	0	220	207	21
2	-9	0	1226	1122	12
3	-9	0	481	413	12
4	-9	0	1324	1266	12
5	-9	0	109	105	-63
6	-9	0	1067	936	12
7	-9	0	378	356	17
0	-8	0	647	682	10
1	-8	0	1024	1007	10
2	-8	0	882	814	10
3	-8	0	659	647	11
4	-8	0	148	117	34
5	-8	0	722	698	11
6	-8	0	831	766	12
7	-8	0	1379	1303	13
8	-8	0	738	683	13
1	-7	0	539	533	9
2	-7	0	961	901	10
3	-7	0	1490	1419	12
4	-7	0	621	558	11
5	-7	0	1374	1301	12
6	-7	0	492	468	12
7	-7	0	558	558	13
8	-7	0	352	327	18
9	-7	0	615	596	13
0	-6	0	1600	1823	12
1	-6	0	290	275	12
2	-6	0	1486	1424	12
3	-6	0	532	534	10
4	-6	0	135	152	32

H	K	L	10FO	10FC	10S
4	-5	0	804	759	10
5	-5	0	1206	1177	11
6	-5	0	575	585	11
7	-5	0	447	439	13
8	-5	0	382	492	15
9	-5	0	474	462	14
10	-5	0	649	645	13
0	-4	0	1222	1346	10
1	-4	0	1670	1661	11
2	-4	0	1083	1023	9
3	-4	0	713	671	9
4	-4	0	294	275	12
5	-4	0	806	805	9
6	-4	0	544	514	11
7	-4	0	1388	1339	12
8	-4	0	789	772	11
9	-4	0	1031	1006	12
10	-4	0	336	425	19
1	-3	0	542	509	7
2	-3	0	1464	1468	11
3	-3	0	574	542	8
4	-3	0	2412	2384	13
5	-3	0	400	334	10
6	-3	0	1230	1252	11
7	-3	0	491	536	12
8	-3	0	509	518	12
9	-3	0	281	362	20
10	-3	0	926	919	12
0	-2	0	1175	1244	7
1	-2	0	2174	2117	8
2	-2	0	1295	1237	10
3	-2	0	252	232	11
4	-2	0	786	809	8
5	-2	0	772	661	8
6	-2	0	1359	1299	11
7	-2	0	1319	1266	10
8	-2	0	893	831	11
9	-2	0	1036	1044	11
10	-2	0	338	289	18
1	-1	0	1329	1258	6
2	-1	0	867	797	6
3	-1	0	1957	1824	10
4	-1	0	1296	1200	9
5	-1	0	2095	1985	13
6	-1	0	515	550	10
7	-1	0	105	113	-54
8	-1	0	524	542	11
9	-1	0	646	661	11

H	K	L	10FO	10FC	10S
8	0	0	1376	1394	10
9	0	0	48	120	-48
10	0	0	991	984	11
1	1	0	1283	1262	6
2	1	0	845	795	6
3	1	0	1923	1851	10
4	1	0	1251	1197	9
5	1	0	2044	1974	13
6	1	0	576	498	9
7	1	0	86	159	-86
8	1	0	430	494	14
9	1	0	684	630	11
10	1	0	405	432	16
0	2	0	1157	1259	6
1	2	0	2105	2112	8
2	2	0	1267	1229	8
3	2	0	219	225	12
4	2	0	831	736	8
5	2	0	682	713	9
6	2	0	1323	1320	11
7	2	0	1331	1277	12
8	2	0	872	862	10
9	2	0	1048	1038	11
10	2	0	274	342	21
1	3	0	503	524	7
2	3	0	1505	1475	8
3	3	0	608	512	7
4	3	0	2423	2385	12
5	3	0	360	381	10
6	3	0	1253	1229	11
7	3	0	552	494	11
8	3	0	530	510	11
9	3	0	386	319	15
10	3	0	922	919	12
0	4	0	1198	1372	7
1	4	0	1595	1634	8
2	4	0	1039	1025	7
3	4	0	733	647	7
4	4	0	297	289	11
5	4	0	821	773	9
6	4	0	540	521	10
7	4	0	1346	1358	12
8	4	0	795	774	10
9	4	0	1005	1053	12
10	4	0	410	386	16
1	5	0	957	978	7
2	5	0	1440	1466	9
3	5	0	1917	1887	11

H	K	L	10FO	10FC	10S
1	6	0	249	275	12
2	6	0	1420	1424	9
3	6	0	554	491	8
4	6	0	103	137	-43
5	6	0	172	178	24
6	6	0	1176	1200	11
7	6	0	265	241	19
8	6	0	1191	1180	12
9	6	0	214	172	24
1	7	0	541	519	9
2	7	0	918	900	9
3	7	0	1412	1415	12
4	7	0	567	564	10
5	7	0	1324	1307	12
6	7	0	495	449	11
7	7	0	578	544	12
8	7	0	300	351	19
9	7	0	593	593	13
0	8	0	601	715	10
1	8	0	951	1021	10
2	8	0	792	813	10
3	8	0	619	650	10
4	8	0	128	121	-36
5	8	0	733	692	10
6	8	0	769	767	11
7	8	0	1295	1310	12
8	8	0	675	691	13
1	9	0	200	214	20
2	9	0	1110	1115	11
3	9	0	434	425	12
4	9	0	1277	1232	12
5	9	0	134	159	-37
6	9	0	941	955	11
7	9	0	359	364	16
0	10	0	231	242	19
1	10	0	1084	1097	11
2	10	0	348	332	14
3	10	0	227	225	20
4	10	0	247	301	21
5	10	0	545	492	12
6	10	0	497	461	13
1	11	0	720	718	11
2	11	0	451	452	13
3	11	0	929	881	11
4	11	0	730	715	11
5	11	0	567	572	13
0	12	0	1059	1218	12
1	12	0	175	142	26

H	K	L	10FO	10FC	10S
1	-12	1	1096	1026	12
2	-12	1	159	130	38
3	-12	1	928	870	12
-5	-11	1	288	276	21
-4	-11	1	625	607	12
-3	-11	1	678	620	12
-2	-11	1	1353	1282	13
-1	-11	1	694	775	12
0	-11	1	707	721	14
1	-11	1	430	413	14
2	-11	1	248	302	22
3	-11	1	567	510	12
4	-11	1	551	538	13
5	-11	1	708	640	13
-7	-10	1	563	521	14
-6	-10	1	1019	917	13
-5	-10	1	570	526	12
-4	-10	1	971	928	12
-3	-10	1	198	89	24
-2	-10	1	48	60	-48
-1	-10	1	146	89	34
0	-10	1	1035	1066	35
1	-10	1	779	756	11
2	-10	1	1354	1259	12
3	-10	1	694	636	11
4	-10	1	505	477	13
5	-10	1	172	204	35
6	-10	1	160	194	-41
-8	-9	1	242	215	25
-7	-9	1	599	572	13
-6	-9	1	288	324	20
-5	-9	1	405	405	14
-4	-9	1	257	217	20
-3	-9	1	1683	1628	14
-2	-9	1	286	245	17
-1	-9	1	1234	1241	12
0	-9	1	259	234	31
1	-9	1	435	411	12
2	-9	1	375	295	13
3	-9	1	638	594	11
4	-9	1	257	175	20
5	-9	1	1226	1184	13
6	-9	1	234	152	24
7	-9	1	1071	1018	13
-8	-8	1	677	671	12
-7	-8	1	854	807	12
-6	-8	1	1195	1131	12
-5	-8	1	647	654	11

H	K	L	10FO	10FC	10S
5	-6	0	221	183	19
6	-6	0	1228	1182	12
7	-6	0	260	244	20
8	-6	0	1213	1170	12
9	-6	0	109	157	-83
1	-5	0	1009	987	9
2	-5	0	1497	1449	12
3	-5	0	1927	1901	14
4	-8	1	488	534	13
5	-8	1	288	240	18
6	-8	1	501	494	13
7	-8	1	491	483	14
8	-8	1	675	691	13
-9	-7	1	397	372	16
-8	-7	1	931	885	12
-7	-7	1	451	427	14
-6	-7	1	91	83	-91
-5	-7	1	131	266	-40
-4	-7	1	1742	1646	14
-3	-7	1	882	830	10
-2	-7	1	2083	2044	15
-1	-7	1	769	806	10
0	-7	1	809	814	45
1	-7	1	183	168	20
2	-7	1	162	214	26
3	-7	1	755	703	10
4	-7	1	967	866	11
5	-7	1	404	387	14
6	-7	1	1583	1513	14
7	-7	1	542	525	13
8	-7	1	560	517	13
9	-7	1	358	337	18
-9	-6	1	317	341	20
-8	-6	1	198	218	28
-7	-6	1	1456	1407	14
-6	-6	1	401	391	13
-5	-6	1	1589	1481	13
-4	-6	1	98	158	-53
-3	-6	1	724	712	9
-2	-6	1	223	186	15
-1	-6	1	930	991	9
0	-6	1	153	111	17
1	-6	1	2349	2358	13
2	-6	1	384	411	10
3	-6	1	1630	1570	12
4	-6	1	217	257	19
5	-6	1	159	141	30
6	-6	1	556	435	11
7	-6	1	491	486	13
8	-6	1	198	282	31

H	K	L	10FO	10FC	10S
10	-1	0	401	411	17
1	0	0	111	56	7
2	0	0	2256	2100	8
3	0	0	271	239	9
4	0	0	708	697	7
5	0	0	344	316	10
6	0	0	1194	1178	9
7	0	0	128	91	-36
3	-5	1	430	436	10
4	-5	1	1213	1201	11
5	-5	1	601	631	11
6	-5	1	1188	1147	11
7	-5	1	699	725	11
8	-5	1	742	706	12
9	-5	1	359	373	18
-10	-4	1	195	179	33
-9	-4	1	278	278	20
-8	-4	1	942	838	11
-7	-4	1	620	604	11
-6	-4	1	1612	1607	13
-5	-4	1	880	882	9
-4	-4	1	1435	1435	11
-3	-4	1	352	251	10
-2	-4	1	275	278	10
-1	-4	1	671	685	7
0	-4	1	1895	1885	81
1	-4	1	529	484	8
2	-4	1	2358	2333	12
3	-4	1	1104	1087	10
4	-4	1	755	730	10
5	-4	1	707	611	10
6	-4	1	442	397	12
7	-4	1	744	784	11
8	-4	1	917	904	11
9	-4	1	663	623	12
10	-4	1	1021	1050	13
-10	-3	1	155	161	-40
-9	-3	1	1435	1402	13
-8	-3	1	234	302	22
-7	-3	1	875	858	11
-6	-3	1	616	543	10
-5	-3	1	860	856	9
-4	-3	1	544	541	9
-3	-3	1	1574	1607	12
-2	-3	1	934	918	8
-1	-3	1	1538	1758	10
0	-3	1	305	289	19
1	-3	1	1261	1245	10
2	-3	1	642	545	8
3	-3	1	1436	1318	11

H	K	L	10FO	10FC	10S
4	5	0	744	780	8
5	5	0	1183	1184	10
6	5	0	575	566	10
7	5	0	467	468	12
8	5	0	508	396	12
9	5	0	465	469	14
10	5	0	637	652	13
0	6	0	1631	1800	9
-4	-2	1	1984	1905	11
-3	-2	1	473	488	7
-2	-2	1	234	232	11
-1	-2	1	248	218	7
0	-2	1	1858	1845	98
1	-2	1	757	794	7
2	-2	1	2366	2246	9
3	-2	1	1645	1533	11
4	-2	1	1853	1697	12
5	-2	1	673	678	8
6	-2	1	449	382	11
7	-2	1	632	595	10
8	-2	1	1485	1520	11
9	-2	1	590	590	12
10	-2	1	892	945	11
-11	-1	1	557	511	14
-10	-1	1	1133	1163	11
-9	-1	1	740	745	11
-8	-1	1	975	956	10
-7	-1	1	421	407	11
-6	-1	1	120	131	-33
-5	-1	1	360	353	10
-4	-1	1	1803	1742	9
-3	-1	1	737	714	7
-2	-1	1	1603	1596	7
-1	-1	1	1189	1265	5
0	-1	1	1971	1898	47
1	-1	1	596	541	6
2	-1	1	552	479	8
3	-1	1	1223	1184	9
4	-1	1	2024	1911	12
5	-1	1	1050	977	9
6	-1	1	1535	1480	11
7	-1	1	830	772	10
8	-1	1	779	721	10
9	-1	1	596	552	11
10	-1	1	389	380	16
-11	0	1	203	292	32
-10	0	1	452	463	14
-9	0	1	955	941	10
-8	0	1	256	252	19
-7	0	1	834	829	9

H	K	L	10FO	10FC	10S
2	12	0	705	741	12
3	12	0	135	135	-41
4	12	0	51	50	-51
-4	-12	1	225	181	28
-3	-12	1	355	343	18
-2	-12	1	146	153	-44
-1	-12	1	460	492	14
0	-12	1	49	59	-35
8	0	1	309	293	17
9	0	1	1299	1285	11
10	0	1	112	60	-65
-11	1	1	541	529	14
-10	1	1	1157	1122	13
-9	1	1	754	740	11
-8	1	1	944	972	11
-7	1	1	419	378	12
-6	1	1	133	91	29
-5	1	1	406	336	9
-4	1	1	1754	1771	10
-3	1	1	741	736	7
-2	1	1	1560	1618	8
-1	1	1	1174	1271	7
0	1	1	1962	1892	4
1	1	1	589	551	6
2	1	1	521	500	7
3	1	1	1255	1148	9
4	1	1	1975	1920	12
5	1	1	1022	995	9
6	1	1	1546	1458	11
7	1	1	818	793	10
8	1	1	747	747	11
9	1	1	552	614	12
10	1	1	403	362	16
-11	2	1	442	459	16
-10	2	1	198	291	29
-9	2	1	430	442	13
-8	2	1	848	804	10
-7	2	1	1102	1065	11
-6	2	1	1721	1727	13
-5	2	1	1291	1266	10
-4	2	1	1923	1929	12
-3	2	1	514	431	7
-2	2	1	204	239	12
-1	2	1	191	241	9
0	2	1	1861	1828	9
1	2	1	826	755	7
2	2	1	2382	2251	9
3	2	1	1640	1516	11
4	2	1	1827	1706	12
5	2	1	735	632	9

H	K	L	10FO	10FC	10S
-4	-8	1	616	567	11
-3	-8	1	184	170	26
-2	-8	1	45	51	-45
-1	-8	1	366	361	13
0	-8	1	614	617	52
1	-8	1	815	779	10
2	-8	1	1675	1559	14
3	-8	1	864	806	11
-1	3	1	1545	1730	6
0	3	1	285	305	6
1	3	1	1281	1254	9
2	3	1	575	595	7
3	3	1	1458	1312	11
4	3	1	430	364	9
5	3	1	2409	2272	14
6	3	1	266	246	16
7	3	1	1392	1371	12
8	3	1	519	520	12
9	3	1	145	157	-38
10	3	1	370	427	16
-10	4	1	195	218	29
-9	4	1	258	281	21
-8	4	1	887	879	10
-7	4	1	621	602	10
-6	4	1	1635	1589	11
-5	4	1	863	875	9
-4	4	1	1446	1437	9
-3	4	1	270	310	11
-2	4	1	281	280	9
-1	4	1	634	678	6
0	4	1	1874	1869	62
1	4	1	559	524	7
2	4	1	2440	2325	11
3	4	1	1086	1095	9
4	4	1	774	733	8
5	4	1	615	673	9
6	4	1	414	425	11
7	4	1	770	747	11
8	4	1	907	923	11
9	4	1	592	634	13
10	4	1	1039	1046	12
-10	5	1	923	906	11
-9	5	1	380	304	16
-8	5	1	719	734	11
-7	5	1	411	433	13
-6	5	1	138	184	32
-5	5	1	179	304	21
-4	5	1	1068	1117	8
-3	5	1	1250	1318	8
-2	5	1	2045	2197	10

H	K	L	10FO	10FC	10S
9	-6	1	1023	1028	13
-10	-5	1	928	909	12
-9	-5	1	278	369	21
-8	-5	1	743	721	11
-7	-5	1	437	428	13
-6	-5	1	177	153	26
-5	-5	1	319	183	14
-4	-5	1	1158	1101	11
-3	-5	1	1274	1310	11
-2	-5	1	2123	2197	12
-1	-5	1	1318	1430	10
0	-5	1	1670	1670	80
1	-5	1	400	324	9
2	-5	1	310	281	11
-6	6	1	396	399	12
-5	6	1	1457	1506	12
-4	6	1	222	112	16
-3	6	1	700	692	8
-2	6	1	160	204	19
-1	6	1	882	993	7
0	6	1	146	132	25
1	6	1	2398	2341	13
2	6	1	393	407	9
3	6	1	1626	1600	11
4	6	1	252	236	15
5	6	1	150	162	29
6	6	1	444	517	12
7	6	1	448	498	14
8	6	1	281	243	20
9	6	1	993	1018	12
-9	7	1	367	350	18
-8	7	1	874	883	12
-7	7	1	431	449	13
-6	7	1	46	84	-46
-5	7	1	255	182	17
-4	7	1	1619	1657	13
-3	7	1	803	839	9
-2	7	1	1894	2063	15
-1	7	1	738	801	8
0	7	1	784	836	29
1	7	1	176	141	20
2	7	1	256	182	14
3	7	1	717	700	10
4	7	1	904	893	10
5	7	1	403	399	13
6	7	1	1512	1485	13
7	7	1	551	526	12
8	7	1	511	492	14
9	7	1	321	345	19
-8	8	1	658	645	13

H	K	L	10FO	10FC	10S
4	-3	1	367	412	10
5	-3	1	2383	2283	14
6	-3	1	288	253	15
7	-3	1	1400	1350	13
8	-3	1	492	535	13
9	-3	1	149	147	-39
10	-3	1	460	380	15
-11	-2	1	520	426	14
-10	-2	1	273	230	21
-9	-2	1	433	421	14
-8	-2	1	817	844	10
-7	-2	1	1049	1076	10
-6	-2	1	1757	1719	11
-5	-2	1	1330	1267	9
-4	9	1	177	253	27
-3	9	1	1560	1617	13
-2	9	1	219	245	20
-1	9	1	1148	1236	10
0	9	1	204	227	23
1	9	1	458	404	11
2	9	1	293	336	17
3	9	1	630	612	11
4	9	1	187	200	24
5	9	1	1167	1168	12
6	9	1	162	181	34
7	9	1	998	1035	12
-7	10	1	539	535	13
-6	10	1	902	932	12
-5	10	1	551	531	12
-4	10	1	940	927	11
-3	10	1	102	131	-56
-2	10	1	95	65	-58
-1	10	1	146	114	28
0	10	1	1035	1062	40
1	10	1	786	764	10
2	10	1	1286	1251	11
3	10	1	656	640	11
4	10	1	473	474	12
5	10	1	197	157	28
6	10	1	190	160	31
-5	11	1	266	276	21
-4	11	1	594	618	12
-3	11	1	599	626	12
-2	11	1	1221	1269	12
-1	11	1	714	751	11
0	11	1	691	733	38
1	11	1	450	407	13
2	11	1	313	277	17
3	11	1	515	521	12
4	11	1	533	542	13

H	K	L	10FO	10FC	10S
-6	0	1	79	38	-79
-5	0	1	1956	1912	11
-4	0	1	157	160	16
-3	0	1	1408	1404	9
-2	0	1	230	204	8
-1	0	1	1070	1186	6
0	0	1	150	155	3
1	0	1	3112	3049	6
2	0	1	140	109	17
3	0	1	1627	1536	10
4	0	1	452	421	9
5	0	1	879	893	9
6	0	1	313	303	13
7	0	1	521	469	11
-2	-11	2	604	620	11
-1	-11	2	1150	1125	12
0	-11	2	742	748	56
1	-11	2	814	823	11
2	-11	2	248	241	23
3	-11	2	235	197	24
4	-11	2	199	185	30
5	-11	2	539	512	14
-7	-10	2	353	308	18
-6	-10	2	256	248	22
-5	-10	2	908	890	12
-4	-10	2	353	354	15
-3	-10	2	1126	1223	12
-2	-10	2	489	506	12
-1	-10	2	191	119	25
0	-10	2	205	175	27
1	-10	2	865	871	11
2	-10	2	452	454	13
3	-10	2	1097	1023	12
4	-10	2	432	381	14
5	-10	2	819	732	12
6	-10	2	216	282	32
-8	-9	2	1189	1175	14
-7	-9	2	186	188	32
-6	-9	2	918	930	12
-5	-9	2	315	256	17
-4	-9	2	221	217	23
-3	-9	2	171	144	28
-2	-9	2	1021	1096	11
-1	-9	2	461	423	12
0	-9	2	1258	1240	58
1	-9	2	265	254	18
2	-9	2	1289	1199	12
3	-9	2	410	328	13
4	-9	2	358	326	15
5	-9	2	251	352	23

H	K	L	10FO	10FC	10S
6	2	1	371	420	11
7	2	1	629	599	10
8	2	1	1570	1493	13
9	2	1	596	568	12
10	2	1	916	910	12
-10	3	1	158	156	37
-9	3	1	1397	1399	12
-8	3	1	338	254	15
-7	3	1	911	845	10
-6	3	1	559	604	9
-5	3	1	841	879	8
-4	3	1	568	504	8
-3	3	1	1554	1596	8
-2	3	1	913	922	6
-8	-7	2	488	475	14
-7	-7	2	1334	1330	13
-6	-7	2	499	481	12
-5	-7	2	457	446	12
-4	-7	2	322	350	14
-3	-7	2	935	974	10
-2	-7	2	645	705	9
-1	-7	2	1153	1099	10
0	-7	2	769	750	43
1	-7	2	1679	1608	14
2	-7	2	481	442	11
3	-7	2	883	816	10
4	-7	2	386	369	13
5	-7	2	1000	928	11
6	-7	2	479	468	13
7	-7	2	1154	1134	13
8	-7	2	538	541	14
-9	-6	2	229	248	26
-8	-6	2	218	227	25
-7	-6	2	143	222	-36
-6	-6	2	753	781	11
-5	-6	2	45	60	-45
-4	-6	2	1735	1797	14
-3	-6	2	150	161	25
-2	-6	2	1412	1583	12
-1	-6	2	402	409	10
0	-6	2	556	565	24
1	-6	2	179	195	19
2	-6	2	1855	1847	13
3	-6	2	234	226	17
4	-6	2	1422	1363	12
5	-6	2	238	267	21
6	-6	2	891	905	12
7	-6	2	422	423	14
8	-6	2	224	228	25
9	-6	2	360	338	18

H	K	L	10FO	10FC	10S
-1	5	1	1252	1434	7
0	5	1	1640	1662	58
1	5	1	377	387	9
2	5	1	296	285	11
3	5	1	443	408	9
4	5	1	1235	1165	9
5	5	1	639	596	9
6	5	1	1162	1140	10
7	5	1	689	694	11
8	5	1	705	748	11
9	5	1	379	384	15
-9	6	1	347	345	17
-8	6	1	228	177	21
-7	6	1	1403	1416	12
-10	-4	2	465	484	15
-9	-4	2	351	377	16
-8	-4	2	244	281	21
-7	-4	2	504	485	11
-6	-4	2	1148	1121	11
-5	-4	2	1236	1302	11
-4	-4	2	1114	1157	9
-3	-4	2	1864	2036	13
-2	-4	2	191	87	15
-1	-4	2	568	530	8
0	-4	2	554	496	26
1	-4	2	1592	1595	11
2	-4	2	567	498	9
3	-4	2	1762	1664	13
4	-4	2	1392	1365	12
5	-4	2	1153	1163	11
6	-4	2	570	577	11
7	-4	2	483	498	12
8	-4	2	485	537	13
9	-4	2	638	654	12
-10	-3	2	879	897	12
-9	-3	2	351	305	16
-8	-3	2	1754	1739	15
-7	-3	2	191	226	24
-6	-3	2	1082	1111	10
-5	-3	2	233	236	14
-4	-3	2	376	388	10
-3	-3	2	80	71	-43
-2	-3	2	1651	1786	11
-1	-3	2	345	306	8
0	-3	2	2262	2229	79
1	-3	2	123	80	20
2	-3	2	1342	1289	10
3	-3	2	530	560	9
4	-3	2	829	785	9
5	-3	2	625	543	10

H	K	L	10FO	10FC	10S
-7	8	1	810	797	11
-6	8	1	1127	1125	12
-5	8	1	619	630	11
-4	8	1	555	604	11
-3	8	1	174	153	24
-2	8	1	75	58	-75
-1	8	1	360	363	11
0	8	1	598	606	23
1	8	1	821	791	10
2	8	1	1613	1551	14
3	8	1	831	804	10
4	8	1	548	461	11
5	8	1	256	276	19
6	8	1	492	464	12
7	8	1	505	465	13
8	8	1	705	678	12
-8	9	1	92	179	-92
-7	9	1	592	561	12
-6	9	1	349	292	16
-5	9	1	392	399	14
4	-2	2	1619	1531	12
5	-2	2	1429	1369	10
6	-2	2	506	467	11
7	-2	2	231	306	21
8	-2	2	608	553	11
9	-2	2	521	557	13
10	-2	2	551	557	14
-11	-1	2	246	314	26
-10	-1	2	620	609	12
-9	-1	2	1177	1247	10
-8	-1	2	594	608	10
-7	-1	2	1142	1114	10
-6	-1	2	655	571	8
-5	-1	2	477	476	8
-4	-1	2	414	429	8
-3	-1	2	792	781	6
-2	-1	2	1499	1631	6
-1	-1	2	2670	2813	8
0	-1	2	1153	1091	14
1	-1	2	2113	2040	8
2	-1	2	674	720	8
3	-1	2	774	759	8
4	-1	2	572	518	8
5	-1	2	989	963	9
6	-1	2	345	310	13
7	-1	2	1315	1323	12
8	-1	2	1081	1023	11
9	-1	2	1150	1146	12
10	-1	2	553	524	13
-11	0	2	185	213	34

H	K	L	10FO	10FC	10S
5	11	1	630	673	12
-4	12	1	192	196	29
-3	12	1	317	339	18
-2	12	1	178	141	28
-1	12	1	474	501	13
0	12	1	57	43	-43
1	12	1	1040	1056	11
2	12	1	118	138	-57
3	12	1	876	877	12
-4	-12	2	1053	1058	13
-3	-12	2	121	128	-58
-2	-12	2	640	679	12
-1	-12	2	123	62	-55
0	-12	2	162	172	29
1	-12	2	232	271	24
2	-12	2	843	803	12
3	-12	2	268	251	23
-5	-11	2	430	410	15
-4	-11	2	127	73	-47
-3	-11	2	442	465	13
-6	1	2	609	601	8
-5	1	2	465	478	8
-4	1	2	460	387	8
-3	1	2	744	833	7
-2	1	2	1498	1651	9
-1	1	2	2640	2844	8
0	1	2	1141	1098	6
1	1	2	2166	2020	8
2	1	2	821	597	7
3	1	2	812	733	8
4	1	2	569	545	8
5	1	2	999	941	9
6	1	2	334	330	13
7	1	2	1346	1300	11
8	1	2	1062	1033	11
9	1	2	1160	1125	12
10	1	2	486	555	14
-11	2	2	778	736	12
-10	2	2	651	657	12
-9	2	2	726	720	11
-8	2	2	302	297	15
-7	2	2	661	630	10
-6	2	2	993	974	9
-5	2	2	1975	2045	13
-4	2	2	1097	1175	8
-3	2	2	1163	1260	8
-2	2	2	789	867	6
-1	2	2	178	77	13
0	2	2	72	87	-30
1	2	2	215	220	11

H	K	L	10FO	10FC	10S
6	-9	2	1248	1162	13
7	-9	2	129	107	-56
-8	-8	2	261	254	23
-7	-8	2	584	589	13
-6	-8	2	549	522	12
-5	-8	2	821	802	11
-4	-8	2	812	813	10
-3	-8	2	1161	1185	11
-2	-8	2	659	640	9
-1	-8	2	442	438	11
0	-8	2	45	106	-32
1	-8	2	923	870	10
2	-8	2	1082	991	11
3	-8	2	1762	1643	14
4	-8	2	992	909	11
5	-8	2	982	940	11
6	-8	2	561	546	13
7	-8	2	254	277	24
8	-8	2	371	330	18
-9	-7	2	765	718	12
7	3	2	100	19	-59
8	3	2	1295	1295	12
9	3	2	262	302	21
10	3	2	538	486	13
-10	4	2	463	471	14
-9	4	2	367	335	15
-8	4	2	256	267	19
-7	4	2	472	496	11
-6	4	2	1134	1126	9
-5	4	2	1274	1240	9
-4	4	2	1086	1160	8
-3	4	2	1930	2011	9
-2	4	2	75	208	-49
-1	4	2	500	558	7
0	4	2	512	540	12
1	4	2	1680	1585	11
2	4	2	546	528	9
3	4	2	1749	1683	12
4	4	2	1417	1339	11
5	4	2	1160	1164	10
6	4	2	573	559	10
7	4	2	505	463	11
8	4	2	565	481	11
9	4	2	649	658	12
-10	5	2	454	451	14
-9	5	2	925	985	11
-8	5	2	699	699	10
-7	5	2	987	964	10
-6	5	2	929	970	9
-5	5	2	631	618	9

H	K	L	10FO	10FC	10S
-10	-5	2	425	451	17
-9	-5	2	1003	959	12
-8	-5	2	688	707	12
-7	-5	2	998	993	11
-6	-5	2	948	946	11
-5	-5	2	606	641	10
-4	-5	2	222	243	17
-3	-5	2	763	791	8
-2	-5	2	1190	1272	10
-1	-5	2	1987	1960	12
0	-5	2	1539	1469	66
1	-5	2	1681	1697	12
2	-5	2	714	730	9
3	-5	2	261	265	15
4	-5	2	493	412	10
5	-5	2	636	603	11
6	-5	2	950	889	11
7	-5	2	1120	1030	12
8	-5	2	540	576	13
9	-5	2	732	750	13
3	6	2	266	223	14
4	6	2	1418	1358	11
5	6	2	289	260	16
6	6	2	936	883	11
7	6	2	422	432	14
8	6	2	187	207	31
9	6	2	317	327	19
-9	7	2	718	705	12
-8	7	2	465	485	14
-7	7	2	1308	1334	12
-6	7	2	447	483	12
-5	7	2	435	447	12
-4	7	2	358	311	12
-3	7	2	899	978	10
-2	7	2	645	701	9
-1	7	2	1002	1104	9
0	7	2	755	737	17
1	7	2	1671	1626	12
2	7	2	454	457	10
3	7	2	887	806	10
4	7	2	380	353	13
5	7	2	949	941	11
6	7	2	463	483	13
7	7	2	1147	1118	12
8	7	2	615	535	12
-8	8	2	295	248	19
-7	8	2	599	590	11
-6	8	2	512	527	12
-5	8	2	776	811	10
-4	8	2	775	797	10

H	K	L	10FO	10FC	10S
6	-3	2	1742	1678	13
7	-3	2	74	17	-74
8	-3	2	1332	1286	13
9	-3	2	325	263	19
10	-3	2	507	528	14
-11	-2	2	710	764	12
-10	-2	2	689	661	11
-9	-2	2	731	729	10
-8	-2	2	290	292	17
-7	-2	2	621	665	10
-6	-2	2	972	1006	9
-5	-2	2	1987	2037	11
-4	-2	2	1136	1157	7
-3	-2	2	1167	1270	7
-2	-2	2	824	844	6
-1	-2	2	167	207	14
0	-2	2	95	97	21
1	-2	2	228	202	11
2	-2	2	768	668	8
3	-2	2	1826	1737	12
6	9	2	1197	1160	12
7	9	2	174	118	32
-7	10	2	288	340	21
-6	10	2	235	201	24
-5	10	2	855	880	11
-4	10	2	371	332	14
-3	10	2	1159	1223	12
-2	10	2	443	506	12
-1	10	2	106	131	-48
0	10	2	179	159	20
1	10	2	913	864	10
2	10	2	462	444	13
3	10	2	1058	1018	11
4	10	2	388	390	15
5	10	2	763	762	11
6	10	2	60	270	-60
-5	11	2	428	398	15
-4	11	2	48	103	-48
-3	11	2	445	460	13
-2	11	2	583	618	11
-1	11	2	1052	1123	11
0	11	2	752	718	14
1	11	2	858	830	10
2	11	2	261	240	20
3	11	2	183	207	31
4	11	2	167	203	35
5	11	2	516	521	14
-4	12	2	1033	1067	12
-3	12	2	50	101	-50
-2	12	2	622	682	11

H	K	L	10FO	10FC	10S
-10	0	2	775	797	11
-9	0	2	326	331	16
-8	0	2	46	43	-46
-7	0	2	178	201	24
-6	0	2	1717	1694	10
-5	0	2	212	233	15
-4	0	2	2967	3082	11
-3	0	2	106	31	22
-2	0	2	2336	2513	9
-1	0	2	104	85	14
0	0	2	216	142	6
1	0	2	353	303	7
2	0	2	2045	1899	9
3	0	2	78	77	-41
4	0	2	2497	2380	12
5	0	2	131	141	26
6	0	2	643	661	10
7	0	2	335	369	15
8	0	2	173	184	29
9	0	2	589	575	12
10	0	2	955	997	11
-11	1	2	281	289	22
-10	1	2	610	620	12
-9	1	2	1223	1213	12
-8	1	2	618	590	11
-7	1	2	1103	1141	10
-2	-10	3	1351	1349	12
-1	-10	3	520	475	12
0	-10	3	505	455	45
1	-10	3	194	204	27
2	-10	3	371	393	16
3	-10	3	220	131	25
4	-10	3	813	791	12
5	-10	3	688	628	12
-8	-9	3	111	107	-90
-7	-9	3	1219	1234	13
-6	-9	3	50	90	-50
-5	-9	3	756	832	11
-4	-9	3	346	329	15
-3	-9	3	325	327	16
-2	-9	3	279	258	18
-1	-9	3	501	468	12
0	-9	3	308	226	30
1	-9	3	1447	1439	13
2	-9	3	113	17	-52
3	-9	3	1063	1071	12
4	-9	3	287	214	19
5	-9	3	52	60	-52
6	-9	3	348	389	19
-8	-8	3	629	603	13

H	K	L	10FO	10FC	10S
2	2	2	705	696	8
3	2	2	1806	1768	11
4	2	2	1606	1522	12
5	2	2	1455	1356	12
6	2	2	480	483	11
7	2	2	294	230	16
8	2	2	546	573	12
9	2	2	549	553	12
10	2	2	568	562	13
-10	3	2	891	902	11
-9	3	2	277	358	20
-8	3	2	1719	1763	13
-7	3	2	206	226	21
-6	3	2	1112	1094	10
-5	3	2	227	249	14
-4	3	2	360	402	9
-3	3	2	102	79	-27
-2	3	2	1614	1806	8
-1	3	2	303	301	8
0	3	2	2210	2231	28
1	3	2	167	116	14
2	3	2	1332	1302	10
3	3	2	627	506	8
4	3	2	850	777	8
5	3	2	568	598	10
6	3	2	1690	1681	13
8	-7	3	797	761	13
-9	-6	3	900	900	12
-8	-6	3	86	182	-86
-7	-6	3	484	460	12
-6	-6	3	132	156	-38
-5	-6	3	784	782	10
-4	-6	3	192	181	22
-3	-6	3	2244	2421	15
-2	-6	3	167	152	22
-1	-6	3	1565	1566	13
0	-6	3	102	130	-28
1	-6	3	108	161	-39
2	-6	3	319	385	13
3	-6	3	770	752	10
4	-6	3	395	353	13
5	-6	3	1474	1469	13
6	-6	3	166	216	33
7	-6	3	1199	1168	13
8	-6	3	480	431	14
-10	-5	3	156	60	-41
-9	-5	3	393	405	15
-8	-5	3	907	882	11
-7	-5	3	661	678	11
-6	-5	3	1296	1345	12

H	K	L	10FO	10FC	10S
-4	5	2	255	228	13
-3	5	2	729	805	7
-2	5	2	1139	1293	7
-1	5	2	1813	1995	9
0	5	2	1496	1495	12
1	5	2	1782	1693	13
2	5	2	742	726	8
3	5	2	335	278	10
4	5	2	433	461	11
5	5	2	609	592	10
6	5	2	904	902	10
7	5	2	1060	1075	11
8	5	2	580	562	12
9	5	2	727	750	12
-9	6	2	239	229	23
-8	6	2	249	233	20
-7	6	2	192	181	25
-6	6	2	730	768	11
-5	6	2	96	98	-50
-4	6	2	1680	1815	10
-3	6	2	157	131	21
-2	6	2	1399	1564	8
-1	6	2	376	395	9
0	6	2	552	568	15
1	6	2	197	206	16
2	6	2	1884	1836	13
7	-4	3	237	360	22
8	-4	3	593	579	12
9	-4	3	436	450	16
-10	-3	3	450	452	14
-9	-3	3	522	486	12
-8	-3	3	342	403	15
-7	-3	3	1552	1590	13
-6	-3	3	289	291	14
-5	-3	3	1357	1458	11
-4	-3	3	252	295	13
-3	-3	3	456	473	8
-2	-3	3	327	364	9
-1	-3	3	956	997	9
0	-3	3	497	453	12
1	-3	3	2348	2302	11
2	-3	3	306	277	11
3	-3	3	2338	2133	13
4	-3	3	548	518	10
5	-3	3	172	159	25
6	-3	3	453	485	12
7	-3	3	1181	1142	12
8	-3	3	181	147	29
9	-3	3	995	1027	12
-11	-2	3	543	538	14

H	K	L	10FO	10FC	10S
-3	8	2	1148	1214	10
-2	8	2	592	655	10
-1	8	2	387	427	11
0	8	2	116	85	-31
1	8	2	901	876	10
2	8	2	997	998	11
3	8	2	1647	1657	13
4	8	2	899	923	11
5	8	2	957	928	11
6	8	2	565	551	12
7	8	2	296	264	18
8	8	2	338	372	18
-8	9	2	1174	1167	13
-7	9	2	214	140	25
-6	9	2	906	911	12
-5	9	2	219	289	23
-4	9	2	216	193	21
-3	9	2	88	157	-88
-2	9	2	974	1089	10
-1	9	2	403	428	11
0	9	2	1211	1238	21
1	9	2	227	250	21
2	9	2	1250	1189	11
3	9	2	339	383	14
4	9	2	347	333	15
5	9	2	384	287	15
0	-1	3	2937	2817	36
1	-1	3	1100	1022	9
2	-1	3	1770	1657	11
3	-1	3	699	643	8
4	-1	3	1151	1088	10
5	-1	3	839	703	9
6	-1	3	739	703	10
7	-1	3	581	609	11
8	-1	3	1035	1039	11
9	-1	3	810	776	12
10	-1	3	673	690	13
-11	0	3	991	938	11
-10	0	3	51	120	-51
-9	0	3	1237	1222	11
-8	0	3	142	109	33
-7	0	3	554	520	10
-6	0	3	231	256	16
-5	0	3	968	1026	8
-4	0	3	153	142	19
-3	0	3	1817	1950	10
-2	0	3	154	81	15
-1	0	3	3270	3307	9
0	0	3	446	404	5
1	0	3	33	54	-33

H	K	L	10FO	10FC	10S
-1	12	2	48	74	-48
0	12	2	120	153	-50
1	12	2	204	227	29
2	12	2	867	797	11
3	12	2	221	242	27
-3	-12	3	901	976	12
-2	-12	3	51	37	-51
-1	-12	3	974	905	13
0	-12	3	432	408	42
1	-12	3	92	120	-92
2	-12	3	130	168	-56
-5	-11	3	679	680	13
-4	-11	3	524	579	13
-3	-11	3	147	194	-37
-2	-11	3	48	49	-48
-1	-11	3	538	513	12
0	-11	3	930	911	42
1	-11	3	649	657	12
2	-11	3	791	798	12
3	-11	3	558	546	13
4	-11	3	377	354	17
-7	-10	3	166	193	40
-6	-10	3	109	67	-66
-5	-10	3	250	287	23
-4	-10	3	887	936	11
-3	-10	3	520	578	12
-10	2	3	1195	1205	12
-9	2	3	698	669	11
-8	2	3	1125	1184	10
-7	2	3	368	391	13
-6	2	3	454	473	10
-5	2	3	859	850	9
-4	2	3	1256	1338	9
-3	2	3	780	857	7
-2	2	3	2003	2101	10
-1	2	3	1182	1196	8
0	2	3	1762	1665	7
1	2	3	542	442	7
2	2	3	1040	950	9
3	2	3	447	337	9
4	2	3	1983	1898	13
5	2	3	1304	1225	12
6	2	3	1229	1166	12
7	2	3	550	603	11
8	2	3	561	571	12
9	2	3	433	488	15
10	2	3	277	297	22
-10	3	3	463	441	14
-9	3	3	475	531	13
-8	3	3	416	364	13

H	K	L	10FO	10FC	10S
-7	-8	3	240	309	23
-6	-8	3	221	230	25
-5	-8	3	361	396	15
-4	-8	3	771	837	10
-3	-8	3	833	923	10
-2	-8	3	941	971	10
-1	-8	3	631	615	11
0	-8	3	643	646	22
1	-8	3	334	361	14
2	-8	3	274	219	18
3	-8	3	649	584	11
4	-8	3	1235	1173	12
5	-8	3	890	792	11
6	-8	3	1260	1170	12
7	-8	3	528	508	14
-9	-7	3	254	276	24
-8	-7	3	1243	1233	13
-7	-7	3	516	517	12
-6	-7	3	1406	1368	13
-5	-7	3	516	550	11
-4	-7	3	637	685	10
-3	-7	3	223	262	20
-2	-7	3	136	76	32
-1	-7	3	634	620	10
0	-7	3	1158	1122	47
1	-7	3	759	739	10
2	-7	3	1867	1786	14
3	-7	3	268	246	18
4	-7	3	576	514	11
5	-7	3	464	462	13
6	-7	3	467	467	15
7	-7	3	463	477	15
5	4	3	707	689	10
6	4	3	1513	1506	12
7	4	3	322	284	16
8	4	3	565	570	12
9	4	3	440	461	15
-10	5	3	146	99	-42
-9	5	3	388	397	15
-8	5	3	865	900	10
-7	5	3	673	678	10
-6	5	3	1298	1316	10
-5	5	3	491	551	10
-4	5	3	1153	1260	8
-3	5	3	445	503	9
-2	5	3	361	371	9
-1	5	3	365	259	9
0	5	3	1575	1591	14
1	5	3	1139	1063	10
2	5	3	1603	1553	12

H	K	L	10FO	10FC	10S
-5	-5	3	538	533	10
-4	-5	3	1192	1233	11
-3	-5	3	466	487	9
-2	-5	3	344	398	10
-1	-5	3	276	362	12
0	-5	3	1567	1572	51
1	-5	3	1078	1076	10
2	-5	3	1593	1551	13
3	-5	3	658	640	9
4	-5	3	700	667	10
5	-5	3	362	353	14
6	-5	3	404	377	14
7	-5	3	314	388	18
8	-5	3	938	932	12
9	-5	3	766	744	13
-10	-4	3	904	878	12
-9	-4	3	833	864	11
-8	-4	3	725	750	11
-7	-4	3	258	171	18
-6	-4	3	127	95	-37
-5	-4	3	646	680	9
-4	-4	3	1272	1424	11
-3	-4	3	706	722	9
-2	-4	3	1894	2034	12
-1	-4	3	1122	1055	10
0	-4	3	462	504	19
1	-4	3	747	697	8
2	-4	3	538	484	9
3	-4	3	1108	1119	10
4	-4	3	1322	1269	12
5	-4	3	658	690	11
6	-4	3	1529	1498	13
4	7	3	534	530	11
5	7	3	447	449	13
6	7	3	474	466	13
7	7	3	450	494	15
8	7	3	757	749	12
-8	8	3	574	633	13
-7	8	3	286	260	19
-6	8	3	220	242	22
-5	8	3	387	384	14
-4	8	3	802	826	10
-3	8	3	859	905	10
-2	8	3	917	965	10
-1	8	3	584	628	10
0	8	3	630	623	7
1	8	3	370	354	13
2	8	3	204	275	22
3	8	3	609	587	11
4	8	3	1213	1150	12

H	K	L	10FO	10FC	10S
-10	-2	3	1178	1224	11
-9	-2	3	680	675	10
-8	-2	3	1133	1168	10
-7	-2	3	417	368	11
-6	-2	3	452	462	10
-5	-2	3	817	879	8
-4	-2	3	1261	1324	7
-3	-2	3	798	866	6
-2	-2	3	1978	2135	7
-1	-2	3	1231	1171	7
0	-2	3	1709	1696	50
1	-2	3	467	492	8
2	-2	3	1012	968	9
3	-2	3	338	432	11
4	-2	3	2012	1897	14
5	-2	3	1289	1250	10
6	-2	3	1207	1208	10
7	-2	3	631	538	11
8	-2	3	594	556	11
9	-2	3	480	459	14
10	-2	3	285	278	23
-11	-1	3	245	202	26
-10	-1	3	195	221	28
-9	-1	3	170	298	30
-8	-1	3	913	926	9
-7	-1	3	445	467	11
-6	-1	3	1945	1963	10
-5	-1	3	1490	1541	9
-4	-1	3	1053	1117	7
-3	-1	3	440	453	7
-2	-1	3	794	808	6
-1	-1	3	2130	2094	9
2	11	3	805	781	11
3	11	3	560	535	13
4	11	3	366	384	17
-3	12	3	949	971	12
-2	12	3	115	49	-51
-1	12	3	897	921	11
0	12	3	405	388	90
1	12	3	50	146	-50
2	12	3	142	164	-46
-3	-12	4	52	89	-52
-2	-12	4	918	909	12
-1	-12	4	230	209	28
0	-12	4	1041	993	27
1	-12	4	192	225	33
-5	-11	4	868	876	11
-4	-11	4	574	607	12
-3	-11	4	862	914	12
-2	-11	4	235	238	23

H	K	L	10FO	10FC	10S
2	0	3	317	299	9
3	0	3	1371	1292	10
4	0	3	203	182	16
5	0	3	1370	1327	11
6	0	3	258	253	17
7	0	3	720	764	10
8	0	3	529	518	12
9	0	3	188	221	32
10	0	3	401	405	17
-11	1	3	154	282	-41
-10	1	3	253	192	22
-9	1	3	276	222	18
-8	1	3	925	922	9
-7	1	3	464	469	11
-6	1	3	1918	1989	11
-5	1	3	1496	1545	9
-4	1	3	1043	1121	7
-3	1	3	434	460	7
-2	1	3	793	822	7
-1	1	3	2121	2089	9
0	1	3	2916	2835	30
1	1	3	1063	1040	8
2	1	3	1761	1682	11
3	1	3	675	644	8
4	1	3	1153	1080	9
5	1	3	727	794	9
6	1	3	727	728	10
7	1	3	607	581	11
8	1	3	1055	1001	11
9	1	3	773	802	12
10	1	3	643	701	13
-11	2	3	520	542	14
-2	-8	4	690	671	11
-1	-8	4	1010	965	11
0	-8	4	955	891	37
1	-8	4	1449	1422	13
2	-8	4	594	599	11
3	-8	4	260	256	19
4	-8	4	482	416	12
5	-8	4	992	980	12
6	-8	4	663	671	13
7	-8	4	766	751	13
-9	-7	4	156	120	-41
-8	-7	4	282	233	19
-7	-7	4	690	677	11
-6	-7	4	340	286	15
-5	-7	4	1124	1111	11
-4	-7	4	770	800	10
-3	-7	4	1267	1323	11
-2	-7	4	363	352	13

H	K	L	10FO	10FC	10S
-7	3	3	1548	1595	12
-6	3	3	261	293	15
-5	3	3	1387	1444	10
-4	3	3	301	270	10
-3	3	3	434	484	8
-2	3	3	351	348	8
-1	3	3	982	955	8
0	3	3	465	488	7
1	3	3	2384	2302	11
2	3	3	281	274	11
3	3	3	2215	2187	13
4	3	3	527	532	9
5	3	3	163	154	25
6	3	3	473	481	11
7	3	3	1138	1169	12
8	3	3	128	112	-45
9	3	3	1011	1014	12
-10	4	3	867	898	11
-9	4	3	873	837	11
-8	4	3	760	732	10
-7	4	3	187	247	23
-6	4	3	144	152	29
-5	4	3	658	663	8
-4	4	3	1325	1379	8
-3	4	3	678	734	7
-2	4	3	1859	1993	10
-1	4	3	1060	1085	7
0	4	3	506	478	8
1	4	3	752	729	8
2	4	3	522	516	9
3	4	3	1141	1095	10
4	4	3	1275	1283	11
1	-5	4	1006	949	9
2	-5	4	807	804	9
3	-5	4	1283	1258	11
4	-5	4	516	536	11
5	-5	4	985	982	12
6	-5	4	671	677	11
7	-5	4	279	289	20
8	-5	4	455	449	15
-10	-4	4	640	601	12
-9	-4	4	923	948	11
-8	-4	4	616	636	11
-7	-4	4	1352	1408	11
-6	-4	4	265	274	17
-5	-4	4	386	383	11
-4	-4	4	230	245	15
-3	-4	4	1213	1268	10
-2	-4	4	725	724	9
-1	-4	4	2066	2043	13

H	K	L	10FO	10FC	10S
3	5	3	663	647	9
4	5	3	681	678	9
5	5	3	353	341	14
6	5	3	386	407	13
7	5	3	423	309	13
8	5	3	925	921	11
9	5	3	788	752	12
-9	6	3	927	905	12
-8	6	3	171	152	31
-7	6	3	489	474	12
-6	6	3	148	132	31
-5	6	3	773	805	10
-4	6	3	210	195	18
-3	6	3	2122	2416	11
-2	6	3	149	145	21
-1	6	3	1458	1559	9
0	6	3	126	110	18
1	6	3	171	161	20
2	6	3	379	317	11
3	6	3	767	758	10
4	6	3	336	385	14
5	6	3	1469	1477	12
6	6	3	208	182	25
7	6	3	1168	1191	12
8	6	3	387	477	17
-9	7	3	301	257	19
-8	7	3	1253	1234	13
-7	7	3	500	528	12
-6	7	3	1334	1404	12
-5	7	3	507	527	11
-4	7	3	634	664	10
-3	7	3	272	249	15
-2	7	3	41	119	-41
-1	7	3	597	613	9
0	7	3	1100	1109	19
1	7	3	716	754	9
2	7	3	1789	1789	14
3	7	3	235	237	19
-3	-2	4	536	559	8
-2	-2	4	579	559	7
-1	-2	4	2013	2038	10
0	-2	4	1192	1171	10
1	-2	4	1373	1341	11
2	-2	4	700	699	8
3	-2	4	315	342	11
4	-2	4	780	714	9
5	-2	4	1015	976	10
6	-2	4	777	735	11
7	-2	4	1363	1341	12
8	-2	4	496	432	13

H	K	L	10FO	10FC	10S
5	8	3	790	811	11
6	8	3	1202	1167	12
7	8	3	480	510	14
-8	9	3	141	147	-45
-7	9	3	1239	1228	13
-6	9	3	150	51	33
-5	9	3	795	811	11
-4	9	3	319	343	16
-3	9	3	333	338	14
-2	9	3	260	272	16
-1	9	3	451	495	11
0	9	3	224	242	14
1	9	3	1441	1430	12
2	9	3	46	54	-46
3	9	3	1087	1034	11
4	9	3	214	278	24
5	9	3	49	33	-49
6	9	3	419	367	15
-7	10	3	197	174	29
-6	10	3	49	111	-49
-5	10	3	281	294	18
-4	10	3	889	918	11
-3	10	3	533	578	12
-2	10	3	1261	1349	12
-1	10	3	473	496	11
0	10	3	436	480	17
1	10	3	221	204	22
2	10	3	385	390	15
3	10	3	136	204	-41
4	10	3	820	776	11
5	10	3	645	634	12
-5	11	3	689	695	12
-4	11	3	572	564	12
-3	11	3	119	177	-48
-2	11	3	89	55	-89
-1	11	3	473	524	13
0	11	3	900	902	8
1	11	3	643	657	12
-10	1	4	315	342	18
-9	1	4	249	280	21
-8	1	4	347	292	15
-7	1	4	707	731	9
-6	1	4	750	756	8
-5	1	4	1863	1971	11
-4	1	4	1102	1201	8
-3	1	4	1359	1404	10
-2	1	4	119	168	21
-1	1	4	1094	1040	8
0	1	4	734	673	7
1	1	4	996	930	8

H	K	L	10FO	10FC	10S
-1	-11	4	172	106	30
0	-11	4	100	158	-49
1	-11	4	742	709	12
2	-11	4	671	621	12
3	-11	4	567	556	13
4	-11	4	620	584	13
-6	-10	4	300	304	20
-5	-10	4	319	312	18
-4	-10	4	301	321	19
-3	-10	4	862	917	11
-2	-10	4	275	285	19
-1	-10	4	1243	1202	12
0	-10	4	497	483	17
1	-10	4	719	682	11
2	-10	4	424	405	14
3	-10	4	103	44	-72
4	-10	4	306	346	20
5	-10	4	455	458	16
-7	-9	4	52	87	-52
-6	-9	4	779	859	12
-5	-9	4	140	157	-37
-4	-9	4	1170	1256	11
-3	-9	4	178	157	28
-2	-9	4	736	728	11
-1	-9	4	137	127	-39
0	-9	4	501	473	25
1	-9	4	239	250	21
2	-9	4	1344	1283	12
3	-9	4	179	104	28
4	-9	4	984	970	12
5	-9	4	369	368	17
6	-9	4	517	474	15
-8	-8	4	689	705	12
-7	-8	4	1024	989	11
-6	-8	4	295	308	17
-5	-8	4	165	121	29
-4	-8	4	251	288	20
-3	-8	4	796	799	10
5	3	4	326	346	13
6	3	4	255	272	19
7	3	4	625	592	12
8	3	4	539	527	12
9	3	4	361	407	17
-10	4	4	613	628	12
-9	4	4	927	965	11
-8	4	4	645	617	10
-7	4	4	1377	1382	11
-6	4	4	274	280	16
-5	4	4	356	377	12
-4	4	4	238	217	15

H	K	L	10FO	10FC	10S
-1	-7	4	289	264	16
0	-7	4	294	334	11
1	-7	4	995	1022	10
2	-7	4	730	674	11
3	-7	4	1075	1038	11
4	-7	4	477	460	12
5	-7	4	759	706	12
6	-7	4	622	546	12
7	-7	4	169	206	38
-9	-6	4	146	198	-42
-8	-6	4	1263	1272	13
-7	-6	4	238	235	22
-6	-6	4	924	973	11
-5	-6	4	302	351	16
-4	-6	4	653	662	10
-3	-6	4	42	11	-42
-2	-6	4	1668	1690	14
-1	-6	4	42	87	-42
0	-6	4	1546	1593	44
1	-6	4	382	431	12
2	-6	4	835	814	10
3	-6	4	309	348	15
4	-6	4	364	359	14
5	-6	4	598	513	11
6	-6	4	1156	1126	12
7	-6	4	104	171	-104
8	-6	4	908	888	13
-10	-5	4	378	359	17
-9	-5	4	230	261	24
-8	-5	4	260	252	20
-7	-5	4	604	636	11
-6	-5	4	685	679	10
-5	-5	4	1412	1523	12
-4	-5	4	1358	1403	12
-3	-5	4	1326	1349	11
-2	-5	4	725	710	9
-1	-5	4	221	170	15
0	-5	4	1223	1181	46
3	6	4	353	282	13
4	6	4	350	344	13
5	6	4	518	578	11
6	6	4	1126	1109	12
7	6	4	165	158	33
8	6	4	888	890	12
-9	7	4	125	156	-56
-8	7	4	267	198	21
-7	7	4	664	688	12
-6	7	4	269	302	18
-5	7	4	1075	1149	11
-4	7	4	761	783	10

H	K	L	10FO	10FC	10S
0	-4	4	1477	1426	36
1	-4	4	1323	1353	10
2	-4	4	709	705	9
3	-4	4	327	291	12
4	-4	4	487	476	11
5	-4	4	1026	986	11
6	-4	4	689	680	11
7	-4	4	1220	1177	12
8	-4	4	558	557	13
9	-4	4	652	696	13
-10	-3	4	837	826	12
-9	-3	4	368	418	15
-8	-3	4	251	224	20
-7	-3	4	245	197	18
-6	-3	4	1623	1648	13
-5	-3	4	101	157	-44
-4	-3	4	1498	1593	12
-3	-3	4	285	296	11
-2	-3	4	975	981	9
-1	-3	4	299	276	11
0	-3	4	429	503	15
1	-3	4	371	339	10
2	-3	4	2411	2458	13
3	-3	4	527	483	9
4	-3	4	2093	2010	15
5	-3	4	311	345	15
6	-3	4	268	283	20
7	-3	4	597	667	11
8	-3	4	538	538	13
9	-3	4	403	363	17
-11	-2	4	557	581	14
-10	-2	4	601	563	12
-9	-2	4	1045	1057	10
-8	-2	4	827	849	10
-7	-2	4	947	924	9
-6	-2	4	414	467	11
-5	-2	4	547	578	8
-4	-2	4	587	633	8
-3	10	4	869	904	11
-2	10	4	242	289	20
-1	10	4	1148	1207	11
0	10	4	461	492	11
1	10	4	686	699	12
2	10	4	417	422	14
3	10	4	141	6	-39
4	10	4	337	305	18
5	10	4	438	466	16
-5	11	4	848	893	12
-4	11	4	569	593	12
-3	11	4	889	896	11

H	K	L	10FO	10FC	10S
9	-2	4	659	663	12
-11	-1	4	726	769	12
-10	-1	4	334	303	18
-9	-1	4	290	258	18
-8	-1	4	312	364	16
-7	-1	4	702	728	10
-6	-1	4	709	767	9
-5	-1	4	1897	1938	10
-4	-1	4	1112	1200	8
-3	-1	4	1346	1418	8
-2	-1	4	195	156	13
-1	-1	4	1088	1061	7
0	-1	4	719	685	5
1	-1	4	924	946	9
2	-1	4	892	844	9
3	-1	4	2238	2121	13
4	-1	4	1001	940	9
5	-1	4	1323	1307	11
6	-1	4	626	566	11
7	-1	4	374	399	15
8	-1	4	526	530	13
9	-1	4	625	671	12
-11	0	4	169	145	37
-10	0	4	1266	1273	11
-9	0	4	158	200	33
-8	0	4	1160	1193	9
-7	0	4	146	78	28
-6	0	4	1198	1262	9
-5	0	4	234	214	14
-4	0	4	216	232	15
-3	0	4	36	10	-36
-2	0	4	2319	2380	11
-1	0	4	549	466	7
0	0	4	2705	2667	10
1	0	4	91	116	-31
2	0	4	510	491	8
3	0	4	679	638	9
4	0	4	317	319	12
5	0	4	471	454	11
6	0	4	1403	1394	11
7	0	4	48	53	-48
8	0	4	1546	1530	12
9	0	4	418	432	16
-11	1	4	787	738	12
-7	-8	5	640	655	12
-6	-8	5	646	661	11
-5	-8	5	508	531	12
-4	-8	5	440	456	13
-3	-8	5	246	244	20
-2	-8	5	201	104	24

H	K	L	10FO	10FC	10S
2	1	4	917	833	8
3	1	4	2244	2116	13
4	1	4	1021	924	9
5	1	4	1330	1267	11
6	1	4	590	594	11
7	1	4	423	386	13
8	1	4	518	517	13
9	1	4	658	630	13
-11	2	4	593	558	13
-10	2	4	559	563	13
-9	2	4	1069	1048	11
-8	2	4	815	829	11
-7	2	4	924	946	10
-6	2	4	415	436	11
-5	2	4	581	549	8
-4	2	4	618	626	8
-3	2	4	522	598	8
-2	2	4	560	592	7
-1	2	4	2015	2023	11
0	2	4	1188	1186	6
1	2	4	1382	1353	11
2	2	4	694	688	9
3	2	4	360	276	10
4	2	4	739	751	9
5	2	4	986	1001	10
6	2	4	749	747	11
7	2	4	1337	1364	13
8	2	4	418	484	15
9	2	4	617	666	13
-10	3	4	826	834	11
-9	3	4	422	383	14
-8	3	4	250	231	19
-7	3	4	204	248	21
-6	3	4	1607	1672	11
-5	3	4	148	143	24
-4	3	4	1474	1605	9
-3	3	4	269	299	11
-2	3	4	945	983	7
-1	3	4	278	301	11
0	3	4	510	426	6
1	3	4	352	368	10
2	3	4	2507	2424	13
3	3	4	501	472	9
4	3	4	2088	1998	15
-2	-5	5	1451	1418	13
-1	-5	5	425	362	11
0	-5	5	714	711	20
1	-5	5	347	306	12
2	-5	5	591	541	10
3	-5	5	301	357	15

H	K	L	10FO	10FC	10S
-3	4	4	1184	1263	8
-2	4	4	704	733	7
-1	4	4	2001	2017	11
0	4	4	1459	1428	18
1	4	4	1376	1349	11
2	4	4	711	706	9
3	4	4	318	294	12
4	4	4	505	474	10
5	4	4	1016	1012	11
6	4	4	695	683	11
7	4	4	1133	1234	12
8	4	4	547	562	12
9	4	4	717	674	12
-10	5	4	372	371	17
-9	5	4	276	204	19
-8	5	4	229	242	23
-7	5	4	603	622	10
-6	5	4	658	700	9
-5	5	4	1429	1510	10
-4	5	4	1306	1420	9
-3	5	4	1245	1393	8
-2	5	4	695	707	7
-1	5	4	134	204	23
0	5	4	1209	1217	6
1	5	4	970	980	9
2	5	4	807	801	10
3	5	4	1269	1258	11
4	5	4	507	521	12
5	5	4	1002	965	11
6	5	4	675	616	11
7	5	4	298	286	18
8	5	4	455	437	15
-9	6	4	173	179	34
-8	6	4	1269	1289	12
-7	6	4	257	258	18
-6	6	4	932	970	11
-5	6	4	372	323	12
-4	6	4	619	687	9
-3	6	4	98	27	-43
-2	6	4	1604	1692	9
-1	6	4	78	74	-78
0	6	4	1582	1558	9
1	6	4	424	397	11
2	6	4	838	810	10
-3	-2	5	600	603	8
-2	-2	5	1047	1079	7
-1	-2	5	744	692	7
0	-2	5	1340	1374	12
1	-2	5	1556	1505	12
2	-2	5	1645	1567	12

H	K	L	10FO	10FC	10S
-3	7	4	1242	1308	11
-2	7	4	342	350	12
-1	7	4	270	261	15
0	7	4	341	290	16
1	7	4	986	991	10
2	7	4	698	677	10
3	7	4	1018	1051	11
4	7	4	482	454	12
5	7	4	702	711	11
6	7	4	541	604	12
7	7	4	197	190	30
-8	8	4	715	686	12
-7	8	4	989	1005	12
-6	8	4	302	282	16
-5	8	4	45	150	-45
-4	8	4	278	279	16
-3	8	4	722	812	10
-2	8	4	645	691	10
-1	8	4	922	968	10
0	8	4	877	901	19
1	8	4	1389	1426	12
2	8	4	561	586	12
3	8	4	237	246	21
4	8	4	381	435	15
5	8	4	997	953	11
6	8	4	665	641	12
7	8	4	714	763	13
-7	9	4	50	94	-50
-6	9	4	843	829	11
-5	9	4	149	133	33
-4	9	4	1169	1258	12
-3	9	4	146	171	32
-2	9	4	682	725	10
-1	9	4	125	137	-39
0	9	4	488	488	18
1	9	4	250	206	20
2	9	4	1312	1292	12
3	9	4	47	126	-47
4	9	4	955	959	12
5	9	4	402	340	16
6	9	4	481	488	15
-6	10	4	299	303	19
-5	10	4	339	331	15
-4	10	4	322	320	16
-10	1	5	1181	1181	12
-9	1	5	596	592	11
-8	1	5	525	581	11
-7	1	5	180	179	25
-6	1	5	655	688	9
-5	1	5	580	602	9

H	K	L	10FO	10FC	10S
-2	11	4	226	190	22
-1	11	4	141	70	-36
0	11	4	170	137	24
1	11	4	702	704	13
2	11	4	637	628	12
3	11	4	513	558	14
-3	12	4	49	64	-49
-2	12	4	894	895	11
-1	12	4	206	194	26
0	12	4	984	1012	40
1	12	4	140	204	-48
-4	-11	5	845	883	12
-3	-11	5	577	601	13
-2	-11	5	864	852	12
-1	-11	5	553	517	13
0	-11	5	190	181	34
1	-11	5	208	185	27
2	-11	5	199	167	32
3	-11	5	475	455	15
-6	-10	5	937	971	12
-5	-10	5	226	239	25
-4	-10	5	567	592	13
-3	-10	5	253	235	22
-2	-10	5	590	589	12
-1	-10	5	341	318	16
0	-10	5	1027	1026	20
1	-10	5	708	690	12
2	-10	5	871	887	12
3	-10	5	357	344	17
4	-10	5	458	443	15
-7	-9	5	263	257	22
-6	-9	5	91	82	-91
-5	-9	5	591	668	12
-4	-9	5	228	202	22
-3	-9	5	1360	1336	11
-2	-9	5	136	65	-39
-1	-9	5	780	744	11
0	-9	5	225	160	15
1	-9	5	135	128	-39
2	-9	5	349	309	16
3	-9	5	963	937	12
4	-9	5	50	112	-50
5	-9	5	1151	1145	13
-8	-8	5	888	902	12
6	3	5	350	297	15
7	3	5	750	783	11
8	3	5	438	501	15
-10	4	5	292	267	19
-9	4	5	411	417	14
-8	4	5	949	941	10

H	K	L	10FO	10FC	10S
-1	-8	5	502	454	12
0	-8	5	1181	1149	11
1	-8	5	1206	1142	11
2	-8	5	1470	1397	13
3	-8	5	599	515	12
4	-8	5	209	321	26
5	-8	5	384	360	17
6	-8	5	456	466	17
-9	-7	5	422	374	16
-8	-7	5	606	562	13
-7	-7	5	151	170	36
-6	-7	5	201	150	25
-5	-7	5	423	328	12
-4	-7	5	1348	1372	12
-3	-7	5	833	831	10
-2	-7	5	1423	1461	11
-1	-7	5	217	285	21
0	-7	5	676	674	21
1	-7	5	333	352	16
2	-7	5	690	682	11
3	-7	5	528	508	12
4	-7	5	1354	1262	13
5	-7	5	584	567	12
6	-7	5	936	910	12
7	-7	5	470	448	16
-9	-6	5	678	683	12
-8	-6	5	256	289	22
-7	-6	5	1404	1373	12
-6	-6	5	119	78	-43
-5	-6	5	1337	1412	12
-4	-6	5	231	259	20
-3	-6	5	275	256	16
-2	-6	5	334	375	14
-1	-6	5	1204	1165	11
0	-6	5	323	288	12
1	-6	5	1854	1874	13
2	-6	5	273	300	17
3	-6	5	1021	978	11
4	-6	5	391	364	15
5	-6	5	96	89	-96
6	-6	5	481	474	14
7	-6	5	746	771	12
-10	-5	5	860	856	12
-9	-5	5	382	323	16
-8	-5	5	526	576	12
-7	-5	5	612	542	11
-6	-5	5	296	346	16
-5	-5	5	462	515	11
-4	-5	5	1437	1534	12
-3	-5	5	1134	1202	11

H	K	L	10FO	10FC	10S
4	-5	5	1082	1137	12
5	-5	5	942	927	11
6	-5	5	1078	1080	12
7	-5	5	560	600	13
8	-5	5	291	308	23
-10	-4	5	247	257	25
-9	-4	5	392	393	16
-8	-4	5	932	961	11
-7	-4	5	586	621	11
-6	-4	5	1161	1241	11
-5	-4	5	641	656	10
-4	-4	5	615	662	9
-3	-4	5	110	111	-34
-2	-4	5	747	683	9
-1	-4	5	417	338	10
0	-4	5	1766	1741	54
1	-4	5	784	736	9
2	-4	5	1358	1319	12
3	-4	5	656	659	10
4	-4	5	424	382	12
5	-4	5	541	547	11
6	-4	5	458	396	12
7	-4	5	580	584	13
8	-4	5	879	935	13
-10	-3	5	162	159	34
-9	-3	5	1122	1106	12
-8	-3	5	333	324	17
-7	-3	5	148	69	32
-6	-3	5	239	205	18
-5	-3	5	943	992	10
-4	-3	5	443	441	10
-3	-3	5	1533	1550	12
-2	-3	5	406	385	10
-1	-3	5	1765	1787	13
0	-3	5	522	425	7
1	-3	5	336	340	10
2	-3	5	436	482	10
3	-3	5	1626	1612	13
4	-3	5	278	253	16
5	-3	5	1503	1487	13
6	-3	5	370	339	14
7	-3	5	776	763	12
8	-3	5	484	458	15
-10	-2	5	334	333	18
-9	-2	5	542	536	12
-8	-2	5	964	950	10
-7	-2	5	818	860	9
-6	-2	5	1467	1528	9
-5	-2	5	607	613	9
-4	-2	5	645	747	8

H	K	L	10FO	10FC	10S
3	-2	5	873	882	10
4	-2	5	856	778	10
5	-2	5	641	565	11
6	-2	5	644	682	11
7	-2	5	534	590	12
8	-2	5	1008	1035	12
9	-2	5	549	557	14
-11	-1	5	535	516	14
-10	-1	5	1171	1175	11
-9	-1	5	568	604	12
-8	-1	5	573	534	11
-7	-1	5	224	172	20
-6	-1	5	654	685	9
-5	-1	5	577	613	9
-4	-1	5	1381	1457	8
-3	-1	5	1213	1249	8
-2	-1	5	1959	1975	10
-1	-1	5	858	806	7
0	-1	5	873	874	9
1	-1	5	326	346	10
2	-1	5	707	698	8
3	-1	5	745	627	9
4	-1	5	1472	1473	12
5	-1	5	639	638	10
6	-1	5	808	813	10
7	-1	5	899	836	11
8	-1	5	554	514	13
9	-1	5	538	486	14
-11	0	5	100	88	-100
-10	0	5	85	121	-85
-9	0	5	534	544	12
-8	0	5	176	165	26
-7	0	5	1519	1541	10
-6	0	5	43	12	-43
-5	0	5	1938	2002	11
-4	0	5	119	126	27
-3	0	5	134	119	23
-2	0	5	199	185	15
-1	0	5	1622	1616	10
0	0	5	321	328	10
1	0	5	1172	1124	9
2	0	5	220	202	14
3	0	5	1687	1607	13
4	0	5	498	529	10
5	0	5	152	91	29
6	0	5	345	323	15
7	0	5	1286	1266	12
8	0	5	238	190	24
9	0	5	1163	1140	13
-11	1	5	508	533	14

H	K	L	10FO	10FC	10S
-4	1	5	1369	1484	9
-3	1	5	1225	1249	9
-2	1	5	1957	1987	12
-1	1	5	816	830	8
0	1	5	884	855	14
1	1	5	357	306	10
2	1	5	703	698	8
3	1	5	662	696	9
4	1	5	1502	1427	12
5	1	5	650	628	10
6	1	5	806	801	11
7	1	5	821	885	11
8	1	5	528	522	13
9	1	5	456	522	15
-10	2	5	323	329	18
-9	2	5	534	528	12
-8	2	5	959	978	10
-7	2	5	858	835	10
-6	2	5	1498	1539	11
-5	2	5	600	617	9
-4	2	5	732	674	8
-3	2	5	608	585	8
-2	2	5	1055	1085	9
-1	2	5	706	730	8
0	2	5	1374	1354	13
1	2	5	1508	1512	12
2	2	5	1597	1591	12
3	2	5	891	879	9
4	2	5	810	802	10
5	2	5	553	651	11
6	2	5	673	641	11
7	2	5	606	525	12
8	2	5	1042	1025	12
9	2	5	563	517	13
-10	3	5	147	138	-38
-9	3	5	1136	1124	11
-8	3	5	322	357	16
-7	3	5	94	138	-65
-6	3	5	231	229	17
-5	3	5	943	995	9
-4	3	5	423	451	9
-3	3	5	1479	1568	10
-2	3	5	431	389	9
-1	3	5	1790	1762	13
0	3	5	464	491	6
1	3	5	357	347	10
2	3	5	475	418	10
3	3	5	1682	1599	13
4	3	5	257	293	17
5	3	5	1528	1475	13

H	K	L	10FO	10FC	10S
-7	4	5	681	579	10
-6	4	5	1176	1213	10
-5	4	5	638	660	10
-4	4	5	628	652	9
-3	4	5	60	81	-60
-2	4	5	681	726	8
-1	4	5	347	408	10
0	4	5	1776	1739	28
1	4	5	773	771	9
2	4	5	1351	1332	11
3	4	5	687	643	10
4	4	5	418	409	12
5	4	5	538	542	11
6	4	5	384	409	14
7	4	5	591	582	12
8	4	5	904	922	12
-10	5	5	892	853	11
-9	5	5	341	333	17
-8	5	5	558	563	12
-7	5	5	579	575	11
-6	5	5	353	293	14
-5	5	5	492	479	11
-4	5	5	1452	1518	9
-3	5	5	1140	1186	8
-2	5	5	1375	1457	9
-1	5	5	343	402	12
0	5	5	723	714	9
1	5	5	322	331	12
2	5	5	552	549	10
3	5	5	406	302	12
4	5	5	1141	1074	11
5	5	5	953	921	11
6	5	5	1105	1070	11
7	5	5	611	574	12
8	5	5	313	299	20
-9	6	5	698	681	12
-8	6	5	325	278	16
-7	6	5	1379	1386	13
-6	6	5	46	54	-46
-5	6	5	1336	1411	12
-4	6	5	239	259	18
-3	6	5	231	245	17
-2	6	5	359	331	11
-1	6	5	1102	1182	9
0	6	5	284	315	10
1	6	5	1874	1894	14
2	6	5	309	270	14
3	6	5	985	1010	10
4	6	5	361	432	14
5	6	5	163	119	31

H	K	L	10FO	10FC	10S
6	6	5	440	491	14
7	6	5	763	760	12
-9	7	5	391	404	17
-8	7	5	560	585	12
-7	7	5	165	156	31
-6	7	5	113	216	-47
-5	7	5	313	370	15
-4	7	5	1251	1383	12
-3	7	5	794	830	10
-2	7	5	1375	1440	11
-1	7	5	302	203	15
0	7	5	652	674	25
1	7	5	361	319	14
2	7	5	671	662	10
3	7	5	525	508	12
4	7	5	1305	1265	12
5	7	5	558	554	12
6	7	5	891	904	12
7	7	5	425	472	16
-8	8	5	938	900	12
-7	8	5	668	641	11
-6	8	5	633	669	11
-5	8	5	510	532	12
-4	8	5	464	456	11
-3	8	5	231	236	20
-2	8	5	131	186	-35
-1	8	5	433	471	12
0	8	5	1142	1139	40
1	8	5	1117	1149	11
2	8	5	1360	1397	12
3	8	5	536	549	12
4	8	5	315	228	17
5	8	5	362	380	16
6	8	5	467	458	15
-7	9	5	229	255	25
-6	9	5	48	79	-48
-5	9	5	627	623	11
-4	9	5	207	199	23
-3	9	5	1286	1357	12
-2	9	5	46	76	-46
-1	9	5	727	744	10
0	9	5	180	197	19
1	9	5	135	120	-39
2	9	5	286	335	20
3	9	5	935	960	11
4	9	5	115	67	-58
5	9	5	1131	1154	12
-6	10	5	980	963	12
-5	10	5	242	263	22
-4	10	5	566	622	12

H	K	L	10FO	10FC	10S
3	10	5	332	346	19
4	10	5	463	427	15
-4	11	5	895	882	12
-3	11	5	545	590	13
-2	11	5	845	860	11
-1	11	5	491	516	14
0	11	5	196	184	23
1	11	5	167	175	36
2	11	5	167	220	36
3	11	5	429	472	17
-3	-11	6	596	582	13
-2	-11	6	668	662	13
-1	-11	6	756	687	12
0	-11	6	565	525	23
1	-11	6	499	502	14
-5	-10	6	956	1020	12
-4	-10	6	477	446	14
-3	-10	6	732	736	12
-2	-10	6	425	394	15
-1	-10	6	183	165	30
0	-10	6	338	352	13
1	-10	6	668	679	12
2	-10	6	338	310	18
3	-10	6	837	822	12
-7	-9	6	186	158	32
-6	-9	6	377	375	16
-5	-9	6	49	118	-49
-4	-9	6	420	444	14
-3	-9	6	382	326	15
-2	-9	6	1050	1002	11
-1	-9	6	76	27	-76
0	-9	6	1286	1223	31
1	-9	6	234	200	24
2	-9	6	493	475	14
3	-9	6	281	358	21
4	-9	6	691	682	13
-8	-8	6	341	341	18
-7	-8	6	608	607	12
-6	-8	6	474	449	13
-5	-8	6	775	812	11
-4	-8	6	750	718	11
-3	-8	6	927	918	11
-2	-8	6	382	372	14
-1	-8	6	88	141	-88
0	-8	6	420	423	28
1	-8	6	917	915	11
2	-8	6	788	800	11
3	-8	6	1004	971	12
4	-8	6	487	432	14
5	-8	6	652	628	13

H	K	L	10FO	10FC	10S
-2	-7	6	622	650	11
-1	-7	6	1173	1167	10
0	-7	6	527	520	9
1	-7	6	1171	1125	12
2	-7	6	382	309	14
3	-7	6	407	363	14
4	-7	6	388	361	16
5	-7	6	926	894	12
6	-7	6	614	586	13
-9	-6	6	174	221	34
-8	-6	6	450	392	14
-7	-6	6	107	105	-62
-6	-6	6	1091	1092	12
-5	-6	6	46	50	-46
-4	-6	6	1551	1608	13
-3	-6	6	272	279	17
-2	-6	6	477	454	12
-1	-6	6	361	389	13
0	-6	6	671	661	17
1	-6	6	325	290	15
2	-6	6	1030	1012	11
3	-6	6	172	198	30
4	-6	6	1054	1075	12
5	-6	6	403	409	15
6	-6	6	446	393	15
7	-6	6	458	471	15
-9	-5	6	1002	1008	12
-8	-5	6	798	820	11
-7	-5	6	890	905	11
-6	-5	6	372	382	14
-5	-5	6	204	190	22
-4	-5	6	573	603	11
-3	-5	6	1170	1195	11
-2	-5	6	714	787	10
-1	-5	6	1279	1241	12
0	-5	6	753	745	10
1	-5	6	802	860	10
2	-5	6	559	615	11
3	-5	6	427	370	13
4	-5	6	568	518	11
5	-5	6	923	841	11
6	-5	6	777	739	12
7	-5	6	966	967	12
-10	-4	6	527	480	13
-9	-4	6	171	156	33
-8	-4	6	273	265	20
-7	-4	6	599	663	11
-6	-4	6	659	707	10
-5	-4	6	1450	1477	12
-4	-4	6	725	707	10

H	K	L	10FO	10FC	10S
3	-4	6	1399	1412	12
4	-4	6	558	564	11
5	-4	6	1029	1030	11
6	-4	6	417	512	15
7	-4	6	226	269	27
8	-4	6	334	289	21
-10	-3	6	1021	1013	12
-9	-3	6	50	121	-50
-8	-3	6	1196	1203	12
-7	-3	6	220	236	22
-6	-3	6	516	485	11
-5	-3	6	331	314	14
-4	-3	6	451	468	10
-3	-3	6	302	320	13
-2	-3	6	1897	1901	14
-1	-3	6	358	341	11
0	-3	6	1863	1941	14
1	-3	6	325	349	12
2	-3	6	439	417	11
3	-3	6	615	643	10
4	-3	6	967	940	10
5	-3	6	442	405	13
6	-3	6	1152	1142	12
7	-3	6	163	81	34
8	-3	6	758	807	13
-10	-2	6	239	350	24
-9	-2	6	427	434	14
-8	-2	6	418	421	14
-7	-2	6	926	919	10
-6	-2	6	642	720	10
-5	-2	6	1338	1393	9
-4	-2	6	581	625	9
-3	-2	6	856	920	8
-2	-2	6	814	781	8
-1	-2	6	142	143	24
0	-2	6	704	634	15
1	-2	6	1301	1299	11
2	-2	6	972	878	9
3	-2	6	1915	1777	14
4	-2	6	589	567	11
5	-2	6	621	637	11
6	-2	6	455	393	13
7	-2	6	267	340	23
8	-2	6	416	490	16
-10	-1	6	440	408	15
-9	-1	6	1115	1084	11
-8	-1	6	476	524	13
-7	-1	6	1102	1090	10
-6	-1	6	509	555	11
-5	-1	6	215	228	18

H	K	L	10FO	10FC	10S
2	-1	6	317	382	12
3	-1	6	291	320	14
4	-1	6	515	387	11
5	-1	6	903	897	11
6	-1	6	671	730	11
7	-1	6	937	959	12
8	-1	6	601	576	13
-10	0	6	684	710	12
-9	0	6	49	58	-49
-8	0	6	294	289	17
-7	0	6	165	139	29
-6	0	6	2023	2171	11
-5	0	6	42	78	-42
-4	0	6	1617	1715	9
-3	0	6	94	74	-42
-2	0	6	397	399	9
-1	0	6	500	505	8
0	0	6	898	898	9
1	0	6	331	344	11
2	0	6	1488	1468	11
3	0	6	44	34	-44
4	0	6	1683	1647	13
5	0	6	438	456	13
6	0	6	205	207	25
7	0	6	604	622	12
8	0	6	545	539	13
-10	1	6	445	401	14
-9	1	6	1116	1102	12
-8	1	6	553	505	11
-7	1	6	1051	1094	10
-6	1	6	513	537	11
-5	1	6	195	223	22
-4	1	6	357	365	11
-3	1	6	1068	1069	9
-2	1	6	1442	1409	10
-1	1	6	2209	2202	13
0	1	6	522	460	6
1	1	6	932	927	9
2	1	6	414	299	10
3	1	6	296	258	14
4	1	6	400	484	13
5	1	6	911	887	10
6	1	6	728	678	11
7	1	6	940	960	11
8	1	6	554	607	14
-10	2	6	324	275	18
-9	2	6	425	414	15
-8	2	6	428	407	13
-7	2	6	876	960	10
-6	2	6	693	694	10

H	K	L	10FO	10FC	10S
-3	10	5	236	251	20
-2	10	5	583	578	11
-1	10	5	325	323	16
0	10	5	964	1016	27
1	10	5	640	682	13
2	10	5	875	870	11
1	2	6	1326	1294	11
2	2	6	889	932	10
3	2	6	1815	1810	14
4	2	6	577	563	11
5	2	6	661	613	11
6	2	6	370	447	15
7	2	6	340	311	17
8	2	6	502	431	14
-10	3	6	1062	1013	11
-9	3	6	50	104	-50
-8	3	6	1209	1215	10
-7	3	6	201	248	24
-6	3	6	459	517	11
-5	3	6	315	320	13
-4	3	6	467	448	10
-3	3	6	318	277	12
-2	3	6	1918	1875	11
-1	3	6	345	335	11
0	3	6	1945	1882	13
1	3	6	348	330	12
2	3	6	407	422	12
3	3	6	644	603	10
4	3	6	941	928	10
5	3	6	406	453	13
6	3	6	1110	1172	12
7	3	6	155	109	36
8	3	6	788	800	12
-10	4	6	523	439	14
-9	4	6	179	150	30
-8	4	6	277	279	18
-7	4	6	631	627	10
-6	4	6	671	677	10
-5	4	6	1435	1495	10
-4	4	6	659	734	9
-3	4	6	1422	1467	10
-2	4	6	461	501	10
-1	4	6	220	242	16
0	4	6	372	412	18
1	4	6	1180	1215	11
2	4	6	1190	1159	11
3	4	6	1370	1433	13
4	4	6	542	538	11
5	4	6	1017	1019	12
6	4	6	504	433	12

H	K	L	10FO	10FC	10S
-8	-7	6	577	546	13
-7	-7	6	720	682	11
-6	-7	6	232	254	23
-5	-7	6	113	98	-51
-4	-7	6	308	292	16
-3	-7	6	628	659	11
1	5	6	863	838	10
2	5	6	648	558	10
3	5	6	391	416	13
4	5	6	530	550	11
5	5	6	841	888	11
6	5	6	766	758	11
7	5	6	961	963	12
-9	6	6	225	183	26
-8	6	6	388	403	15
-7	6	6	83	124	-83
-6	6	6	1086	1113	11
-5	6	6	44	25	-44
-4	6	6	1552	1602	11
-3	6	6	265	266	17
-2	6	6	447	467	11
-1	6	6	371	343	12
0	6	6	687	658	18
1	6	6	279	308	17
2	6	6	1011	1033	11
3	6	6	205	195	23
4	6	6	1058	1059	12
5	6	6	385	397	15
6	6	6	422	404	15
7	6	6	426	457	17
-8	7	6	567	571	12
-7	7	6	683	700	12
-6	7	6	228	238	23
-5	7	6	74	87	-74
-4	7	6	293	284	16
-3	7	6	636	648	10
-2	7	6	644	629	10
-1	7	6	1144	1146	11
0	7	6	495	516	11
1	7	6	1062	1121	11
2	7	6	290	356	17
3	7	6	328	386	17
4	7	6	344	383	17
5	7	6	873	890	12
6	7	6	555	588	14
-8	8	6	345	334	18
-7	8	6	609	623	12
-6	8	6	460	464	14
-5	8	6	755	792	11
-4	8	6	703	721	11

H	K	L	10FO	10FC	10S
-3	-4	6	1468	1438	12
-2	-4	6	485	468	10
-1	-4	6	215	218	18
0	-4	6	422	352	27
1	-4	6	1184	1184	10
2	-4	6	1190	1156	11
-4	9	6	433	421	13
-3	9	6	324	353	16
-2	9	6	1012	1033	10
-1	9	6	47	68	-47
0	9	6	1204	1229	40
1	9	6	137	229	-42
2	9	6	472	467	14
3	9	6	321	314	19
4	9	6	703	665	12
-5	10	6	1016	995	12
-4	10	6	426	453	15
-3	10	6	708	724	11
-2	10	6	380	419	15
-1	10	6	153	178	34
0	10	6	345	338	12
1	10	6	617	678	14
2	10	6	277	308	22
3	10	6	792	824	12
-3	11	6	585	590	12
-2	11	6	691	645	12
-1	11	6	705	711	12
0	11	6	540	538	26
1	11	6	440	491	18
-4	-10	7	1029	1032	12
-3	-10	7	446	438	15
-2	-10	7	720	752	12
-1	-10	7	273	260	21
0	-10	7	231	218	19
1	-10	7	299	284	21
2	-10	7	386	343	17
-6	-9	7	192	186	30
-5	-9	7	658	576	12
-4	-9	7	148	110	-38
-3	-9	7	50	54	-50
-2	-9	7	248	200	23
-1	-9	7	1048	947	11
0	-9	7	59	204	-43
1	-9	7	1218	1235	13
2	-9	7	114	125	-65
3	-9	7	394	440	17
-7	-8	7	50	29	-50
-6	-8	7	360	326	17
-5	-8	7	449	421	14
-4	-8	7	978	982	11

H	K	L	10FO	10FC	10S
-4	-1	6	345	374	12
-3	-1	6	1065	1093	9
-2	-1	6	1413	1425	9
-1	-1	6	2240	2191	12
0	-1	6	479	505	9
1	-1	6	972	906	9
-5	-7	7	357	384	15
-4	-7	7	545	567	12
-3	-7	7	215	232	23
-2	-7	7	347	352	15
-1	-7	7	396	438	14
0	-7	7	1545	1535	39
1	-7	7	577	539	12
2	-7	7	972	940	12
3	-7	7	422	371	14
4	-7	7	246	171	24
5	-7	7	492	455	15
-8	-6	7	145	127	-44
-7	-6	7	206	182	27
-6	-6	7	134	149	-43
-5	-6	7	1214	1233	13
-4	-6	7	216	228	22
-3	-6	7	1469	1491	14
-2	-6	7	47	29	-47
-1	-6	7	788	739	11
0	-6	7	399	364	13
1	-6	7	48	61	-48
2	-6	7	289	328	17
3	-6	7	774	840	11
4	-6	7	196	154	28
5	-6	7	1299	1322	13
6	-6	7	218	179	29
-9	-5	7	502	447	14
-8	-5	7	968	941	11
-7	-5	7	676	709	11
-6	-5	7	1204	1267	12
-5	-5	7	351	363	15
-4	-5	7	427	408	13
-3	-5	7	123	159	-44
-2	-5	7	633	649	11
-1	-5	7	813	807	10
0	-5	7	1090	1122	9
1	-5	7	694	675	11
2	-5	7	1006	1015	11
3	-5	7	399	402	14
4	-5	7	558	500	12
5	-5	7	322	364	18
6	-5	7	670	690	13
-9	-4	7	269	320	22
-8	-4	7	493	511	13

H	K	L	10FO	10FC	10S
-5	2	6	1331	1400	11
-4	2	6	574	622	9
-3	2	6	870	896	9
-2	2	6	786	785	9
-1	2	6	148	151	21
0	2	6	645	694	6
5	-4	7	246	272	23
6	-4	7	890	837	12
7	-4	7	501	463	15
-10	-3	7	156	189	-43
-9	-3	7	700	727	12
-8	-3	7	198	198	26
-7	-3	7	1291	1324	12
-6	-3	7	133	53	-36
-5	-3	7	994	1043	11
-4	-3	7	166	167	27
-3	-3	7	167	106	24
-2	-3	7	198	210	20
-1	-3	7	1446	1447	12
0	-3	7	178	162	27
1	-3	7	1792	1837	13
2	-3	7	264	258	18
3	-3	7	837	835	11
4	-3	7	428	464	14
5	-3	7	341	327	16
6	-3	7	443	470	14
7	-3	7	782	773	13
-10	-2	7	1047	959	11
-9	-2	7	449	441	14
-8	-2	7	303	314	18
-7	-2	7	149	95	32
-6	-2	7	596	592	11
-5	-2	7	509	525	10
-4	-2	7	1027	1084	9
-3	-2	7	1034	1010	9
-2	-2	7	1597	1623	10
-1	-2	7	1068	1057	9
0	-2	7	528	500	7
1	-2	7	487	500	11
2	-2	7	1103	1117	10
3	-2	7	894	898	10
4	-2	7	1179	1175	11
5	-2	7	562	578	11
6	-2	7	824	812	12
7	-2	7	551	544	13
-10	-1	7	223	357	28
-9	-1	7	208	206	26
-8	-1	7	883	879	10
-7	-1	7	874	886	10
-6	-1	7	1300	1384	10

H	K	L	10FO	10FC	10S
7	4	6	262	238	23
8	4	6	258	354	25
-9	5	6	1041	986	11
-8	5	6	803	833	11
-7	5	6	892	887	10
-6	5	6	388	372	13
-5	5	6	153	211	30
-4	5	6	559	602	10
-3	5	6	1129	1184	9
-2	5	6	751	740	9
-1	5	6	1204	1279	10
0	5	6	750	732	8
7	-1	7	754	756	12
-10	0	7	51	26	-51
-9	0	7	944	938	11
-8	0	7	49	120	-49
-7	0	7	123	134	-46
-6	0	7	47	150	-47
-5	0	7	1145	1179	10
-4	0	7	158	132	26
-3	0	7	1667	1708	11
-2	0	7	135	135	30
-1	0	7	1414	1391	10
0	0	7	345	339	8
1	0	7	204	203	20
2	0	7	406	398	12
3	0	7	1243	1201	11
4	0	7	71	95	-71
5	0	7	1389	1405	12
6	0	7	468	454	13
7	0	7	700	705	12
-10	1	7	431	365	16
-9	1	7	189	161	28
-8	1	7	864	908	10
-7	1	7	873	881	10
-6	1	7	1340	1366	10
-5	1	7	760	792	10
-4	1	7	464	453	10
-3	1	7	359	356	12
-2	1	7	739	659	9
-1	1	7	749	789	9
0	1	7	1384	1356	24
1	1	7	661	691	9
2	1	7	1194	1181	10
3	1	7	900	938	10
4	1	7	306	293	17
5	1	7	506	528	12
6	1	7	759	764	11
7	1	7	769	729	12
-10	2	7	1010	991	12

H	K	L	10FO	10FC	10S
-3	8	6	908	913	10
-2	8	6	358	359	14
-1	8	6	138	154	33
0	8	6	400	399	18
1	8	6	850	922	11
2	8	6	761	764	11
3	8	6	922	970	11
4	8	6	411	466	16
5	8	6	586	633	13
-7	9	6	160	167	35
-6	9	6	353	384	16
-5	9	6	49	112	-49
-9	3	7	730	705	12
-8	3	7	197	193	26
-7	3	7	1318	1317	11
-6	3	7	105	46	-50
-5	3	7	997	1037	10
-4	3	7	159	191	26
-3	3	7	131	135	32
-2	3	7	211	207	18
-1	3	7	1455	1440	11
0	3	7	183	189	24
1	3	7	1874	1835	14
2	3	7	241	265	18
3	3	7	850	832	10
4	3	7	404	466	14
5	3	7	332	355	16
6	3	7	470	426	13
7	3	7	726	815	13
-9	4	7	320	314	18
-8	4	7	511	515	13
-7	4	7	217	191	21
-6	4	7	612	606	10
-5	4	7	160	146	28
-4	4	7	1403	1492	10
-3	4	7	624	643	10
-2	4	7	1049	1067	10
-1	4	7	905	913	9
0	4	7	130	169	23
1	4	7	607	553	10
2	4	7	601	558	11
3	4	7	754	726	11
4	4	7	1156	1115	12
5	4	7	281	263	19
6	4	7	836	871	12
7	4	7	491	451	14
-9	5	7	422	453	16
-8	5	7	1012	916	11
-7	5	7	673	698	10
-6	5	7	1247	1245	10

H	K	L	10FO	10FC	10S
-3	-8	7	824	751	11
-2	-8	7	826	791	11
-1	-8	7	544	529	13
0	-8	7	315	321	12
1	-8	7	276	300	20
2	-8	7	562	566	13
3	-8	7	573	533	13
4	-8	7	809	814	12
5	-8	7	540	529	15
-8	-7	7	1030	997	13
-7	-7	7	503	467	14
-6	-7	7	730	750	12
-2	6	7	45	21	-45
-1	6	7	764	770	9
0	6	7	391	395	9
1	6	7	78	80	-78
2	6	7	318	276	15
3	6	7	814	826	11
4	6	7	151	151	36
5	6	7	1280	1309	12
6	6	7	53	229	-53
-8	7	7	1039	1018	12
-7	7	7	469	483	14
-6	7	7	713	755	11
-5	7	7	378	341	14
-4	7	7	539	537	11
-3	7	7	194	201	25
-2	7	7	347	341	14
-1	7	7	441	416	12
0	7	7	1508	1517	40
1	7	7	523	549	13
2	7	7	925	949	11
3	7	7	359	379	16
4	7	7	144	248	-42
5	7	7	455	494	15
-7	8	7	50	27	-50
-6	8	7	312	339	18
-5	8	7	426	439	13
-4	8	7	965	968	11
-3	8	7	748	780	11
-2	8	7	809	793	11
-1	8	7	554	519	11
0	8	7	306	321	13
1	8	7	269	281	20
2	8	7	528	571	13
3	8	7	495	543	14
4	8	7	795	807	12
-6	9	7	180	196	32
-5	9	7	481	615	14
-4	9	7	49	129	-49

H	K	L	10FO	10FC	10S
-7	-4	7	158	178	33
-6	-4	7	569	618	11
-5	-4	7	46	149	-46
-4	-4	7	1437	1460	12
-3	-4	7	676	630	10
-2	-4	7	1091	1065	10
-1	-4	7	932	887	11
0	-4	7	147	121	22
1	-4	7	541	610	11
2	-4	7	542	591	11
3	-4	7	724	745	11
4	-4	7	1140	1139	12
-5	-9	8	245	198	25
-4	-9	8	1146	1077	12
-3	-9	8	229	176	25
-2	-9	8	189	219	32
-1	-9	8	224	209	25
0	-9	8	761	740	9
1	-9	8	230	243	27
2	-9	8	937	955	13
-6	-8	8	122	174	-62
-5	-8	8	131	128	-50
-4	-8	8	372	358	16
-3	-8	8	751	731	11
-2	-8	8	668	631	11
-1	-8	8	1043	1011	12
0	-8	8	628	619	11
1	-8	8	647	624	12
2	-8	8	366	282	18
3	-8	8	452	477	15
-7	-7	8	542	479	14
-6	-7	8	487	484	14
-5	-7	8	1081	1037	12
-4	-7	8	565	569	12
-3	-7	8	879	866	11
-2	-7	8	146	193	-37
-1	-7	8	323	295	17
0	-7	8	350	338	13
1	-7	8	1141	1107	12
2	-7	8	518	538	13
3	-7	8	760	722	12
4	-7	8	530	519	14
-8	-6	8	1115	1051	13
-7	-6	8	190	167	29
-6	-6	8	314	327	17
-5	-6	8	124	165	-49
-4	-6	8	800	804	12
-3	-6	8	275	293	18
-2	-6	8	979	1003	11
-1	-6	8	281	259	18

H	K	L	10FO	10FC	10S
-5	-1	7	776	793	9
-4	-1	7	446	474	11
-3	-1	7	326	394	13
-2	-1	7	675	714	9
-1	-1	7	826	739	9
0	-1	7	1367	1361	16
1	-1	7	681	678	10
2	-1	7	1235	1150	11
3	-1	7	951	905	11
4	-1	7	300	308	17
5	-1	7	517	513	11
6	-1	7	762	750	11
4	-5	8	681	729	13
5	-5	8	582	596	14
6	-5	8	370	451	19
-9	-4	8	994	958	12
-8	-4	8	277	244	20
-7	-4	8	888	838	11
-6	-4	8	360	350	15
-5	-4	8	183	229	28
-4	-4	8	276	244	18
-3	-4	8	1042	1018	11
-2	-4	8	871	887	11
-1	-4	8	1383	1403	12
0	-4	8	712	678	11
1	-4	8	905	940	11
2	-4	8	339	410	16
3	-4	8	359	385	16
4	-4	8	411	375	15
5	-4	8	913	925	12
6	-4	8	474	447	15
-9	-3	8	50	47	-50
-8	-3	8	519	544	13
-7	-3	8	127	106	-42
-6	-3	8	1165	1159	12
-5	-3	8	139	106	-38
-4	-3	8	1180	1202	12
-3	-3	8	201	206	24
-2	-3	8	476	500	11
-1	-3	8	529	438	11
0	-3	8	911	891	16
1	-3	8	367	400	13
2	-3	8	1531	1533	13
3	-3	8	135	71	-38
4	-3	8	824	857	11
5	-3	8	393	438	16
6	-3	8	237	173	25
-9	-2	8	849	739	11
-8	-2	8	492	510	13
-7	-2	8	583	596	12

H	K	L	10FO	10FC	10S
-9	2	7	469	416	13
-8	2	7	288	316	18
-7	2	7	92	105	-92
-6	2	7	569	633	11
-5	2	7	513	516	10
-4	2	7	1093	1068	9
-3	2	7	993	1022	10
-2	2	7	1595	1622	12
-1	2	7	1066	1060	10
0	2	7	507	544	11
1	2	7	510	503	9
2	2	7	1134	1064	11
3	2	7	914	894	10
4	2	7	1198	1165	12
5	2	7	543	563	12
6	2	7	793	834	12
7	2	7	521	553	14
-10	3	7	202	178	29
-6	-1	8	765	816	10
-5	-1	8	1328	1362	10
-4	-1	8	313	338	15
-3	-1	8	923	908	9
-2	-1	8	100	217	-58
-1	-1	8	273	285	16
0	-1	8	311	219	11
1	-1	8	1105	1121	11
2	-1	8	842	798	10
3	-1	8	1266	1278	12
4	-1	8	714	650	11
5	-1	8	372	358	16
6	-1	8	389	471	17
7	-1	8	362	407	18
-10	0	8	1026	1002	12
-9	0	8	194	109	29
-8	0	8	1086	1095	11
-7	0	8	93	64	-93
-6	0	8	578	580	11
-5	0	8	45	45	-45
-4	0	8	944	956	9
-3	0	8	265	259	16
-2	0	8	1710	1692	12
-1	0	8	163	142	26
0	0	8	912	917	7
1	0	8	448	407	12
2	0	8	527	515	11
3	0	8	680	688	11
4	0	8	594	570	11
5	0	8	184	198	31
6	0	8	1228	1247	12
7	0	8	81	202	-81

H	K	L	10FO	10FC	10S
-5	5	7	355	331	14
-4	5	7	391	430	13
-3	5	7	192	171	22
-2	5	7	655	612	10
-1	5	7	855	792	10
0	5	7	1114	1106	25
1	5	7	674	693	10
2	5	7	991	1023	11
3	5	7	434	406	12
4	5	7	508	527	12
5	5	7	329	329	17
6	5	7	686	682	12
-8	6	7	173	114	31
-7	6	7	196	180	26
-6	6	7	90	153	-90
-5	6	7	1201	1250	12
-4	6	7	180	219	26
-3	6	7	1430	1501	11
-3	2	8	1205	1163	11
-2	2	8	833	870	10
-1	2	8	1384	1356	12
0	2	8	763	740	9
1	2	8	645	661	11
2	2	8	456	527	12
3	2	8	262	316	18
4	2	8	643	659	11
5	2	8	779	802	12
6	2	8	274	261	22
7	2	8	916	940	12
-9	3	8	50	62	-50
-8	3	8	561	516	12
-7	3	8	116	88	-52
-6	3	8	1182	1159	11
-5	3	8	94	123	-72
-4	3	8	1228	1202	10
-3	3	8	211	197	21
-2	3	8	503	464	11
-1	3	8	454	515	11
0	3	8	898	899	15
1	3	8	384	367	13
2	3	8	1600	1522	13
3	3	8	46	76	-46
4	3	8	849	841	11
5	3	8	419	417	15
6	3	8	139	204	-47
-9	4	8	1026	951	12
-8	4	8	249	263	22
-7	4	8	830	881	11
-6	4	8	336	364	15
-5	4	8	247	214	18

H	K	L	10FO	10FC	10S
-3	9	7	49	62	-49
-2	9	7	177	253	29
-1	9	7	941	970	11
0	9	7	192	150	19
1	9	7	1161	1234	12
2	9	7	171	120	33
3	9	7	420	406	16
-4	10	7	1064	1016	11
-3	10	7	436	435	14
-2	10	7	781	734	10
-1	10	7	263	239	21
0	10	7	211	224	19
1	10	7	53	302	-53
2	10	7	319	379	20
-3	-10	8	762	739	13
-2	-10	8	321	291	19
-1	-10	8	778	730	12
0	-10	8	412	413	12
5	5	8	590	591	13
6	5	8	401	416	18
-8	6	8	1158	1058	12
-7	6	8	171	169	31
-6	6	8	332	319	15
-5	6	8	200	162	23
-4	6	8	781	795	10
-3	6	8	304	261	16
-2	6	8	986	992	10
-1	6	8	277	266	16
0	6	8	1084	1082	21
1	6	8	355	353	14
2	6	8	195	229	25
3	6	8	296	353	18
4	6	8	742	748	12
5	6	8	245	222	24
-7	7	8	493	510	14
-6	7	8	463	490	14
-5	7	8	1051	1033	12
-4	7	8	561	555	12
-3	7	8	864	857	11
-2	7	8	145	159	-37
-1	7	8	314	304	15
0	7	8	343	350	14
1	7	8	1062	1102	11
2	7	8	522	523	14
3	7	8	721	741	12
4	7	8	494	519	15
-6	8	8	160	198	36
-5	8	8	164	135	33
-4	8	8	409	353	14
-3	8	8	704	733	12

H	K	L	10FO	10FC	10S
0	-6	8	1116	1072	62
1	-6	8	355	374	15
2	-6	8	198	200	29
3	-6	8	328	322	18
4	-6	8	736	761	12
5	-6	8	190	230	35
-8	-5	8	126	135	-54
-7	-5	8	725	755	12
-6	-5	8	649	685	11
-5	-5	8	1218	1241	12
-4	-5	8	762	805	11
-3	-5	8	542	546	12
-2	-5	8	216	155	22
-1	-5	8	383	289	15
0	-5	8	599	578	18
1	-5	8	879	806	11
2	-5	8	563	537	12
3	-5	8	931	984	12
-3	-8	9	52	86	-52
-2	-8	9	558	572	13
-1	-8	9	579	554	13
0	-8	9	1068	1007	25
1	-8	9	606	604	13
2	-8	9	433	441	17
-6	-7	9	435	372	15
-5	-7	9	356	372	17
-4	-7	9	1002	1000	12
-3	-7	9	375	357	17
-2	-7	9	827	785	12
-1	-7	9	302	310	19
0	-7	9	259	281	16
1	-7	9	411	348	15
2	-7	9	616	629	13
3	-7	9	426	425	17
-7	-6	9	1024	984	12
-6	-6	9	156	149	38
-5	-6	9	691	668	12
-4	-6	9	164	218	35
-3	-6	9	149	189	-39
-2	-6	9	370	336	15
-1	-6	9	901	906	12
0	-6	9	239	214	20
1	-6	9	1119	1159	12
2	-6	9	257	200	23
3	-6	9	504	571	14
4	-6	9	471	462	15
-8	-5	9	284	254	22
-7	-5	9	51	40	-51
-6	-5	9	564	519	12
-5	-5	9	771	761	11

H	K	L	10FO	10FC	10S
-6	-2	8	151	144	32
-5	-2	8	197	147	24
-4	-2	8	168	185	28
-3	-2	8	1157	1181	9
-2	-2	8	878	845	9
-1	-2	8	1385	1375	10
0	-2	8	745	756	7
1	-2	8	748	648	9
2	-2	8	521	472	11
3	-2	8	299	279	17
4	-2	8	674	631	11
5	-2	8	814	819	11
6	-2	8	233	304	26
7	-2	8	944	937	12
-10	-1	8	178	310	38
-9	-1	8	114	97	-60
-8	-1	8	316	311	19
-7	-1	8	987	1009	10
-9	-3	9	619	591	13
-8	-3	9	181	185	32
-7	-3	9	182	200	30
-6	-3	9	238	204	23
-5	-3	9	1015	976	11
-4	-3	9	147	81	34
-3	-3	9	1636	1602	14
-2	-3	9	211	174	23
-1	-3	9	744	778	11
0	-3	9	309	389	28
1	-3	9	598	605	12
2	-3	9	478	545	13
3	-3	9	1004	1043	12
4	-3	9	340	310	17
5	-3	9	823	814	12
-9	-2	9	440	431	16
-8	-2	9	961	961	11
-7	-2	9	578	537	12
-6	-2	9	991	1059	11
-5	-2	9	498	466	12
-4	-2	9	117	111	-46
-3	-2	9	369	422	15
-2	-2	9	889	917	10
-1	-2	9	901	881	10
0	-2	9	1094	1085	16
1	-2	9	722	687	11
2	-2	9	1001	973	11
3	-2	9	430	400	14
4	-2	9	329	309	18
5	-2	9	303	392	21
6	-2	9	607	628	14
-9	-1	9	403	436	17

H	K	L	10FO	10FC	10S
-10	1	8	329	279	19
-9	1	8	140	104	-42
-8	1	8	327	330	17
-7	1	8	986	1023	10
-6	1	8	796	815	10
-5	1	8	1347	1330	10
-4	1	8	359	300	14
-3	1	8	928	912	9
-2	1	8	206	183	20
-1	1	8	299	252	15
0	1	8	207	324	31
1	1	8	1107	1141	10
2	1	8	837	811	10
3	1	8	1305	1272	12
4	1	8	660	677	11
5	1	8	367	375	16
6	1	8	458	429	14
7	1	8	448	373	16
-9	2	8	802	797	11
-8	2	8	505	502	13
-7	2	8	624	587	11
-6	2	8	175	122	26
-5	2	8	195	183	22
-4	2	8	164	184	27
0	0	9	54	19	-39
1	0	9	1114	1097	11
2	0	9	254	263	20
3	0	9	898	863	11
4	0	9	434	460	14
5	0	9	503	520	14
6	0	9	328	355	20
-9	1	9	471	421	14
-8	1	9	191	169	31
-7	1	9	260	264	20
-6	1	9	570	553	11
-5	1	9	578	597	11
-4	1	9	1039	1009	10
-3	1	9	654	675	11
-2	1	9	1183	1192	11
-1	1	9	444	488	12
0	1	9	156	218	26
1	1	9	337	353	15
2	1	9	714	738	10
3	1	9	680	695	11
4	1	9	856	867	11
5	1	9	575	584	13
6	1	9	537	592	15
-9	2	9	477	431	14
-8	2	9	981	972	11
-7	2	9	529	550	12

H	K	L	10FO	10FC	10S
-4	4	8	242	256	19
-3	4	8	1005	1070	10
-2	4	8	915	871	10
-1	4	8	1396	1375	11
0	4	8	682	694	7
1	4	8	952	915	11
2	4	8	371	340	15
3	4	8	391	366	14
4	4	8	385	420	15
5	4	8	905	919	12
6	4	8	465	469	15
-8	5	8	120	174	-53
-7	5	8	740	730	11
-6	5	8	691	662	11
-5	5	8	1212	1244	10
-4	5	8	792	785	10
-3	5	8	542	529	11
-2	5	8	46	191	-46
-1	5	8	330	337	14
0	5	8	579	597	14
1	5	8	799	870	11
2	5	8	515	573	12
3	5	8	956	974	11
4	5	8	733	716	11
-6	4	9	735	780	11
-5	4	9	465	466	13
-4	4	9	249	256	19
-3	4	9	369	357	14
-2	4	9	679	713	10
-1	4	9	571	571	11
0	4	9	1185	1149	22
1	4	9	513	513	12
2	4	9	782	790	11
3	4	9	479	444	13
4	4	9	50	168	-50
5	4	9	505	504	14
-8	5	9	210	273	28
-7	5	9	86	67	-86
-6	5	9	538	504	12
-5	5	9	760	758	11
-4	5	9	1057	1082	11
-3	5	9	566	575	12
-2	5	9	714	711	10
-1	5	9	321	327	16
0	5	9	351	331	10
1	5	9	281	221	18
2	5	9	531	555	12
3	5	9	662	688	12
4	5	9	889	894	12
5	5	9	631	623	13

H	K	L	10FO	10FC	10S
-2	8	8	638	639	11
-1	8	8	1043	1011	11
0	8	8	629	599	23
1	8	8	583	635	13
2	8	8	271	343	21
3	8	8	462	442	16
-5	9	8	233	218	24
-4	9	8	1081	1097	11
-3	9	8	96	207	-96
-2	9	8	192	204	29
-1	9	8	220	202	24
0	9	8	719	739	41
1	9	8	142	220	-45
2	9	8	928	963	12
-3	10	8	726	746	12
-2	10	8	239	305	24
-1	10	8	700	730	12
0	10	8	434	409	14
-3	-9	9	995	949	12
-2	-9	9	167	114	38
-1	-9	9	476	454	15
0	-9	9	290	297	19
-5	-8	9	442	409	16
-4	-8	9	351	344	19
-3	9	9	952	948	12
-2	9	9	162	151	35
-1	9	9	466	443	14
0	9	9	283	295	30
-3	-8	10	516	450	15
-2	-8	10	113	105	-70
-1	-8	10	454	454	16
-5	-7	10	224	240	29
-4	-7	10	273	319	23
-3	-7	10	703	709	12
-2	-7	10	382	410	18
-1	-7	10	941	920	12
0	-7	10	476	441	10
1	-7	10	342	327	19
-6	-6	10	1029	1012	13
-5	-6	10	154	176	-41
-4	-6	10	797	771	12
-3	-6	10	200	176	28
-2	-6	10	168	56	35
-1	-6	10	425	368	15
0	-6	10	611	610	16
1	-6	10	51	151	-51
2	-6	10	849	863	12
-7	-5	10	532	492	14
-6	-5	10	187	144	30
-5	-5	10	333	319	18

H	K	L	10FO	10FC	10S
-4	-5	9	1090	1061	12
-3	-5	9	576	585	12
-2	-5	9	710	721	11
-1	-5	9	303	303	18
0	-5	9	327	322	15
1	-5	9	194	297	29
2	-5	9	536	542	12
3	-5	9	675	661	13
4	-5	9	889	895	13
5	-5	9	619	611	14
-8	-4	9	899	894	12
-7	-4	9	473	469	14
-6	-4	9	782	746	11
-5	-4	9	468	452	13
-4	-4	9	245	239	21
-3	-4	9	386	380	14
-2	-4	9	704	697	11
-1	-4	9	562	587	11
0	-4	9	1156	1158	20
1	-4	9	501	520	12
2	-4	9	777	805	12
3	-4	9	416	489	15
4	-4	9	131	142	-52
5	-4	9	537	500	14
2	-3	10	75	77	-75
3	-3	10	506	496	14
4	-3	10	515	524	14
-8	-2	10	162	207	40
-7	-2	10	915	888	11
-6	-2	10	486	509	14
-5	-2	10	834	875	11
-4	-2	10	556	571	12
-3	-2	10	527	525	12
-2	-2	10	358	326	15
-1	-2	10	323	316	17
0	-2	10	638	617	9
1	-2	10	1038	1042	11
2	-2	10	483	480	13
3	-2	10	845	882	12
4	-2	10	305	324	20
-8	-1	10	464	417	16
-7	-1	10	685	711	12
-6	-1	10	131	104	-44
-5	-1	10	196	199	25
-4	-1	10	447	457	14
-3	-1	10	1115	1144	11
-2	-1	10	561	503	12
-1	-1	10	1210	1167	11
0	-1	10	464	429	9
1	-1	10	449	427	14

H	K	L	10FO	10FC	10S
-8	-1	9	168	207	34
-7	-1	9	248	266	22
-6	-1	9	503	566	13
-5	-1	9	604	588	11
-4	-1	9	1000	1052	10
-3	-1	9	640	672	11
-2	-1	9	1215	1161	10
-1	-1	9	506	466	11
0	-1	9	224	163	18
1	-1	9	345	350	14
2	-1	9	743	730	10
3	-1	9	689	692	11
4	-1	9	869	881	11
5	-1	9	593	603	13
6	-1	9	572	592	14
-9	0	9	653	637	13
-8	0	9	50	43	-50
-7	0	9	1466	1477	11
-6	0	9	85	70	-85
-5	0	9	727	735	10
-4	0	9	96	133	-65
-3	0	9	554	523	11
-2	0	9	319	314	16
-1	0	9	1050	1024	10
4	1	10	516	521	14
5	1	10	753	807	12
-8	2	10	160	211	-40
-7	2	10	889	889	11
-6	2	10	525	526	12
-5	2	10	874	841	11
-4	2	10	569	567	12
-3	2	10	536	528	12
-2	2	10	337	341	15
-1	2	10	316	333	16
0	2	10	645	632	15
1	2	10	1063	1036	12
2	2	10	493	463	13
3	2	10	854	857	12
4	2	10	293	322	21
-8	3	10	789	737	12
-7	3	10	148	136	-41
-6	3	10	243	261	22
-5	3	10	203	272	25
-4	3	10	738	719	11
-3	3	10	235	163	20
-2	3	10	1469	1411	12
-1	3	10	98	47	-71
0	3	10	765	778	19
1	3	10	432	407	14
2	3	10	74	76	-74

H	K	L	10FO	10FC	10S
-6	2	9	1069	1035	11
-5	2	9	479	474	12
-4	2	9	67	96	-67
-3	2	9	427	349	12
-2	2	9	909	875	11
-1	2	9	861	893	11
0	2	9	1069	1078	11
1	2	9	674	701	11
2	2	9	966	1002	11
3	2	9	417	437	14
4	2	9	281	320	20
5	2	9	396	379	16
6	2	9	606	623	13
-9	3	9	604	591	13
-8	3	9	249	190	21
-7	3	9	204	187	25
-6	3	9	226	236	21
-5	3	9	961	1003	11
-4	3	9	46	101	-46
-3	3	9	1634	1636	13
-2	3	9	208	204	22
-1	3	9	824	740	10
0	3	9	364	334	10
1	3	9	620	627	11
2	3	9	557	486	12
3	3	9	991	1052	12
4	3	9	324	331	17
5	3	9	782	842	12
-8	4	9	918	867	11
-7	4	9	456	468	14
-1	6	10	365	417	16
0	6	10	632	608	8
1	6	10	160	105	35
2	6	10	853	872	12
-5	7	10	221	241	27
-4	7	10	317	304	19
-3	7	10	677	702	13
-2	7	10	446	419	15
-1	7	10	939	926	12
0	7	10	483	458	22
1	7	10	278	330	22
-3	8	10	489	478	14
-2	8	10	51	126	-51
-1	8	10	441	426	15
-4	-6	11	124	153	-67
-3	-6	11	741	739	13
-2	-6	11	179	157	34
-1	-6	11	435	446	16
0	-6	11	370	348	16
-5	-5	11	281	240	22

H	K	L	10FO	10FC	10S
-7	6	9	1020	988	12
-6	6	9	187	131	29
-5	6	9	687	671	11
-4	6	9	247	179	20
-3	6	9	211	152	23
-2	6	9	363	327	15
-1	6	9	855	898	10
0	6	9	220	227	18
1	6	9	1133	1163	12
2	6	9	188	256	30
3	6	9	589	548	12
4	6	9	418	486	17
-6	7	9	438	394	15
-5	7	9	389	362	15
-4	7	9	1062	993	12
-3	7	9	376	365	15
-2	7	9	774	805	11
-1	7	9	334	286	16
0	7	9	305	274	18
1	7	9	275	391	21
2	7	9	587	613	13
3	7	9	416	422	16
-5	8	9	451	411	15
-4	8	9	335	371	18
-3	8	9	128	70	-45
-2	8	9	625	552	12
-1	8	9	591	559	12
0	8	9	1025	1017	51
1	8	9	587	569	13
2	8	9	401	446	17
-3	-3	11	502	470	14
-2	-3	11	317	294	17
-1	-3	11	1113	1103	13
0	-3	11	128	199	-38
1	-3	11	880	886	12
2	-3	11	284	307	22
3	-3	11	260	301	25
-7	-2	11	208	177	30
-6	-2	11	539	504	14
-5	-2	11	575	550	12
-4	-2	11	994	982	11
-3	-2	11	610	617	12
-2	-2	11	846	808	11
-1	-2	11	196	209	30
0	-2	11	234	223	16
1	-2	11	555	535	13
2	-2	11	650	646	12
3	-2	11	500	496	15
-7	-1	11	632	614	13
-6	-1	11	656	706	13

H	K	L	10FO	10FC	10S
-4	-5	10	408	379	15
-3	-5	10	808	776	11
-2	-5	10	509	493	13
-1	-5	10	807	840	12
0	-5	10	672	651	10
1	-5	10	398	381	16
2	-5	10	303	369	20
3	-5	10	332	355	20
-7	-4	10	779	799	12
-6	-4	10	505	502	14
-5	-4	10	1001	998	12
-4	-4	10	534	508	13
-3	-4	10	547	525	12
-2	-4	10	364	326	16
-1	-4	10	384	383	15
0	-4	10	568	599	8
1	-4	10	813	849	12
2	-4	10	510	533	13
3	-4	10	861	925	12
4	-4	10	258	293	25
-8	-3	10	786	733	12
-7	-3	10	103	129	-103
-6	-3	10	274	255	20
-5	-3	10	221	215	26
-4	-3	10	738	709	11
-3	-3	10	170	205	30
-2	-3	10	1443	1414	13
-1	-3	10	48	35	-48
0	-3	10	775	757	8
1	-3	10	398	443	15
3	0	11	951	925	12
-7	1	11	624	618	13
-6	1	11	753	676	12
-5	1	11	137	112	-43
-4	1	11	152	188	37
-3	1	11	270	281	21
-2	1	11	663	629	11
-1	1	11	283	329	19
0	1	11	787	825	11
1	1	11	721	718	12
2	1	11	632	624	12
3	1	11	495	514	15
-7	2	11	194	167	29
-6	2	11	565	497	12
-5	2	11	561	563	12
-4	2	11	1014	975	12
-3	2	11	609	609	12
-2	2	11	828	824	12
-1	2	11	243	241	21
0	2	11	246	213	15

H	K	L	10FO	10FC	10S
2	-1	10	462	399	13
3	-1	10	414	398	15
4	-1	10	508	550	14
5	-1	10	786	784	13
-8	0	10	653	621	13
-7	0	10	180	156	30
-6	0	10	1220	1248	11
-5	0	10	48	112	-48
-4	0	10	829	828	11
-3	0	10	327	308	17
-2	0	10	318	305	16
-1	0	10	538	504	12
0	0	10	753	765	11
1	0	10	49	170	-49
2	0	10	1337	1356	13
3	0	10	114	145	-58
4	0	10	653	656	13
5	0	10	595	547	14
-8	1	10	463	431	15
-7	1	10	752	679	11
-6	1	10	108	91	-62
-5	1	10	166	176	33
-4	1	10	503	446	12
-3	1	10	1142	1127	11
-2	1	10	510	545	12
-1	1	10	1162	1198	11
0	1	10	434	436	34
1	1	10	410	469	14
2	1	10	405	454	14
3	1	10	355	412	17
-1	4	11	407	403	15
0	4	11	123	119	-51
1	4	11	500	477	14
2	4	11	681	696	12
-5	5	11	256	248	23
-4	5	11	168	181	37
-3	5	11	233	197	23
-2	5	11	554	499	12
-1	5	11	631	650	12
0	5	11	812	809	17
1	5	11	512	532	14
-4	6	11	134	159	-48
-3	6	11	732	734	12
-2	6	11	142	164	-44
-1	6	11	456	439	15
0	6	11	317	382	14
-4	-4	12	509	504	15
-3	-4	12	743	734	13
-2	-4	12	415	450	17
-1	-4	12	819	826	13

H	K	L	10FO	10FC	10S
3	3	10	507	522	13
4	3	10	472	525	15
-7	4	10	794	781	12
-6	4	10	498	488	13
-5	4	10	976	1010	11
-4	4	10	508	513	12
-3	4	10	526	511	12
-2	4	10	312	371	17
-1	4	10	393	396	14
0	4	10	608	568	33
1	4	10	827	856	12
2	4	10	523	542	13
3	4	10	930	891	12
4	4	10	288	278	22
-7	5	10	503	488	14
-6	5	10	192	180	29
-5	5	10	297	335	18
-4	5	10	394	365	15
-3	5	10	791	790	11
-2	5	10	503	478	12
-1	5	10	837	818	11
0	5	10	667	656	9
1	5	10	376	405	16
2	5	10	349	324	18
3	5	10	325	357	20
-6	6	10	1064	983	12
-5	6	10	125	171	-53
-4	6	10	815	769	11
-3	6	10	169	140	33
-2	6	10	95	91	-95
-2	-1	12	200	246	30
-1	-1	12	414	401	16
0	-1	12	402	387	16
1	-1	12	860	811	12
-6	0	12	53	66	-53
-5	0	12	266	300	23
-4	0	12	741	695	12
-3	0	12	181	182	31
-2	0	12	1078	1052	11
-1	0	12	153	105	-39
0	0	12	670	629	9
1	0	12	339	349	19
-6	1	12	283	404	22
-5	1	12	691	725	13
-4	1	12	206	171	27
-3	1	12	469	460	14
-2	1	12	191	284	30
-1	1	12	403	430	15
0	1	12	397	386	40
1	1	12	819	828	12

H	K	L	10FO	10FC	10S
-4	-5	11	203	211	30
-3	-5	11	173	222	36
-2	-5	11	573	503	13
-1	-5	11	662	637	13
0	-5	11	832	814	16
1	-5	11	512	522	14
-6	-4	11	677	622	13
-5	-4	11	390	352	17
-4	-4	11	870	852	12
-3	-4	11	573	568	12
-2	-4	11	620	650	12
-1	-4	11	437	412	15
0	-4	11	125	152	-39
1	-4	11	467	511	15
2	-4	11	657	687	13
-7	-3	11	999	973	13
-6	-3	11	143	72	-42
-5	-3	11	548	571	14
-4	-3	11	148	189	-39

H	K	L	10FO	10FC	10S
-5	-1	11	129	150	-49
-4	-1	11	154	182	37
-3	-1	11	296	297	18
-2	-1	11	663	656	12
-1	-1	11	321	315	18
0	-1	11	827	814	8
1	-1	11	724	726	12
2	-1	11	619	625	12
3	-1	11	558	471	14
-7	0	11	376	357	17
-6	0	11	167	206	34
-5	0	11	794	814	11
-4	0	11	74	81	-74
-3	0	11	1090	1055	11
-2	0	11	89	132	-89
-1	0	11	489	448	13
0	0	11	314	326	13
1	0	11	549	500	12
2	0	11	396	381	16

H	K	L	10FO	10FC	10S
1	2	11	514	516	13
2	2	11	649	658	12
3	2	11	508	471	14
-7	3	11	999	976	12
-6	3	11	51	82	-51
-5	3	11	591	562	12
-4	3	11	223	138	24
-3	3	11	483	483	13
-2	3	11	257	307	22
-1	3	11	1110	1095	12
0	3	11	218	189	19
1	3	11	884	907	12
2	3	11	262	303	23
3	3	11	305	298	21
-6	4	11	707	627	12
-5	4	11	357	380	17
-4	4	11	838	871	12
-3	4	11	582	546	12
-2	4	11	663	607	12

H	K	L	10FO	10FC	10S
0	-4	12	184	241	31
-5	-3	12	123	56	-59
-4	-3	12	730	679	13
-3	-3	12	235	220	25
-2	-3	12	88	152	-88
-1	-3	12	315	321	19
0	-3	12	703	712	27
-5	-2	12	386	393	18
-4	-2	12	235	404	28
-3	-2	12	965	950	12
-2	-2	12	601	553	13
-1	-2	12	577	580	14
0	-2	12	236	270	31
1	-2	12	248	294	25
-6	-1	12	482	389	15
-5	-1	12	734	710	13
-4	-1	12	52	195	-52
-3	-1	12	513	435	14

H	K	L	10FO	10FC	10S
-5	2	12	424	376	15
-4	2	12	467	407	14
-3	2	12	986	952	12
-2	2	12	618	550	13
-1	2	12	610	578	12
0	2	12	267	263	32
1	2	12	294	273	22
-5	3	12	51	64	-51
-4	3	12	761	698	12
-3	3	12	194	239	31
-2	3	12	191	144	28
-1	3	12	320	332	18
0	3	12	749	716	26
-4	4	12	550	506	14
-3	4	12	728	732	12
-2	4	12	472	440	15
-1	4	12	871	808	12
0	4	12	221	208	20